

Novel Anti-oxidant properties of Cobalamin

Thesis submitted in accordance with the requirements of
The University of Liverpool
for the degree of Doctor of Philosophy by

Ala Altaie

**September 2009
University of Chester**

Table of contents

Title page	i
Declaration	iii
Acknowledgment	iv
Dedication	v
Abstract	vi
Publications and postrs	vii
Thesis contents	viii
List of Figures	xvi
List of Tables	xxix
Abbreviations	xxx

DECLARATION

The work presented in this thesis is original and has not been submitted previously in support of any qualification or course.

Signed:

Date:

Acknowledgments

I would like to express my gratitude to all those whom their support made it possible to complete this thesis;

My supervisors, Professor John Williams and Professor Sarah Andrew for their continued support and advice.

Everyone in the research lab for their endless encouragement and support: Francesca Leoni, Elyse Ireland, Helen Williams, Rob Coleman, Ian Hurly, Neil Pickles, Hong-Mei and Nina Dempsey

Servel Miler and Alison Morgan for listening to me, comforting me and always ensuring that I stay positive.

My parents and family for being supportive and patience, and for facilitating everything I need.

And

Firas, for being in my life!

Dedication

To Mum and Dad for their immense support.

To Firas For everything.

Abstract

Oxidative stress has been associated with a wide range of diseases, including cardiovascular diseases, Alzheimer's disease, atherosclerosis, Parkinson's disease and cancer. It also plays a role in the ageing process. Hyperhomocysteimia is commonly found to be associated with these diseases. The hyperhomocysteimia is a result of a deficiency in both folate and cobalamin. Folate is known to reduce Hcy and protect cells from apoptosis, but there are no studies investigating the impact of cobalamin on apoptosis induced by oxidative stress or the mechanism(s) of the protection. The aims of the research are to investigate the protective role of cobalamin and the possible mechanism(s) for this protection. It also examines the protective role of novel cobalamin and investigates their superior protection. The methods used in this research for apoptosis detection we used caspase-3 and the annexin-V, while for necrosis we used PI staining, where cell viability were detected using MTS assay. We also measured the generation of superoxide by Lucigenin-enhanced chemiluminescence and reactive oxygene species by using the redox active prob DCFH-DA. Moreover, the intracellular proteins were measured via staining with specific fluorescent-conjugated antibodies were detected using flowcytometry. Our result demonstrated that 25 μ M of cobalamin protects cells from apoptosis. The protection by cobalamin was associated with induction of iHsp72 and iHO-1, and these are shown to be essential for the protection. Furthermore, our research demonstrated a novel mechanism of cobalamin-apoptosis protection involving induction of Nf κ B, ERK1/2 and AKT signal transduction pathways. In order to protect cells from apoptosis induced by oxidative stress, cobalamin induces the pNf κ B which in turn regulate the iNOS and HO-1 induction. Cobalamin also induces the pERK1/2 which regulates the induction of Hps72 and Nrf2. And finally, pAKT induced by cobalamin which regulate the Nrf2 and HO-1 induction. The inhibition of any of theses pathways leads to loss the protection. The GSCbl and NACCbl provide a superior protection against oxidative stress, this protection involved induction of the signal transduction pathways and Hsps. To conclude; cobalamin provides protection against cells death induced by oxidative stress. Cobalamin achieves this by multiple pathways which include direct antioxidant stimulation and induction of signal transduction pathways. Different cobalamin

derivatives have superior protections. These finding are a useful pharmaceutical tool in the treatment of the oxidative stress related diseases.

Publications

Ireland, H.E., Leoni, F., Altaie, O., Birch, C. S., Coleman, R. C., Hunter-Lavin, C. & Williams, J. H. H. (2007). Measuring of heat shock proteins from cells. *Methods*, 43 (3):176-183.

Posters

Functional assays for Hsp70 using Surface Plasmon Resonance (2006). Prism conference, Lancaster University, UK.

Characterisation the effect of oxidative stress on apoptosis, necrosis, and cellular location and release of Hsp72. (2007). Cell Stress Society International Congress on Stress Responses in in Biology and Medicine and 2nd World Conference of Stress, Budapest, Hungary.

Chapter	Page
1. Introduction	
1.1 Background to study	1
1.2 Oxidative stress and diseases	2
1.3 Oxidative stress generation	2
1.4 Hydrogen peroxide (H ₂ O ₂)	3
1.5 Homocysteine (Hcy)	3
1.6 Mechanism of cell death	6
1.6.1 Apoptosis	6
1.6.2 Necrosis	7
1.7 Folate and cobalamin	8
1.7.1 Folate	8
1.7.2 Cobalamin (Vit B ₁₂)	10
1.7.3 Glutathionylcobalamin (GSCbl) and N-acetyl-L-Cysteinylcobalamin (NACCbl)	11
1.8 Protective role of folate and cobalamin	11
1.9 Heat shock proteins	12
1.9.1 Hsps Nomenclature	14
1.9.2 Hsps regulation and expression	15
1.9.3 Hsp27	16
1.9.4 Hemoxxygenase-1	16
1.9.5 Hsp70 family	17
1.9.6 Hsp90	18
1.10 Signal transduction pathways	18
1.10.1 Nf _κ B	21
1.10.2 MAPK family	21
1.10.2.1 ERK1/2	24
1.10.2.2 JNK & P38	24
1.10.3 AKT/PI3	25
1.10.4 Nrf2	26
1.10.5 iNOS	27
1.11 Aims and objectives	30

Chapter	Page
2. Material and methods	31
2.1 Equipment	31
2.2 Reagents	34
2.3 Buffers	38
2.3.7 Freeze media solution (v/v)	38
2.3.8 MTS Working Solution (w/v)	38
2.3.9 pH solutions	39
2.3.10 4 % Paraformaldehyde (PFA) buffer	39
2.3.11 0.15M Phosphate buffered saline pH 7.4 (PBS) (w/v)	39
2.3.14 Propidium Iodide stock solution (1mg/ml) (w/v)	39
2.3.15 Red blood cells Lysing Buffer 10X solution (w/v)	39
2.3.21 Tissue culture media (v/v)	40
2.3.22 Wash buffer 1X	40
2.4 Methods	40
2.4.1 Cell culture: Sk-Hep1	40
2.4.2 Cell culture: Jurkat	41
2.4.3 Freezing storage and thawing of sk-hep1 and Jurkat	41
2.4.4 Whole blood collection	41
2.4.5 Whole blood isolation	42
2.4.6 Trypan blue exclusion test cell viability	42
2.4.7 Sterilisation of equipment	43
2.4.8 Treatment's Solution preparation	43
2.4.8.1 Hydrogen peroxide	43
2.4.8.2 Homocysteine	43
2.4.8.3 Folic acid	43
2.4.8.4 Cobalamin	44
2.4.9 MTS assay: Cells viability	44
2.4.10 Caspase-3/7 fluorimetric assay	45
2.4.11 Caspase-3 assay FC	45

Chapter	Page
2.4.12 Necrosis detection with Propidium Iodide fluorescent assay	46
2.4.13 Annexin-v and Propidium Iodide	46
2.4.14 Measure Intracellular Protein by FC	47
2.4.15 Measurement of super peroxide generation	47
2.4.16 Measurement of super oxide generation by Lucigenin-enhanced chemiluminescence	47
2.4.17 statistical analyses	48
3 Protection from oxidative stress	49
3.1 Introduction	49
3.2 Methods	51
3.2.1 Sk-hep1 cells preparation	51
3.2.2 Jurkat cells preparation	51
3.2.3 Leukocyte cells preparation	51
3.2.4 Determine cell viability	51
3.2.5 Determination of apoptosis	51
3.2.6 Determination of necrosis	51
3.2.7 Cells count and viability test by trypan blue exclusion	51
3.2.8 Caspase-3 activity via flow cytometry	52
3.2.1 Annexin-V and PI	52
3.2 Result	53
3.3.1 Induction of apoptosis and necrosis in Sk- Hep1cells <i>via</i> exposure to Hydrogen peroxide and Homocysteine.	53
3.3.2 Folate and Cobalamin protect cells from apoptosis and necrosis induced by oxidative stress:	57
3.3.2.1 Folate protects cells from apoptosis and necrosis induced by oxidative stress	57
3.3.2.2 Cobalamin protects cells from apoptosis and necrosis induced by oxidative stress	63

Chapter	Page
3.3.2.3 ROS and cobalamin apoptosis protection	68
3.3.2.3.1 Measurement of mitochondrial membrane potential ($\Delta\Psi$) (ROS generation).	
3.3.2.3.2 Measurement of superoxide under oxidative stress and anti oxidative stress conditions	69
3.3.3 Induction apoptosis and necrosis in Jurkat cells <i>via</i> Hydrogen peroxide and Homocysteine	70
3.3.4 Folate protects cells from apoptosis and necrosis induced by oxidative stress	80
3.3.5 Induction of apoptosis and necrosis in normal blood cells <i>via</i> exposure to Hydrogen peroxide and Homocysteine	84
3.3 Discussion	106
4 Hsps induction by Cobalamin	110
4.1 Introduction	110
4.2 Methods	111
4.2.1 Sk-hep1 cells preparation	111
4.2.2 Jurkat cells preparation	
4.2.3 Cells count and viability test by trypan blue exclusion	111
4.2.4 Measurement of intracellular Hsps	111
4.2.5 Inhibition of HO-1 and Hsp72	111
4.2.6 Induction of HO-1 and Hsp72	112
4.2.7 Determination of apoptosis	112
4.2.8 Determination of necrosis	
4.3 Result	113
4.3.1 Induction of intracellular Hsps under oxidative stress-induced apoptosis and under apoptosis protection conditions	113
4.3.1.1 Impact of cobalamin on intracellular Hsps	113

4.3.1.2 Induction of intracellular Hsps under oxidative stress and under protection from apoptosis via folate in sk-hep1	120
4.3.2 The impact of overexpression and inhibition of Hsp72 on apoptosis induced by oxidative stress and protected by cobalamin	123
4.3.2.1 Induction of Hsp72 and oxidative stress	123
4.3.2.2 Effect of Hsp72 inhibition by KNK437 on cobalamin protection	132
4.3.3 Impact of inhibition and induction of HO-1 on cobalamin and folate apoptosis-protection:	136
4.3.3.1 The effect of iHO-1 induction by hemin on apoptosis induced by oxidative stress	136
4.3.3.2 The impact of iHO-1 inhibition by Sn(IV) Protoporphyrin IX dichloride on cobalamin-apoptosis protection	138
4.3.4 Intracellular Hsps under antioxidant protection in Jurkat	142
4.4 Discussion	145
5 Cobalamin protection mechanism	
5.1 Introduction	148
5.2 Methods	150
5.2.1 The inhibitory study	150
5.2.2 Cells count and viability test by trypan blue exclusion	151
5.2.3 Measurement of intracellular Hsps	151
5.2.4 Measurement of pNf κ B induction	151
5.2.5 Measurement of pERK1/2 induction	151
5.2.6 Measurement of pAKT induction	152
5.2.7 Measurement of Nrf2 induction	152
5.2.8 Measurement iNOS induction	152
5.2.10 Measurement of super oxide generation	152
5.2.11 Measurement of ROS generation	152

Chapter	Page
5.2.12 Determination of apoptosis	152
5.3 Result	153
5.3.1 Impact of signal transduction pathways on cobalamin apoptosis-protection	153
5.3.2 Impact of cobalamin on phosphorelated level of signal transduction pathways	160
5.3.3 Effect of cobalamin protection on Nrf2	166
5.3.4 Effect of signals transduction inhibitors on intracellular Hsps	169
5.3.4.1 Effect of NfκB inhibition on intracellular Hsps	169
5.3.4.2 Effect of ERK1/2 inhibition on intracellular Hsps	172
5.3.4.3 Effect of P38 inhibition on intracellular Hsps	175
5.3.4.4 Effect of (PI3 /AKT) inhibition on intracellular Hsps	178
5.3.4.5 Effect of Nrf2 inhibitor (Wortmanin) on intracellular Hsps under cobalamin apoptosis protection	181
5.3.5 Impact of signal transduction pathways on Nrf2 induction	184
5.3.6 Effect of signal transduction pathways on ROS reduction by cobalamin	188
5.3.7 Effect of signal transduction pathways on super oxide reduction by cobalamin	192
5.3.8 Impact cobalamin on iNOS induction	196
5.4 Discussion	200

Chapter	Page
6. Novel cobalamin mechanism	203
6.1 Introduction	203
6.2 Methods	204
6.3 Results	207
6.3.1 Effect of GSCbl and NACCbl on the apoptosis, necrosis induced by oxidative stress	207
6.3.2 The impact of GSCbl and NACCbl on ROS and super oxide generation	211
6.3.3 Induction of Hsps by novel cobalamin NACCbl and GSCbl	214
6.3.4 The NACCbl and GSCbl and signal transduction pathways	217
6.3.4.1 The impact of signal transduction inhibitor on NACCbl and GSCbl-apoptosis protection	217
6.3.4.2 Impact of NACCbl and GSCbl on pNfkb, pERK1/2 and pAKT induction	223
6.3.4.3 Impact of NACCbl and GSCbl on Nrf2 induction	225
6.3.4.4 Impact of GSCbl and NACCbl on iNOS induction	226
6.4 Discussion	229
7 General Discussions	231
8 References	241

List of Figures	Page
Figure 1.1: Major pathways of Hcy metabolism.	4
Figure 1.2: folate cycle.	9
Figure 1.3: Structure of cobalamin.	10
Figure 1.4: Activation of Nf_kB .	20
Figure 1.5: Activation of the MAPK family.	23
Figure 1.6: Activation of AKT/Nrf2 pathways.	25
Figure 1.7 Generation of NO	27
Figure 2.1: Haemocytometer.	43
Figure 3.1: Effect of oxidative stress on viability of sk-hep1 cells.	54
Figure 3.2: Effect of Hcy on viability of sk-hep1 cells.	54
Figure 3.3: Effect of Hydrogen peroxide on caspase-3 level in Sk-Hep1.	55
Figure 3.4: Effect of Hcy on caspase-3 level in Sk-Hep1.	55
Figure 3.5: Induction of necrosis in Sk-Hep1 by H_2O_2 .	56
Figure 3.6: Induction of necrosis in Sk-Hep1 Hcy.	56
Figure 3.7: Effect of folate on caspase-3 in Sk-hep1 cells.	58
Figure 3.8: Effect of folate on necrosis activity in Sk-hep1 cells.	58
Figure 3.9: Effect of folate pre-treatment on Sk-Hep1 cells surviving oxidative stress.	59
Figure 3.10: Effect of folate pre-treatment on Sk-Hep1 cells surviving oxidative stress.	60
Figure 3.11: The effect of folate pre-treatment on the caspase-3 activity.	61
Figure 3.12: The effect of folate pre-treatment on the caspase-3 activity.	61
Figure 3.13: Effect of folate pre-treatment on necrosis induction in Sk-hep1.	62
Figure 3.14: Effect of folate pre-treatment on necrosis induction in Sk-hep1.	62
Figure 3.15: Effect of cobalamin on caspase-3 in Sk-hep1 cells.	64
Figure 3.16: Effect of cobalamin on caspase-3 in Sk-hep1 cells.	64
Figure 3.17: Primary study of cobalamin apoptosis protection.	65

	Page
Figure 3.18: The effect of cobalamin on the caspase-3 activity induced by H ₂ O ₂ .	66
Figure 3.19: The effect of cobalamin pre-treatment on the caspase-3 activity.	66
Figure 3.20: The effect of cobalamin pre-treatment on necrosis activity.	67
Figure 3.21: The effect of cobalamin pre-treatment on necrosis activity.	67
Figure 3.22: Effect of cobalamin on generation of reactive oxygen species.	68
Figure 3.23: Effect of cobalamin on the superoxide generation.	69
Figure 3.24: Time course study effect of H ₂ O ₂ on caspase-3 activity in Jurkat cells	72
Figure 3.25: Time course study the effect of H ₂ O ₂ on necrosis level of Jurkat cells	72
Figure 3.26: Time course study the effect of homocysteine on caspase-3 activity in Jurkat cells.	73
Figure 3.27: Time course study the effect of homocysteine on necrosis level of Jurkat cells	73
Figure 3.28: Time course study the effect of H ₂ O ₂ on the PS externalization in Jurkat cells.	75
Figure 3.29: Time course study the effect of Hcy on the PS externalization in Jurkat cells.	75
Figure 3.30: Time course study the effect of H ₂ O ₂ on the necrosis activity of Jurkat cells.	76
Figure 3.31: Time course study the effect of Hcy on the necrosis activity of Jurkat cells.	76
Figure 3.32: The effect of Hcy on the PS externalization in Jurkat cells.	77
Figure 3.33: Mechanisms of cell of Jurkat cells death after exposure to hydrogen peroxide.	79

	Page
Figure 3.34: Mechanisms of cell of Jurkat cells death after exposure to homocysteine.	79
Figure 3.35: Effect of folate on caspase-3 in Jurkat cells.	81
Figure 3.36: Effect of folate on necrosis of Jurkat cells.	81
Figure 3.37: The effect of folate pre-treatment on the caspase-3 activity.	82
Figure 3.38: The effect of folate pre-treatment on the caspase-3 activity.	82
Figure 3.39: Effect of folate pre-treatment on necrosis.	83
Figure 3.40: Effect of folate pre-treatment on necrosis.	83
Figure 3.41: Time course study the effect of H ₂ O ₂ on PS translocation in neutrophil cells.	86
Figure 3.42: Time course study the effect of Hcy on PS translocation in neutrophil cells.	86
Figure 3.43: Time course study the effect of H ₂ O ₂ on caspase-3 level in neutrophil cells.	87
Figure 3.44: Time course study the effect of Hcy on caspase-3 level in neutrophil cells.	87
Figure 3.45: Time course study the effect of H ₂ O ₂ on necrosis level of neutrophil cells.	88
Figure 3.46: Time course study the effect of Hcy on necrosis level of neutrophil cells.	88
Figure 3.47: Induction of apoptosis and necrosis in neutrophil cells.	90
Figure 3.48: Mechanisms of neutrophil cells death subjected to H ₂ O ₂ or Hcy.	91
Figure 3.49: Time course study the effect of H ₂ O ₂ on PS translocation in monocyte cells.	93
Figure 3.50: Time course study the effect of Hcy on PS translocation in monocyte cells.	94
Figure 3.51: Time course study the effect of H ₂ O ₂ on caspase-3 level in Monocyte cells.	94

	Page
Figure 3.52: Time course study the effect of Hcy on caspase-3 level in Monocyte cells.	95
Figure 3.53: Time course study the effect of H ₂ O ₂ on necrosis level of monocyte cells.	95
Figure 3.54: Time course study the effect of Hcy on necrosis level of monocyte cells.	96
Figure 3.55: Induction of apoptosis and necrosis in monocyte cells.	97
Figure 3.56: Mechanisms of monocyte cells death subjected to H ₂ O ₂ or Hcy.	98
Figure 3.57: Time course study the effect of H ₂ O ₂ on PS translocation in lymphocyte cells.	100
Figure 3.58: Time course study the effect of Hcy on PS translocation in lymphocyte cells.	101
Figure 3.59: Time course study the effect of H ₂ O ₂ on caspase-3 level in lymphocyte cells.	101
Figure 3.60: Time course study the effect of Hcy on caspase-3 level in lymphocyte cells.	102
Figure 3.61: Time course study the effect of H ₂ O ₂ on necrosis level of lymphocyte cells.	102
Figure 3.62: Time course study the effect of Hcy on necrosis level of lymphocyte cells.	103
Figure 3.63: Induction of apoptosis and necrosis in lymphocyte cells.	104
Figure 3.64: Mechanisms of lymphocyte cells death subjected to H ₂ O ₂ or Hcy.	105
Figure 4.1: Effect of cobalamin on the iHsp27 and iHO-1 level.	114
Figure 4.2: Effect of cobalamin on iHsp72 and iHsp90.	115
Figure 4.3: Effect of cobalamin on intracellular Hsps level.	116

	Page
Figure 4.4: Intracellular Hsp27 and HO-1 during cobalamin apoptosis-protection.	118
Figure 4.5: Intracellular Hsp72 and Hsp90 during cobalamin apoptosis-protection.	119
Figure 4.6: Effect of folate on iHsp27 and iHO-1 induction.	121
Figure 4.7: Effect of folate on iHsp72 and iHsp90 induction.	122
Figure 4.8: Induction of iHsp27 and iHsp72 in sk-hep1.	124
Figure 4.9: Effect induction of Hsp72 on caspase-3 activity induced by Hcy or H ₂ O ₂ .	125
Figure 4.10: Effect of induction of the Hsp72 on necrosis activity under oxidative stress.	126
Figure 4.11: The intracellular Hsp27 after heat shock and apoptosis induction by oxidative stress.	128
Figure 4.12: The intracellular HO-1 after heat shock and apoptosis induction by oxidative stress.	129
Figure 4.13: The intracellular Hsp72 after heat shock and apoptosis induction by oxidative stress.	130
Figure 4.14: The intracellular Hsp90 after heat shock and apoptosis induction by oxidative stress.	131
Figure 4.15: inhibition of Hsp72 by KNK437 in sk-hep1 cells.	133
Figure 4.16: Effect of Hsp72 inhibition on necrosis activity under oxidative stress.	133
Figure 4.17: Effect of Hsp72 inhibition on cobalamin apoptosis-protection.	134
Figure 4.18: Effect of Hsp72 inhibition on folate apoptosis-protection.	135
Figure 4.19: The induction of iHO-1 by Hemin.	136
Figure 4.20: Effect of iHO-1 induction on caspase-3 under oxidative stress.	137
Figure 4.21: Effect of HO-1 induction on necrosis activity under oxidative stress induces.	137

	Page
Figure 4.22: Inhibition of iHO-1 with SN (IV) Protoporphyrin IX dichloride in sk-hep1.	138
Figure 4.23: Effect of iHo-1inhibition on folate –apoptosis protection in sk-hep1 cells.	139
Figure 4.24: Effect of iHO-1 inhibition on folate –apoptosis protection in sk-hep1 cells.	140
Figure 4.25: Effect of iHO-1 inhibition on necrosis activity under oxidative stress	141
Figure 4.26: Effect of folate on iHsp27 and iHO-1 level in Jurkat cells	143
Figure 4.27: Effect of folate on iHsp72 and iHsp90 level in Jurkat cells	144
Figure 5.1: Effect of gene transcription inhibitor on cobalamin apoptosis protection.	153
Figure 5.2: Effect of Bay-117082 on cobalamin apoptosis-protection.	154
Figure 5.3: Effect of U0126 on cobalamin apoptosis-protection.	155
Figure 5.4: Effect of LY294002 cobalamin apoptosis-protection.	156
Figure 5.5: Effect of wortmanin cobalamin apoptosis-protection.	157
Figure 5.6: Effect of SB202190 cobalamin apoptosis-protection.	158
Figure 5.7: Effect of SP600125 on cobalamin apoptosis-protection.	159
Figure 5.8: induction of pNf _k B by cobalamin.	161
Figure 5.9: Induction of pERK1/2 by cobalamin.	163
Figure 5.10: induction of pAKT by cobalamin.	165
Figure 5.11: Effect of cobalamin on Nrf2 induction.	166
Figure 5.12: Induction of Nrf2 under cobalamin apoptosis protection.	167
Figure 5.13: Induction of Nrf2 under oxidative stress and apoptosis protection conditions.	168

	Page
Figure 5.14: Effect of Bay-117082 on intracellular Hsp27 and HO-1 under cobalamin apoptosis-protection.	170
Figure 5.15: Effect of Bay-117082 on intracellular Hsp72 and Hsp90 under cobalamin apoptosis-protection.	171
Figure 5.16: Effect of U0126 on intracellular Hsp27 and HO-1 under cobalamin apoptosis-protection.	173
Figure 5.17: Effect of U0126 on intracellular Hsp72 and Hsp90 under cobalamin apoptosis-protection.	174
Figure 5.18: Effect of SB202190 on intracellular Hsp27 and HO-1 under cobalamin apoptosis-protection.	176
Figure 5.19: Effect of SB202190 on intracellular Hsp72 and Hsp90 under cobalamin apoptosis-protection.	177
Figure 5.20: Effect of LY294002 on intracellular Hsp27 and HO-1 under cobalamin apoptosis-protection.	179
Figure 5.21: Effect of LY294002 on intracellular Hsp72 and Hsp90 under cobalamin apoptosis-protection.	180
Figure 5.22: Effect of wortmanin on intracellular Hsp27 and HO-1 after cobalamin apoptosis-protection.	181
Figure 5.23: Effect of wortmanin on intracellular Hsp72 and Hsp90 under cobalamin apoptosis-protection.	183
Figure 5.24: effect of Bay-11 and U0126 on Nrf2 induction under cobalamin-apoptosis protection.	185
Figure 5.25: Effect of LY294002 on Nrf2 induction under cobalamin-apoptosis protection.	186
Figure 5.26: Effect of SB202190 on Nrf2 induction under cobalamin-apoptosis protection.	187
Figure 5.27: Effect of Actinomycin and Bay-110782 on generation of ROS.	189
Figure 5.28: Effect of U0126 and LY294002 on generation of ROS.	190

	Page
Figure 5.29: Effect of SB202190 and SP600125 on generation of ROS.	191
Figure 5.30: Effect of Actinomycin or Bay-11 on the superoxide generation.	193
Figure 5.31: Effect of U0126 or LY294002 on the superoxide generation.	194
Figure 5.32: Effect of SB202190 or SP600125 on the superoxide generation.	195
Figure 5.33: Effect of cobalamin on iNOS induction.	196
Figure 5.34: Effect cobalamin apoptosis protection on iNOS induction.	197
Figure 5.35: Effect of Bay-117082 on iNOS induction.	198
Figure 5.36: Effect of U0126 on iNOS induction.	199
Figure 5.37: Effect of LY294002 on iNOS induction.	199
Figure 6.1: The effect of GSCbl pre-treatment on the caspase-3 activity.	208
Figure 6.2: The effect of NACCbl pre-treatment on the caspase-3 activity.	209
Figure 6.3: The effect of GSCbl pre-treatment on necrosis.	210
Figure 6.4: The effect of NACCbl pre-treatment on necrosis.	210
Figure 6.5: Effect of GSCbl and NACCbl on generation of reactive oxygen species.	212
Figure 6.6: Effect of GSCbl and NACCbl on the superoxide generation.	213
Figure 6.7: Effect of cobalamin, NACCbl and GSCbl on iHsps level.	215
Figure 6.8: Effect of cobalamin, NACCbl and GSCbl on intracellular Hsps.	216
Figure 6.9: Effect of Bay-117082 on NACCbl or GSCbl-apoptosis-protection.	217
Figure 6.10: Effect of U0126 on NACCbl or GSCbl-apoptosis protection.	218

Figure 6.11: Effect of LY294002 NACCbl or GSCbl-apoptosis protection.	219
Figure 6.12: Effect of wortmanin NACCbl or GSCbl-apoptosis protection.	220
Figure 6.13: Effect of SB202190 on NACCbl or GSCbl-apoptosis protection.	221
Figure 6.14: Effect of SP600125 on NACCbl or GSCbl-apoptosis-protection.	222
Figure 6.15: Effect of GSCbl, NACCbl and cobalamin on pNf _κ B induction.	223
Figure 6.16: Effect of GSCbl, NACCbl and cobalamin on pERK1/2 induction.	224
Figure 6.17: Effect of GSCbl, NACCbl and cobalamin on pAKT induction.	224
Figure 6.18: Effect of GSCbl, NACCbl on Nrf2 induction.	225
Figure 6.19: Effect of GSCbl, NACCbl on iNOS induction.	227
Figure 6.20: Effect of GSCbl, NACCbl on iNOS induction.	228
Figure 7.1: The mechanism of cobalamin-apoptosis protection	235

List of Tables	Page
Table 1.1: Classification of the caspases according to their function	7
Table 1.2: Classification of Hsps, their location and function	14
Table 1.3 Nomenclatures of the Hsps	15

Abbreviations

AdoCbl	Adenosylecobalamin
BV	Briverdin
BSA	Bovine serum albumin
BACH-1	Transcription regulator protein BACH-1
Cbl	Cobalamin
C β C	Cystathionine β -synthase
CO	Carbon monoxide
COX-2	Cyclooxygenase-2
DHF	Dihydrofolate
DMSO	Dimethylsulfoxide
DCFH-DA	2,7-Dichlorofluorescein diacetate
dH ₂ O	Distilled water
dUMP	2'-deoxyuridine-5'-phosphate
dTMP	2'-deoxythymidine-5'-phosphate
ER	Endoplasmic Reticum
ERK1/2	Extracellular signal regulated kinase 1/2
EM	Emission wavelength
EX	Excitation wavelength
GSCbl	Glutathionylcobalamin
H ₂ OCbl	Aquacobalamin
HOcbl	Hydroxylcobalamin
H ₂ O ₂	Hydrogen peroxide
Hcy	Homocysteine
HOCl	Hypochlorous acid
HSF-1	Heat shock factor-1
JNK	Jun N-terminal kinase
KDa	Kilo Dalton
MS	Methionine synthesis
MAPK	Mitogen-activated protein kinases
MeCbl	Methylcobalamin
NO	Nitric oxide
NACCbl	N-acetyl-L-Cysteinylcobalamin
NAC	N-acetyl-L-Cysteine

NO ₂ Cbl	NitroCobalamin
Nf _k B	Nuclear factor kappa B
Nrf2	Nuclear factor erythroid 2-related factor 2
O ₂ ⁻	Super oxide
·O ₂	Single oxygen
·OH	Hydroxyl radical
ONOO ⁻	Peroxynitrite
PKC	Protein Kinase C
ROS	Reactive oxygen species
SO ₃ Cbl	SubphititoCobalamin
Sn(IX)PP	Sn Protoporphyrin (IX) dihydrochloride
THF	Tetrahydrofolate
VCAM-1	Vascular Cell Adhesion Molecule-1
v/v	Volume-by volume
w/v	weight-by-volume
w/w	weight-by-wieght
ΔΨ _m	Mitochondrial membrane potential

1. Introduction:

1.1 Background to study:

Oxidative stress is associated with a variety of diseases such as cardiovascular diseases, which are one major cause of mortality in Europe as cardiovascular diseases statistics in 2008 showed that nearly half of all deaths in Europe (48%) caused by cardiovascular disease. It was recently reported that one of the factors leading to oxidative stress is homocysteine (Hcy), which is also considered as an independent risk factor for vascular diseases (Jacobsen, 2000). Hcy is a sulphur-containing intermediate product, which is a result of the normal metabolism of methionine. A reduction in folate or cobalamin (vitamin B₁₂) supply should lead to a reduced methionine synthase activity, and as a result reduced conversion of Hcy to methionine and cysteine and increases the cellular level of Hcy. Hyperhomocysteimism leads to cell death by either apoptosis or necrosis (Mujumdar *et al.*, 2001; Zhang *et al.*, 2001). Apoptosis is a programmed cell death while necrosis is non-physiological cell death. Numerous studies have reported that the majority of oxidative stress related disease mortality is associated with the increase in apoptotic cells as a result of high level of Hcy (Cattaneo, 1999; Malinow *et al.*, 1989; Verhoef *et al.*, 1996; Clarke *et al.*, 1998; Miller, 1999; Blandini *et al.*, 2001; Duan *et al.*, 2002; Kuhn *et al.*, 1998; Yasui *et al.*, 2003). The cellular response to oxidative stress involves upregulation of specific proteins, including heat shock proteins (Hsps) (Huot *et al.*, 1991; Mehlen *et al.*, 1993). Hsps are known as molecular chaperones, with roles which include repair of denatured proteins and protein transport across intracellular membranes. It has also been reported that the upregulation of the Hsps under different stressor protects the cells from the damage induced by a variety of stressors (Musch *et al.*, 1996; Otani *et al.*, 1997; Ren *et al.*, 2001). The upregulation of Hsps is controlled by a variety of signal transduction pathways dependent on the stressor.

The work in this thesis aims to evaluate the protective effect of cobalamin provided against apoptosis and necrosis induced by oxidative stress, and to characterise the molecular mechanisms and the possible involvement of Hsps. This study will also investigate the protection efficiency of glutathionylcobalamin (GSCbl) and N-acetyl-L-cysteinylcobalamin (NACCbl). Increased understanding of these mechanisms may lead to new tools for treatment and drug design that could lead to preservation and

restoration of health. The works reported in this thesis have been carried out on various cell types, using cell culture methods and blood taken from healthy volunteers. A mechanistic-based approach has been employed to study cell death and the protection from cell death induced by oxidative stress, using pharmacologically relevant concentrations of oxidants and antioxidants.

1.2 Oxidative stress and diseases

Oxidative stress is associated with several diseases, such as Parkinson's disease (Miller, 1999), Alzheimer's disease (Scalabrino, 2005), cardiovascular diseases (Forouhi *et al.*, 2006), stroke progression (Alexandrova *et al.*, 2005), diabetes (Szabo, 2005), atherosclerosis and cancer (Schwartz *et al.*, 1993). The majority of oxidative stress related diseases are associated with mitochondrial dysfunction (Bostantjopoulou *et al.*, 2005; Blennow *et al.*, 2006; Alexandrova *et al.*, 2005), which triggers a cascade of events resulting in apoptosis and necrosis which in turn lead to progression of the disease and organ dysfunction (Kim-Han *et al.*, 2005; Pamplona *et al.*, 2006). There is not as yet a full understanding of cell death pathways induced by reactive oxygen species (ROS) generation, and therefore the means to decrease the damaging effects of oxidative stress in disease pathologies is limited.

1.3 Oxidative stress generation:

Oxidative stress is caused by imbalance of antioxidant generation and ROS, which plays a vital role in vascular physiology and pathology. The ROS family includes; superoxide (O_2^-), nitric oxide (NO), the hydroxyl radical ($\cdot OH$), hydrogen peroxide (H_2O_2), hypochlorous acid (HOCl), peroxynitrite ($ONOO^-$) and single oxygen (1O_2). Under stress and pathological conditions, the production of ROS is higher than in normal conditions (Behrendt *et al.*, 2002; Barja 2004; Bitar, *et al.*, 2005; Frank *et al.*, 2005; Lyle *et al.*, 2006). The production of O_2^- mainly occurs within the mitochondrial of a cell, as the mitochondrial electron transport chain is the main source of ATP in mammalian cells, so the redox status get to be maintained (Kovacic *et al.*, 2005). In all cell types, O_2^- can be produced by enzymes such as NADPH oxidase, xanthine oxidase, cyclooxygenases, NO synthases, cytochrome P450 monooxygenases and enzymes from the mitochondrial respiratory chain (Griendling *et al.*, 1997; Atarod *et al.*, 2004; Ceriello *et al.*, 2004). O_2^- is reduced to uncharged H_2O_2 by superoxide dismutase (SOD), and H_2O_2 in the presence of catalase or glutathione peroxidase is converted into water and oxygen (Valko *et al.*,

2006). ROS levels are elevated in many vascular disease states and also associated with a reduction of antioxidants which reduces the ability to scavenge oxygen-derived free radicals. All of these factors contribute to generations of oxidative stress (Touyz, 2004).

1.4 Hydrogen peroxide (H_2O_2):

H_2O_2 is one of the abundant ROS which plays a different role in the cellular system such as signalling (Davies, 1999). After dismutation of super oxide, H_2O_2 can be generated directly or indirectly by NADPH oxidase, which is located in the mitochondrial respiratory system. H_2O_2 is regulated by cellular glutathione peroxidase (cGPx) and catalase (Dringen *et al.*, 2005).

1.5 Homocysteine (Hcy)

Hcy is an amino acid formed from S-adenosyl-methionine (Herman *et al.*, 1999; Finkelstein *et al.*, 2000; Mattson *et al.* 2002), which is converted to S-adenosyl-Hcy (Figure 1.1). Subsequent hydrolysis of S-adenosyl-Hcy leads to Hcy formation which then may be transformed to cysteine by vitamin B₆ and cystathionine β -synthase (C β S). Alternately, Hcy can be remethylated and converted back to methionine by folate and cobalamin dependent reaction catalysed by methionine synthase (MS). The side chains of all amino acid residues of proteins, in particular cysteine and methionine residues of proteins, are susceptible to oxidation by the action of ROS (Stadtman, 2004).

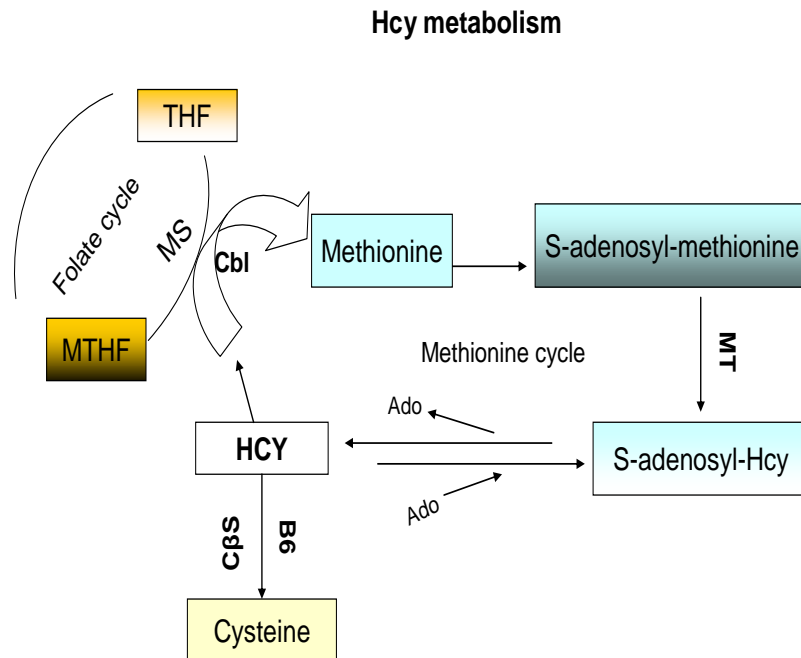


Figure 1.1: Major pathways of Hcy metabolism. Hcy is generated in a cycle through S-adenosylmethionine and S-adenosylhcy. Remethylation of Hcy back to methionine is carried out by cobalamin-dependent methionine synthase (Cbl-MS). Hcy is also converted to cysteine, initiated by B₆-dependent cystathionine β-synthase (CβS). The folate cycle generates methyltetrahydrofolate (MTHF) for the remethylation of Hcy back to methionine. Each molecule in the diagram was given its unique colour and form. The colour of the molecule changed to black when the methyl group was added. Other abbreviations: Ado, adenosine; THF, tetrahydrofolate.

As shown in (Figure 1.1) Hcy metabolism is dependent on folate and cobalamin and any deficiency in them might lead to hyperhomocysteinemia (Jacobsen, 1998; Selhub, 1999; Chambers *et al.*, 2000; Jacobsen, 2000; Selhub *et al.*, 2000; Herrmann *et al.*, 2002; Lee *et al.*, 2003; Mattson & Shea, 2003;; McCully, 2005). Defects in the MS or CBS genes also result in hyperhomocysteinemia (Carmel *et al.*, 2003). Moreover, the genetic variation of 677C/T in the gene coding of the enzyme methylenetetrahydrofolate reductase which is required in the Hcy-methionine cycle for the formation of 5-methylenetetrahydrofolate. The carriers of the TT genotype have high level of the Hcy (Frosst *et al.*, 1995).

It has been reported recently that an increase of the plasma Hcy level has been classified as a risk factor of several age related diseases, including vascular and neurodegenerative diseases, atherosclerosis and diabetes (Bousser & Ferro, 2007; Mattson *et al.*, 2002; Seshadri *et al.*, 2002; Hoffmann *et al.*, 2001; Abdella *et al.*, 2002; McCaddon *et al.*, 2006; Lentz, 2005). Moreover, Hcy metabolism might be affected by different biological, environmental or pathological factors such as aging, inflammation, renal insufficiency and smoking (Mattson *et al.*, 2002).

Hyperhomocysteinemia may lead to cell death either by apoptosis or necrosis as has been demonstrated by *in vivo* and *in vitro* studies (Mujumdar *et al.* 2001; Zhang *et al.* 2001). Several studies have demonstrated the effect of Hcy on cells, such as high levels of Hcy induce apoptosis in primary human bone marrow stromal cells, HS-5 cell line (Kim *et al.*, 2006), H9C2 cardiomyocytes (Levrant *et al.*, 2007) and lymphocytes (Picerno *et al.*, 2007). The induction of apoptosis by Hcy is caspase-dependent including activation of caspase-9 and caspase-3, and Hcy also increases cytochrome c release into the cytosol, indicating that Hcy also induces apoptosis *via* the mitochondria pathway (Tyagi *et al.*, 2006). Furthermore, it has been demonstrated that moderate levels of H₂O₂ should result in cells dying through apoptosis, while high concentration causes necrosis cell death (Lennon *et al.*, 1991; Dypbukt *et al.*, 1994; Davies, 1999; Hampton & Orrenius, 1997; Gardner *et al.*, 1997; Lee & Shacter, 1999). The induction of apoptosis by H₂O₂ is associated with activation of caspase-3, caspase-9 and phosphatidylserine appearance on the surface of the cells and release of cytochrome c (Wang, 2001).

1.6 Mechanism of cell death:

There are two forms of cell death known as apoptosis and necrosis. They are characterised according to morphological and biochemical features (Kerr *et al.*, 1972).

1.6.1 Apoptosis:

Apoptosis is known as a programmed cell death (PCD), which is a regulated physiological type of death that gets rid of senescent, abnormal and potentially harmful cells (Schwartz *et al.*, 1993). Apoptotic cell death is required for cell and tissue development as well as cellular defence, and occurs during normal morphogenesis and as a result of pathogenic infections or any excessive stressor causing cell damage. Apoptosis is therefore helping to remove potentially harmful cells affected by disease or toxic agents (Fiers *et al.*, 1999).

Apoptotic cell death can be triggered by two known pathways: the mitochondrial or intrinsic pathway, which is activated by internal cellular signals; the death receptor or extrinsic pathway, activated by external signals; (Hengartner, 2000; Danial *et al.*, 2004; Nicotera *et al.*, 2004; Beere, 2005; Ciriolo, 2005; Berger *et al.*, 2006; Hail *et al.*, 2006). Generally, apoptosis is characterised by membrane blebbing, cell shrinkage, nuclear condensation, breakdown of nuclear DNA, and the formation of apoptotic bodies (Schweichel *et al.*, 1973).

Apoptotic cell death is classically associated with the activation of proteases known as caspases; the caspase family consists of 14 members. They are broadly classified as either initiator caspases or effector caspases (Table 1.1). Their names reflect the active cysteine group and the feature cleave of their targets at aspartate residues (Alnemri *et al.*, 1996). When caspases are activated they lead to the cleavage of different types of intracellular proteins, including major structural elements of the cytoplasm and nucleus, components of the DNA repair machinery and a number of protein kinases (Earnshaw *et al.*, 1999).

Table 1.1: Classification of the caspases according to their function

Types	Names	Function
Initiator	Caspase-2 Caspase-8 Caspase-9 Caspase-10	Cleavage of the inactive forms of the effector caspases.
Effector	Caspase-3 Caspase-6 Caspase-7	Cleavage of other protein substrates within the cells to trigger apoptosis.

Adapted from (Alnemri *et al.*, 1973)

The intrinsic and extrinsic pathways involve activation of caspases (Reed, 2000; Strasser *et al.*, 2000). The extrinsic pathway is activated by members of the tumor necrosis factor-family (TNF) of cytokine receptors such as TNFR1, Fas and TRAIL receptors. Stimulation of these receptors leads to the activation of initiator caspases, specifically caspase-8. Once caspase-8 is activated it cleaves and activates effector caspases such as caspase -3, -6 or -7, which leads to apoptosis. The intrinsic pathway is activated by release of cytochrome c from the mitochondria into the cytosol. The cytochrome c then binds to Apaf1 resulting in the activation of the initiator caspase-9, which then cleaves and activates caspase-3, and apoptosis occur. The extrinsic pathway is suppressed in the presence of the caspase inhibitor known as zVAD-Fmk, which enhances mitochondrial membrane potential ($\Delta\Psi_m$) that maintains the plasma membrane integrity during apoptotic processes ensuring that the intracellular contents remain in the cell, thus restricting any potentially harmful inflammatory immune responses (Banki *et al.*, 1999). In contrast, intrinsic pathway is blocked by anti-apoptotic Bcl-2 family proteins, which prevents cytochrome c release (Facchinetti *et al.*, 2002; Yamakawa *et al.*, 2000; Chandra *et al.*, 2000). It has been reported that H₂O₂ induce apoptosis *via* extrinsic and intrinsic pathways in neuronal cells (Yamakawa *et al.*, 2000; Chandra *et al.*, 2000; Facchinetti *et al.*, 2002).

1.6.2 Necrosis:

Necrosis is a non-physiological type of death is known as a passive mechanism (Loscalzo, 1996). Necrosis takes place when cells under severe stress or exposed to

cytotoxic agents sustain cell injury (Patel *et al.*, 2000). Necrotic cell death is characterized by cell swelling and interruption of the cell membrane, leakiness of the cell membrane leading to loss of cell membrane integrity and of cellular contents, cell collapse (Majno *et al.*, 1995; Leist *et al.*, 1997; Nicotera & Melino, 2004; Wilson *et al.*, 2005). The release of the cellular content has the potential to lead to a harmful inflammatory response.

1.7 Folate and cobalamin

1.7.1 Folate (Vitamin B₉)

Folate is also known as folic acid or vitamin B₉. It has essential cellular activities such as nucleotide synthesis, conversion of 2'-deoxyuridine-5'-phosphate (dUMP) to 2'-deoxythymidine-5'-phosphate (dTMP) and metabolism of Hcy to methionine (Fenech *et al.*, 2001). The reduction of folate leads to formation of dihydrofolate (DHF), and further reduction by dihydrofolate reductase catalyses resulted in formation of tetrahydrofolate (THF). NADPH is required in the synthesis of both steps (Figure 1.2). THF can be converting to methylene-THF by the addition of methylene groups. A reduction of methylene-THF by NADPH leads to formation of methyl-THF. In turn, methyl-THF is important cofactor as a methyl donor transforming cobalamin to methylcobalamin which is essential in the Hcy metabolism (Lucock *et al.*, 1996).

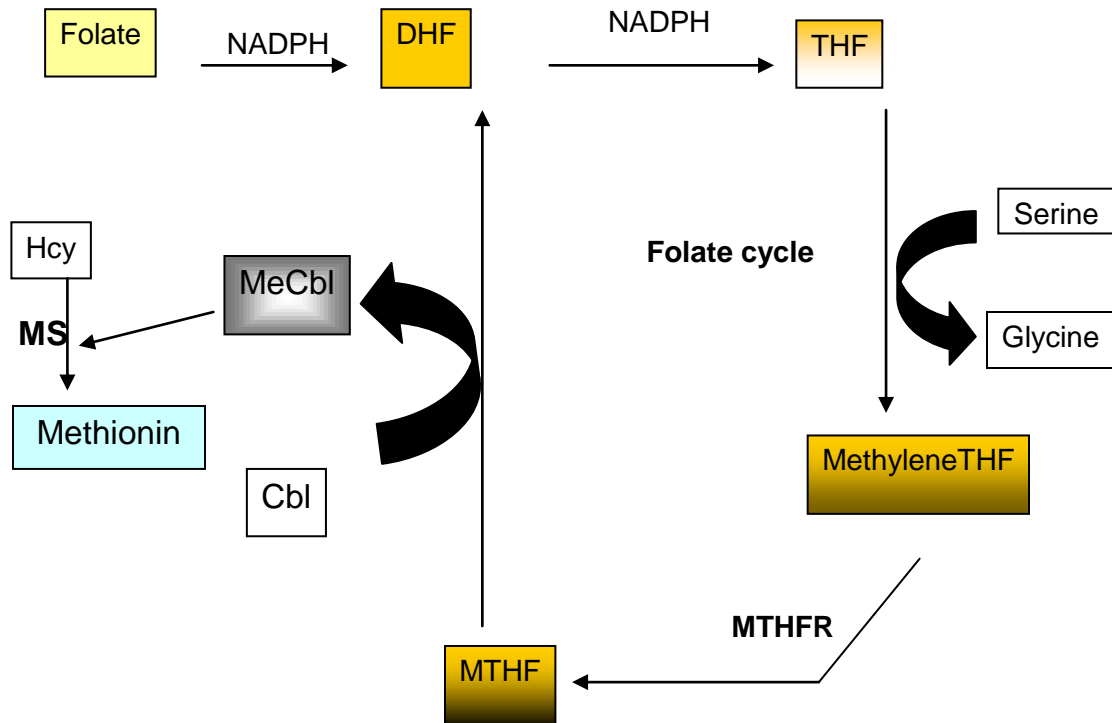


Figure 1.2: folate cycle. Dihydrofolate (DHF) is resulted from a reduction of folate by NADPH and further reduction form tetrahydrofolate (THF). The additions of methylene to THF by conversion of serine to glycine produce methylenetetrahydrofolate (MethyleneTHF). By methyltetrahydrofolate trasferase (MTHFR), methyleneTHF converted to methyltetrahydrofolate (MTHF) that acts as a methyl donor to convert Hcy to methionine and cobalamin (Cbl) and methion synthesis (MS). Each molecule in the diagram was given a unique colour and form, and subsequently the colour has changed according to the process such as the black colour was added when the molecule had methyl group on it.

1.7.2 Cobalamin (Vitamin B₁₂)

Cobalamin is the largest and most complex of the vitamins which contains a cobalt metal ion (Figure 1.3). It was first isolated in 1950s by Dorothy Hodgkin from liver and bacterial broths. The cobalamin derivatives are adenosylcobalamin (AdoCbl), methylcobalamin (MeCbl), aquacobalmin (H₂OCbl) and subphitocobalamin (SO₃Cbl), hydroxycobalamin (HOCbl) and nitrocobalamin (NO₂Cbl) (Smith *et al.*, 1952; Gimsing & Nexø, 1983; Anes *et al.*, 1994).

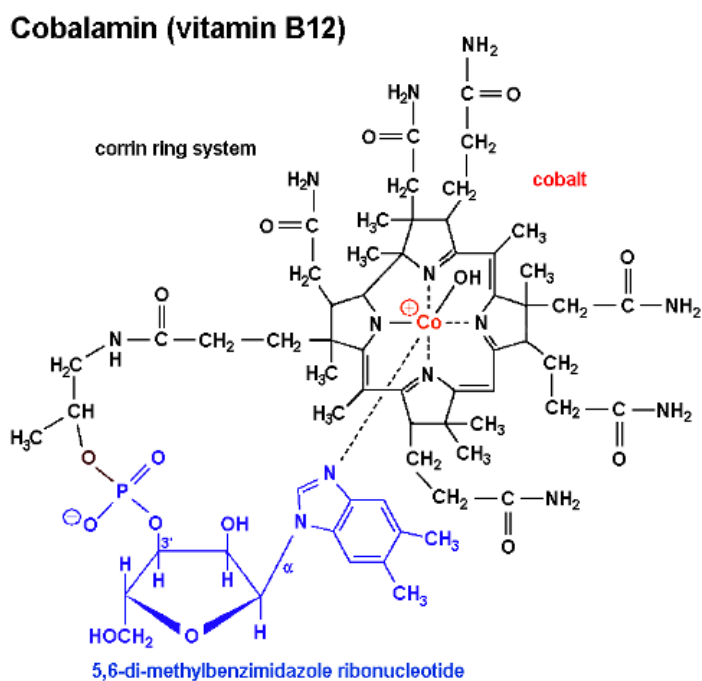


Figure 1.3: Structure of cobalamin. Reproduced from C. Birch PhD thesis (2007).

As shown in Figure 1.2 by remethylation process, methyl-THF converts cobalamin to MeCbl that transform Hcy to methionine, and this step required MS enzyme (Lucock *et al.*, 1996 & Refsum, 2001). The generation of methionine is essential for the synthesis of S-adenosylmethionine, which is required by many biological methylation reactions within DNA and RNA (Shane, 2000).

1.7.3 Glutathionylcobalamin (GSCbl) and N-acetyl-L-Cysteinylcobalamin (NACCbl)

Recently attention has been drawn to thiolatocobalamins – principally GSCbl and NACCbl. Glutathione can be found in cells at concentration up to 10mM (Zhao *et al.*, 1997), and it can interact with H_2OCbl^+ that is formed upon the removal of β -ligand from MeCbl and AdoCbl and finally resulting in formation of GSCbl (Pezacka, 1993). Since GSCbl is more active than other cobalamins in terms of support of MS activity, so GSCbl is the preferred substrate for the reductase enzymes reaction that transform the vitamin to its metabolically active form (Pezacka *et al.*, 1990). GSCbl might be more efficient than other cobalamins in reducing and treatment of diseases associated with hyperhomocysteinemia and oxidative stress, such as Alzheimer's disease (McCaddon & Hudson, 2007). However, McCaddon and Davies in 2005 had suggested that combination of NAC and H_2OCbl^+ has a clinical benefit in Alzheimer's patients. NACCbl synthesis has recently been reported by combination of the NAC and HOCbl.HCl , the NAC ligand form Co-S bound with cobalamin by binding to the sulphur atom (Suarez-Moreira *et al.*, 2006). So NACCbl might provide a protection against oxidative stress. Interestingly GSCbl and NACCbl provided a significant protection, superior to that given by cobalamin, against cell death induced by Hcy (Birch *et al.*, 2009). So while the thiolatocobalamins has suggested having a protective role against oxidative stress, the mechanism of the protection is not fully understood yet.

1.8 Protective role of folate and cobalamin:

Neither folate or cobalamin can be synthesised in mammals, so a rich diet of these cofactors is necessary (Liu *et al.*, 2006). As previously shown in Figures 1.1& 1.2; folate and cobalamin are essential for the Hcy metabolism (Yamada *et al.*, 2006) an imperfection in Hcy metabolism caused by folate and cobalamin deficiency may lead to oxidative stress and endothelium dysfunction in the microcirculation and induces apoptosis *in vitro* (James *et al.*, 1994; Koury *et al.*, 1997; Huang *et al.*, 1999; McCaddon, 2006). Hyperhomocysteinemia may also result from neutrinos reasons as populations with folate-lack-diet have a different Hcy level than population with rich-folate-diet (Wallace *et al.*, 2009). Moreover, the lack of methyl donor precursors in the diet, have been monitored to induce DNA hypomethylation (Liu *et al.*, 2006). It has been suggested that DNA hypomethylation is essential for apoptosis induction

which leads to induce SLE-like autoimmune diseases (Wen *et al.*, 2007). DNA hypomethylation can also be resulted from hyperhomocysteinemia as it is an independent risk factor of atherosclerosis (Jiang *et al.*, 2007).

In 1997, Ward and colleagues showed that 0.2mg -0.4mg/d of folate provides a significant reduction of the Hcy. Moreover, there are several studies demonstrated the association of folate and cobalamin with a variety of diseases such as Alzheimer's disease and increased risk of vascular diseases (Ashfield-Watt *et al.*, 2001; Bailey, 2003; Carmel *et al.*, 2003; Allen, 2004; Bailey, 2005; Antoniadou *et al.*, 2006; de Lau *et al.*, 2006). A recent study by Luchsinger *et al.*, 2007, suggested that increasing folate intake for people > 65y without dementia, over a period of ~6y would decrease the risk of Alzheimer's disease. Furthermore it has been proposed that oral supplementation of folate and cobalamin can reduce hyperhomocysteinemia and provide a direct protective effect for the vessel wall (Chambers *et al.*, 1999; Woo *et al.*, 1999; Fenech, 1999; Doshi *et al.*, 2002; Vermeulen *et al.*, 2000). Folate and cobalamin treatments suppress Hcy-induced oxidative stress and inflammatory responses in macrophages (Au-Yeung *et al.*, 2006), and reduce Hcy level and caspase-3 cleavage in the neurodegenerative disease amyotrophic lateral sclerosis disease (Zhang *et al.*, 2008). It has been suggested that folate and cobalamin reduced hyperhomocysteinemia in cardiovascular patients (Quinlivan *et al.*, 2002).

It is obvious that cobalamin has a significant protective role despite being known as a cofactor enzyme in the Hcy metabolism cycle Figure 1.1. The protection mechanism of cobalamin, however, remains poorly understood.

1.9 Heat shock proteins:

The heat shock response was first identified in 1962 by Ritossa when *Drosophila melanogaster* larvae were subjected to a 30°C heat stimulus and found to increase the expression of certain genes in the salivary gland cells. These genes were later shown to lead to an increase in the expression of proteins with molecular weights of 27 and 70 kDa (Tissieres *et al.*, 1974) and these proteins are known as heat shock proteins (Hsps). Several studies have demonstrated that Hsp expression is highly conserved in most of prokaryotes and eukaryotes, (Boorestein *et al.*, 1994; Hartl, 1996). Hsps are up-regulated under different environmental and physiological

stressors such as heat, heavy metal exposure, oxidative stress infection and ischemia (Lang *et al.*, 2000; Menoret *et al.*, 2002; Pockley, 2003; Ireland *et al.*, 2004; Binder *et al.*, 2004).

The Hsps are known to function as molecular chaperones within the cell by helping the correct folding of denatured proteins, prevention of improper protein aggregation, mediating transport of proteins across intra-cellular membranes, assistance to the correct folding of newly synthesised proteins, and are capable of repairing damage (Bukau & Horwich, 1998; Mayer & Bukau, 1998; Lindquist *et al.*, 1988; Beere, 2005). Hsps assist the stabilization and correct folding of polypeptides through their binding to the hydrophobic amino acid side chain of partially unfolded polypeptides following heat stress and therefore prevent aggregation (Hartl, 1996; Tavaría *et al.*, 1996). Furthermore, Hsps have the ability to provide vital protection in cellular processes by removing damaged intracellular proteins and maintaining the correct proteins configuration against any environmental and physiological effects (Tytell *et al.*, 2005). The response of the cellular system to stress is not derived from the chemical and the physiological character of the stress but is also due to accumulation of denatured proteins which act as a signal to induce Hsp gene expression (DeMaio, 1999; Kültz, 2005; Diller, 2006; Wheeler *et al.*, 2007).

Hsps are classified according to their molecular weight in Kilo Dalton (KDa) and gene sequences homology as follows; the small Hsp family is between (Hsp10, Hsp27), HO-1, Hsp60, Hsp70, Hsp90 and Hsp100. They are located in different locations within the intracellular and their functions varies as shown in Table1.2

Table 1.2: Classification of Hsps, their location and function.

Name	Location	Function
Small Hsps		
Hsp10	Mitochondria	Cofactor for Hsp60
Hsp27	Cytoplasm/nucleus	Cytoskeleton stabilization
Hsp32 (HO-1)		
Hsp32 (HO-1)	Microsome	Oxidative stress inducible, tissue protective
HO-2	Microsome	Non-inducible
Hsp60		
Hsp60	Mitochondria	Molecular chaperone
Hsp70		
Hsp72	Cytoplasm/nucleus	Stress inducible, protective
Hsp73	Cytoplasm/nucleus	Constitutively expressed molecular chaperone
Hsp90		
Hsp90 α	Cytoplasm	Stress inducible chaperone
Hsp90 β	Cytoplasm	Molecular chaperone

Adapted from (Fink, 1999; Pockley, 2003)

1.9.1 Hsps Nomenclature

Hsps are classically named according to their molecular weight but are assigned to the different families based on their sequence homologies. Recently, new nomenclature for the Hsps has been proposed, and agreed by the HUGO Gene nomenclature committee, as shown in Table1.3. The study of this thesis is carried out before the new nomenclature, so we will be using the old nomenclature to report the work of this thesis.

Table 1.3 Nomenclatures of the Hsps

Protein name	Old name
Small Hsps family Hsp27	HSPB family HSPB1
Hsp70 family Hsp72 Hsp73	HSPA family HSPA1A HSPA8
Hsp90 family Hsp90 α Hsp90 β	HSPC HSPC2 HSPC3
Hsp32	HO-1

Adapted from (Kampinga *et al.*, 2009)

1.9.2 Hsps regulation and expression:

The cellular response to the heat shock is regulated by transcription factors known as heat shock factors (HSF). HSF1 plays a central role as transcription factor to regulate the stress response (Uchiyama *et al.*, 2007). It has been reported that HSF1 is required to regulate the expression of Hsp27 and Hsp72 under stress conditions (Christians *et al.*, 2002; Ahn *et al.*, 2003; Trinklein *et al.*, 2004). The HSF1 is found as monomer bound to Hsps and other chaperone proteins under non-stress conditions (Shi *et al.*, 1998). Under stress conditions, HSF1 is traslocated to the nucleus and converted to trimer *via* their leucine zipper domains. The trimer binds with Heat shock elements (HSEs) that are located within the promoter regions of the Hsp genes, resulting in transcriptional activation and synthesis of Hsps (Zou *et al.*, 1998; Uchiyama *et al.*, 2007). Moreover, the HO-1 can be regulated at the transcriptional level, the promoter of the HO-1 gene (the 5' distal flanking region) has several response elalement located in it including NF- κ B, and HSF-1 (Maines,1997; Choi *et al.*, 2004).

There is a negative feedback mechanism control the expression of the Hsps, when the cellular level of the Hsps increase, Hsp72 or other chaperone protein such as Hsp90, relocate to the nucleus and bind to the HSF-1 trans-activation domain by which the transcription of Hsps is suppressed.

1.9.3 Hsp27

Heat shock protein 27 (Hsp27), with a molecular weight of 27kD in human and 25kD in rodents, is an adenosine triphosphate-independent molecular chaperone that can facilitate the repair of degradation and damaged proteins, regulate actin cytoskeleton organization and modulate redox parameters potentially produced in stressed cells (Hout *et al.*, 1996; Mehlen *et al.*, 1996; Ehrnsperger *et al.*, 1997).

Recently it has been suggested that overexpression of Hsp27 provides protection from oxidative stress in different cell lines; H9c2 cells, hippocampal progenitor cells, HeLa cells and breast cancer cells (Casado *et al.*, 2007; Son *et al.*, 2005; Tsuchiya *et al.*, 2005). These studies also demonstrated that Hsp27 has an anti-apoptosis effect by reducing generation of ROS, prevent the loss of membrane potential and suppressing the release of cytochrome c (Mehlen *et al.*, 1995; Ito *et al.*, 1998; Concannon *et al.*, 2001). The protective role of Hsp27 might be due to its ability to regulate the redox status in the cells through maintaining antioxidant enzyme activity such as glutathione reductase and glutathione transferase (Wheeler *et al.*, 2007).

1.9.4 Hemoxygenase-1 (HO-1)

Hemoxygenase-1 (HO-1), also known as Hsp32, is an enzyme that breaks down the heme molecule (Fe-protoporphyrin IX) by releasing the chelated iron from the tetrapyrrole macromolecule to form Carbon monoxide (CO) and biliverdin IX α (BV) isomer (Balla *et al.*, 1992; Yamaguchi *et al.*, 2002; Kravets *et al.*, 2004; Maines, 2005). All the outcome products of HO-1 activity have antioxidant properties (Ryter *et al.*, 2002).

The initial response of the cells to oxidative stress is up-regulation of HO-1 which has an anti-inflammatory, anti-apoptosis, anti-proliferation and cytoprotective effect (Maines, 1997; Yamada *et al.*, 2000; Tulis *et al.*, 2001, Shibahara 2003; Maines *et al.*, 2005). Moreover, there are several studies demonstrated that HO-1 has a role in maintaining antioxidant homeostasis during cellular stress (Alam & Cook, 2003; Choi *et al.*, 2003; Otterbein *et al.*, 2000).

There are negative and positive feedback mechanisms regulating the induction of HO-1. When the cells exposed to a stressor such as hypoxia or heat, HO-1 is upregulated to protect the cells from damage and produces CO and BV (Shibahara, 2003). However, the accumulation of CO and BV can be toxic, but the transcription factor BACH-1 is known to suppress the induction of HO-1 and prevent the accumulation of BR and CO (Sun *et al.*, 2002; Shibahara, 2003). Moreover, HO-1 can be regulated at transcriptional level and most of the response elements of HO-1 gene located in the promoter at 5' distal flanking region which include the binding site of transcription factors such as HSF-1 and Nf- κ B (Maines, 1997; Choi, *et al.* 2004).

Several studies have demonstrated the cytoprotection role of HO-1 against oxidative stress (Siow *et al.*, 1999; Prohászka, *et al.*, 2004). However, inhibition of HO-1 is believed to induce cell death (Otterbein *et al.*, 2000; Soares *et al.*, 2002). It has been shown by Yet and co-worker in 2003, that depletion of HO-1 in mice leads to an advanced atherosclerotic lesion development. The induction of HO-1 has been indicated in several diseases such as Alzheimer's disease, Parkinson's disease, ischemic stroke, atherosclerosis and renal insufficiency (Agarwal *et al.*, 2000; Abraham *et al.*, 2005; Bach, 2005; Deshane *et al.*, 2005; Maines, *et al.* 2005; Morita, 2005), so a treatment that leads to induction of HO-1 could be a significant approach for the treatment of these diseases.

1.9.5 Hsp70 family:

Hsp70 is the major inducible heat shock protein in many vertebrate cells and it has been widely studied among the Hsps families. The Hsp70 family is known to confer thermotolerance and also provides a protection against different stress conditions including oxidative stress (Minowada *et al.*, 2005; Musch *et al.*, 1996; Musch *et al.*, 1999).

In mammalian systems, the Hsp70 family includes; the constitutive cytosolic Hsc70 (Hsp73), the stress induced cytosolic form (Hsp72), Grp78 (BiP) which is located in the endoplasmic reticulum (ER), and the mitochondrial Grp75 (Gebauer *et al.*, 1997; Liu *et al.*, 2005). These proteins contain two domains: the N-terminal domain which is also known as the ATPase domain due to its ability to hydrolyse ATP to ADP, and the C-terminal domain, which has a substrate binding domain that binds to

hydrophobic peptides (Hartl, 1996; Tavaría *et al.*, 1996; Sriram *et al.*, 1997; Hartl & Hayer-Hartl, 2002; Ruchalski *et al.*, 2006).

It has been reported that Hsp72 is induced under different stimuli such as hyperthermia (Landry, 1989), oxidative stress (Huot *et al.*, 1999; Mehlen *et al.*, 1993), and by several commonly used anti-cancer drugs (Garrido *et al.*, 1997). The overexpression of Hsp72 has been reported in several studies that provide protection against apoptosis induced by different stimuli (Samali *et al.*, 1996; Lindquist, 1986; Creagh & Cotter, 1999; Grasso *et al.*, 2003; Kim *et al.*, 2005; Doulias *et al.*, 2007).

1.9.6 Hsp90

Heat shock protein 90 (Hsp90) mainly functions as a cellular chaperone (Pratt *et al.*, 2003). Hsp90 assists proteins to correctly fold and maintains the function of various complex chaperone proteins such as Hsp70, Hop (Hsp70 and Hsp90 organising protein) and Hsp40.

The Hsp90 family includes; Hsp90 β which is required for cell survival and it is essential for ATP-dependent refolding of denatured proteins (Pearl *et al.*, 2002). Also, it has been reported that Hsp90 is over-expressed in many cancer cells, and it has been proposed to have the potential as anticancer treatment (Schilb *et al.*, 2004; Whitesell & Lindquist, 2005).

1.10 Signal transduction pathways

Signal transduction pathways are defined as any process by which a cell converts one kind of signal or stimulus into an action or response, so they control essential processes in all eukaryotic cells, including gene transcription, protein translation, cytoskeletal remodelling, endocytosis, cell metabolism, cell proliferation and survival (Cano *et al.*, 1994, Widmann *et al.*, 1999). These processes involve ordered sequences of biochemical reactions within the cells. Oxidative stress is known to induce apoptosis in different cell types which trigger cell death signaling cascades (Martindale *et al.*, 2002). At the same time, oxidative stress can also activate certain signaling pathways that provide protection against cell death (Wang *et al.*, 1998; Qin & Chock, 2003). Nf κ B, ERK1/2 and AKT are considered as survival signals, they activate anti-apoptosis signaling pathways. JNK and p38, on the other hand, are

known as cell death signals pathways inducing the death cascade (inducing apoptosis) (Xia *et al.*, 1995; Harper & LoGrasso., 2001; Crossthwaite *et al.*, 2002).

1.10.1 Nf_κB

Nuclear factor kappa B (Nf_κB) is a family of inducible transcription factors present in all mammalian cells (Chen & Greene, 2004; Hayden & Ghosh, 2006; Hoffmann *et al.*, 2006; Perkins, 2006). The phrase Nf_κB is referring to a family of inducible dimeric transcription factors that recognize a common sequence pattern, the _κB site. There are seven subunits related to Nf_κB polypeptides: Nf_κB1:p105 and p50, Nf_κB2:p100 and p52, RelA(p65), c-Rel and RelB, and these subunits can form large numbers of homo- and heterodimers (Ghosh & Karin, 2002; Hayden *et al.*, 2006).

Under normal conditions in the cytoplasm, Nf-_κB is usually found in an inactive form bound to an inhibitory protein known as I_κB (Figure 1.4). When cells are exposed to a different type of stress, I_κB is phosphorylated, resulting in subsequent degradation of I_κB and translocation of Nf_κB to the nucleus (Baeuerle, 1998; Mattson *et al.*, 2000; Kaltschmidt *et al.*, 2005).

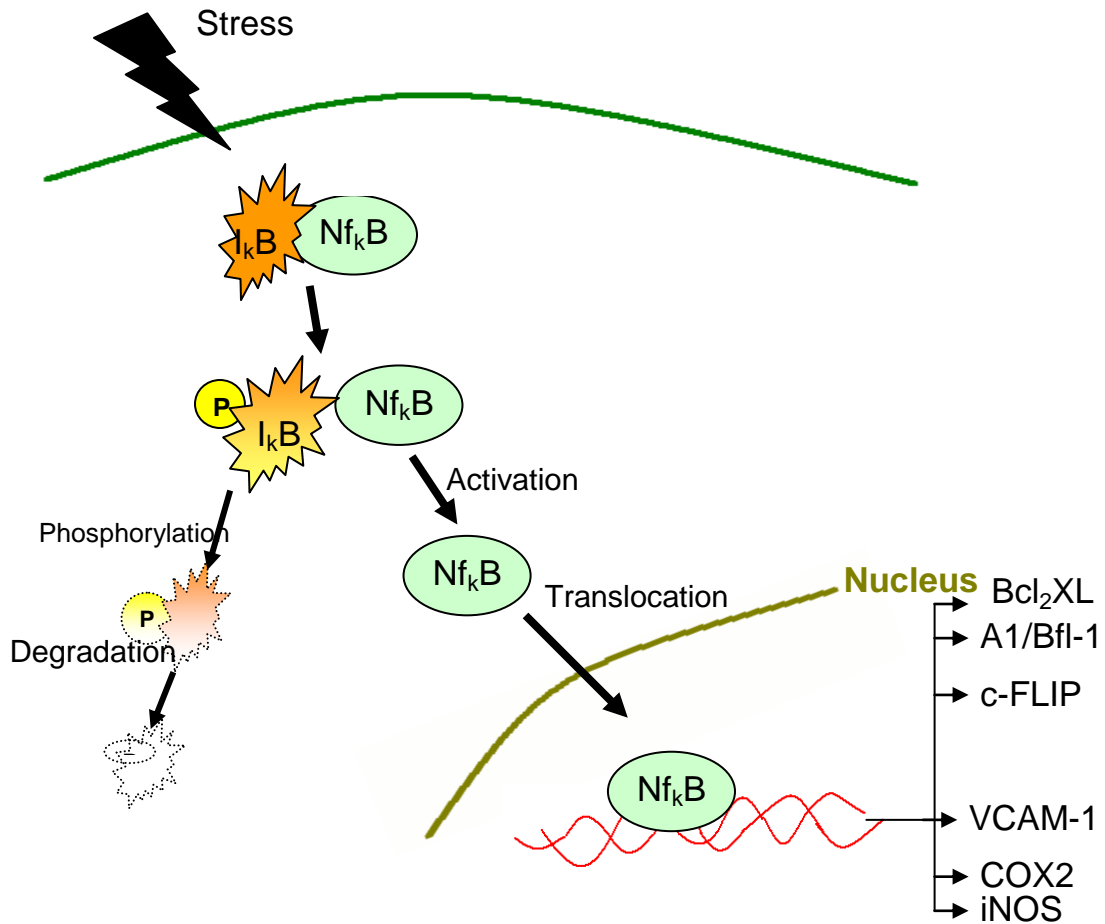


Figure 1.4; Activation of NF κ B. The phosphorylation of I κ B leads to dissociation with NF κ B and translocation to the nucleus. NF κ B then bind to the gene promoter to upregulated gene expression of proteins such as inducible nitric oxide (iNOS), cyclooxygenase-2 (COX-2), Vascular Cell Adhesion Molecule-1 (VCAM-1), Intercellular Cell Adhesion Molecule-1(ICAM-1) and glutathione (Glu). Each molecule in the diagram has a unique colour and form, and the colour was changed according to the process to yellow when the molecule was phosphorelated.

Recently, several research studies have investigated Nf_κB activation under different stress conditions. The central cellular roles of Nf_κB are; maintaining tissue homeostasis, activation of innate and adaptive immune responses, and control of the development of disease through its ability to suppress apoptosis and promote cell survival signals (Sun & Karin, 2008; Lin & Karin, 2003). Nf_κB activation regulates the expression of anti-apoptosis gene proteins such as Bcl-XL, c-FLIP, A1/Bfl-1 (Lin & Karin, 2003). Moreover, Nf_κB is also known to control expression of iNOS and other inducible genes such as cyclooxygenase-2 (COX-2), Vascular Cell Adhesion Molecule-1 (VCAM-1), and Intercellular Cell Adhesion Molecule-1(ICAM-1) in immune and inflammatory responses (Pham *et al.*, 2004; Xia *et al.*, 2001). Furthermore, it has been reported that Nf_κB activation is associated with neurodegenerative diseases including Alzheimer's disease, Parkinson's disease, Huntington's disease, and active multiple sclerosis (Bonettie *et al.*, 1999; Mattson & Camandola, 2001; Memet, 2006).

1.10.2 Mitogen-Activated Protein Kinases family (MAPK)

The function and regulation of mitogen-activated protein kinases (MAPK) have been highly conserved (Widmann *et al.*, 1999). MAPKs are serine/threonine kinases and include extracellular signal regulated kinase 1/2 (ERK1/2), c-Jun N-terminal kinase (JNK), and p38 MAPK. These MAPKs are upregulated by kinases and inactivated by phosphatases (Hommes *et al.*, 2003). MAPK plays a vital role in the cellular system including proliferation, differentiation and cell death (Singh & Czaja, 2006; Dhanasekaran *et al.*, 2007). They are triggered by various factors such as growth factors, cytokines, oxidative stress and hyperthermia (Aikawa *et al.*, 1997; Chen *et al.*, 1998; Kamata & Hirata, 1999; Ng & Bogoyevitch, 2000).

The MAPK signals are triple kinase pathways that include a MKKK (MAPK kinase kinase), a MKK (MAPK kinase) and the terminal MAPK (Raman *et al.*, 2007). The first well defined MKKK was Raf-1, which is a proto-oncogene serine/threonine protein kinase (Figure 1.5). Under stress Ras binds directly to Raf-1 leading to phosphorylation and activation of Raf-1 (Wellbrock *et al.*, 2004). The phosphorylated Raf-1 activates and phosphorylates MAPK (Muslin, 2005). This then leads to phosphorylation of

MKK4/7, MKK 3/6 and MKK1/2 in order to phosphorylate the JNK, P38 and ERK1/2 respectively.

Generally, it is known that MAPKs are associated with the oxidative stress- signaling (Avogaro *et al.*, 2008) and control the mitochondrial pathway of apoptosis (Torres *et al.*, 2003; McCubrey *et al.*, 2006). More specifically they promote cell survival, while the activation JNK and p38 MAPK is associated with death signaling pathways (Xia *et al.*, 1995; Brunet *et al.*, 2001; Harper & LoGrasso, 2001).

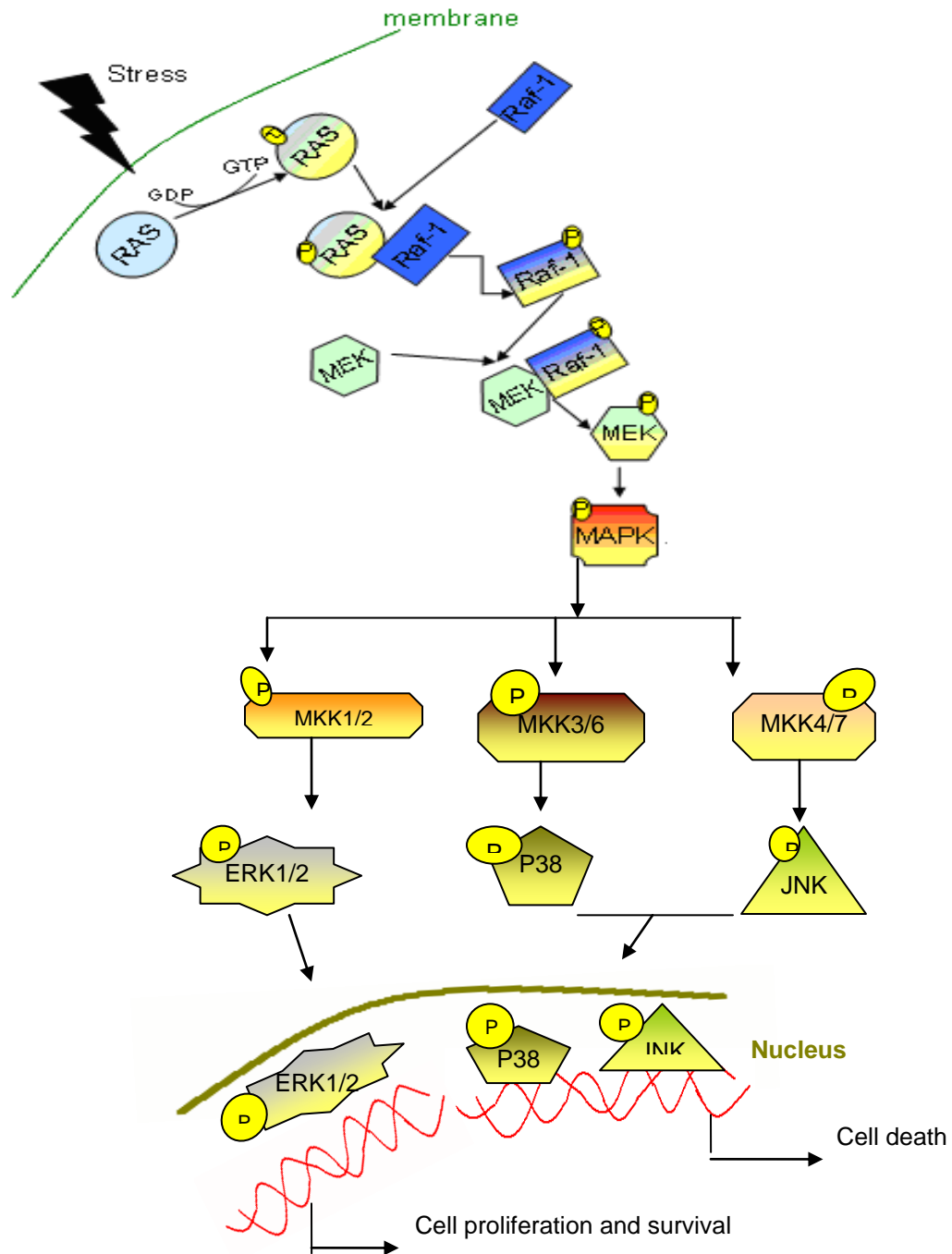


Figure1.5: Activation of the MAPK family. Under stress, Ras phosphorylate and bid to Raf-1. The activation of Raf-1 leads to phosphorylation of MEK, which in turn phosphorylate MAPK. MKK4/7 activates N-terminal kinase (JNK), MKK3/6 activates P38 and MKK1/2 activates extracellular signal regulated kinase 1/2 (ERK1/2). Each of them traslocated to the nucleas and transcript related genes. Each molecule in the diagram has its unique colour and form, and the colour changed according to the process to yellow when the molecule was phosphorelated.

1.10.2.1 Extracellular Signal Regulated Kinases (ERK1/2)

Extracellular signal regulated kinases (ERK1/2) are highly conserved signalling pathways. The ERK1/2 is known to be activated by heat shock stimuli, oxidative stress and growth factors (Xia *et al.*, 1995; Lapadat, 2002; Kurland *et al.*, 2003; Kurland *et al.*, 2003; Monick *et al.*, 2008; Yan *et al.*, 2007; Junttila *et al.*, 2008; Johnson & Monick *et al.*, 2008;).

The activation of ERK1/2 requires the activated form of Raf-1 which activates and phosphorylates the MKK1/2. In turn, the ERK1/2 was phosphorylated on the threonine and tyrosine residue (Kurland *et al.*, 2003; Monick *et al.*, 2008). Activation of the ERK1/2 has several cellular functions such as; regulation of cell growth and proliferation, cell death protection (Figure 1.5). Moreover, the role of ERK1/2 to promote cell survival also has been demonstrated under oxidative stress in different cell types such as osteoblastic cells (Yung *et al.*, 2007) and SH-SY5Y neuroblastoma cells (Ruffel *et al.*, 2004) rat PC12 cells (Guyton *et al.*, 1996) and primary cortical neurons (Crossthwaite *et al.*, 2002).

1.10.2.2 JNK and P38

The c-Jun N-terminal kinase (JNK) and P38 are members of the MAPK family. There are different stimuli triggering these pathways such as; growth factors, cytokines, heat shock and oxidative stress (Hibi *et al.*, 1993; De'rijard *et al.*, 1994; Westwick *et al.*, 1994; Davis, 1994; Prasad *et al.*, 1995; Cano *et al.*, 1994). As shown in Figure 1.5, the activation of the JNK and P38 is required for the phosphorylation of Raf-1 that leads to activation and phosphorylation of the MAPK. MKK4 and MKK7 are required in order to phosphorylate JNK, and MKK3 and MKK6 are needed for P38 activation (Dhanasekaran & Reddy, 1998).

It is believed that activation of JNK and P38 is essential for control of cell proliferation (Rangneaud *et al.*, 1995; Miyazawa *et al.*, 1998; Rincon *et al.*, 1998). JNK and P38 are activated when the cells undergoes apoptosis (Xia *et al.*, 1995; Matsuzaki *et al.*, 1999; Uchiyama *et al.*, 2004).

1.10.3 AKT/PI3

Akt/PI3 is a serine/threonine protein kinase that is associated with anti-apoptosis signal transduction pathways (Hatano & Brenner, 2001). Upon a variety of stimuli such as oxidative stress, Akt/PI3 is activated by phosphorylation at Thr 308 and Ser 473, (Figure 1.6). The phosphorylation of AKT/PI3K mediates Nrf2 translocation to the nucleus (Kang *et al.*, 2002). Moreover, the PI3K cascade controls the regulation of antioxidant response element (ARE) dependent genes in H4II rat hepatoma cells (Kang *et al.*, 2001), and in IMR-32 human neuroblastoma cells (Lee *et al.*, 2001). Several studies shows that AKT/PI3K has the ability to upregulate HO-1 under oxidative stress conditions (Martin *et al.*, 2003; Pischke *et al.*, 2005; Salina *et al.*, 2003; Chung *et al.*, 2005).

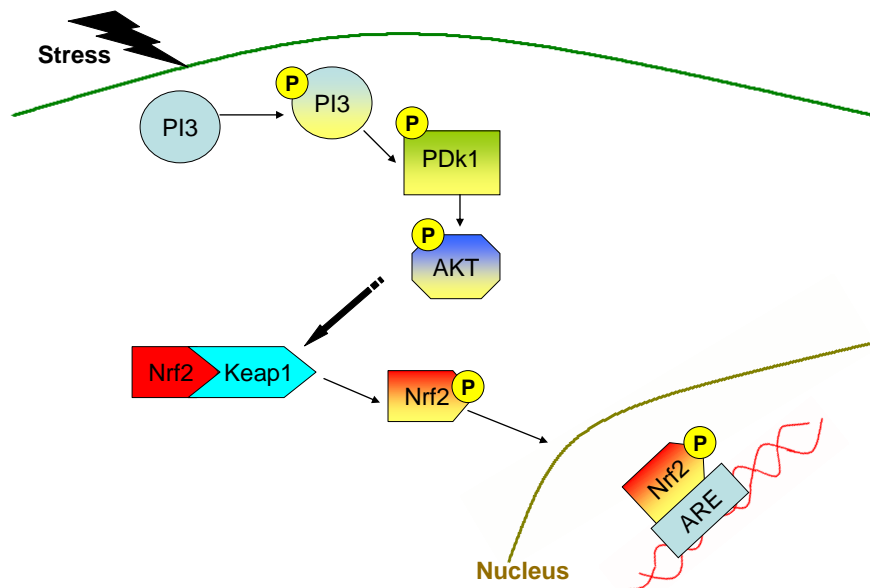


Figure1.6: Activation of AKT/Nrf2 pathways. Under stress, PI3 phosphorelated and consequently leads to phosphorylation of AKT. The phosphorylate AKT activate the Nuclear factor erythroid 2-related factor 2 (Nrf2), which then traslocated to the nucleus to bind with promoter gene of antioxidant response element (ARE). Each molecule in the diagram has its unique colour and form, and the colour changed according to the process to yellow when the molecule was phosphorelated.

1.10.4 NRF2

Nuclear factor erythroid 2-related factor 2 (Nrf2) is a critical transcription factor that belongs to the Cap'n'Collar family, basic leucine zipper transcription factors. As shown in Figure 1.6, Nrf2 has the ability to bind and activate the ARE, antioxidant enzymes and other stress-inducible genes in response to oxidative or electrophilic stress (Itoh *et al.*, 2005; Chan & Kan, 1999; Chan *et al.*, 2001; Kim *et al.*, 2001; Kwak *et al.*, 2002).

ARE is a cis-acting enhancer sequence which regulates the transcriptional activation of many antioxidant and detoxification-related genes that contain the ARE in their promoters under oxidative stress (Rushmore *et al.*, 1991). Genes that are ARE regulated include glutathione transferase, HO-1, SOD, and thioredoxin (Lee *et al.*, 2003). As a result, the ARE is involved in controlling the cellular redox status and the provision of protection to the cell against oxidative stress (Hayes & McLellan, 1999)

Nrf2 activity can be regulated at several levels: transcription, degradation, translocation, and *via* post-translational modifications such as phosphorylation (Huang *et al.*, 2000; Kong *et al.*, 2001; Kwak *et al.*, 2003; Zhang & Hannink, 2003; Nioi & Hayes, 2004). The activation of Nrf2 can be triggered by different stimuli (Nguyen *et al.*, 2003). Normally, Nrf2 presents in the cytoplasm as an inactive complex form with Kelch-like ECH-associated protein 1 (Keap1) (Kobayashi & Yamamoto, 2005). Activation of Nrf2 occurs upon alteration in the intracellular redox state or when cells are exposed to compounds that possess the ability to oxidize or covalently modify thiol groups or other exogenous stressor (Dinkova-Kostova *et al.*, 2001). As shown in (Figure 1.6), the Nrf2-Keap1 complex is discharged leading to release of the Nrf2 that can then translocate into the nucleus and bind to the ARE to induce expression of defensive proteins (Kobayashi & Yamamoto, 2005; Cullinan *et al.*, 2004; Furukawa & Xiong 2005; Kobayashi *et al.*, 2004; Sun *et al.*, 2007), such as the glutathione peroxidase-2, and HO-1 genes (Chan & Kwong, 2000; Cho *et al.*, 2002; Hayes *et al.*, 2000; Kwak *et al.*, 2001; McMahon *et al.*, 2001). However, recently it has been proposed that several signal transduction pathways, including MAPKs and $\text{Nf}\kappa\text{B}$ pathways are required for activation of Nrf2 nuclear translocation (Kong *et al.*, 2001; Huang *et al.*, 2000; Numazawa *et al.*, 2003; Nakaso *et al.*, 2003).

1.10.5 iNOS

The iNOS is the inducible form of nitric oxide synthase (NOS), which is a member of the nitric oxide synthase family present in macrophages and other cells. The NOS family includes the constitutive form present in neurons (nNOS) or endothelial cells (eNOS) and iNOS. The constitutive NOS form is a calcium-dependent enzyme, while iNOS is inducible calcium-independent enzyme. NOS are mainly responsible for nitric oxide (NO) generation. NO is a highly reactive nitrogen radical associated with different biological processes, such as regulating platelet aggregation and leukocyte adhesion, mediating the excessive vasodilatation and cytotoxic actions of macrophages against microbes and tumor cells, and acting in neurotransmission, (Moncada *et al.*, 1991; Nathan & Xie, 1994). However, the free radical (NO \cdot) can act as a cytotoxic agent in pathological processes, especially in inflammatory disorders (Alderton *et al.*, 2001; Bogdan, 2001; Dawn & Bolli, 2002; Moncada & Higgs, 1991).

NO synthesis requires L-arginine, the electron donor NADPH, oxygen, and cofactors heme, FMN, FAD and tetrahydrobiopterin (H4B) (Alderton *et al.*, 2001; Mayer and Hemmens, 1997; Stuehr *et al.*, 1991). The oxidation of L-arginine by NADPH and oxygen leads to formation of an intermediate product Nw-hydroxy-L-arginine (NOHarginine), followed by another oxidation step resulting in formation of L-citrulline and NO (Figure 1.7).

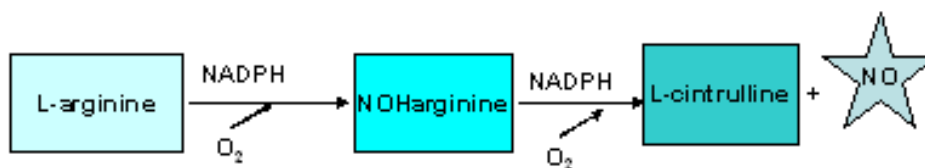


Figure 1.7: Generation of NO.

The iNOS is a bi-domain protein consisting of a C-terminal half, which acts as a reductase domain that contains the binding sites for CaM, NADPH, FAD and FMN; and the N-terminal half of the enzyme acts as an oxygenase domain that contains the binding sites for heme, H4B, and L-arginine (Sennequier & Stuehr, 1996). The iNOS can be induced in response to cytokines, bacterial products or infection in different cell types, including endothelium, hepatocytes, monocytes, mast cells, macrophages and smooth muscle cells (Nathan, 1992; Jaffrey & Snyder, 1995; Mayer & Hemmens, 1997; Alderton *et al.*, 2001). Moreover, it is believed that iNOS is a vital factor in the regulation of vascular disease (Kirkeboen & Strand, 1999; Ortega Mateo *et al.*, 2000). However, it has been suggested that there is an association between hyperhomocysteinemia and iNOS in atherosclerosis (Yla-Herttuala *et al.*, 1986). So the overproduction of iNOS can provide either protective or damaging effects, which depend on the cell type. (Cosentino *et al.*, 1998; Huk *et al.*, 1998; Marla *et al.*, 1997; Blatter *et al.*, 1995; Bogdan, 2001).

The iNOS can be regulated at the transcriptional level via Nf_κB pathway (Xia *et al.*, 2001). Upon stimulation such as by Lipopolysaccharide (LPS), cytokines, interferon- γ (IFN γ), and tumor necrosis factor- α (TNF α), Nf_κB is phosphorylated and then translocates to the nucleus to facilitate the iNOS gene expression (Huang *et al.*, 1998; Marks-Konczalik *et al.*, 1998; Obermeier *et al.*, 1999). However, iNOS can be regulated by different signal pathways that activate transcription factors such as protein kinase C (PKC), tyrosine kinase, JNK, raf-1 protein kinase, and MAPK. This activation is dependent on the stimulus and cell type (Lahti *et al.*, 2002; Marks-Konczalik *et al.*, 1998; Momose *et al.*, 2000; Muller *et al.*, 2001; Wang *et al.*, 1999).

The activation of Nf_κB - I_κB binding is the negative feedback mechanism that controls iNOS expression by NO production in macrophages and hepatocytes (Aktan, 2004). Overproduction of the iNOS leads to inhibition of the Nf_κB activation through stabilization of I_κB and increased transcription of the I_κB gene (Peng *et al.*, 1995b). Furthermore, it has also been suggested that exposure of human vascular endothelial cells to NO-generating compounds such as sodium nitroprusside (SNP), S-nitroso-N-acetylpenicillamine (SNAP) and S-nitrosoglutathione (GSNO), leads to inhibition of Nf_κB - I_κB dissociation, inactivation of Nf_κB (Peng *et al.*, 1995a). The binding of the Nf_κB - I_κB is controlled by the redox state of the cysteine residue C62 in

the Nf_κB p50 subunit (Kumar *et al.*, 1992; Matthews *et al.*, 1992; Toledano *et al.*, 1993; Hayashi *et al.*, 1993; Matthews *et al.*, 1993), which is found within the α polypeptide loop, and specifically binds to I_κB (Ghosh *et al.*, 1995; Müller *et al.*, 1995).

Recently, it has been suggested that cobalamin regulates the iNOS activity through OH-Cbl directly scavenging NO leading to inhibition of the NOS activity (Weinberg *et al.*, 2005). Also $\text{CN}_2\text{-Cbl}$ interacts directly with iNOS and therefore inhibits activity. On the other hand, Me-Cbl and Ado-Cbl have no inhibitory activity (Weinberg *et al.*, 2009). It has recently been hypothesized that cobalamin might induce the iNOS activity (Wheatley, 2007) but to date there are no data to support this hypothesis.

1.11 Aims and objectives:

The role of cobalamin in the oxidative stress protection and the mechanism of the protection are not fully understood.

The thesis aims to examine the protective role of cobalamin against cell death induced by oxidative stress, and investigate the possible mechanism(s) of the protection. Furthermore, it examines the novel cobalamin protection against cells death induced by oxidative stress and investigates the mechanism(s) of their superior protection.

The objectives of this thesis are:

- Determine the mechanisms of cell death induced by oxidative stress in different cell types.
- Investigate protective role of cobalamin against cell death induced by oxidative stress in different cell lines.
- Investigate the possible mechanisms of the protection provided against oxidative stress by:
 - Examine the possible involvement of the Hsps in the cobalamin protection.
 - Examine involvement of signal transduction in the cobalamin apoptosis protection
- Examine the efficiency of novel cobalamins in the oxidative stress protection and the mechanism(s) of their superior protection.

Chapter 2

Materials and Methods

2.1 Equipment

1.5 mL Microcentrifuge Tubes

Thermo Fisher Scientific Inc.

Part no. TUL-918-014G

12-well Cell Culture Plates

Thermo Fisher Scientific Inc.

Part no. TKT-520-070H

15 mL Centrifuge Tubes

StarLab.

Part no. E1415-0200

25 cm² Cell Culture Flasks

Thermo Fisher Scientific Inc.

Part no. TKT-130-050P

48-well Cell Culture Plates

Thermo Fisher Scientific Inc.

Part no. TKT-522-070S

96-well Cell Culture Plates

Thermo Fisher Scientific Inc.

Part no. DPS-130-010N

BD Eclipse Blood Collection Needle, 21g

Southern Syringe Services Ltd.

Part no. 268609

BD Vacutainer® One Use Holder

Southern Syringe Services Ltd.

Part no. 364815

BD Vacutainer® Whole Blood Tube, K₂EDTA, 10 mL

Southern Syringe Services Ltd.

Part no. 367895

BD Vacutainer® Whole Blood Tube, K₂EDTA, 6 mL

Southern Syringe Services Ltd.

Part no. 367873

Bio-Rad ChemiDoc XRS Molecular Imaging System

Bio-Rad Laboratories Ltd.

Part no.170-8070

Bio-Rad Radiance 2100 AGR-3Q AOFT confocal microscope (Argon 488, Green He/Ne 500, Red Diode 535) with following lasers: Argon (514, 488, 476, 457), Green (543), Red (637) Blue (405)

Bio-Tek Synergy™ HT Multi-Detection Microplate Reader

Labtech International Ltd.

Part no. SIAFR

Bright-Line™ Hemacytometer

Sigma-Aldrich Ltd.

Part no. Z359629

Circulating Water Bath

Wolf Laboratories Ltd.

Part no. GD100-P5

E100 Binocular Microscope

Jencons (Scientific) Ltd.

Part no. 450-951

BD FACS Canto™ Flow Cytometer

BD Biosciences™.

Part no. 337175

Hermle Z323K Refrigerated Centrifuge

VWR International Ltd.

Part no. 521-0221

Including:

Swing-out Rotor (8 X 15 mL)

Part no. 521-0189

Fixed-angle Rotor (24 X 1.5 mL)

Part no. 521-0201

Fixed-angle Rotor (8 X 50 mL)

Part no. 521-0194

High Speed Mini Orbital Shaker

Wolf Laboratories Ltd.

Part no. SSM5

HTS Transwell-96 Well Permeable Support System

Thermo Fisher Scientific Inc.

Part no. HTS-106-050J

Inverted TE2000-U Microscope System

Nikon Corporation Ltd:

Eclipse TE2000-U Basic Unit Part no. MEA51010

Eposcopic Fluorescence Attachment (Hg) Part no. MEE54000

CFI Plan Fluor ELWD Objectives

Part nos. MRH38220/MRH38420/MRH18620

Hamamatsu Orca – 285 Digital CCD Camera

Part no.1HMOC285

Coolpix Digital Colour Camera Part no. 85400RUK

IPLAB Suite Software Part no. 1SCSUITE

Microplate 96 well V bottom polystyrene clear 0.415 mL

Thermo Fisher Scientific Inc. Part no. FB-56424

Microplate 384 well square shape polystyrene solid black

Thermo Fisher Scientific Inc. Part no. FB-58050

Microscope slide Polysine adhesion glass 25mm x 75mm x 1mm

Thermo Fisher Scientific Inc. Part no. MNJ-800-010F

Nunc Immuno Maxisorp 96-well Plates

Thermo Fisher Scientific Inc. Part no. DIS-971-030J

Nitrocellulose Membrane, 0.45 µm

Bio-Rad Laboratories Inc. Part. No. 162-0115

Sigma 1-14 Microcentrifuge

Wolf Laboratories Ltd. Part no. 10016

Temperature-controlled, Stirred Water Bath, GD100-S5

Thermo Fisher Scientific Inc. Part no. BLE-650-010G

Vortex Mixer, mini

Thermo Fisher Scientific Inc. Part no. GBI-900-010E

2.2 Reagents

Actinomycin D

Sigma-Aldrich Ltd.

Part no. A9415

Annexin V: FITC Apoptosis Detection Kit I (100 Tests)

BD Biosciences™.

Part no. 556547

Antibiotic/Antimycotic Solution (100X)

Sigma-Aldrich Ltd.

Part no. A-5955

Anti-Goat IgG (whole molecule)–FITC antibody produced in rabbit

Sigma-Aldrich Ltd.

Part no. F-2016

Anti-Rabbit IgG (whole molecule)–FITC antibody

Sigma-Aldrich Ltd.

Part no. F-0382

Anti-Nrf2 Goat IgG polyclonal antibody

Santa cruz biotechnology, INC.

Part no. sc-30915

Anti- pNf_κB Rabbit IgG monoclonal antibody

Santa cruz biotechnology, INC.

Part no. sc-3033

Anti- pERK1/2 Rabbit IgG monoclonal antibody

Santa cruz biotechnology, INC.

Part no. sc-101760

Anti- pAKT Rabbit IgG monoclonal antibody

Santa cruz biotechnology, INC.

Part no. sc-4058

Anti- iNOS rabbit IgG monoclonal antibody

Santa cruz biotechnology, INC.

Part no. sc-2977

Bay-117082

Sigma-Aldrich Ltd.

Part no. B-5556

BD FACS Lysing Solution

BD Biosciences™

Part no. 349202

Bovine Serum Albumin

Sigma-Aldrich Ltd.

Part no. A-7906

Caspase-3, Active Form (100 Tests)

BD Biosciences™.

Part no. 559341

CellTiter® Aqueous One Solution Cell Proliferation Assay

Promega UK Ltd.

Part no. G3580

Methylcobalamin

Sigma-Aldrich Ltd.

Part no. M-9756

Coomassie (Bradford) Protein Assay Kit

Pierce Biotechnology.

Part no. 23200

Dulbecco's Phosphate Buffered Saline (DPBS)

Cambrex Corporation.

Part no. BE17 – 513F

E6.1, Human Leukemic T cell lymphoblast Cell Line,

European Collection of Cell Cultures ECACC Part no. 88042803

Enzolyte™ Rh110 Caspase-3 Assay kit

Anaspec Inc.

Part no. 71141

Ethylenediaminetetraacetic acid, anhydrous (EDTA)

Sigma-Aldrich Ltd.

Part no. E-6758

EMEM media

Lonza

Part no. 12-611F

Fixation/Permeabilization Solution (250 Test)		
BD Biosciences™.		Part no. 554722
Foetal Bovine Serum (FBS) (75 mL)		
Cambrex Corporation.		Part no. 14-810F
Folic acid		
Sigma-Aldrich Ltd.		Part no. F-7876
Formaldehyde Solution 37 wt. % in H₂O (500 mL)		
Sigma-Aldrich Inc.		Part no. 533998
HEPES (50 G)		
Sigma-Aldrich Ltd.		Part no. H-3375
Histopaque®-1077 Hybri-max Solution		
Sigma-Aldrich Inc.		Part no. H-8889
Hsp27 Mouse Monoclonal Antibody: FITC conjugate (100 µg)		
Cambridge Bioscience.		Part no. SPA-800FI
HO-1 Mouse Monoclonal Antibody: FITC conjugate (100µg)		
Cambridge Bioscience		Part no. OSA-111HI
Hsp72 Mouse Monoclonal Antibody: FITC conjugated (400 µg)		
Cambridge Bioscience.		Part no. SPA- 810FI
Hsp90 Mouse Monoclonal Antibody: PE Conjugate (100 µg)		
Cambridge Bioscience.		Part no. SPA-830PE
Hydrochloric Acid		
Sigma-Aldrich Inc.		Part no.H-1758

KNK423, Heat shock protein inhibitor II,	
Calbiochem,	Part no. 373265
LY-249002, AKT/PI3 inhibitor	
Sigma Aldrich Inc.	Part no.L-9908
Paraformaldehyde powder 95%	
Sigma-Aldrich Ltd.	Part no. 158127
Propidium Iodide Minimum 95% (HPLC)	
Sigma-Aldrich Inc.	Part no. P-4170
RPMI-1640 Medium (500 mL)	
Cambrex Corporation.	Part no. BE12-702F
RPMI-1640 Medium, Phenol Red-Free (500 mL)	
Cambrex Corporation.	Part no. BE12-918F
SB202190, P38K inhibitor	
Sigma Aldrich Inc.	Part no.S-7067
SensoLyte Homogeneous Rh110 Caspase-3/7 Assay Kit	
Cambridge Bioscience.	Part no. ANA-71141
Sodium Bicarbonate	
Sigma-Aldrich Ltd.	Part no. S-6297
Sodium Carbonate	
Sigma-Aldrich Ltd.	Part no. S-7795
Sodium Chloride	
Sigma-Aldrich Ltd.	Part no. S-7653

Sodium Hydroxide

Sigma-Aldrich Ltd.

Part no. S-8045

SP600125, JNK inhibitor

Sigma-Aldrich Ltd.

Part no. S5567

SK-hep1 cells line

ECACC (European Collection Cell Culture)

Part no.91091816

Triton® X-100

Sigma-Aldrich Ltd.

Part no. T-8787

Tween® 20

Sigma-Aldrich Ltd.

Part no. P-1379

U0126, ERK1/2 inhibitor

Sigma-Aldrich Ltd.

Part no. U120

Wortmanin, Nrf2 inhibitor

Sigma-Aldrich Ltd.

Part no. 95455

2.3 Buffers**2.3.1 Freeze media solution (v/v)**

10 ml of DMSO was diluted into 40ml of FBS; the solution was kept cold at 4°C during the whole freezing process.

2.3.2 MTS Working Solution (w/v)

MTS Stock solution was prepared by dissolving 0.042g of MTS powder in 21ml DPBS and pH was adjusted to 6.5 with 1M HCl. The Phenazyl-Etho-Sulfate (PES) stock solution was prepared by dissolving 0.0092g of the powder in 10ml DPBS. The MTS working solution was obtained by adding 1ml of PES stock solution in each 20ml of MTS Stock solution and then the solution was stored at -20°C.

2.3.9 pH solutions

1M HCl (v/v)

A volume of 9.8 ml of 37% hydrochloric acid (HCl) was mixed with dH₂O to obtain up to 100 ml of solution, which was stirred until dissolved.

1M NaOH (w/v)

4g of sodium hydroxide (NaOH) was added to 80ml of dH₂O and stirred until dissolved. The solution was then made up to 100 ml with dH₂O.

2.3.10 4 % Paraformaldehyde (PFA) buffer

2g of Paraformaldehyde (PFA) and 100µl of 5M sodium hydroxide (NaOH) were diluted in 40ml of phosphate buffer saline (PBS); the solution was stirred and heated at 56°C in a water bath until PFA was completely dissolved. The pH was adjusted with 100µl 5M HCl to 7.4, and then filled up to 50 ml final volume with PBS and stored at 4°C for maximum a week.

2.3.11 15M Phosphate buffered saline, pH 7.4 (PBS) (w/v)

8g of Sodium chloride (NaCl), 0.2g of potassium chloride (KCl), 0.24g of potassium dihydrogen orthophosphate (KH₂PO₄) and 1.44g of sodium dihydrogen orthophosphate (Na₂HPO₄) were added to 1L of dH₂O and pH adjusted to 7.2.

2.3.12 Propidium Iodide stock solution (1mg/ml) (w/v)

0.001g of Propidium iodide (PI) dissolved in 1ml DPBS. 100µg/ml stock solutions was prepared and stored at -20°C into single use aliquots.

2.3.13 Blood cells Lysing Buffer 10X solution (w/v)

8.02g of ammonium chloride (NH₄Cl), 84g of sodium carbonate (NaHCO₃) and 0.37g EDTA disodium were dissolved in 50 ml of dH₂O. The 1X working dilution was obtained by diluting 1/10 the concentrated solution with dH₂O.

2.3.14 Tissue culture media (v/v)

10% FBS was added to RPMI 1640 or EMEM media and stored at - 20°C. The

media was regularly transfer to 24 well plates and examined under light microscope for infection and integrity of the culture media.

2.3.15 Wash buffer 1X

5ml of foetal bovine serum (FBS) was diluted in 100ml PBS

All chemicals unless otherwise indicated are obtained from Sigma-Aldrich Company Limited, Poole, Dorset, UK.

2.4 Method

2.4.1 Cell culture: Sk-Hep1

Sk-hep1 is carcinoma liver endothelial cells. The cells were purchased frozen. The cryostats containing the cells were removed from the cryostat, soaked with alcohol and placed in a 37°C water bath immediately. The vial opened and the contents were placed in a 25cm² flask containing 5ml of pre-warmed EMEM media with 10% serum. The cells were then counted with the haemocytometer and cell density was adjusted to 3-9x10⁵cells ml⁻¹. Cells were kept at 37°C in the incubator with 5% CO₂. A cell viability test was performed after 24h using trypan blue assay on haemocytometer. The cell line was passage every 3 days and viability was always tested by trypan blue assay.

Cells were sub-cultured 1:2 in culture flask at density, as required for the experiment. For passaging the Sk-Hep1 cells, medium was removed and cells were washed with 1 ml of trypsin/EDTA 0.4% solution. 1ml or 2ml of trypsin/EDTA 0.4% solution per 25cm² or 75cm² flasks respectively added. After 90s trypsin removed. The digestion was stopped after further 3 min by the addition of 5ml of fresh EMEM media. For the experiment cells were grown in monolayer until approximately 90% confluent in 6-96-well plates. Cells were cultured at 37°C in 5%CO₂ humidified Heracell incubator.

2.4.2 Cell culture: Jurkat

One of the cells line was used in this study was derived from blood malignancies: the E6.1 Jurkat is human leukemic T-cell lymphoblast cell line and it is a suspended cell. Briefly the cells were purchased frozen and, the cryostats containing the cells were removed from the cryostat, soaked with alcohol and quickly placed in a 37°C water bath. The vial was quickly opened and the contents were placed in a 25cm² flask containing 5ml of pre-warmed PRMI 1940 media with 10% serum. The cells were then counted with the haemocytometer and cell density was adjusted to 3-9x10⁵cells ml⁻¹. Cells were kept at 37°C in the incubator, 5% CO₂. The cell viability test was performed after 24h using trypan blue assay on haemocytometer. The cell line was passage every 3 days. For experimental use cells were plated in 6-12-24 well plates and the cells were sub cultured at density required for the experiment use.

2.4.3 Freezing storage and thawing of sk-hep1 and Jurkat

For long-term storage cells were kept at low density at 5x10⁵ cells/ml, in which cells were in the log phase of the growth curve and they were actively growing. SK-Hep1 cells were detached with trypsin/EDTA 0.4% solution, and centrifuge at 218g for 5 min, for the Jurkat cells; cells were centrifuged at 400xg for 5min at 25°C. The culture media was removed and cell pellet was re-suspended in 1ml of freeze media. The cells suspension was transferred to cryostats and frozen immediately at -20°C for 24hr, then at -80°C for 7 days, prior to storage at -196°C in liquid nitrogen. This procedure was performed in order to ensure gradual freezing of the cells to avoid ice –crystal formation within the cell structure.

For thawing, cells were defrosted in 37°C water bath and the cell suspension was immediately transferred to a 25cm² cell culture flask containing 9ml fresh complete media. Cells were cultured at 37°C in a 5 CO₂ humidified Heracell incubator.

2.4.4 Whole blood collection

The venous blood provided for these studies came from healthy voluntary people (non-smoker, clear from any infection and no alcohol). The blood samples were collected by venepuncture in 7ml K₂ EDTA vacutainers.

2.4.5 Whole blood isolation

Whole blood was washed with two volumes of DPBS and centrifuged at 500g for 5 min at 25°C. The supernatant was discarded and the red blood cells were lysed using 1x lysing buffer. The lysed whole blood was then centrifuged at 500xg for 5 min and the supernatant discarded. The cell pellet was washed with DPBS and the cells counted using the trypan Blue exclusion. The experiments were performed when the percentage of dead cells was <1%. Concentration of the viable cells was adjusted to 1×10^6 cells/ml and the cells were centrifuged at 500xg for 5 min. Supernatant was discarded and cells were re-suspended with 1 ml of wash buffer (DPBS 5%FCS) and kept on ice for flow cytometry analysis.

2.4.6 Trypan blue exclusion test cell viability

The dye exclusion test is employed to determine the viability and cell counts. It is based on the principle that Trypan Blue is a non-permeable cell membrane DNA dye, so the viable cells will not interact with dye whereas dead cells or necrotic cells allow the dye to stain the DNA inside the cells. As a result viable cells would appear clear white whereas dead cells would show up blue. Cells suspended in media were diluted 1:1 with Trypan Blue, and then 50µl of the suspension mixture was loaded in to both chambers of the haemocytometer. Cells were counted in the 0.04 mm centre square and four 0.04 mm corner squares, as presented in the (Figure 2.1) Cell number/ ml was obtained using the following formula:

$$\text{Cells/ml} = \text{Cell count} \times 5 \times \text{dilution factor} \times 10000$$

When the dead cells percentage exceeded 5% cells were discarded and not used for the experiments.

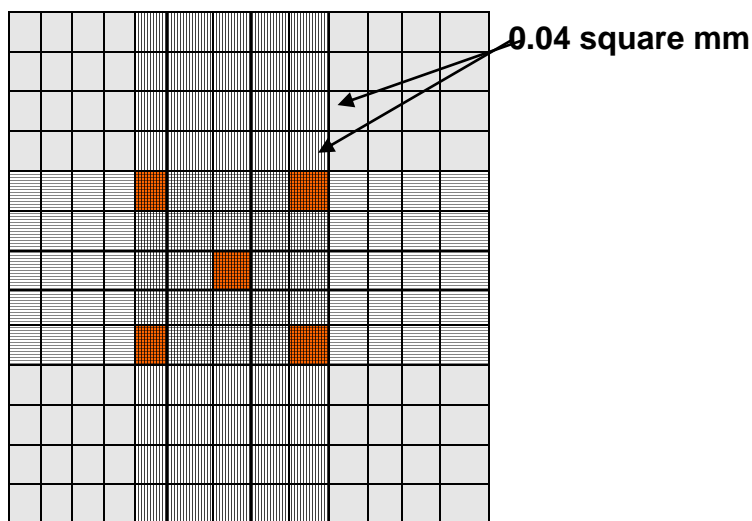


Figure 2.1: Haemocytometer

2.4.7 Sterilisation of equipment

Filter units containing 0.2 filters were autoclaved for filter serialisation of all reagents used under experimental conditions in culture media.

2.4.8 Treatment's Solution preparation

2.4.8.1 Hydrogen peroxide: The stock solution was 8.8M, diluted to 100mM, 10mM, 1mM and 0.1mM in media and Stored at 4°C.

2.4.8.2 Homocysteine: The stock solution made out in 1M HCl at concentration 100mM. The stock diluted to 1mM, 500 μ M, 250 μ M, 125 μ M, 65 μ M, 31.25 μ M and 13 μ M in media on the same day of the experiments because the Hcy is not stable in the media.

2.4.8.3 Folic acid: The stock solution made out in 1M NaOH at concentration 100mM. The stock diluted to the required concentration in media and store at -20°C.

2.4.8.4 Cobalamin

Stock of 1M prepared with ethanol, and then the stock diluted with media to the required concentration 200 μ M, 100 μ M, 50 μ M, 25 μ M, 12.5 μ M, 6.25 μ M and 3.125 μ M. Store at -20°C.

2.4.9 MTS assay: Cells viability

The cell viability in proliferation was performed using a colorimetric assay from Promega; CellTiter ® MTS Aqueous solution. The solution contain a tetrazolium compound called MTS (3-(4,5-dimethylthiazol-2yl)-5-(3-carboxymethoxyphenyl)-2-(4-sulfophenyl)-2H-tetrazolium) and an electron coupling agent PES (Phenazyl-Etho-Sulphate). MTS solution is bio-reduced by dehydrogenases enzymes in metabolically active cells, into formazan detected by colure developed at 490nm using a Bio-Tek Synergy H.T Multi-detection Microplate Reader, ruining KC-4 v3.4 software. Test conditions were as follows:

For the SK-Hep1 cells, 100 μ l cells were plated on 96-well plate at approximately 5×10^5 cells per well and cultured for 24hr. The cell media was removed from test wells and replaced with 100 μ l media containing various concentrations of test compounds. Plates were incubated for indicated time.

For the Jurkat cells, cells were seeded on 12-24 well plate on the day before at cell density 1×10^5 . Then cells treated with media containing various concentrations of test compounds and incubated for indicated time. After the incubation time 100 μ l of Jurkat cells transferred to black 96-well plate.

After incubation time for both cells lines, 20 μ l of MTS solution was added to each test well. Cells were incubated at 37°C with 5% CO₂ for the required time (2.5 hours for Jurkat and 1 hour for SK-hep1). The absorbance was measured at 490nm and comparison with control was performed. Controls were included a blank control; media, positive control; viable cells and negative control; dead cells killed by microwave irradiation for 10sec.

.

2.4.10 Caspase-3/7 fluorimetric assay:

The activation of downstream caspase-3, which is an effector of caspase, have the ability to cleave poly-(ADP ribose) polymerase (PARP), DNA-dependent protein kinase (DNA-PK), topoisomerases, and protein kinase C. This activity determined with an assay using the synthetic peptide substrate DEVD (asp-glu-val-asp). The DEVD substrate is labelled with a fluorophore, 7-amino-4-methylcoumarin (AFC), allowing the detection of the cleavage of caspase-3. The release of this fluorophore resulted in a shift from blue to green fluorescence, measured at an excitation wavelength of 390nm and an emission wavelength of 505nm. ($\text{Ex}=496\text{nm}/\lambda$, $\text{Em}=520\text{nm}/\lambda$) as described by the manufacture. The reaction has a linear progression over approximately two hours, provided the enzyme is saturated with substrate. Caspases need a thiol group for their catalytic function; therefore they are susceptible to changes in redox potential. This can allow the thiol group to be oxidized by agents such as air, oxygen and traces metal ions. To counteract this effect, the substrate buffer contains dithiothreitol (DTT) as reducing agent.

Briefly cell incubated under test condition of the experiment, and then 100 μl of Jurkat cells were transferred into a 96-well black plate while sk-hep1 were seeded in the 96-well black plate. The entire reagents needed were thawed at 25°C and a working solution of the substrate was prepared by diluting 5ml assay buffer with 200 μl DTT and 50 μl caspase-3 substrate solution. The 20 μl of working solution was added to each cell well and incubate for 1hour at 37°C. The result compared to controls; negative control: no treated cells, blank; media.

2.4.11 Caspase-3 assay FC:

Active caspase-3 was also tested using a polyclonal anti- active form of caspase-3-FITC conjugated rabbit antibody. Cells were treated under test condition then washed with wash buffer and centrifuged at 500 $\times g$ for 5 min at 25°C. Cell pellet re-suspended in 70 μl of fix/perm and incubated at 4°C for 20 min to allow the cells to fix biochemistry reaction inside the cells and permeabilise the cells membrane. The cell suspension was then washed with wash buffer, centrifuged at 500 $\times g$ for 5 min at 25°C. Then cells pellet were incubated with 20 μl /1 $\times 10^6$ cells/ml caspase-3-FITC conjugated antibody and incubated for 40 min at 4°C in dark. The unbound antibody

was washed with wash buffer, centrifuged at 500xg for 5 min at 25°C, the pellet then re-suspended with fresh DPBS buffer. Cells were analysed on the FACS Canto dual laser flow cytometry in the FITC channel.

2.4.12 Necrosis detection with Propidium Iodide fluorescent assay:

DNA fragmentation is considered to be a characteristic hallmark of necrosis; therefore necrotic cells can be detected and quantified by propidium iodide. PI interacts with DNA content of the cells. The cells were seeded at concentration of $0.2-0.7 \times 10^6$ cells/ml in black 96-well plate and treated under test conditions. The stock solution of propidium iodide kept at -20°C at 100 µg/ml concentration and the working solution 5 µg/ml was prepared before each analysis in DPBS. The 100 µl per well of working solution was then added and incubated at room temperature for 20 min in the dark. The PI fluorescence was detected at $\lambda_{Ex}=535\text{nm}/\lambda_{Em}=617\text{nm}$. The controls were positive control; cells incubated in the microwaves for 15 seconds, negative control; viable cells and blank: media.

2.4.13 Annexin-v and Propidium Iodide:

One of the early events of apoptotic cell death is the membrane changing, such as loss of membrane asymmetry and attachment. Phosphatidylserine (PS), usually present as an internal membrane lipid, when apoptosis occurs, it is translocated to outside the plasma membrane. Annexin V is a 35-36 kDa Ca^{2+} dependent phospholipid-binding protein that has a high affinity for PS, and binds to cells with exposed PS. Using this protein conjugated with FITC labelled combined with propidium iodide PE-labelled, it is possible to distinguish cells the apoptotic cells or necrotic cells using flowcytometry.

Cells were treated under test conditions and washed twice with cold PBS which centrifuged at 500g for 5 min at 25°C. And then cells were re-suspended in 1x binding buffer at density of 1×10^5 cells/ml, and 5 µl of Annexin V-FITC was added and incubated for 15 min at 25°C in the dark. Before the analysis 5 µl Propidium Iodide (PI 5 µg/ml) solution was added to the cell. The samples were analysed immediately by flow cytometry Annexin V was detected at $\text{Ex}=490/\text{Em}=520\text{nm}$ and PI was detected using a $>520\text{nm}$ long phase filter; 10000 events were recorded for each samples and compensation controls were applied for each experiment.

2.4.14 Measurement of intracellular Protein by FC:

Cells were treated under test condition and harvest as mentioned previously at concentration 1×10^6 cells/ml prior labelling. The cell washed with wash buffer (5% FBS in PBS), and centrifuged at 500xg for 5 min. Cells were then fixed and permeabilised with 50 μ l of Fix/Perm solution and incubated for 20 min at 25°C. Followed by adding 1ml wash buffer to the cells and centrifuged at 500xg for 5 min and supernatant removed. Cells were then labelled for the intracellular (Hsp27, HO-1, Hsp72 and Hsp90) by adding 1 μ l of antibody+49 μ l wash buffer and incubated for 40 min at 25°C in the dark. The incubation time was followed by a wash with 1 ml of wash buffer, centrifuged at 500xg for 5 min and the supernatant discard. Cell pellet was re-suspended in 20 μ l of wash buffer and analysed by the flow cytometry. The same dilution applied for measuring Nrf2, Nfkb, ERK1/2, AKT and iNOS. Compensation controls for each experiment panel was run in the first experiment and settings same were applied throughout all the study.

2.4.15 Measurement of Reactive Oxygen species:

Cells were cultured in 96-well plates for 24hr and then treated with reagents under test conditions. The redox active probe 2'7'-dichlorofluorescein-diacetate (DCFH-DA) was added to the cells at a concentration of 10mM and then incubated in the dark for 30min. Following treatment samples were solubilised in NaOH (0.1N). DCFH-DA activity was measured at $\lambda_{ex}=485\text{nm}/\lambda_{em}=530\text{nm}$.

2.4.16 Measurement of super oxide generation by Lucigenin-enhanced chemiluminescence:

Cells were cultured in white 96-well plates for 24hr and then treated with reagents under test conditions. The generation of superoxide ($\cdot\text{O}_2^-$), was demonstrated by added 5 μ M Lucigenin to each test well and the plate was incubated for 45min at 37°C in dark conditions. Absorbance was measured at 550nm.

2.4.17 statistical analyses

All statistical analyses were performed using Prism™ 5.01 (GraphPad Software Inc., San Diego, USA).

Initially all the data were tested to determine if the results were normally distributed. Depending on the size of the population, either the Shapiro-Wilk (when $n < 50$) or Kolmogorov-Sirnov (when $n > 50$) statistical test was employed. Data were considered as normally distributed if $p \geq 0.05$.

Everywhere the data normally distributed, reported measures one-way or two-way analysis of variance (ANNOVA) between samples test was employed adopting a 5% level of significance. Post hoc testing was carrying out using the Tukey test or Bonferroni test for pairwise comparisons between means.

All data are represented as the mean \pm standard deviation (SD). Numbers of replicates (n) are shown in parentheses in figure legends where appropriate.

Chapter 3

Protection From Oxidative Stress

3.1 Introduction:

Oxidative stress has been associated with a wide range of diseases, such as cardiovascular (Diaz-Arrastia, 2000; Refsum *et al.*, 1998), Alzheimer's Disease (Clarke *et al.*, 1998; Miller, 1999), atherosclerosis, Parkinson's Disease (Blandini *et al.*, 2001; Duan *et al.*, 2002; Kuhn *et al.*, 1998; Yasui *et al.*, 2000) cancer (Jacobson *et al.*, 1996), and also plays a role in the ageing process (Jacobson, 1996). Hcy has been demonstrated to be an inducer of apoptosis in different cell types such as primary human bone marrow stromal cells and the HS-5 cell line (Duk *et al.*, 2006), H9C2 cardiomyocytes (Levrant *et al.*, 2007) and lymphocyte cells (Picerno *et al.*, 2006), (Mujumdar *et al.*, 2001; Zhang *et al.*, 2001). The trigger of apoptosis by Hcy was associated with activation of caspase-3, caspase-9 and release of cytochrome c, (Liu *et al.*, 2005; Obeid & Herrmann 2006; Duk *et al.*, 2006). Low concentrations of H₂O₂ have been reported to induce apoptosis and high concentrations induce necrosis (Jacobson, 1996; Wolj, 1994; Vanags *et al.*, 1996). The induction of apoptosis induced by H₂O₂ is associated with caspase-9 and caspase-3 activation and with phosphotidylserine appearance on the surface of the cells (Saito *et al.*, 2006; Hampton & Orrenius, 1997).

Several ways have been suggested to reduce the lethal effects of oxidative stress, including reduction of oxidative agents and maintenance of trans-methylation pathways (Szeto & Benzie, 2002). Hyperhomocysteinemia is associated with folate and cobalamin deficiency results in high levels of apoptotic cells (Selhub *et al.*, 2000; Mattson & Shea, 2003). Folate is a methyl donor in one-carbon metabolism, which helps to promote the remethylation of Hcy (Lucock *et al.*, 1996), while cobalamin acts as a methionine synthase cofactor (Refsum, 2001). Therefore therapy with folate and cobalamin can reduce hyperhomocysteinemia by significant inhibition of caspase cleaved (Zhang *et al.*, 2008). Moreover, *In vivo* and *in vitro*, studies have demonstrated that supplementation with folate has a significant effect on reducing apoptotic and necrotic cells (Chambers *et al.*, 1999; Vermeulen *et al.*, 2000; Woo *et al.*, 1999; Fenech, 1999), and reduced Hcy in the blood of hyperhomocysteinemic patients (B-Vitamin Treatment Trialists', 2006; Rosenberg, 2007; Kazerooni *et al.*,

2008; Nagaraja *et al.*, 2008). However there are limited studies investigating whether cobalamin has a protection role against oxidative stress.

In this chapter the aim is to investigate mechanisms of cells death under oxidative stress and the impact of folate and cobalamin on cell death induced by oxidative stress. Different cell models will be used: initially an endothelial cell line - sk-hep-1 (known to be highly sensitive to oxidative stress), a T-cell lymphoma cell line – Jurkat; and primary leukocytes from healthy volunteers (non-smoker, clear from any infection and no alcohol consumed).

3.2 Methods

All preparations and cell culture experiments were carried out within a class II tissue culture hood.

3.2.1 Sk-hep1 cells preparation:

Cells were passed every 3 days as described in (section 2.4.1).

3.2.2 Jurkat cells preparation:

Cells were passed every 3 days as described in (section 2.4.2).

3.2.3 Leukocyte cells preparation:

Blood was taken from healthy volunteers (section 2.4.4), and leukocyte cells were isolated as described in (section 2.4.5). Cells were then transferred to 12 or 24 well plates and treated under test conditions.

3.2.4 Determine cell viability

Cells were plated on to a black 96 well cell plate and treated under test conditions then cell viability measured by MTS assay as described in (section 2.4.9).

3.2.5 Determination of apoptosis

Cells were plated on to a black 96 well cell plate and treated under test conditions then analysed for apoptosis by caspase-3/7 detection (section 2.4.9).

3.2.6 Determination of necrosis:

Cells were plated on to a black 96 well cell plate and treated under test conditions then analysed for apoptosis by caspase-3/7 detection (section 2.4.11).

3.2.7 Cells count and viability test by trypan blue exclusion:

Upon treatment finished, cells were re-suspended in to the media by pipetting. Cells were then counted and assessed by trypan blue exclusion (section 2.4.6)

3.2.8 Caspase-3 activity *via* flow cytometry

Cells were treated under test condition and processed as described in (section 2.4.10)

3.2.9 Annexin-V and PI

Cells were treated under test condition and then processed for annexin-V and PI analysis as described in (section 2.4.12)

3.3 Results

3.3.1 Induction of apoptosis and necrosis in Sk-hep1cells via exposure to Hydrogen peroxide and Homocysteine.

In order to investigate the mode of Sk-hep1 cell death, cells were incubated with a range of H₂O₂ and Hcy concentrations for 2 hours. Cell viability reduced significantly with increasing concentrations (0-50μM H₂O₂ or Hcy) ($p < 0.001$, as determined by ANOVA) (Figures 3.1 & 3.2). Upon further analysis, Tukey pairwise testing showed significant reduction in cells viability and reached less than 20% ($P < 0.001$) at 25μM H₂O₂ and 10% ($P < 0.001$) at 25μM Hcy as compared to the basal values (control – state what the controls where here).

Control cells had no detectable caspase-3 activity. However, the H₂O₂ or Hcy have a significant effect on caspase-3 ($p < 0.001$, as determined by ANOVA) (Figures 3.3 & 3.4). And Tukey pairwise testing showed at low concentrations such at 1.325 of H₂O₂ or Hcy caspase-3 activity increased significantly to peak at 3.125μM H₂O₂ or Hcy ($P < 0.001$), after which activity declined.

There was a significant effect on necrosis activity induced by H₂O₂ and Hcy ($p < 0.001$, as determined by ANOVA) (Figures 3.5 & 3.6). Post-hoc pairwise comparison showed at concentrations above 6.25μM H₂O₂ ($P < 0.001$) or 6.25μM Hcy ($P < 0.001$) that there was a significant increase in necrosis as indicated by PI. Also higher concentration such at 50μM H₂O₂ or Hcy resulted in 100% necrosis ($P < 0.001$) as compared to control cells.

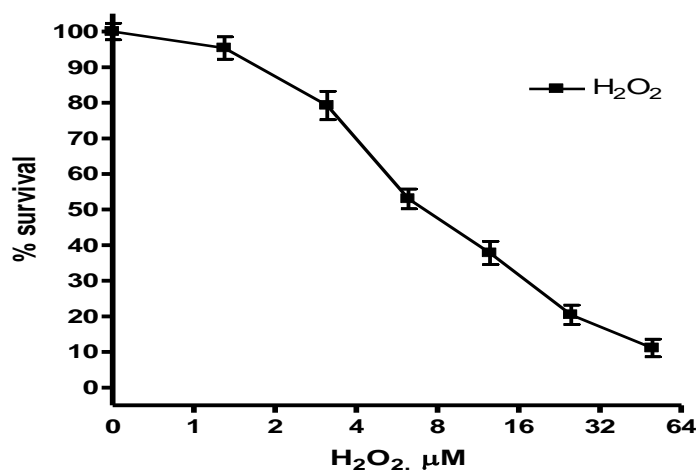


Figure 3.1: Effect of oxidative stress on viability of sk-hep1 cells. Cells were treated with a range of H₂O₂ (0-50μM) for 2 hours, control cells are non-treated cells. Cell viability was determined by MTS® assay at 490nm. Data are means ± SD n=3, p< 0.001 as determined by one-way ANOVA. Baseline (control) vs 3.125μM (p<0.001), 6.25 μM (p<0.001), 12.5 μM (p<0.001), 25 μM (p<0.001) and 50 μM (p<0.001) as determined by Tukey *post hoc*.

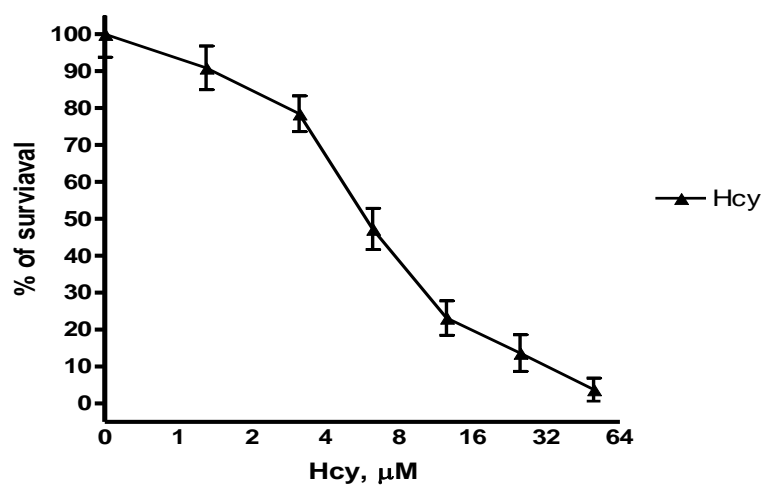


Figure 3.2: Effect of Hcy on viability of sk-hep1 cells. Cells were treated with a range of Hcy (0-50μM) for 2 hours, control cells are non-treated cells. Cell viability was determined by MTS® assay. Data are means ± SD n=3, p< 0.001 as determined by one-way ANOVA. Baseline (control) vs 3.125μM (p<0.001), 6.25 μM (p<0.001), 12.5 μM (p<0.001), 25 μM (p<0.001) and 50 μM (p<0.001) as determined by Tukey *post hoc*.

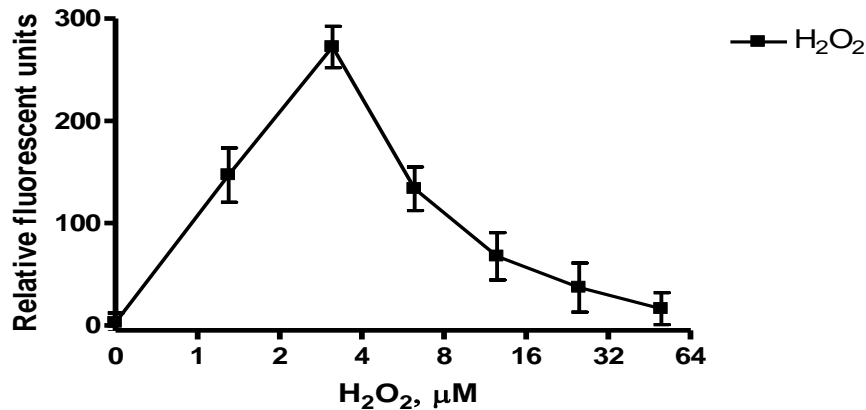


Figure 3.3: Effect of Hydrogen peroxide on caspase-3 level in Sk-Hep1. Cells were treated with a range of H₂O₂ concentrations (0-50μM) for 2 hours. Control cells are non-treated cells. Caspase-3 measured at EX=496nm/EM=520nm. Data are means ± SD n=3, p< 0.001 as determined by one-way ANOVA. Baseline (control) vs 1.325 (p<0.001), 3.125μM (p<0.001), 6.25 μM (p<0.001), 12.5 μM (p<0.001), as determined by Tukey *post hoc*.

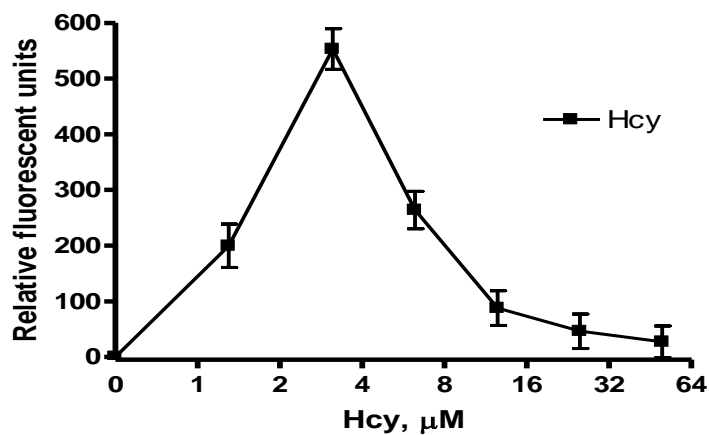


Figure 3.4: Effect of Hcy on caspase-3 level in Sk-Hep1. Cells were treated with a range of concentrations of H₂O₂ (0-50μM) for 2 hours, control cells were non-treated cells. Caspase-3 measured at EX=496nm/EM=520nm. Data are means ± SD n=3, p< 0.001 as determined by one-way ANOVA. Baseline (control) vs 1.325 (p<0.001), 3.125μM (p<0.001), 6.25 μM (p<0.001), 12.5 μM (p<0.001), as determined by Tukey *post hoc*.

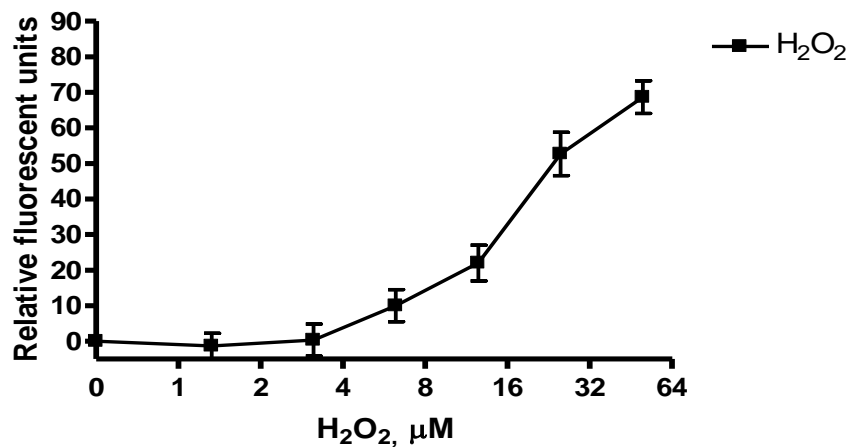


Figure 3.5: Induction of necrosis in Sk-Hep1 by H₂O₂. Cells were treated with a range of H₂O₂ concentrations (0-50μM) for 2 hours, control cells were non-treated cells. Necrosis measured at EX=535/EM=617. Data are means ± SD n=3, p< 0.001 as determined by one-way ANOVA. Baseline (control) vs 6.25 μM (p<0.001), 12.5 μM (p<0.001), 25 μM (p<0.001), and 50 μM (p<0.001) as determined by Tukey *post hoc*.

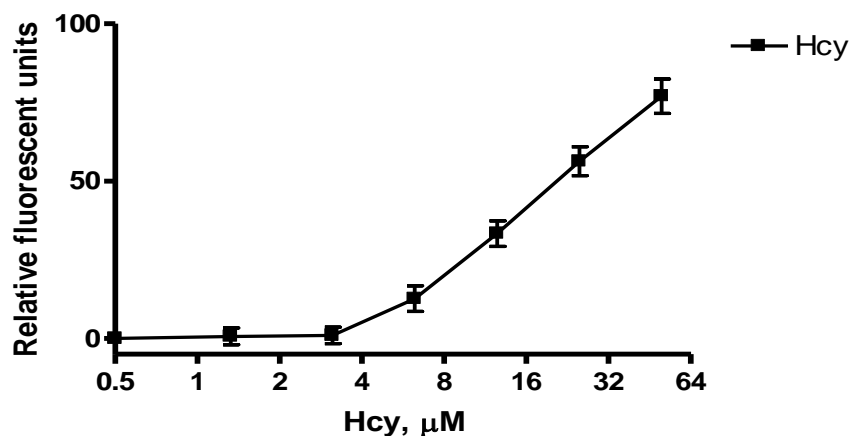


Figure 3.6: Induction of necrosis in Sk-Hep1 Hcy. Cells were treated with a range of Hcy concentrations (0-50μM) for 2 hours. Control cells: were non-treated cells. Necrosis measured at EX=535/EM=617. Data are means ± SD n=3, p< 0.001 as determined by one-way ANOVA. Baseline (control) vs 6.25 μM (p<0.001), 12.5 μM (p<0.001), 25 μM (p<0.001), and 50 μM (p<0.001) as determined by Tukey *post hoc*.

3.3.2 Folate and Cobalamin protect cells (SK-hep1) from apoptosis and necrosis induced by oxidative stress:

3.3.2.1 Folate protects cells (Sk-hep1) from apoptosis and necrosis induced by oxidative stress:

After determining the concentrations required of H_2O_2 or Hcy to induce apoptosis and necrosis in sk-hep1 cells, the effect of folate on cell death induced by oxidative stress was investigated. Cells were subjected to a range of folate concentrations (0-100 μM) for 2 hours, none of which caused significant caspase-3 activity detected as compared to control cells (non-treated) ($P > 0.05$, as determined by one-way ANOVA) (Figure 3.7). Also there was no significant necrosis activity observed with folate treated cells compared to control cells ($P > 0.05$, as determined by one-way ANOVA) (Figure 3.8).

Pre-incubation of cells with 30 μM folate for 2 hours followed by 2 hours incubation with a range of H_2O_2 or Hcy (0-50 μM) has showed significant effect ($P < 0.001$, as determined by Two-way ANNOVA) (Figures 3.9 & 3.10). Further analysis with Bonferroni pairwise resulted in significant increases in cell viability at $\geq 3.125\mu\text{M}$ H_2O_2 or Hcy ($P < 0.001$), and cells viability reached more than 60% ($P < 0.001$) and 55% ($P < 0.001$) at 50 μM H_2O_2 or Hcy respectively as compared to control cells (non-treated). Folate pre-treatment provided a significant protection against oxidative stress induced apoptosis ($P < 0.001$, as determined by Two-way ANNOVA) (Figures 3.11 & 3.12). Furthermore, analysis with Bonferroni pairwise showed a significant reduction in the caspase-3 activity at low concentrations of H_2O_2 or Hcy ($P < 0.001$). Caspase-3 reduced by 62% ($P < 0.001$) and 63% ($P < 0.001$) at 3.125 μM H_2O_2 or Hcy respectively with pre-incubation of folate compared to cells treated with H_2O_2 or Hcy alone. Additionally, folate treatment provides a significant protection against necrosis induced by H_2O_2 or Hcy ($P < 0.001$, as determined by Two-way ANNOVA) (Figures 3.13 & 3.14). The analysis with Bonferroni pairwise showed significant induction of caspase by 6.25 μM H_2O_2 or Hcy ($P < 0.001$), after which necrosis activity declined by 61% ($P < 0.001$) and 65% ($P < 0.001$) at 25 μM H_2O_2 or Hcy compared to H_2O_2 or Hcy alone.

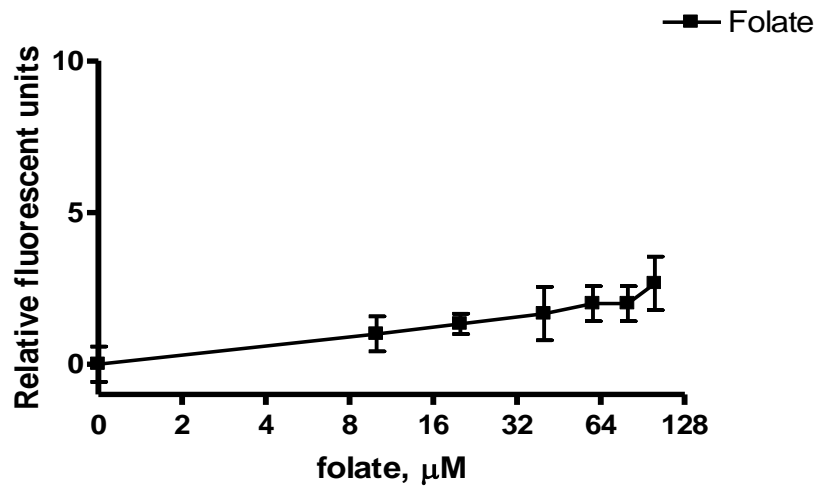


Figure 3.7: Effect of folate on caspase-3 in Sk-hep1 cells. Cells were pre-incubated with a range of folate concentrations (0-100 μM) for 2 hours, control cells were non-treated cells. Caspase-3 measured at EX=496nm/EM=520nm. The data presents are means \pm SD n=3. $p > 0.05$ as determined by one-way ANOVA.

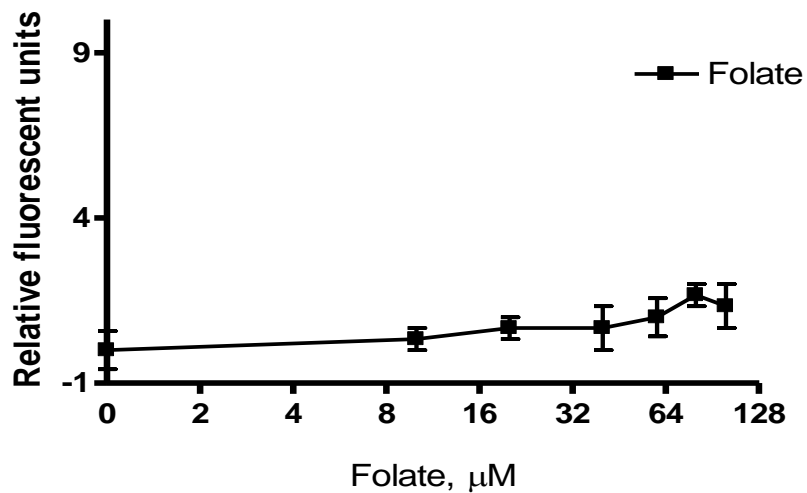


Figure 3.8: Effect of folate on necrosis activity in Sk-hep1 cells. Cells were pre-incubated with a range of folate concentrations (0-100 μM) for 2 hours, control cells were non-treated cells. Necrosis measured at EX=535/EM=617. The data presents are means \pm SD n=3. $p > 0.05$ as determined by one-way ANOVA.

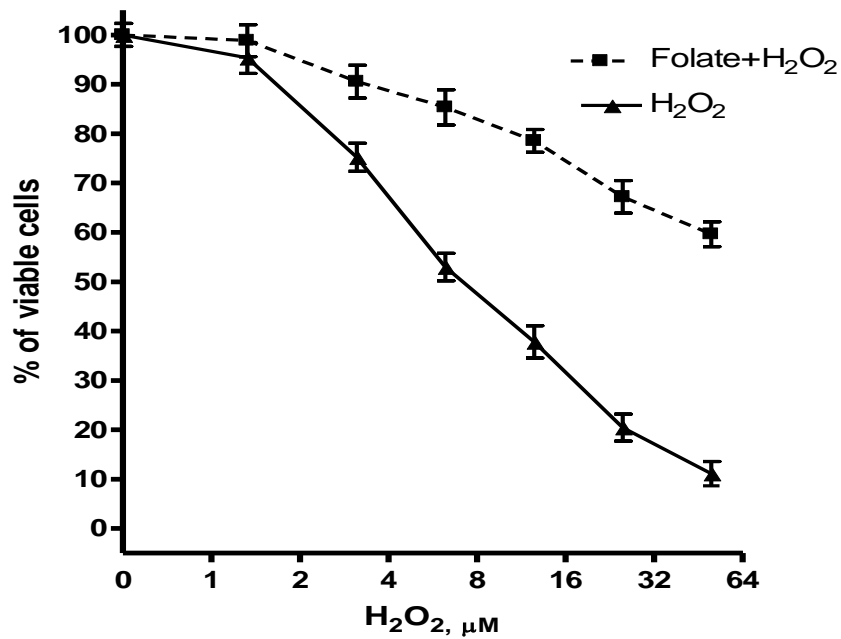


Figure 3.9: Effect of folate pre-treatment on Sk-Hep1 cells surviving oxidative stress.

Cells were pre-incubated with 30μM folate for 2 hours followed by treatment with a range of H₂O₂ concentrations for 2 hours and control; cells were treated with a range of H₂O₂ concentrations (0-50μM) for 2 hours. Cell viability was determined by MTS® assay at 490nm. Data are means ± SD n=3, p< 0.001 as determined by two-way ANOVA. H₂O₂ (control) vs 3.125μM (p<0.001), 6.25 μM (p<0.001), 12.5 μM (p<0.001), 25 μM (p<0.001), 50 μM (p<0.001), as determined by Bonferroni *post hoc*.

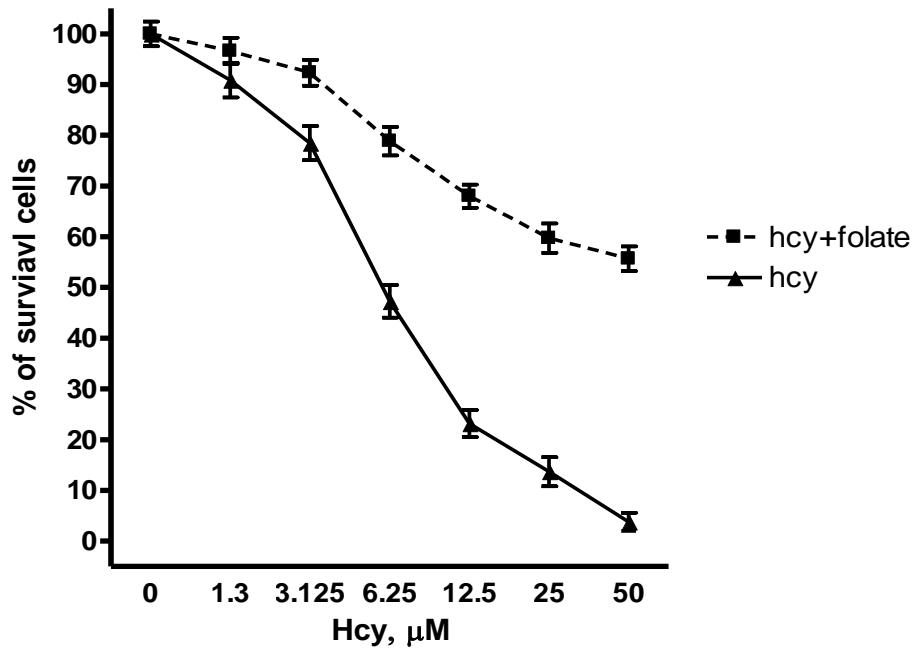


Figure 3.10: Effect of folate pre-treatment on Sk-Hep1 cells surviving oxidative stress.

Cells were pre-incubated with 30 μM folate for 2 hours. Followed by treatments with a range of Hcy concentrations for 2 hours and control cells were treated with a range of Hcy concentrations (0-50 μM) for 2 hours. Cell viability was determined by MTS® assay at 490nm. Data are means \pm SD $n=3$, $p < 0.001$ as determined by two-way ANOVA. Hcy (control) vs 3.125 μM ($p < 0.001$), 6.25 μM ($p < 0.001$), 12.5 μM ($p < 0.001$), 25 μM ($p < 0.001$), 50 μM ($p < 0.001$), as determined by Bonferroni *post hoc*.

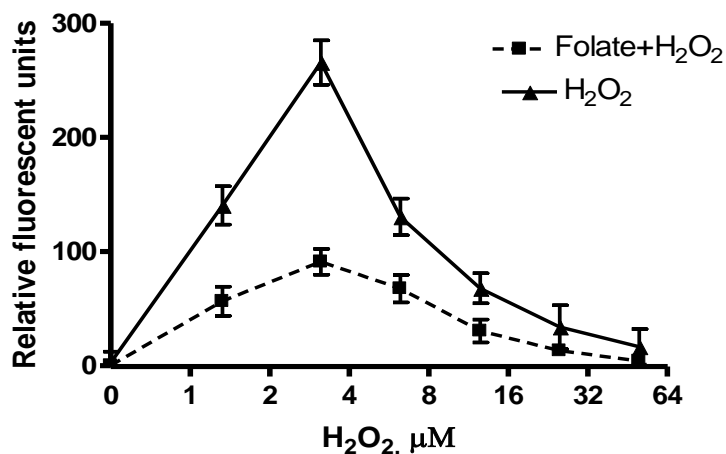


Figure 3.11: The effect of folate pre-treatment on the caspase-3 activity. Sk-hep1 cells were pre-incubated with 30μM folate for 2 hours and then treated with a range of H₂O₂ concentrations for 2hours. The control cells were treated with H₂O₂ only. Caspase-3 measured at EX=496nm/EM=520nm. Data are means ± SD n=3, p< 0.001 as determined by two-way ANOVA. H₂O₂ (control) vs 1.325 μM (p<0.001), 3.125μM (p<0.001), 6.25 μM (p<0.001), as determined by Bonferroni *post hoc*.

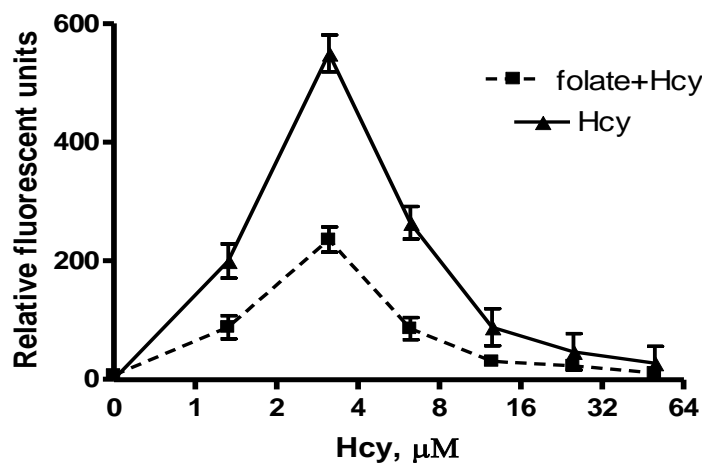


Figure 3.12: The effect of folate pre-treatment on the caspase-3 activity. Sk-hep1 cells were pre-incubated with 30μM folate for 2 hours and then treated with a range of Hcy concentrations for 2hours. The control cells were treated with Hcy alone. Caspase-3 measured at EX=496nm/EM=520nm. Data are means ± SD n=3, p< 0.001 as determined by two-way ANOVA. Hcy (control) vs 1.325 μM (p<0.001), 3.125μM (p<0.001), 6.25 μM (p<0.001), as determined by Bonferroni *post hoc*.

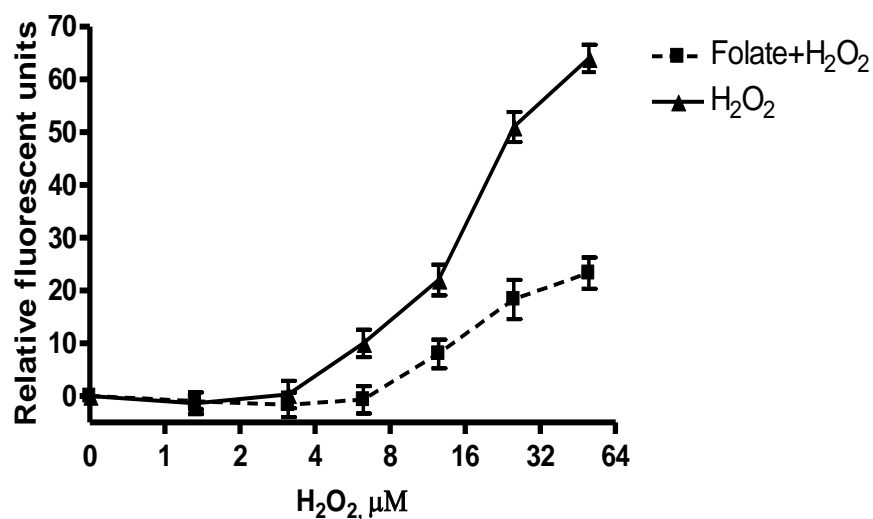


Figure 3.13: Effect of folate pre-treatment on necrosis induction in Sk-hep1. Cells were pre-incubated with 30μM folate for 2 hours and then treated with a range of concentrations of H₂O₂ for 2 hours. The control cells were treated with H₂O₂ alone. Necrosis measured at EX=535/EM=617. Data are means ± SD n=3, p< 0.001 as determined by two-way ANOVA. H₂O₂ (control) vs 6.25μM (p<0.05), 12μM (p<0.01), 25μM (p<0.001), 50μM (p<0.001) as determined by Bonferroni *post hoc*

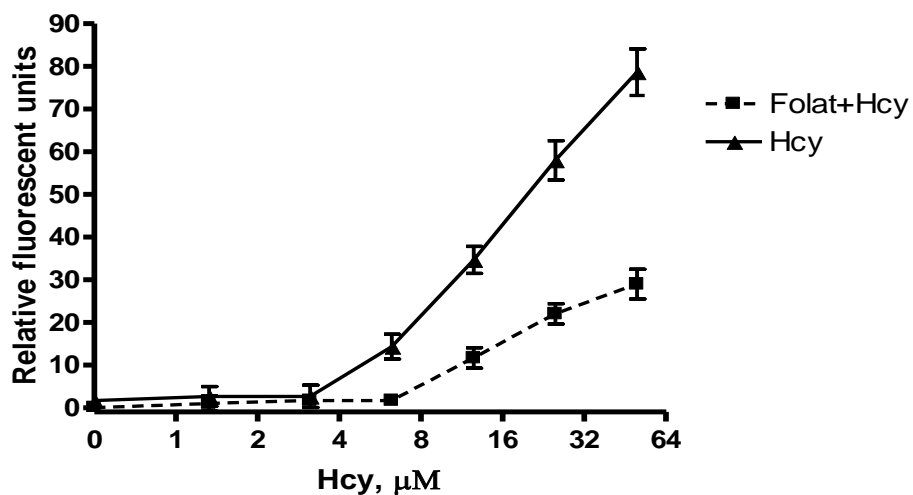


Figure 3.14: Effect of folate pre-treatment on necrosis induction in Sk-hep1. Cells were pre-incubated with 30μM folate for 2 hours and then treated with a range of concentrations of Hcy for 2 hours. The control cells were treated with H₂O₂ alone. Necrosis measured at EX=535/EM=617. Data are means ± SD n=3, p< 0.001 as determined by two-way ANOVA. Hcy (control) vs 6.25μM (p<0.05), 12μM (p<0.001), 25μM (p<0.001), 50μM (p<0.001) as determined by Bonferroni *post hoc*.

3.3.2.2 Cobalamin protects cells (Sk-hep1) from apoptosis and necrosis induced by oxidative stress:

Cobalamin had no significant effect on neither caspase-3 nor necrosis activity in sk-hep1 cells when they were treated with a range of cobalamin concentrations (0-100 μ M) for 2 hours, when compared to the control cells ($P > 0.05$, as determined by one-way ANOVA), (Figures 3.15 & 3.16).

In order to optimize concentration required for optimum cell protection from apoptosis, Cells were subjected to a range of cobalamin concentrations for 2 hours prior treatment with 3.125 μ M H₂O₂ or Hcy for further 2 hours: which previously had been shown to induce apoptosis in sk-hep1 cells. This treatment resulted in a significant reduction in caspase-3 as compared to H₂O₂ or Hcy only (control) ($P < 0.001$, as determined by two-way ANNOVA) (Figure 3.17). Further analysis by Bonferroni pairwise showed a significant reduction of caspase-3 at low concentration of cobalamin (1.325 μ M $P < 0.01$, 3.125 μ M $P < 0.001$, 6.25 μ M $P < 0.001$, 12.5 μ M $P < 0.001$), and there was a further reduction in caspase-3 up to 70% at $\geq 25\mu$ M cobalamin compared to H₂O₂ or Hcy treated cells ($P < 0.001$). There was no further increase in protection provided by higher concentrations; therefore 25 μ M cobalamin was an appropriate concentration to be applied to all oxidative stress protection studies. SK-hep1 cells pre-incubated with 25 μ M cobalamin for 2 hours followed by 2 hours incubation with a range of H₂O₂ or Hcy concentrations (0-50 μ M) resulted in significant effect on caspase-3 ($P < 0.001$, as determined by two-way ANNOVA) (Figures 3.18 & 3.19). Post-hoc pairwise comparisons showed caspase-3 was less than 30% ($P < 0.001$) and 28% ($P < 0.001$) at 3.125 μ M H₂O₂ and Hcy respectively, followed by significant decline of caspase-3 activity at $\geq 12.5\mu$ M H₂O₂ or Hcy as compared to control cells (H₂O₂ or Hcy alone) . At the same time cobalamin treatment provides a significant protection against necrosis ($P < 0.001$, as determined by two-way ANNOVA) (Figures 3.20 & 3.21). And Bonferroni pairwise showed at $\geq 6.25\mu$ M H₂O₂ and Hcy ($P < 0.001$), necrosis decreased up to 40% and 45% at 50 μ M H₂O₂ and Hcy with pre-incubation of cobalamin compared to H₂O₂ and Hcy alone ($P < 0.001$).

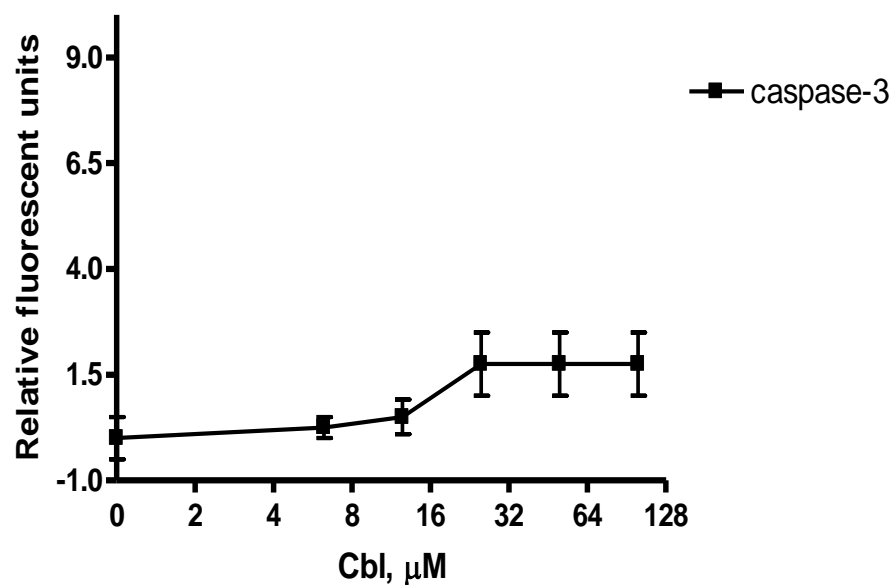


Figure 3.15: Effect of cobalamin on caspase-3 in Sk-hep1 cells. Cells were pre-incubated with a range of cobalamin concentrations (0-100 μM) for 2 hours, control cells were non-treated. Caspase-3 measured at EX=496nm/EM=520nm. The data presents are means \pm SD n=3. $p > 0.05$ as determined by one-way ANOVA.

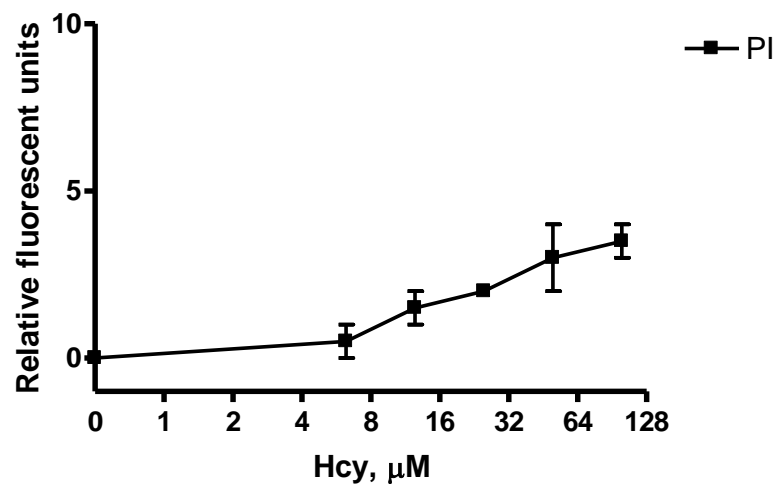
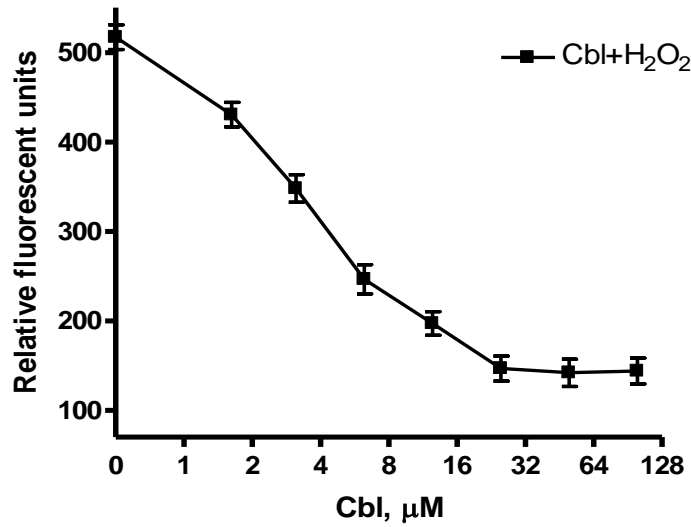


Figure 3.16: Effect of cobalamin on caspase-3 in Sk-hep1 cells. Cells were pre-incubated with a range of cobalamin concentrations (0-100 μM) for 2 hours, control cells were non-treated. Caspase-3 measured at EX=496nm/EM=520nm. The data presents are means \pm SD n=3. $p > 0.05$ as determined by one-way ANOVA.

A.



B.

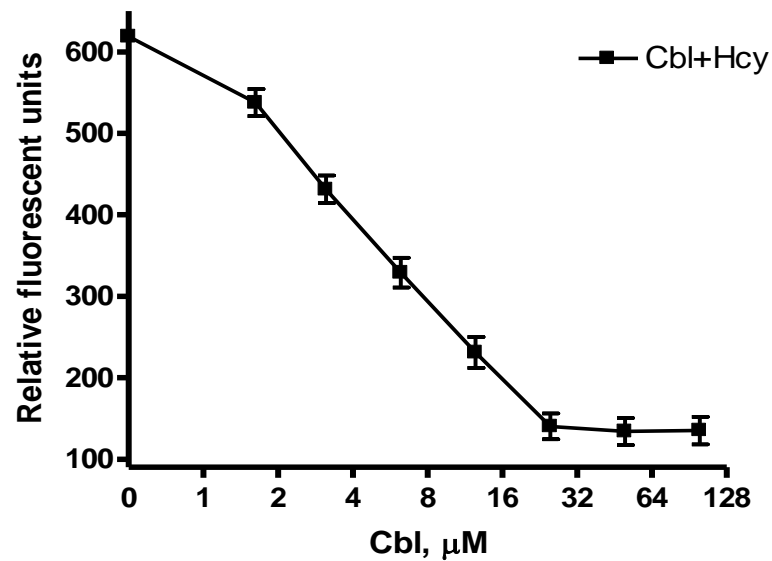


Figure 3.17: Primary study of cobalamin apoptosis protection. Sk-hep1 cells were pre-incubated with a range of cobalamin concentrations (0-100 μM) for 2 hours, followed by treatments with **A.** 3.125 μM H_2O_2 or **B.** 3.125 μM Hcy for further 2 hours. Caspase-3 measured at EX=496nm/EM=520nm. Data are means \pm SD n=3, $p < 0.001$ as determined by one-way ANOVA. H_2O_2 or Hcy, (control) vs 1.325 μM ($p < 0.001$), 3.125 μM ($p < 0.001$), 6.25 μM ($p < 0.001$), 12.5 μM ($p < 0.001$), 25 μM ($p < 0.001$), 50 μM ($p < 0.001$), 100 μM ($p < 0.001$), as determined by Tukey *post hoc*.

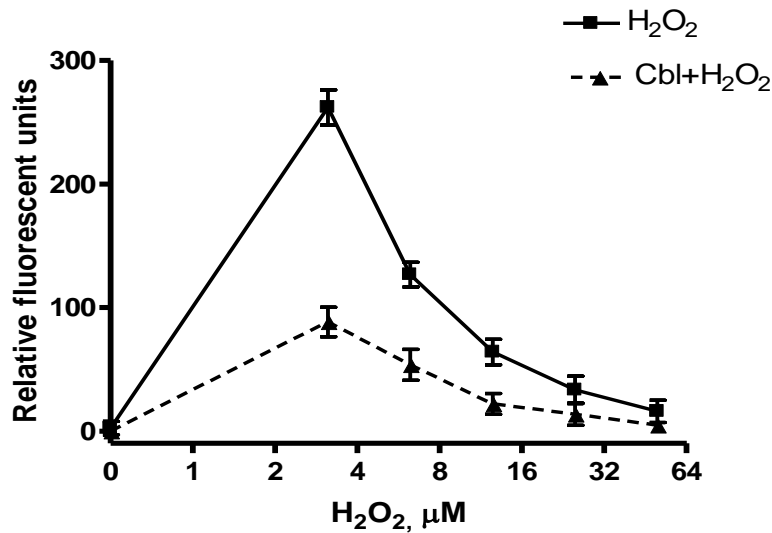


Figure 3.18: The effect of cobalamin on the caspase-3 activity induced by H₂O₂. Sk-hep1 cells were pre-incubated with 25μM cobalamin for 2 hours and treated with a range of H₂O₂ concentrations for 2 hours and control cells were treated with H₂O₂ alone; Caspase-3 measured at EX=496nm/EM=520nm. Data are means ± SD n=3, p< 0.001 as determined by two-way ANOVA. H₂O₂ (control) vs 3.125μM (p<0.001), 6.25 μM (p<0.001), 12.5 μM (p<0.05) as determined by Bonferroni *post hoc*.

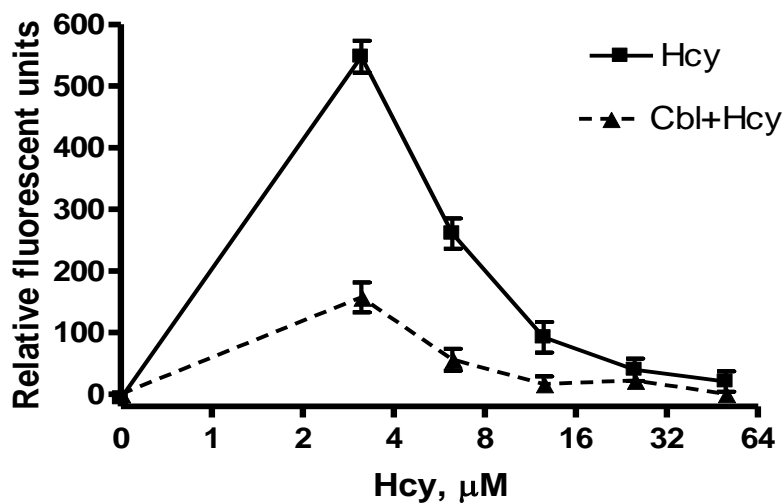


Figure 3.19: The effect of cobalamin pre-treatment on the caspase-3 activity. Sk-hep1 cells were pre-incubated with 25μM cobalamin for 2 hours and treated with a range of Hcy concentrations for 2 hours and control cells were treated with Hcy alone, Caspase-3 measured at EX=496nm/EM=520nm. Data are means ± SD n=3, p< 0.001 as determined by two-way ANOVA. Hcy (control) vs 3.125μM (p<0.001), 6.25 μM (p<0.001), 12.5 μM (p<0.05) as determined by Bonferroni *post hoc*.

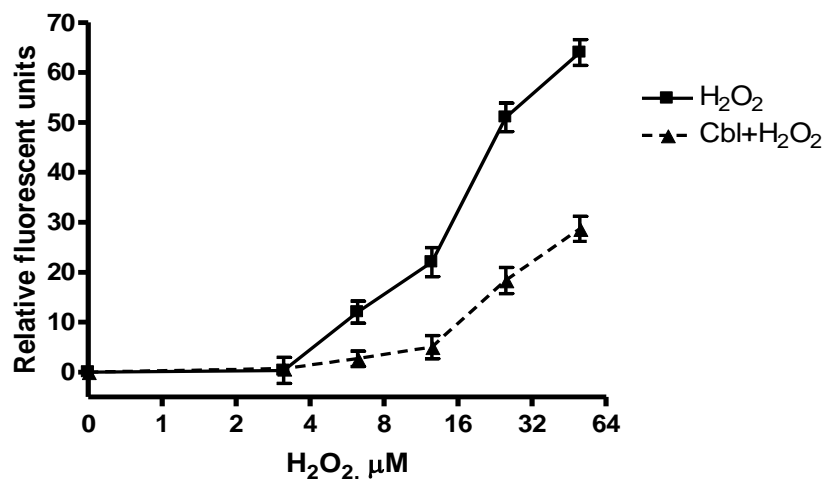


Figure 3.20: The effect of cobalamin pre-treatment on necrosis activity. Sk-hep1 cells were pre-incubated with 25μM cobalamin for 2 hours and treated with a range of H₂O₂ concentrations for 2 hours and control cells were treated with H₂O₂ alone. Necrosis measured at EX=535/EM=617. Data are means ± SD n=3, p< 0.001 as determined by two-way ANOVA. Hcy (control) vs 6.25μM (p<0.05), 12.5 μM (p<0.001) 25μM (p<0.001), 50μM (p<0.001) as determined by Bonferroni *post hoc*.

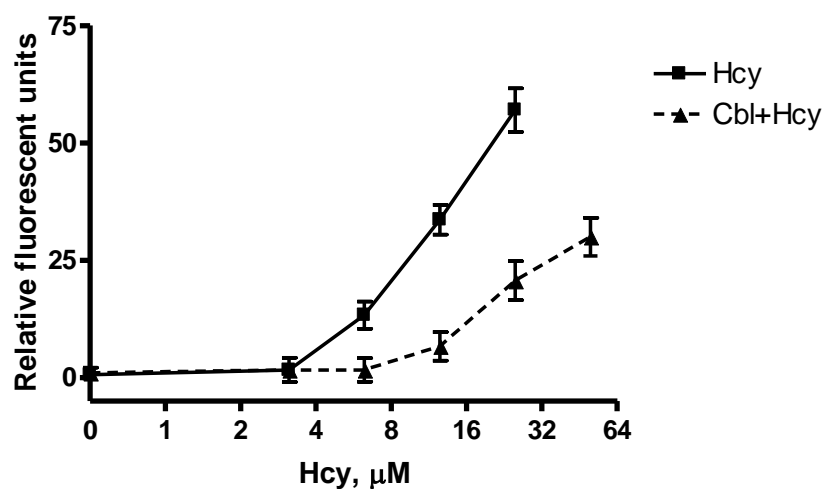


Figure 3.21: The effect of cobalamin pre-treatment on necrosis activity. Sk-hep1 cells were pre-incubated with 25μM cobalamin for 2 hours and treated with a range of Hcy concentrations for 2 hours and control cells were treated with Hcy alone. Necrosis measured at EX=535/EM=617. Data are means ± SD n=3, p< 0.001 as determined by two-way ANOVA. Hcy (control) vs 6.25μM (p<0.05), 12.5 μM (p<0.001) 25μM (p<0.001), 50μM (p<0.001) as determined by Bonferroni *post hoc*.

3.3.2.3 ROS and cobalamin apoptosis protection:

3.3.2.3.1 Measurement of mitochondrial membrane potential ($\Delta\Psi$) (ROS generation).

The measurement of intracellular ROS was achieved by the use of fluorescence redox active probe 2', 7'-dichlorofluorescein-diacetate (DCFH-DA). Intracellular levels of ROS generation were determined using the non-fluorescence probe 2', 7'-dichlorofluorescein-diacetate group. The action of intracellular esterases results in the release of dichlorofluorescein, which on exposure to ROS, is oxidised to fluorescence probe dichlorofluorescein, allowing for quantification. The intensity of fluorescence was measured at Ex=485/Em=530nm using a 37°C pre-warmed fluorescence microplate reader.

The treatment with Cbl, Hcy and Cbl+Hcy had a significant effect on the fluorescence intensity of DCFH-AC ($P<0.001$, as determined by on-way ANNOVA), (Figure 3.22). ($P<0.001$, as determined by one-way ANNOVA), Post-hoc pairwise comparisons showed cells were subjected to Hcy had a significant increase in the ROS production ($P<0.001$) compared to control (non-treated) and when cells were pre-treated with cobalamin and then were further treated with Hcy, there was a significant reduction in the ROS production compared to Hcy alone ($P<0.001$). Cobalamin alone had no significant effect on ROS production above control cells ($P>0.05$)

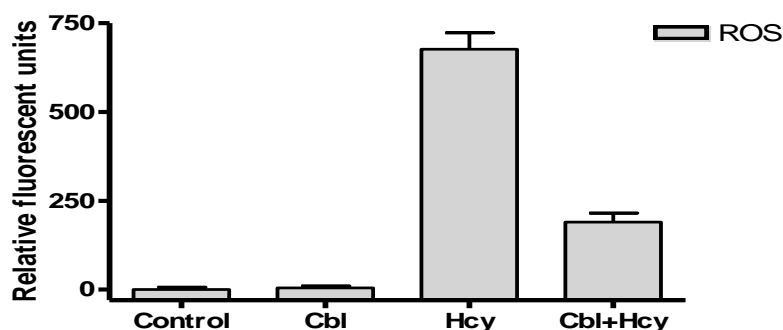


Figure 3.22: Effect of cobalamin on generation of reactive oxygen species. Sk-hep1 cells were pre-incubated in black 96-well plate with 10mM DCFH-diacetate, then 25 μ M Cbl for 2 hours followed by 2 hours treatments with 3.125 μ M Hcy, control cells were non-treated and then all cells solubilised in 0.1N NaOH. DCFH-DA activity was measured at EX=485/EM=530nm following incubation Data are means \pm SD n=3, $p<0.001$ as determined by two-way ANOVA. Hcy vs Cbl+Hcy ($p<0.001$) Tukey *post hoc*.

3.3.2.3.2 Measurement of superoxide under oxidative stress and anti oxidative stress conditions:

Generation of O_2^- production was demonstrated by measurement of the chemiluminescence of Lucigenin at 550nm using a 37°C pre-warmed fluorescence microplate reader. The treatment with Cbl, Hcy and Cbl+Hcy had a significant effect on the O_2^- generation ($P<0.001$, as determined by one-way ANNOVA), (Figure 3.23). Further analysis with Tukey pairwise showed cells exposed to 3.125 μ M Hcy had a significant increase of O_2^- generation compared to control cells ($P<0.001$). In contrast cells which were subjected to 25 μ M cobalamin prior 3.1.25 μ M Hcy showed a significant reduction in the O_2^- generation compared to Hcy alone ($P<0.001$), while there was no detectable difference in O_2^- generation in cobalamin alone treatment compared to control cells (non-treated) ($P>0.05$).

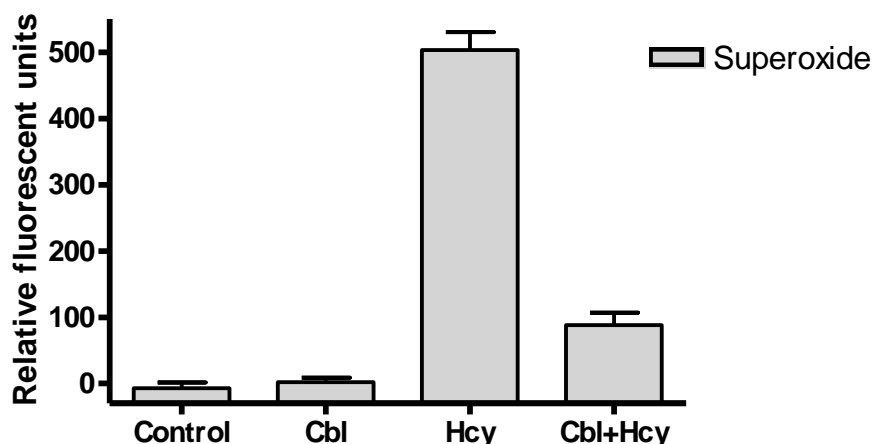


Figure 3.23: Effect of cobalamin on the superoxide generation. Sk-hep1 cells were pre-treated in 96-well plate with Lucigenin (5 μ M), and then treated with 25 μ M cobalamin for 2 hours followed by 2hours treatments with 3.125 μ M Hcy. Lucigenin chemiluminescence was measured at 550nm following incubation. Data presented are \pm SEM $n=4$. $P>0.05$, *** $p<0.001$, one-way ANOVA, Tukey *post hoc*.

3.3.3 Induction apoptosis and necrosis in Jurkat cells *via* Hydrogen peroxide and Homocysteine.

The mode of Jurkat cell death was investigated to determine if apoptosis or necrosis was being initiated by H₂O₂ or Hcy. In order to examine caspase-3 activity under oxidative stress, Jurkat cells were subjected to range of H₂O₂ and Hcy concentrations in a time-dependant study.

In Figures 3.24 & 3.25, cells were exposed to a range of H₂O₂ concentrations for different times showed a significant effect on caspase-3 and necrosis activity ($P < 0.001$, as determined by two-way ANNOVA). The Bonferroni pairwise analysis showed control vs 2 hours incubation at 0-10mM H₂O₂ had no significant effect on caspase-3 activity ($P > 0.05$). While there was a significant increase of caspase-3 activity at low concentrations (0.001mM, $P < 0.001$) with 4 hours incubation to peak at 0.01mM H₂O₂ ($P < 0.001$), after which activity declined such that at ≥ 1 mM H₂O₂ showed no detectable caspase-3 activity ($P > 0.05$). However, after 6 hour caspase-3 activity was elevated significantly at low concentrations (0.001mM, $P < 0.001$) to peak at 0.01mM H₂O₂ ($P < 0.001$) compared to 2 hour and 4 hour treatments, after which activity decreased significantly. At 1mM H₂O₂ cells had no caspase-3 activity detected compared to control cells ($P > 0.05$). Control cells had no significant caspase-3 activity ($P > 0.05$).

On the other hand, the post-hoc comparison showed no significant necrosis activity after 2 hours incubation as compared to control ($P > 0.05$). However, after 4 hours, necrosis significantly increased at ≥ 0.1 mM H₂O₂ ($P < 0.001$) and treatment with 10mM H₂O₂ showed significant increase of necrosis which reached 100% (Figure 3.25). Furthermore, exposing cells to a range of H₂O₂ concentrations for 6 hours, resulted in a significant increase in necrosis activity at ≥ 0.1 mM H₂O₂ ($P < 0.001$), and there was a significant difference at 10mM H₂O₂ in necrosis

activity compared to 2 and 4 hours treatments ($P < 0.001$), although control cells showed no necrosis activity.

Jurkat cells were then treated with a range of Hcy concentrations (0-100 μ M) for 3 and 6 hours showed a significant effect on apoptosis and necrosis activity ($P < 0.001$, as determined by two-way ANNOVA) (Figure 3.26). The Bonferroni pairwise analysis resulted in; Caspase-3 activity significantly peaked at 3.125 μ M Hcy after 3 hours ($P < 0.001$), then activity declined with no significant activity of caspase-3 at $\geq 12.5\mu$ M Hcy ($P < 0.05$) However, after 6 hours treatments caspase-3 peaked at 3.125 μ M Hcy which were significantly different from the 3 hours treatments ($P < 0.001$), then activity decreased at $\geq 12.5\mu$ M Hcy with no significant activity detected ($P < 0.05$).

Moreover, the cells had significant necrosis activity at 12.5 μ M Hcy after 3 hours treatment ($P < 0.01$) followed by increasing necrosis activity by increasing concentrations such at 100 μ M Hcy 65% of the cells were necrotic. However, after 6 hours incubation, cells were significantly necrotic at $\geq 12.5\mu$ M Hcy ($P < 0.001$) compared to 3 hours treatment and reached 100% necrosis at 100 μ M Hcy (Figure 3.27).

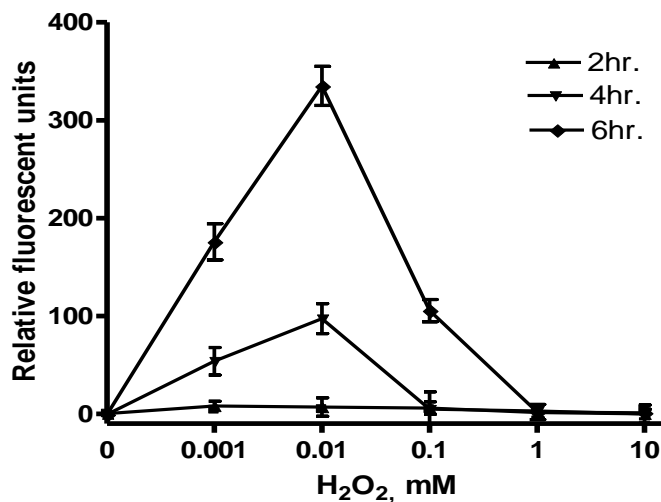


Figure 3.24: Time course study effect of H₂O₂ on caspase-3 activity in Jurkat cells. Cells were exposed to increasing concentrations of H₂O₂ (0-10mM) for 2, 4, and 6 hours, control were non-treated cells, caspase-3 measured after at EX=496/Em=520. Data are means \pm SD n=4, $p < 0.001$ as determined by two-way ANOVA. Baseline (control) vs 4h; 0.001mM ($p < 0.001$), 4h; 0.01mM, 6h; 0.001mM ($p < 0.001$), 6h; 0.01mM ($p < 0.001$), and 6h; 0.1mM ($p < 0.001$) as determined by Bonferroni *post hoc*.

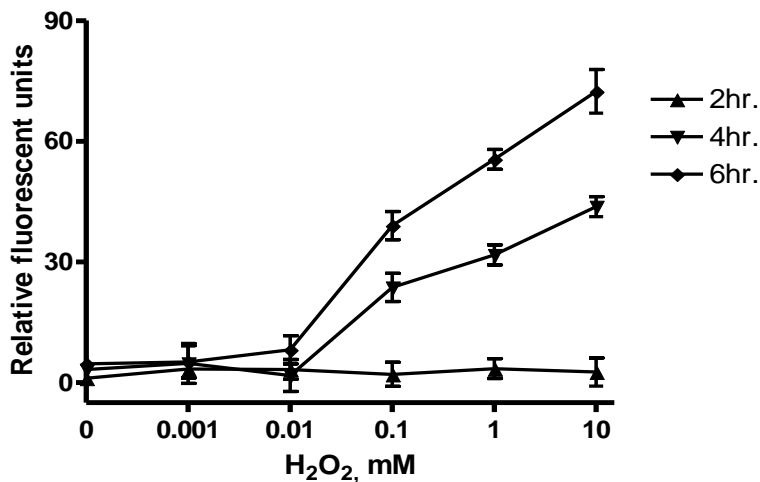


Figure 3.25: Time course study the effect of H₂O₂ on necrosis level of Jurkat cells. Cells were exposed to increasing concentrations of H₂O₂ (0-10mM) for 3, and 6 hours, control cells were non-treated. Followed by staining with PI which measured at EX=535/EM=617. Data are means \pm SD n=4, $p < 0.001$ as determined by two-way ANOVA. Baseline (control) vs 4h; 0.1mM, ($p < 0.001$), 4h; 1mM ($p < 0.001$), 4h; 10mM ($p < 0.001$), 6h; 0.1mM ($p < 0.001$), 6h; 1mM ($p < 0.001$), and 6h; 10mM ($p < 0.001$) as determined by Bonferroni *post hoc*.

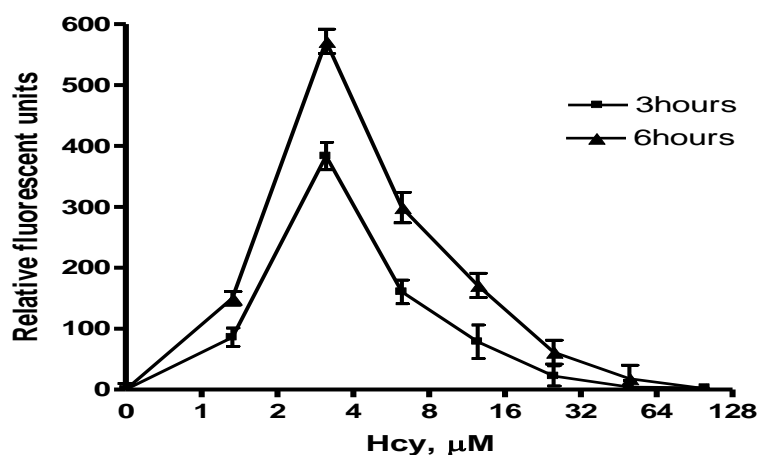


Figure 3.26: Time course study the effect of homocysteine on caspase-3 activity in Jurkat cells. Cells were exposed to increasing concentrations of Hcy (0-100 μM) for 3, and 6 hours, control cells were non-treated. Caspase-3 measured at Ex=496/Em=520. Data are means \pm SD n=4, $p < 0.001$ as determined by two-way ANOVA. Baseline (control) vs 3h; 1.325 μM ($p < 0.001$), 3h; 3.125 μM ($p < 0.001$), 3h; 6.25 μM ($p < 0.001$), 6h; 1.325 μM ($p < 0.001$), 6h; 3.125 μM ($p < 0.001$), 6h; 6.25 μM ($p < 0.001$) as determined by Bonferroni *post hoc*.

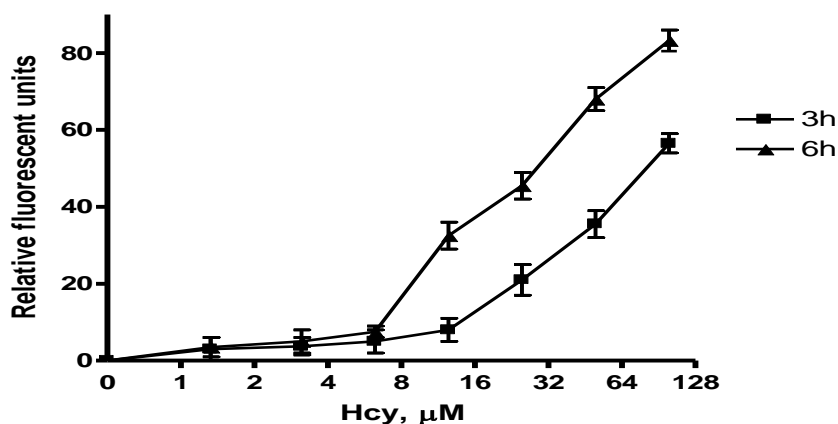


Figure 3.27: Time course study the effect of homocysteine on necrosis level of Jurkat cells. Cells were exposed to increasing concentrations of Hcy (0-100 μM) for 3, and 6 hours followed by PI staining measured at Ex=535/Em=617. Data are means \pm SD n=4, $p < 0.001$ as determined by two-way ANOVA. Baseline (control) vs 3h; 6.25 μM ($p < 0.001$), 3h; 12.5 μM ($p < 0.001$), 3h; 25 μM ($p < 0.001$), 50 μM ($p < 0.001$), 100 μM ($p < 0.001$), 6h; ; 6.25 μM ($p < 0.001$), 3h; 12.5 μM ($p < 0.001$), 3h; 25 μM ($p < 0.001$), 50 μM ($p < 0.001$), 100 μM ($p < 0.001$) as determined by Bonferroni *post hoc*.

In order to confirm that apoptosis is the main cell death in Jurkat at 0.01mM H₂O₂ or 3.125μM Hcy and cells mainly died by necrosis at 10mM H₂O₂ or 100μM Hcy after 6 hours incubation, cells were double stained with Annexin-V and PI prior subjecting cells for 24 hours to 0.01mM H₂O₂ or 3.125μM Hcy for apoptosis detection and 10mM H₂O₂ or 100μM Hcy for necrosis in a time-course study showed a significant effect on apoptosis activity and necrosis (P<0.001, as determined by one-way ANNOVA) . Further analysis with Tukey pairwise showed PS was significantly increased on the surface of the cells after 4 hours of H₂O₂ (P<0.05) or Hcy (P<0.001) treatments, the majority of cells were positive to Annexin-v with 6 hours treatment, and PS externalization declined such that after 24 hours there was no significant difference compared to control cells (P<0.05), (Figures 3.28 & 3.29). PI detection showed significant increase in necrosis activity with ≥ 4hours treatment of H₂O₂ or Hcy (P<0.001), followed by significant increase such that after 6 hours 90% of the cells were necrotic and 100% of cells were necrotic after 24 hours (Figures 3.30 & 3.31).

The scatter plot illustrates the distribution of the cells depending on if they are Annexin-V positive or PI positive (x-axis -Annexin-v and y-axis - PI). Cells in C area are viable, cells were Annexin-V positive when they shifted to the D area, cells were late apoptotic/necrotic at B area, and cells became late necrotic at A area. As it shown in Figure 3.32, the majority of the cells were shifted to annexin-V positive area when they treated with 3.125μM Hcy for 6 hours with no necrosis activity, while 100μM Hcy result it in majority of the cells allocated in the late apoptotic/necrosis area.

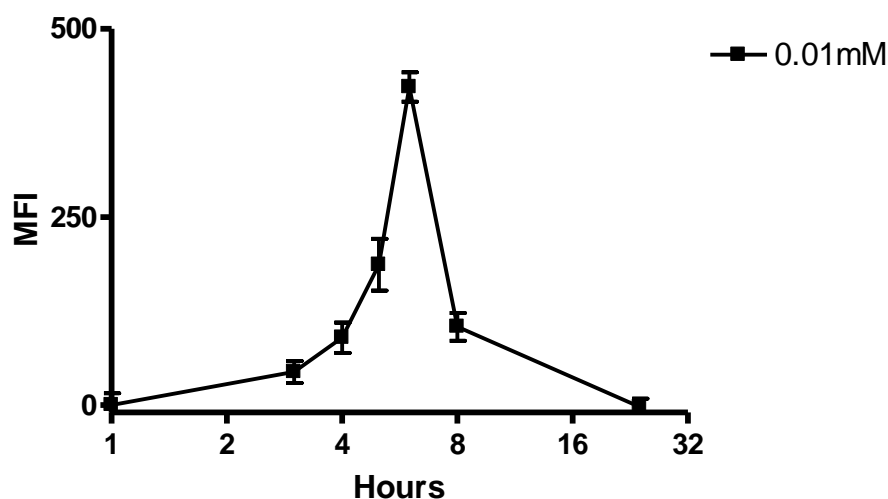


Figure 3.28: Time course study the effect of H₂O₂ on the PS externalization in Jurkat cells. Cells were treated with 0.01mM H₂O₂ for (0-24hours), control cells were non-treated. Cells were double stained to Annexin-v FITC and PI as an early apoptosis marker and necrosis then analysed by flow cytometry and BD FACSDiva software. Data are means \pm SD n=4, $p < 0.001$ as determined by one-way ANOVA. Baseline (control) vs 3h ($p < 0.001$), 4h ($p < 0.001$), 5h ($p < 0.001$), 6h ($p < 0.001$) and 8h ($p < 0.001$) as determined Tukey *post hoc*.

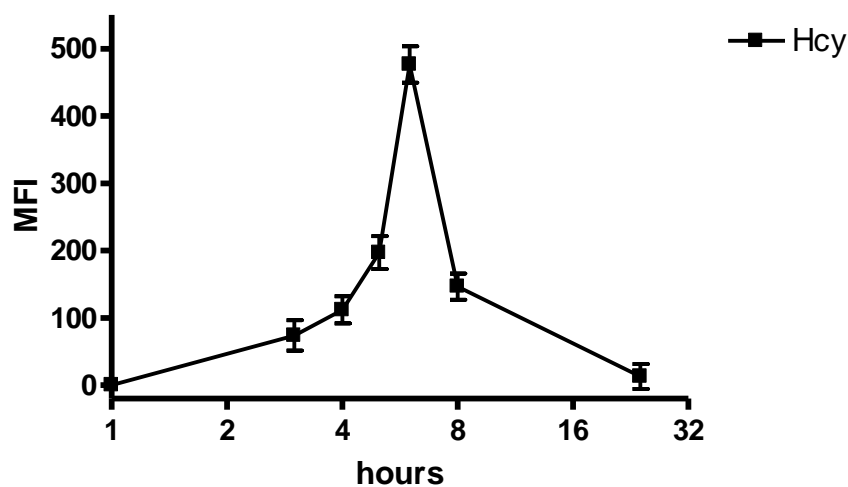


Figure 3.29: Time course study the effect of Hcy on the PS externalization in Jurkat cells. Cells were treated with 3.125 μ M Hcy for (0-24hours), control cells were non-treated. Cells were double stained to Annexin-v FITC and PI as an early apoptosis marker and necrosis then analysed by flow cytometry and BD FACSDiva software. Data are means \pm SD n=4, $p < 0.001$ as determined by one-way ANOVA. Baseline (control) vs 3h ($p < 0.001$), 4h ($p < 0.001$), 5h ($p < 0.001$), 6h ($p < 0.001$) and 8h ($p < 0.001$) as determined Tukey *post hoc*.

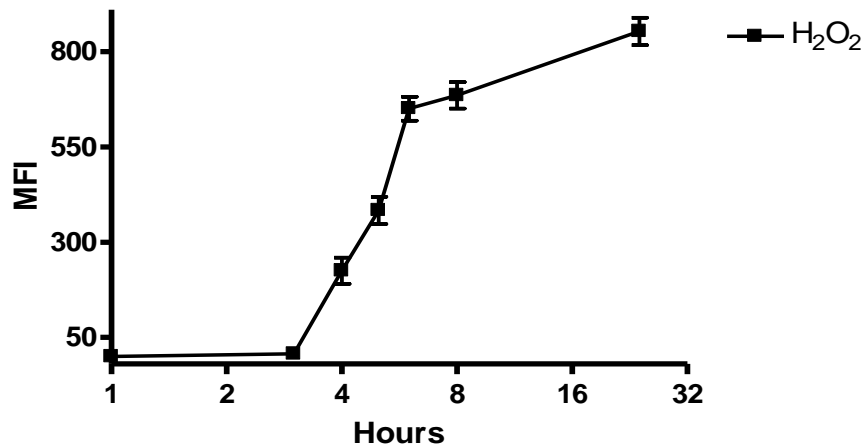


Figure 3.30: Time course study the effect of H₂O₂ on the necrosis activity of Jurkat cells. Cells were treated with 10mM for (0-24hours), control cells were non-treated. Cells were stained with PI for necrosis detection then analysed by flow cytometry and BD FACSDiva software. Data are means \pm SD n=4, $p < 0.001$ as determined by one-way ANOVA. Baseline (control) vs 3h ($p < 0.001$), 4h ($p < 0.001$), 5h ($p < 0.001$), 6h ($p < 0.001$) and 8h ($p < 0.001$) as determined Tukey *post hoc*.

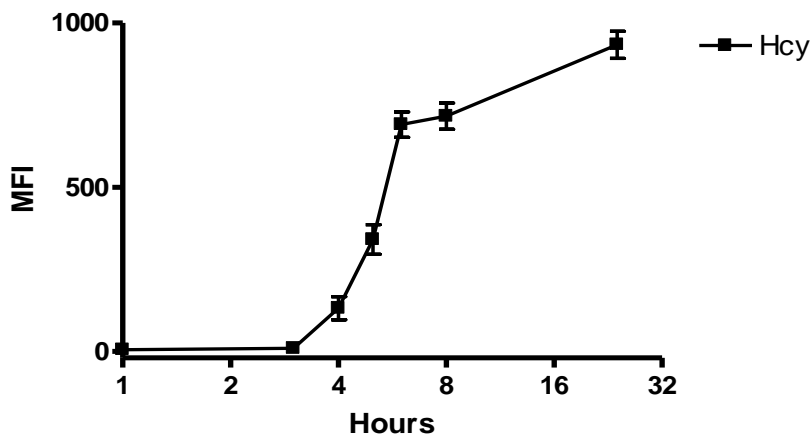
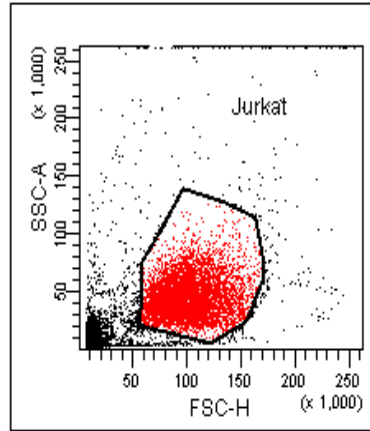
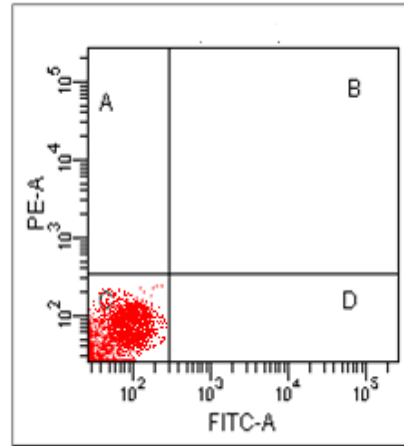


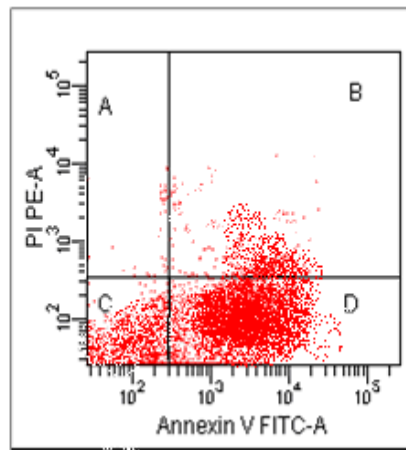
Figure 3.31: Time course study the effect of Hcy on the necrosis activity of Jurkat cells. Cells were treated with 50 μ M Hcy for (0-24hours), control cells were non-treated. Cells were stained with PI for necrosis detection. And then samples analysed by flow cytometry and BD FACSDiva software. Data are means \pm SD n=4, $p < 0.001$ as determined by one-way ANOVA. Baseline (control) vs 3h ($p < 0.001$), 4h ($p < 0.001$), 5h ($p < 0.001$), 6h ($p < 0.001$) and 8h ($p < 0.001$) as determined Tukey *post hoc*.



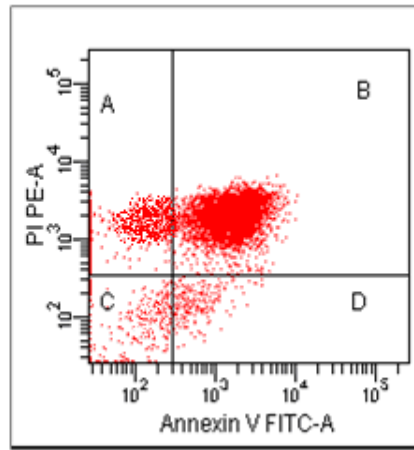
Cell distribution



Non stained cells



Cells treated with 3.125 μ M Hcy



Cells treated with 100 μ M Hcy

Figure 3.32: The effect of Hcy on the PS externalization in Jurkat cells. Cells were subjected to (3.125 μ M Hcy for Annexin-v and 100 μ M for necrosis detection) for 2 hours. Cells were stained to Annexin-v FITC and PI as an early apoptosis marker and necrosis then analysed by flow cytometry and BD FACSDiva software. **A:** late necrotic cells, **B:** late apoptotic and early necrosis, **C:** viable cells and **D:** apoptotic cells.

After determining the required time to induce apoptosis and necrosis, the concentrations needed to induce apoptosis or necrosis as a main cell death pathway were confirmed. In Jurkat cells treatment with H_2O_2 showed a significant effect on caspase-3 and necrosis activity ($P < 0.001$, as determined by one-way ANNOVA) (Figure 3.34). And the Tukey pairwise showed that after 6 hours, caspase-3 significantly increased at $\geq 0.01\text{mM}$ H_2O_2 ($P < 0.001$), and the cells were mostly apoptotic at 0.01mM H_2O_2 ($P < 0.001$) with no significant necrosis activity ($P < 0.05$). Followed by reduction in caspase-3 such at above 1mM there was no significant caspase-3 activity ($P < 0.05$).

In contrast, Tukey pairwise analysis showed that necrosis was significantly induced at $\geq 0.1\text{mM}$ H_2O_2 ($P < 0.001$) when the caspase-3 activity declined, then cells reached 100% necrosis at 10mM H_2O_2 with no caspase-3 activity detected (Figure 3.33). When the cells were treated with a range of Hcy concentrations for 6 hours resulted in the majority of the cells were apoptotic at $3.125\mu\text{M}$ Hcy with no detection of necrosis activity, followed by decline in the casapse-3 activity such that at $\geq 12.5\mu\text{M}$ Hcy necrosis induced significantly ($P < 0.001$) compared to control cells. Furthermore, necrosis reached 100% at $100\mu\text{M}$ Hcy ($P < 0.001$) with no caspase-3 activity detected ($P > 0.05$) (Figure 3.34)

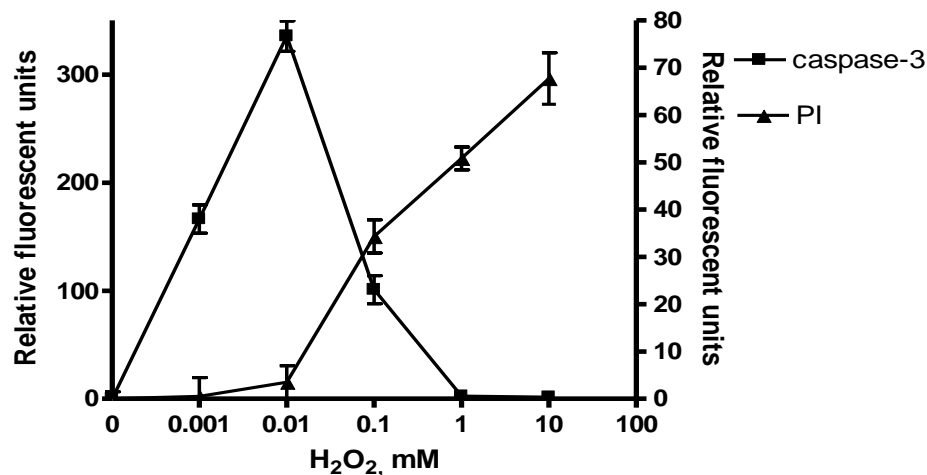


Figure 3.33: Mechanisms of cell of Jurkat cells death after exposure to H₂O₂. Cells were exposed to increasing concentrations of H₂O₂ (0-10mM) for 6 hours, caspase-3 measured at Ex=496/520 and PI staining was measured at EX=535/EM=617. Data are means \pm SD n=4, $p < 0.001$ as determined by one-way ANOVA. Baseline (control) vs 0.001mM-caspase ($p < 0.001$), 0.01mM-caspase, 0.1mM-caspase ($p < 0.001$), 0.1mM-PI, ($p < 0.001$), 1mM-PI ($p < 0.001$), 10mM-PI ($p < 0.001$) as determined by Tukey *post hoc*.

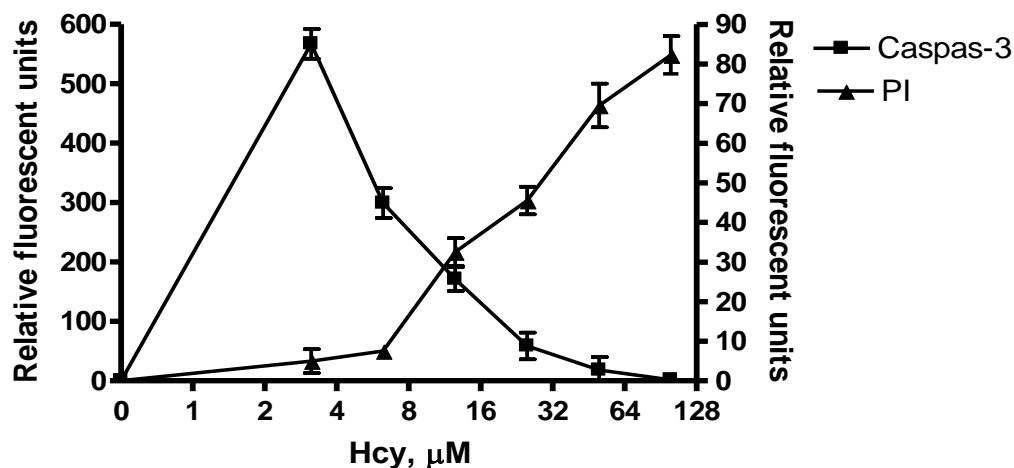


Figure 3.34: Mechanisms of cell of Jurkat cells death after exposure to Hcy. Cells were exposed to increasing concentrations of Hcy (0-100μM) for 6 hours, caspase-3 measured at EX=496/EM=520 and PI staining was measured at EX=535/EM=617. Data are means \pm SD n=4, $p < 0.001$ as determined by one-way ANOVA. Baseline (control) vs 3.125μM-caspase ($p < 0.001$), 6.25μM-caspase ($p < 0.001$), 12.5μM-caspase ($p < 0.001$), 12.5μM ($p < 0.001$)-PI, 25μM ($p < 0.001$)-PI, 50μM ($p < 0.001$)-PI, 100μM ($p < 0.001$)-PI as determined by Tukey *post hoc*.

3.3.4 Folate protects cells from apoptosis and necrosis induced by oxidative stress:

As previously demonstrated, majority of the cells died by apoptosis at 0.01mM H₂O₂ and 3.125μM Hcy after 6 hours of incubation. Also, majority of the cells died by necrosis at 10mM H₂O₂ and 100μM Hcy with 6 hours treatments.

In order to examine the protection role of folate, the effect of folate on caspase-3 and necrosis activity was determined. Folate had no significant effect on caspase-3 or necrosis activity, since addition up to 100μM folate to the cells for 2 hours, resulted in no significant difference in caspase-3 activity and PI labelling comparing to control cells ($P>0.05$, as determined by one-way ANNOVA), (Figures 3.35 & 3.36).

Pre-incubation of cells with 30μM folate has provided significant protection against apoptosis induced by H₂O₂ and Hcy ($P<0.001$, as determined by two-way ANNOVA), (Figures 3.37 & 3.38). The post-hoc comparison showed that at 0.01mM H₂O₂ and 3.125μM Hcy 68% ($P<0.001$) and 75% ($P<0.001$) of the cells, respectively, were protected. Also, significant protection was provided at higher concentrations of H₂O₂ and Hcy such as 0.1mM H₂O₂ and 6.25μM Hcy ($P<0.001$) as compared to H₂O₂ and Hcy alone.

Moreover, the same dose of folate protects Jurkat cells from necrosis induced by H₂O₂ and Hcy significantly ($P<0.001$, as determined by two-way ANNOVA), (Figures 3.39 & 3.40). The Bonferroni pairwise comparison showed that pre-incubation with 30μM folate provided a significant protection at $\geq 0.1\text{mM}$ H₂O₂ or 12.5μM Hcy ($P<0.001$). Additionally, at 10mM H₂O₂ or 100μM Hcy protect 65% ($P<0.001$) and 70% ($P<0.001$) of the cells from necrosis respectively compared to control cells, H₂O₂ or Hcy alone treated cells

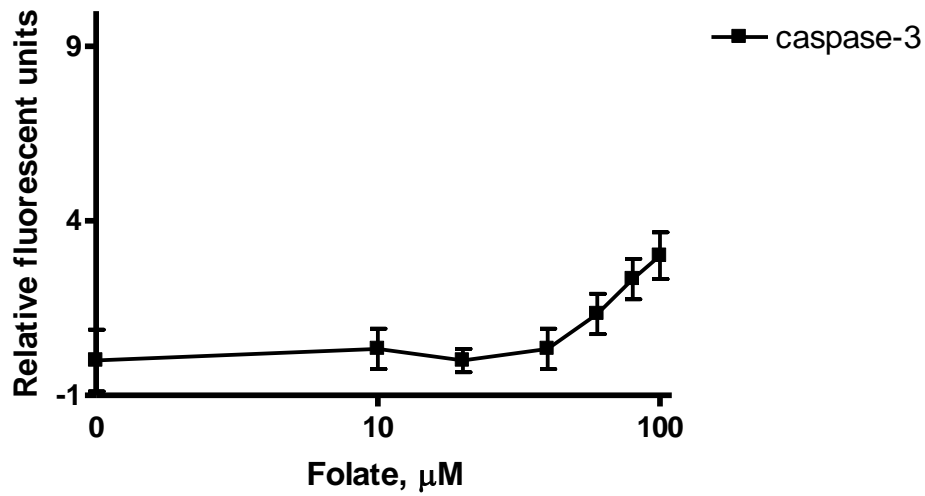


Figure 3.35: Effect of folate on caspase-3 in Jurkat cells. Cells were pre-incubated with a range of folate concentrations (0-100 μM) for 2 hours, caspase-3 was measured at Ex=496/Em=617. The data presents are means \pm SD n=3. $p > 0.05$ as determined by one-way ANOVA.

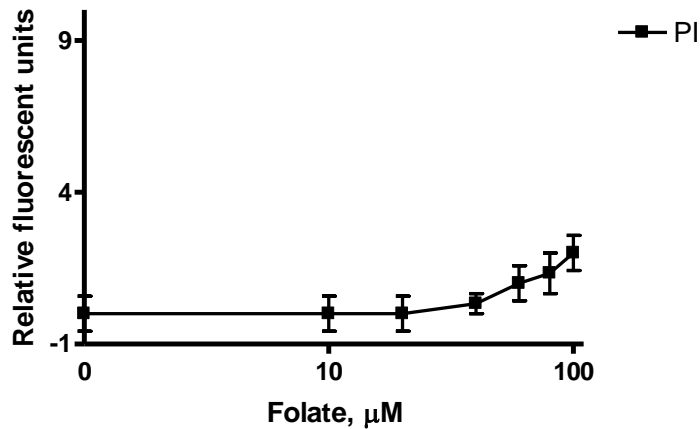


Figure 3.36: Effect of folate on necrosis of Jurkat cells. Cells were pre-incubated with a range of folate concentrations (0-100 μM) for 2 hours, necrosis activity was measured after at Ex=496/Em=520. The data presents are means \pm SD n=3. $p > 0.05$ as determined by one-way ANOVA.

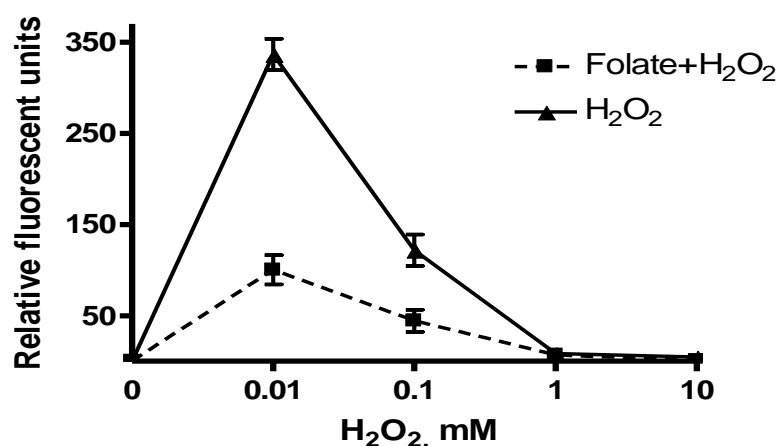


Figure 3.37: The effect of folate pre-treatment on the caspase-3 activity. Jurkat cells were pre-incubated with 30 μ M folate for 2 hours then treated with a range of H₂O₂ concentrations for 6 hours and the control cells were treated with H₂O₂ only. Caspase-3 was measured after at EX=496/EM=520. Data are means \pm SD n=4, $p < 0.001$ as determined by two-way ANOVA. H₂O₂ vs folate+ 0.001mM H₂O₂ ($p < 0.001$), Folate+0.01mM, ($p < 0.001$), as determined by Bonferroni *post hoc*.

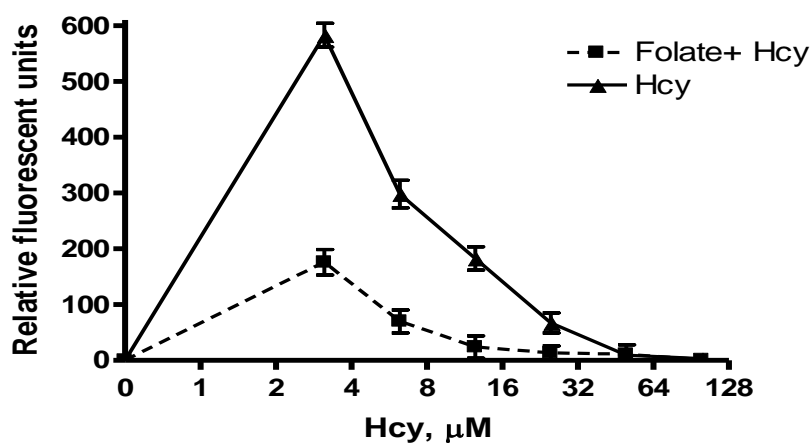


Figure 3.38: The effect of folate pre-treatment on the caspase-3 activity. Jurkat cells were pre-incubated with 30 μ M folate for 2 hours then treated with a range of Hcy concentrations for 6 hours and the non-treated cells were the control cells, caspase-3 was measured after at EX=496/EM=520. Data are means \pm SD n=4, $p < 0.001$ as determined by two-way ANOVA. Hcy vs Folate 3.125 μ M ($p < 0.001$), Folate+6.25 μ M ($p < 0.001$), folate+12.5 μ M ($p < 0.001$), as determined by Bonferroni *post hoc*.

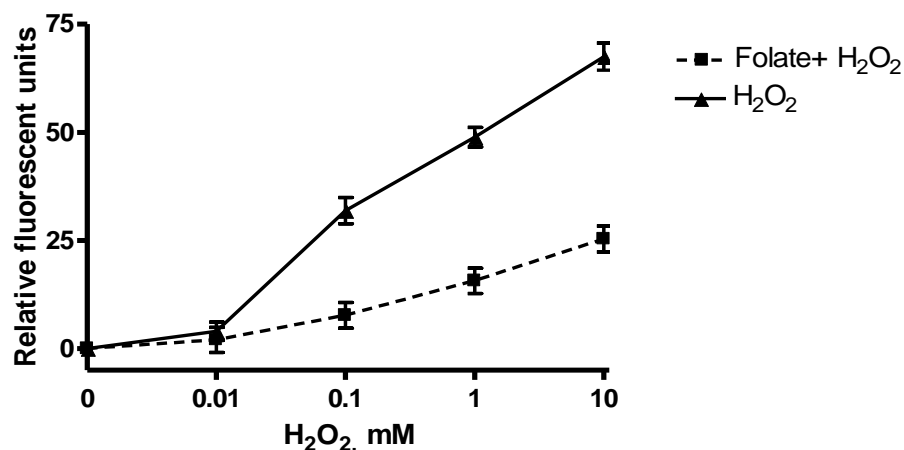


Figure 3.39: Effect of folate pre-treatment on necrosis. Jurkat cells were pre-incubated with 30 μ M folate for 2 hours then cells treated with a range of H₂O₂ concentrations for 6 hours and the control cells were treated with H₂O₂ alone, necrosis activity was measured at EX=535/EM=617. The Data are means \pm SD n=4, $p < 0.001$ as determined by two-way ANOVA. H₂O₂ vs folate+0.1mM H₂O₂ ($p < 0.001$), Folate+1mM, ($p < 0.001$), Folate+10mM, ($p < 0.001$), as determined by Bonferroni *post hoc*.

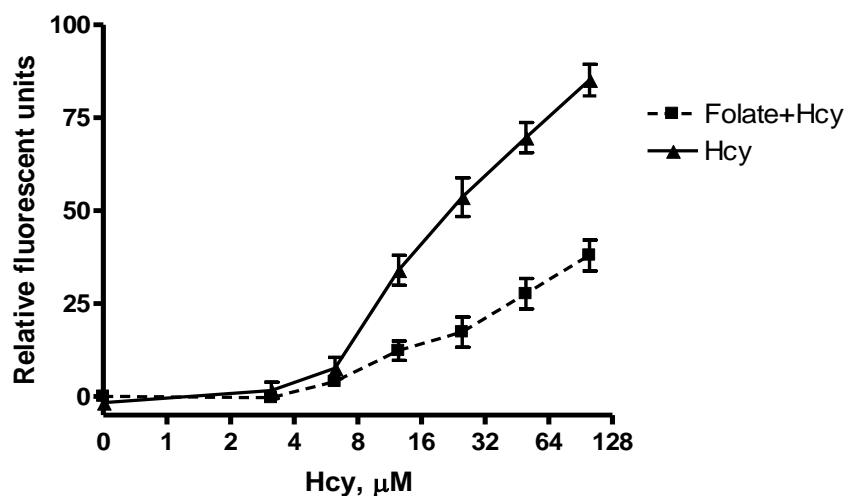


Figure 3.40: Effect of folate pre-treatment on necrosis. Jurkat cells were pre-incubated with 30 μ M folate for 2 hours then cells were treated with a range of concentrations of Hcy for 6 hours and the control cells were treated with Hcy alone. Necrosis activity was measured at EX=535/EM=617. The Data are means \pm SD n=4, $p < 0.001$ as determined by two-way ANOVA. Hcy vs Folate 3.125 μ M ($p < 0.001$), Folate+6.25 μ M ($p < 0.001$), folate+12.5 μ M ($p < 0.001$), as determined by Bonferroni *post hoc*.

3.3.5 Induction of apoptosis and necrosis in normal blood cells *via* exposure to Hydrogen peroxide and Homocysteine.

After investigating the effect of oxidative stress and death pattern in Sk-hep1 and Jurkat cells, we examined further the effect of oxidative stress on healthy peripheral blood cells. Whole blood was collected from healthy volunteers and peripheral blood cells were isolated and treated with a range of concentrations of H₂O₂ or Hcy to induce apoptosis and necrosis. Caspase-3 activity, Annexin-V and PI uptake were used to detect apoptosis and necrosis *via* flow cytometry.

The treatments with H₂O₂ or Hcy have a significant effect on the PS externalisation and PI uptake ($P < 0.001$, as determined by two-way ANNOVA), (Figures 3.41 & 3.42). Further analysis with Bonferroni pairwise showed that After 1 hour exposing neutrophil cells to a range of H₂O₂ concentrations (0-10mM) there was no significant effect on the PS externalisation on the cells compared to control cells ($P > 0.05$). However, with 2, 3, 4 hours treatment, PS externalisation peaked at 0.01mM H₂O₂ to reach 33%, 60% and 23% respectively, and then declined at 0.1mM with significant difference ($P < 0.001$) while at 1mM H₂O₂ and above there was no significant difference ($P > 0.05$) compared to control cells (Figure 3.41). Furthermore, subjecting neutrophil cells to a range of Hcy concentration for 1, 2, and 3 hours resulted in; PS externalisation significantly increased such that at 0.01mM Hcy reach 73% ($P < 0.001$), 39% ($P < 0.001$), and 35% ($P < 0.001$) after 1, 2 and 3 hours respectively. This was followed by a reduction in the PS appearance on the surface of the cells at 0.05mM Hcy with a significant difference compared to control cells ($P < 0.001$), while above 0.1mM Hcy ($P > 0.05$) there was no significant effect on PS externalisation compared to control cells which have no significant activity of PS translocation (Figure 3.42).

Caspase-3 activity was significantly affected by H₂O₂ and Hcy ($P < 0.001$, as determined by two-way ANNOVA), (Figures 3.43 & 3.44). Post-hoc comparison showed there is a significant increase at low concentration of H₂O₂ in neutrophil cells, hence at 0.01mM H₂O₂ caspase-3 reached 60% 93%,

and 25% after 2, 3 and 4 hours treatment ($P < 0.001$), followed by decrease in caspase-3 activity such as at above 1mM H_2O_2 there was no significant difference ($P > 0.05$) compared to control cells (Figure 3.43). On the other hand, at low concentrations of Hcy there was a significant effect on caspase-3 after 1, 2, and 3 hours incubation; such that at 0.01mM Hcy caspase-3 reached 91%, 64% and 46% respectively as compared to control cells ($P < 0.001$). Although above 0.1mM Hcy ($P > 0.05$) treatment have no detectable effect on caspase-3 activity (Figure 3.44).

Moreover, the H_2O_2 and Hcy treatment induced a significant effect on necrosis activity of neutrophils ($P < 0.001$, as determined by two-way ANNOVA), (Figures 3.45 & 3.46). The Bonferroni pairwise analysis showed that when neutrophils were exposed to range of H_2O_2 concentrations no significant effect on necrosis activity was observed after 1 hour ($P > 0.05$). However, at 0.1mM H_2O_2 a significant increase in necrosis activity was observed after 2, 3, and 4 hours treatments, and at 10mM necrosis reached 79% ($P < 0.001$), 91% ($P < 0.001$) and 97% ($P < 0.001$) after 2, 3, and 4 hours exposing compared to control cells (Figure 3.45). Also Hcy has a significant effect on necrosis such that at above 0.05mM Hcy there was a significant elevation of necrosis detected with 1, 2 and 3 hours exposure ($P < 0.001$), followed by a significant increase in necrosis activity with increasing Hcy concentrations and more than 91%, 94%, 96% of the cells were dying neurotically at 1mM Hcy ($P < 0.001$) after 1, 2 and 3 hours exposure (Figure 3.46).

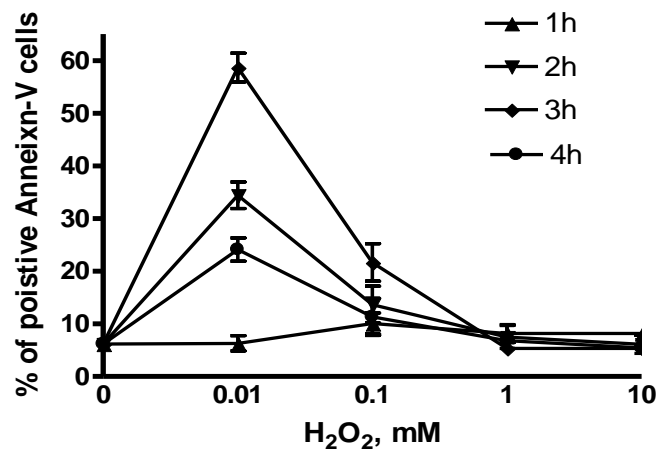


Figure 3.41: Time course study the effect of H₂O₂ on PS translocation in neutrophil cells. Cells were incubated with a range of H₂O₂ concentrations (0-10mM) for 1, 2 and 3 hours. Control cells were non-treated. Then cells were stained Annexin-v FITC labelled and analysed using flowcytometry and BD FACSDiva software. The Data are means \pm SD n=4, $p < 0.001$ as determined by two-way ANOVA. Baseline (control) vs 2h; 0.01mM ($p < 0.001$), 3h; 0.01mM ($p < 0.001$), 3h; 0.1mM ($p < 0.001$), 4h; 0.01mM ($p < 0.001$), as determined by Bonferroni *post hoc*.

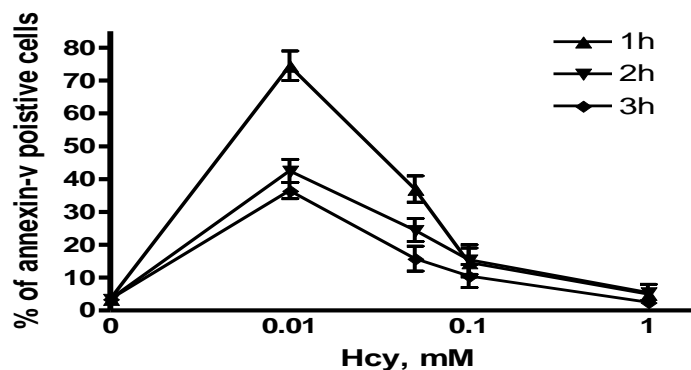


Figure 3.42: Time course study the effect of Hcy on PS translocation in neutrophil cells. Cells were treated with a range of concentrations of Hcy (0-10mM) for 1, 2 and 3 hours. Control cells were non-treated. Then cells were stained Annexin-v FITC labelled and analysed using flowcytometry and BD FACSDiva software. The Data are means \pm SD n=4, $p < 0.001$ as determined by two-way ANOVA. Baseline (control) vs 1h; 0.01mM ($p < 0.001$), 1h; 0.05mM ($p < 0.001$), 2h; 0.01mM ($p < 0.001$), 2h; 0.1mM ($p < 0.001$), 2h; 0.01mM ($p < 0.001$), as determined by Bonferroni *post hoc*.

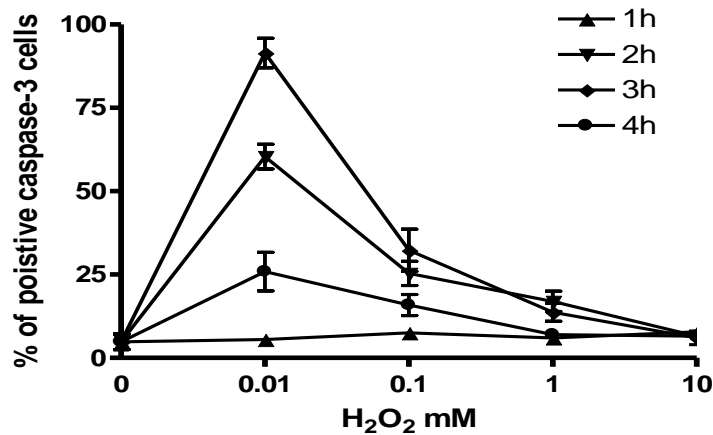


Figure 3.43: Time course study the effect of H₂O₂ on caspase-3 level in neutrophil cells.

Cells were treated with a range of H₂O₂ concentrations (0-10mM) for 1, 2 and 3 hours. Cells were then stained with monoclonal anti-rabbit caspase-3 FITC labelled antibody. Control cells: Non-treated cells. The Data are means \pm SD n=4, $p < 0.001$ as determined by two-way ANOVA. Baseline (control) vs 2h; 0.01mM ($p < 0.001$), 3h; 0.01mM ($p < 0.001$), 3h; 0.1mM ($p < 0.001$), 4h; 0.01mM ($p < 0.001$), 4h; 0.1mM ($p < 0.001$), as determined by Bonferroni *post hoc*.

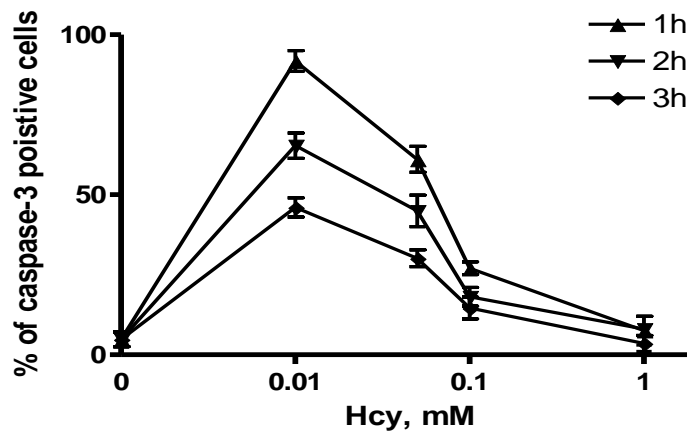


Figure 3.44: Time course study the effect of Hcy on caspase-3 level in neutrophil cells.

Cells were treated with a range of concentrations Hcy (0-1mM) for 1, 2 and 3 hours. Cells were then stained with monoclonal anti-rabbit caspase-3 FITC labelled antibody. Control cells; non-treated cells. The data are means \pm SD n=4, $p < 0.001$ as determined by two-way ANOVA. Baseline (control) vs 1h; 0.01mM ($p < 0.001$), 1h; 0.05mM ($p < 0.001$), 1h; 0.1mM ($p < 0.001$), 2h; 0.01mM ($p < 0.001$), 2h; 0.05mM ($p < 0.001$), 3h; 0.01mM ($p < 0.001$), 2h; 0.05mM ($p < 0.001$), as determined by Bonferroni *post hoc*.

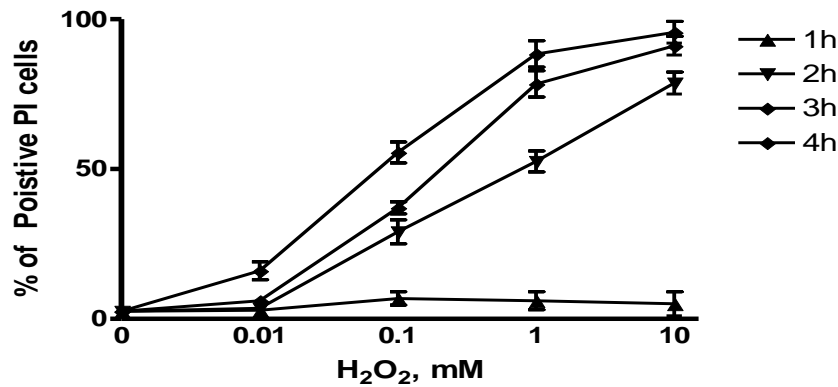


Figure 3.45: Time course study the effect of H₂O₂ on necrosis level of neutrophil cells.

Cells were incubated with range of H₂O₂ concentrations (0-10mM) for 1, 2 and 3 hours. Then cells were stained with PI and analysed using flowcytometry and BD FACSDiva. Control cells were non-treated. The data are means \pm SD n=4, p< 0.001 as determined by two-way ANOVA. Baseline (control) vs 2h; 0.1mM (p<0.001), 2h; 1mM (p<0.001), 2h; 10mM (p<0.001), 3h; 0.1mM (p<0.001), 3h; 1mM (p<0.001), 3h; 10mM (p<0.001), 4h; 0.1mM (p<0.001), 4h; 1mM (p<0.001), 4h; 10mM (p<0.001), as determined by Bonferroni *post hoc*.

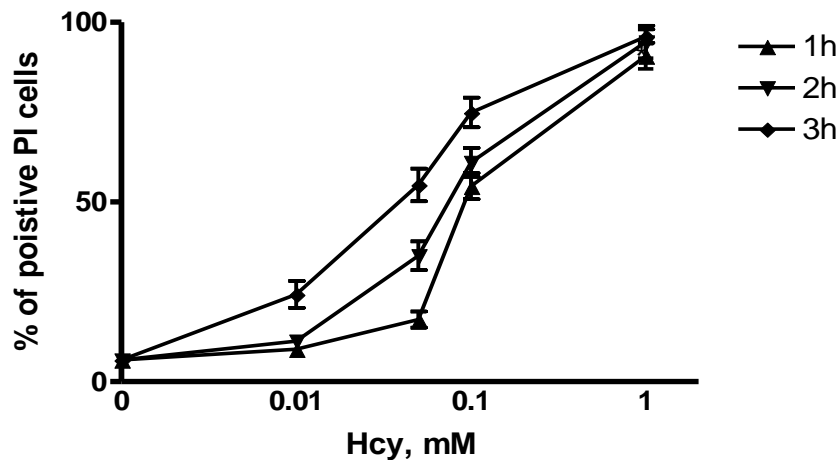
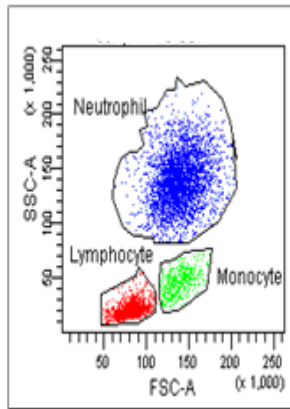


Figure 3.46: Time course study the effect of Hcy on necrosis level of neutrophil cells.

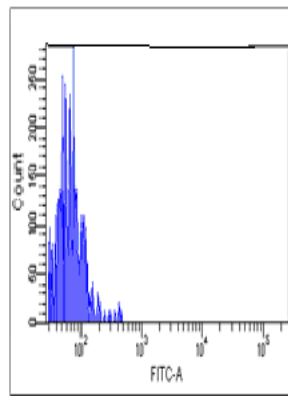
Cells were treated with a range of Hcy concentrations (0-1mM) for 1, 2 and 3 hours. Then cells were stained with PI and analysed using flowcytometry and BD FACSDiva. Control cells; non-treated cells. The data are means \pm SD n=4, p< 0.001 as determined by two-way ANOVA. Baseline (control) vs 1h; 0.1mM (p<0.001), 1h; 1mM (p<0.001), 2h; 0.1mM (p<0.001), 2h; 1mM (p<0.001), 3h; 0.01mM (p<0.001), 3h; 0.1mM (p<0.001), 3h; 1mM (p<0.001) as determined by Bonferroni *post hoc*.

In Figure 3.47, the scatter plot demonstrated the distribution of the blood cells according to size neutrophils presented by blue colour. The histogram showed that the cells had significant increase of the fluorescence intensity after exposing the cells for 1 hour to 0.01mM Hcy, compared to control cells and most of the cells were shifted to the annexin-v positive area. Also the majority of the cells shifted to the necrotic/late apoptotic area after 1 hour exposure to 1mM Hcy, in comparison to the control cells.

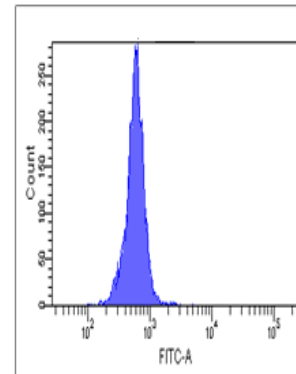
The neutrophil cells that were subjected to a range of H_2O_2 concentrations for 3 hours or Hcy for 1 hour showed significant effect in caspase-3 and necrosis activity ($P < 0.001$, as determined by one-way ANNOVA), (Figure 3.48). The Tukey pairwise analysis showed that at 0.01mM most of the cells were caspase-3 positive ($P < 0.001$), followed by a reduction in both of them such that at above 0.1mM H_2O_2 or 0.05mM Hcy showed no significant increase in casapse-3 activity as compared to control cells ($P > 0.05$). In contrast, necrosis was increased significantly at $\geq 0.1\text{mM}$ H_2O_2 or 0.05mM Hcy ($P < 0.001$) when casapse-3 reduced, and at 10mM H_2O_2 or 1mMHcy resulted in cells were mostly necrotic with no caspase-3 activity (Figure 3.48).



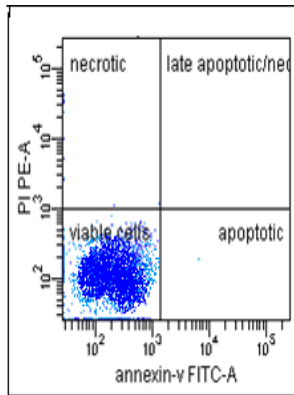
A. Distribution of the cells according cell size



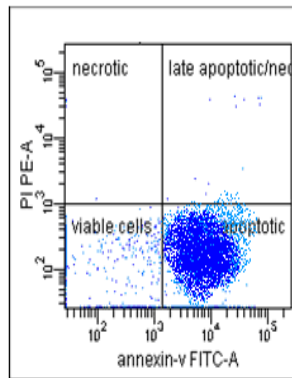
B. Caspase-3 control



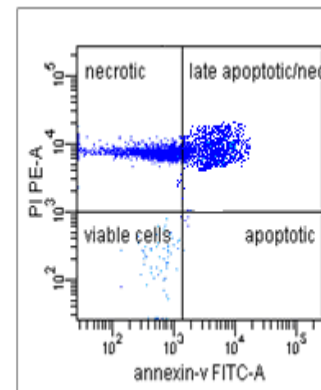
C. Cells treated with 0.01mM Hcy



D. control cells for Annexin-v and PI



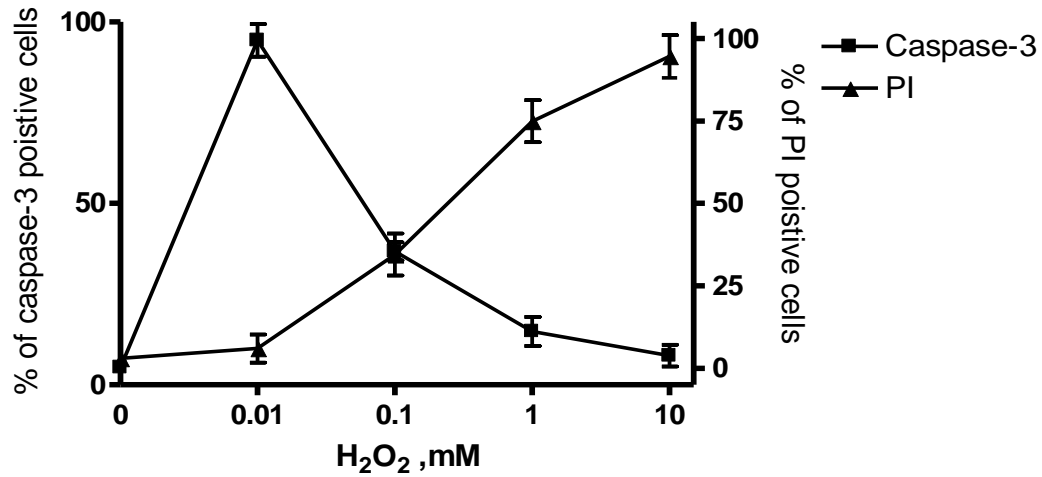
E. Cells treated with 0.01mM Hcy



F. cells treated with 1mM Hcy

Figure 3.47: Induction of apoptosis and necrosis in neutrophil cells. Cells were treated for 1 hour with 0.01mM Hcy for apoptosis induction and 1mM Hcy for necrosis induction. Then cells were stained with monoclonal anti-rabbit caspase-3 FITC labelled antibody for caspase activity measurement and doubled stain with Annexin-v and PI for early apoptosis and necrosis measurements using flowcytometry and BD FACSDiva software to analyse. **A.** distribution of the cells according cell size, **B.** Caspase-3 control (non-treated), **C.** Cells treated with 0.01mM Hcy, **D.** control cells for Annexin-v and PI (non-treated), **E.** Cells treated with 0.01mM Hcy and **F.** cells treated with 1mM Hcy.

A.



B.

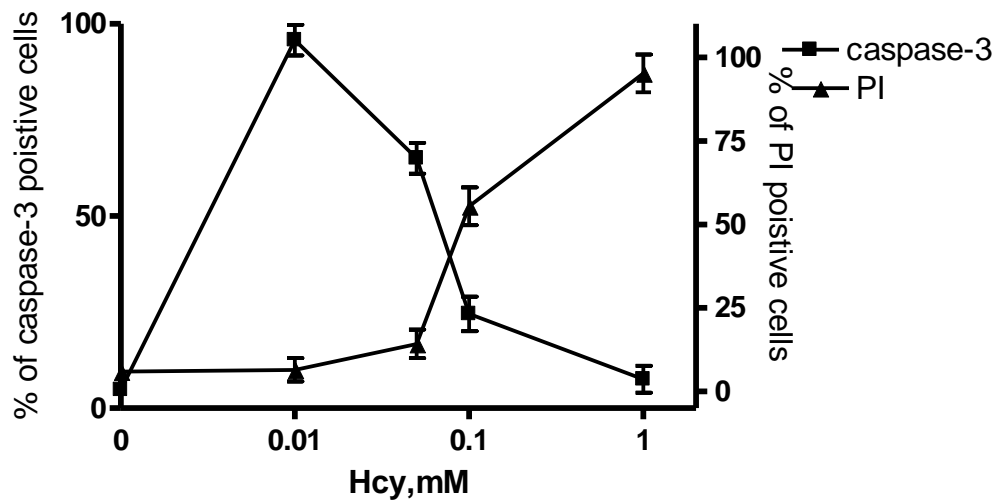


Figure 3.48: Mechanisms of neutrophil cells death subjected to H_2O_2 or Hcy. Cells were exposed to increasing concentrations of **A.** H_2O_2 (0-10mM) for 3 hours or **B.** Hcy (0-1mM) for 1 hour. Then cells were stained with monoclonal anti-rabbit caspase-3 FITC labelled antibody for caspase activity measurement using flowcytometry and BD FACSDiva software to analyse. The present data are means \pm SD n=4, $p < 0.001$ as determined by two-way ANOVA.

The H₂O₂ and Hcy had a significant effect on the PS exposure in monocyte cells ($P < 0.001$, as determined by two-way ANNOVA), (Figure 3.49 & 3.50). The analysis with Bonferroni pairwise resulted in PS externalisation increased significantly in monocyte cells at 0.01mM H₂O₂ after 1, 2 and 3 hours incubation ($P < 0.001$). There were further increases in PS translocation at 0.1mM H₂O₂ which reached 31% ($P < 0.001$), 72% ($P < 0.001$) and 53% ($P < 0.001$) after 1, 2 and 3 hours treatment. This was followed by a reduction in the PS appearances such that at 10mM there was no significant increase in the PS externalisation ($P > 0.05$) compared to control cells (Figure 3.49). However, at 0.01mM Hcy PS externalisation reached 82%, 67% and 33% after 1, 2, and 3 hours treatment respectively ($P < 0.001$), followed by reduction such that at ≥ 0.1 mM Hcy showed no significant increase in the PS externalisation after 1, 2, and 3 hours incubation ($P > 0.05$), (Figure 3.50).

Caspase-3 activities were significantly affected in monocyte by H₂O₂ and Hcy treatment ($P < 0.001$, as determined by two-way ANNOVA), (Figures 3.51 & 3.52). The post-hoc comparison showed that when monocyte cells were exposed to a range of H₂O₂ concentrations (0-10mM) for 1 hour incubation, there was no significant increase of caspase-3 activity ($P > 0.05$) as compared to control cells (non-treated). However, exposing cells to a range of H₂O₂ concentrations for up to 2 and 3 hours resulted in a significant increase in the caspase-3 at 0.01mM H₂O₂ ($p < 0.001$). And at higher concentrations such as 0.1mM H₂O₂ caspase-3 activity reached 50% and 91% after 2, and 3 hours respectively ($P < 0.001$), followed by decreases such that at 10mM H₂O₂ there was no significant effect on caspase-3 activity ($P > 0.05$) compared to control cells (Figure 3.51). Exposing cells to a range of Hcy concentrations for 1 hour showed significant effect at 0.01mM Hcy ($p < 0.001$). However, higher concentrations such as 0.1mM and 1mM showed no significant effect on caspase-3 activity as compared to control cells (non-treated) ($P > 0.05$). While after 2 and 3 hours of exposing cells to a range of Hcy resulted in a significant increase of caspase-3 to reach 94% and 76% at 0.01mM Hcy respectively ($P < 0.001$), after which caspase-3 reduced and there was no significant difference at 0.1mM Hcy ($P > 0.05$) compared to control cells (Figure 3.52).

Also H_2O_2 and Hcy had a significant effect on necrosis activity in monocyte ($P < 0.001$, as determined by two-way ANNOVA), (Figure 3.53 & Figure 3.54). However, further analysis with Bonferroni pairwise indicated no significant effect on necrosis when monocyte were exposed to a range of H_2O_2 concentrations after 1 hour ($P > 0.05$). While at $\geq 0.1mMH_2O_2$ there was a significant increase in necrosis activity observed after 2, and 3 hours treatments, and at 10mM necrosis reached 74% ($P < 0.001$) and 92% ($P < 0.001$) after 2, and 3 hours of treatments compared to control cells (Figure 3.53). Moreover, 1 hour treatment of Hcy showed no significant effect on necrosis ($P > 0.05$). However, Hcy has a significant effect on necrosis such as at above 0.05mM Hcy there was significant necrosis detected with 2 and 3 hours exposure ($P < 0.001$), followed by a significant increase in necrosis activity with increasing Hcy concentrations and more than 92% ($P < 0.00$) and 98% ($P < 0.001$) of the cells were dying neurotically at 1mM Hcy after 2 and 3 hours exposure (Figure 3.54).

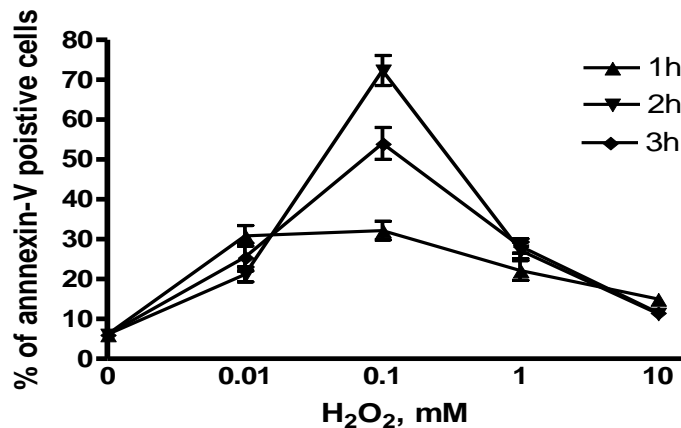


Figure 3.49: Time course study the effect of H_2O_2 on PS translocation in monocyte cells. Cells were incubated with a range of H_2O_2 concentrations (0-10mM) for 1, 2 and 3 hours. Control cells were non-treated. Then cells were stained by Annexin-v FITC, labelled and analysed using flowcytometry and BD FACSDiva software. The Data are means \pm SD $n=4$, $p < 0.001$ as determined by two-way ANOVA. Baseline (control) vs 1h; 0.01mM ($p < 0.001$), 1h; 0.1mM ($p < 0.001$), 1h; 1mM ($p < 0.001$), 2h; 0.01mM ($p < 0.001$), 2h; 0.1mM ($p < 0.001$), 2h; 1mM ($p < 0.001$), 3h; 0.01mM ($p < 0.001$), 3h; 0.1mM ($p < 0.001$), 3h; 1mM ($p < 0.001$), as determined by Bonferroni *post hoc*.

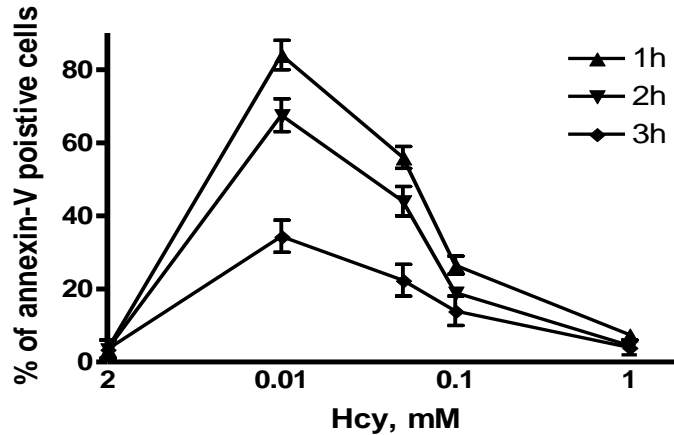


Figure 3.50: Time course study the effect of Hcy on PS translocation in monocyte cells.

Cells were incubated with a range of Hcy concentrations (0-1mM) for 1, 2 and 3 hours. Control cells were non-treated. Then cells were stained with Annexin-v FITC, labelled and analysed using flowcytometry and BD FACSDiva software. The Data are means \pm SD n=4, $p < 0.001$ as determined by two-way ANOVA. Baseline (control) vs 1h; 0.01mM ($p < 0.001$), 1h; 0.05mM ($p < 0.001$), 1h; 0.1mM ($p < 0.001$), 2h; 0.01mM ($p < 0.001$), 2h; 0.05mM ($p < 0.001$), 2h; 0.1mM ($p < 0.001$), 3h; 0.01mM ($p < 0.001$), 3h; 0.05mM ($p < 0.001$) as determined by Bonferroni *post hoc*.

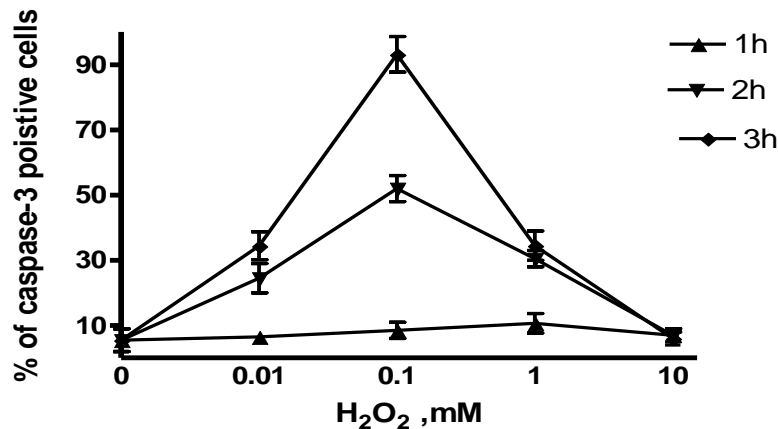


Figure 3.51: Time course study the effect of H₂O₂ on caspase-3 level in Monocyte cells.

Cells were treated with a range of H₂O₂ concentrations (0-10mM) for 1, 2 and 3 hours. Cells were then stained with monoclonal anti-rabbit caspase-3 FITC labelled antibody. Control cells: Non-treated cells. The Data are means \pm SD n=4, $p < 0.001$ as determined by two-way ANOVA. Baseline (control) vs 2h; 0.01mM ($p < 0.001$), 2h; 0.1mM ($p < 0.001$), 2h; 1mM ($p < 0.001$), 3h; 0.01mM ($p < 0.001$), 3h; 0.1mM ($p < 0.001$), 3h; 1mM ($p < 0.001$), as determined by Bonferroni *post hoc*.

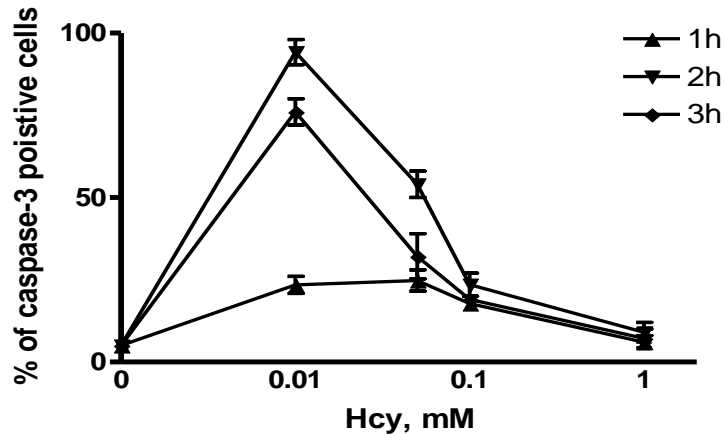


Figure 3.52: Time course study the effect of Hcy on caspase-3 level in Monocyte cells.

Cells were treated with a range of Hcy concentrations (0-10mM) for 1, 2 and 3 hours. Cells were then stained with monoclonal anti-rabbit caspase-3 FITC labelled antibody. Control cells: Non-treated cells. The Data are means \pm SD $n=4$, $p < 0.001$ as determined by two-way ANOVA. Baseline (control) vs 1h; 0.01mM ($p < 0.001$), 1h; 0.05mM ($p < 0.001$), 2h; 0.01mM ($p < 0.001$), 2h; 0.05mM ($p < 0.001$), 3h; 0.01mM ($p < 0.001$), 3h; 0.05mM ($p < 0.001$), 3h; 0.1mM ($p < 0.001$), as determined by Bonferroni *post hoc*.

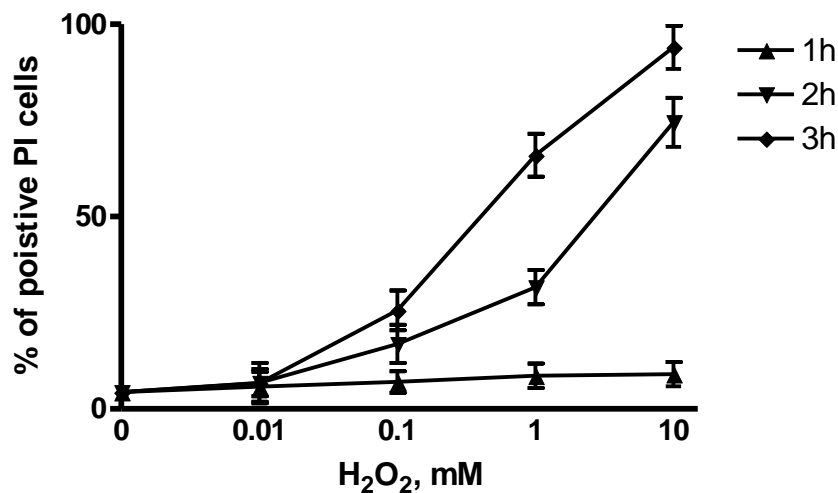


Figure 3.53: Time course study the effect of H₂O₂ on necrosis level of monocyte cells.

Cells were incubated with a range of H₂O₂ concentrations (0-10mM) for 1, 2 and 3 hours. Then cells were stained with PI and analysed using flowcytometry and BD FACSDiva. Control cells; non-treated cells. The Data are means \pm SD $n=4$, $p < 0.001$ as determined by two-way ANOVA. Baseline (control) vs 2h; 1mM ($p < 0.001$), 2h; 10mM ($p < 0.001$), 3h; 0.1mM ($p < 0.001$), 3h; 1mM ($p < 0.001$), 3h; 10mM ($p < 0.001$), as determined by Bonferroni *post hoc*.

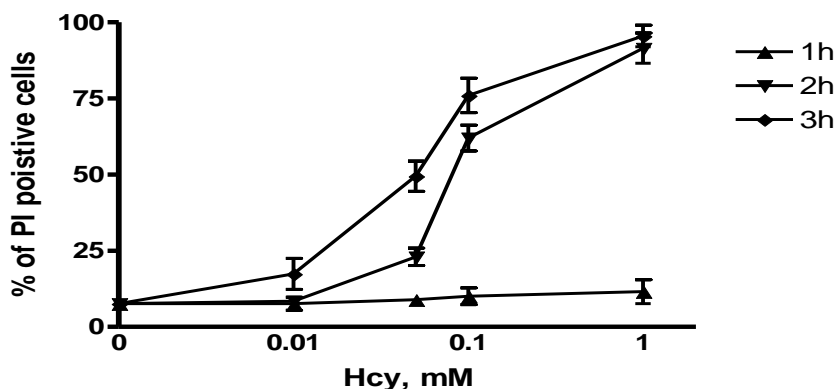
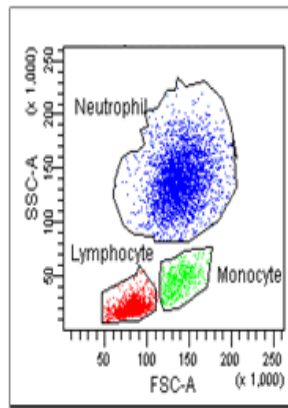


Figure 3.54: Time course study the effect of Hcy on necrosis level of monocyte cells.

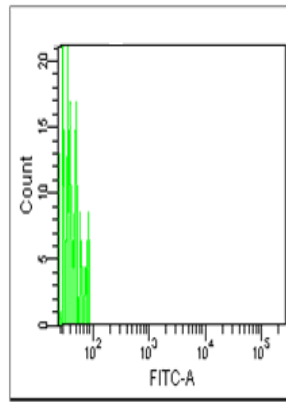
Cells were incubated with a range of Hcy concentrations (0-10mM) for 1, 2 and 3 hours. Then cells were stained with PI and analysed using flowcytometry and BD FACSDiva. Control cells were non-treated. The Data are means \pm SD $n=4$, $p < 0.001$ as determined by two-way ANOVA. Baseline (control) vs 2h; 0.05mM ($p < 0.001$), 2h; 0.1mM ($p < 0.001$), 2h; 1mM ($p < 0.001$), 3h; 0.05mM ($p < 0.001$), 3h; 0.1mM ($p < 0.001$), 3h; 1mM ($p < 0.001$) as determined by Bonferroni *post hoc*.

In Figure 3.55, the scatter plot demonstrated the distribution of the blood cells according to size, and the monocyte cells were presented in green. The histogram showed a significant increase of the fluorescence intensity after 2 hours of exposing the cells to 0.01mM Hcy, in comparison to the control cells and most of the cells were shifted to the annexin-v positive area. Also, the majority of the cells were shifted to the necrotic/late apoptotic area after 1 hour of exposing the cells to 1mM Hcy (in comparison to the control cells). When monocyte cells were subjected to range of H_2O_2 concentrations for 3 hours or Hcy for 2 hours, it resulted in a significant effect on caspase-3 and necrosis activity ($P < 0.001$, as determined by one-way ANNOVA), (Figure 3.56). The Tukey pairwise analysis showed that when cells were exposed to a range of concentrations of H_2O_2 for 3 hours or Hcy for 2 hours, they showed significant increase in caspase-3 activity which peaked at 0.1mM ($P < 0.001$), followed by a reduction in caspase-3 activity with both treatments and at higher concentrations of H_2O_2 or Hcy (10mM H_2O_2 and 1mM Hcy) there was no significant increase in casapse-3 activity as compared to control cells ($P > 0.05$).

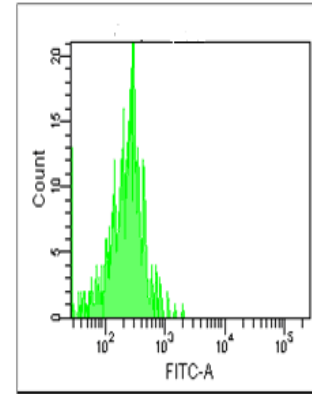
In contrast, necrosis has increased significantly at $\geq 0.1\text{mM H}_2\text{O}_2$ or $>0.05\text{mM Hcy}$ when caspase-3 activity reduced ($P < 0.001$), and at $10\text{mM H}_2\text{O}_2$ or 1mM Hcy resulted in 100% necrosis with no caspase-3 activity (Figure 3.56).



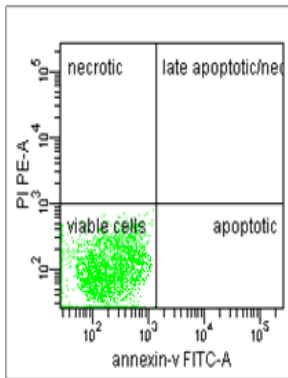
A. Distribution of the cells according cell size



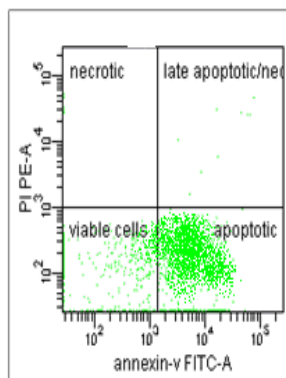
B. Caspase-3 control



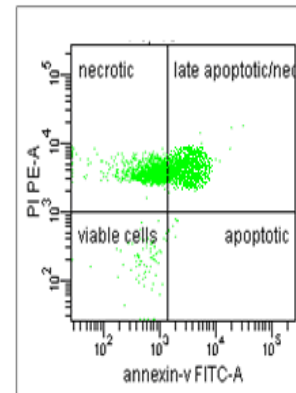
C. Cells treated with 0.01mM Hcy



D. control cells for Annexin-v and PI



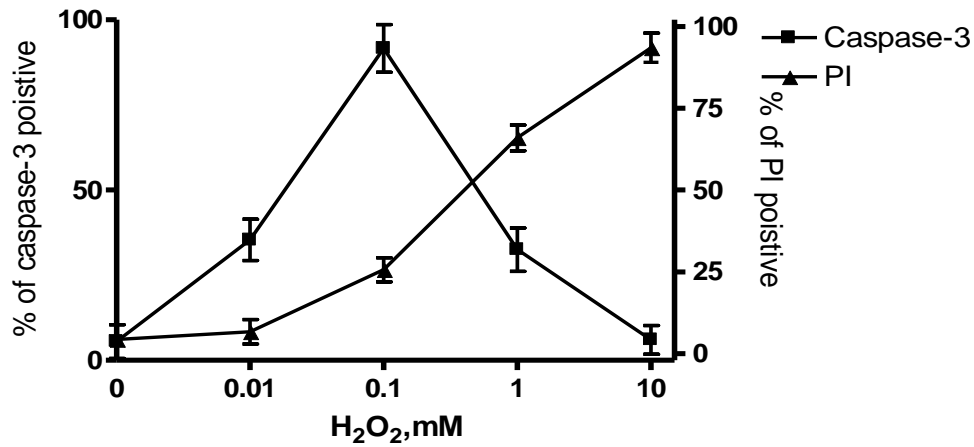
E. Cells treated with 0.01mM Hcy



F. cells treated with 1mM Hcy.

Figure 3.55: Induction of apoptosis and necrosis in monocyte cells. Cells were treated for 2 hours with 0.01mM Hcy for apoptosis induction and 1mM Hcy for necrosis induction. Then cells were stained with monoclonal anti-rabbit caspase-3 FITC labelled antibody for caspase activity measurement and doubled stain with Annexin-v and PI for early apoptosis and necrosis measurements using flowcytometry and BD FACSDiva software to analyse.: **A.** distribution of cells according cell size, **B.** Caspase-3 control (non-treated), **C.** Cells treated with 0.01mM Hcy , **D.** control cells for Annexin-v and PI (non-treated), **E.** Cells treated with 0.01mM Hcy and **F.** cells treated with 1mM Hcy .

A.



B.

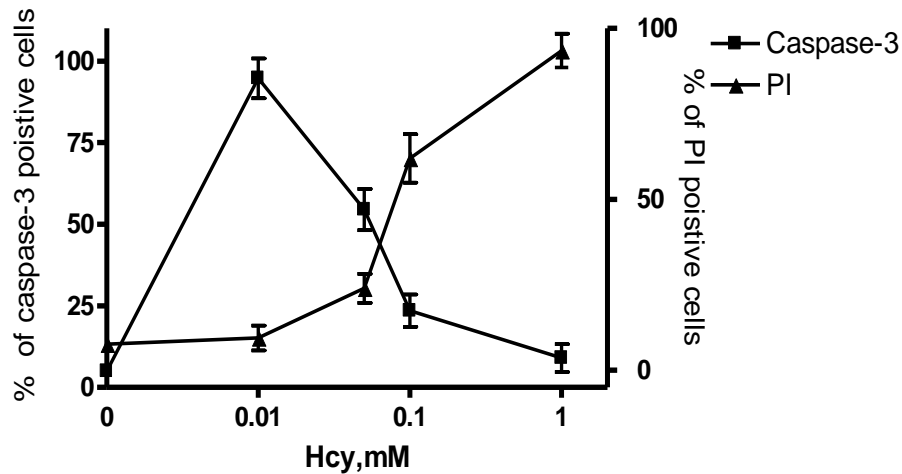


Figure 3.56: Mechanisms of monocyte cells death subjected to H₂O₂ or Hcy. Cells were exposed to increasing concentrations of **A.** H₂O₂ (0-10mM) for 3 hours or **B.** Hcy (0-1mM) for 2 hours. Then cells were stained with monoclonal anti-rabbit caspase-3 FITC labelled antibody for caspase activity, and for PI detection cells were stained with PI and measured using flowcytometry and BD FACSDiva software to analyse. The present data are means \pm SD n=4, p< 0.001 as determined by two-way ANOVA.

Lymphocyte cells also showed a significant activity of PS after treatment with a range of H_2O_2 and Hcy concentrations ($P < 0.001$, as determined by two-way ANNOVA), (Figures 3.57 & 3.58). The comparison with post-hoc showed that when lymphocyte cells exposed to a range of H_2O_2 concentrations (0-10mM), they showed a significant effect on the PS externalisation into the surface of the cells, to reach 74%, 64% and 53% at 0.01mM after 1, 2 and 3 hours respectively, in comparison to the control cells ($P < 0.001$), and then declined at 0.1mM ($P < 0.001$), while above 1mM H_2O_2 , there was no significant difference in the PS ($P > 0.05$) compared to control cells (non-treated) (Figure 3.57). Furthermore, subjecting lymphocyte cells to a range of Hcy concentration for 1, 2, and 3 hours resulted in increased PS externalisation such that at 0.01mM Hcy reach 84% , 76% and 48% after 1, 2 and 3 hours respectively. Followed by a reduction in the PS appearance on the surface of the cells at 0.05mM Hcy with a significant difference, when compared to control cells ($P < 0.001$), while above 0.1mM Hcy had no significant effect on the PS externalisation ($P > 0.05$) compared to control cells (non-treated) (Figure 3.58).

In the same time caspase-3 and necrosis activity were significantly affected by the H_2O_2 and Hcy exposure ($P < 0.001$, as determined by two-way ANNOVA), (Figures 3.59, 3.60, 3.61 & 3.62). Further analysis with Bonferroni pairwise indicated that caspase-3 significantly increased at low concentrations of H_2O_2 , hence at 0.01mM H_2O_2 caspase-3 reached 62% 95%, and 75% after 1, 2 and 3 hours treatment respectively ($P < 0.001$), followed by a decrease in caspase-3 activity such that at above 1mM H_2O_2 there was no significant difference ($P > 0.05$) compared to control cells (Figure 3.59). At low concentrations of Hcy there was a significant effect on caspase-3 activity after 1, 2, and 3 hours incubation such that at 0.01mM Hcy caspase-3 reached 50%, 97% and 72% respectively as compared to control cells ($P < 0.001$). Although above 0.1mM Hcy had no detectable effect on caspase-3 ($P > 0.05$) compared to control cells (Figure 3.60).

Also the Post-hoc comparison showed that when lymphocyte were exposed to a range of H_2O_2 concentrations, they showed a significant effect on necrosis activity observed after 1 hour at 0.1mM H_2O_2 ($P < 0.001$), while 2 and 3 hours treatment induced necrosis at 0.1mM H_2O_2 significantly ($P < 0.001$). However, necrosis activity was increased with increasing concentrations which reached 58% ($P < 0.001$), 92% ($P < 0.001$) and 95% ($P < 0.001$) at 10mM H_2O_2 after 1, 2, and 3 hours treatment when compared to control cells (Figure 3.61). Also, Hcy has a significant effect on necrosis that at above 0.1mM Hcy there was a significant increase of necrosis detected after 1 hour exposing ($P < 0.001$), whereas after 2 and 3 hours treatments it showed a significant increase in necrosis activity at ≥ 0.05 mM Hcy, and then necrosis activity increased with higher concentration such at 1mM Hcy reached 34% ($P < 0.001$), 90% ($P < 0.001$) and 96% ($P < 0.001$) necrosis after 1, 2 and 3 hours (Figure 3.62).

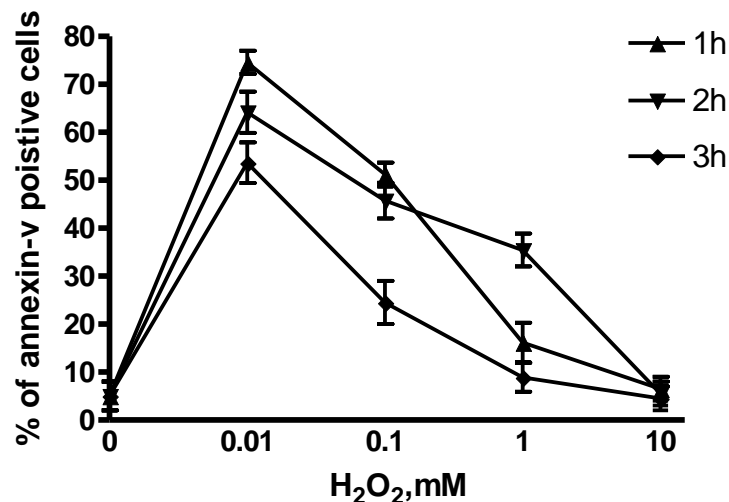


Figure 3.57: Time course study the effect of H_2O_2 on PS translocation in lymphocyte cells. Cells were incubated with a range of H_2O_2 concentrations (0-10mM) for 1, 2 and 3 hours. Control cells were non-treated. Then cells were stained Annexin-v FITC labelled and analysed using flowcytometry and BD FACSDiva software. The Data are means \pm SD $n=4$, $p < 0.001$ as determined by two-way ANOVA. Baseline (control) vs 1h; 0.01mM ($p < 0.001$), 1h; 0.1mM ($p < 0.001$), 2h; 0.01mM ($p < 0.001$), 2h; 0.1mM ($p < 0.001$), 2h; 1mM ($p < 0.001$), 3h; 0.01mM ($p < 0.001$), 3h; 0.1mM ($p < 0.001$), as determined by Bonferroni *post hoc*.

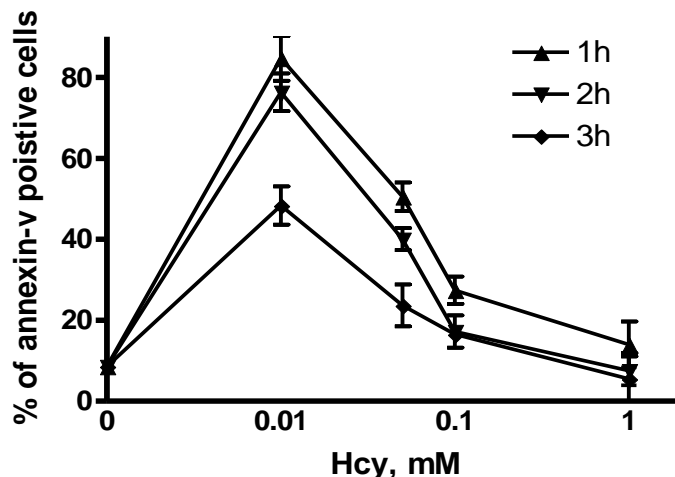


Figure 3.58: Time course study the effect of Hcy on PS translocation in lymphocyte cells. Cells were incubated with a range of Hcy concentrations (0-1mM) for 1, 2 and 3 hours. Control cells werenon-treated. Cells were then stained by Annexin-v FITC labelled and analysed using flowcytometry and BD FACSDiva software. The Data are means \pm SD n=4, $p < 0.001$ as determined by two-way ANOVA. Baseline (control) vs 1h; 0.01mM ($p < 0.001$), 1h; 0.05mM ($p < 0.001$), 1h; 0.1mM ($p < 0.001$), 2h; 0.01mM ($p < 0.001$), 2h; 0.05mM ($p < 0.001$), 3h; 0.01mM ($p < 0.001$), 3h; 0.05mM ($p < 0.001$) as determined by Bonferroni *post hoc*.

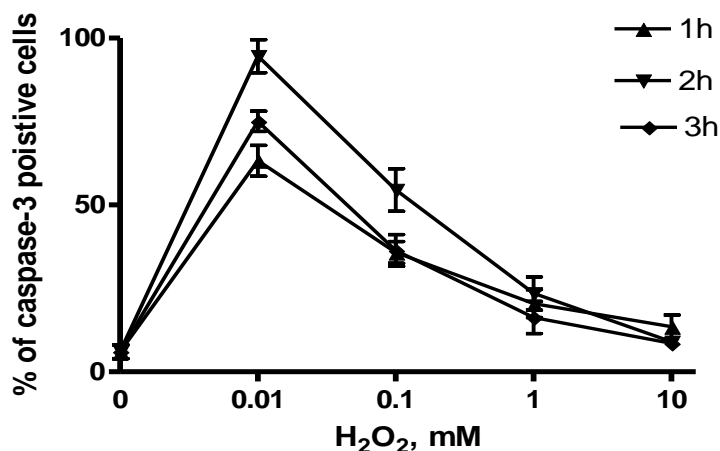


Figure 3.59: Time course study the effect of H₂O₂ on caspase-3 level in lymphocyte cells. Cells were treated with a range of H₂O₂ concentrations (0-10mM) for 1, 2 and 3 hours. Cells were then stained with monoclonal anti-rabbit caspase-3 FITC labelled antibody. Control cells were non-treated. The Data are means \pm SD n=4, $p < 0.001$ as determined by two-way ANOVA. Baseline (control) vs 1h; 0.01mM ($p < 0.001$), 1h; 0.1mM ($p < 0.001$), 2h; 0.01mM ($p < 0.001$), 2h; 0.1mM ($p < 0.001$), 2h; 1mM ($p < 0.05$), 3h; 0.01mM ($p < 0.001$), 3h; 0.1mM ($p < 0.001$), as determined by Bonferroni *post hoc*.

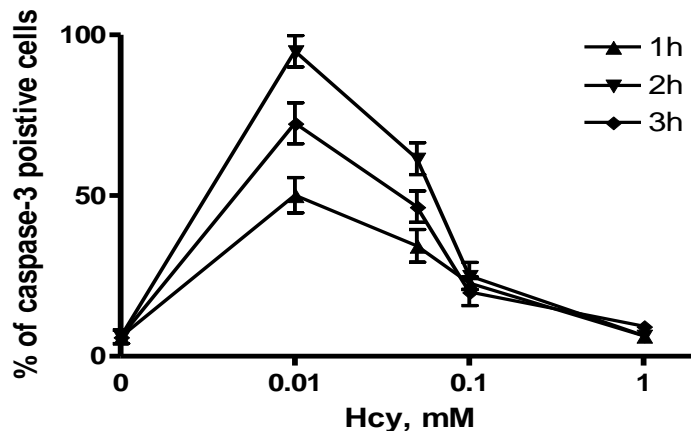


Figure 3.60: Time course study the effect of Hcy on caspase-3 level in lymphocyte cells. Cells were treated with a range of Hcy concentrations (0-1mM) for 1, 2 and 3 hours. Cells were then stained with monoclonal anti-rabbit caspase-3 FITC labelled antibody. Control cells were non-treated. The Data are means \pm SD $n=4$, $p < 0.001$ as determined by two-way ANOVA. Baseline (control) vs 1h; 0.01mM ($p < 0.001$), 1h; 0.05mM ($p < 0.001$), 1h; 0.1mM ($p < 0.01$), 2h; 0.01mM ($p < 0.001$), 2h; 0.05mM ($p < 0.001$), 2h; 0.1mM ($p < 0.001$), 3h; 0.01mM ($p < 0.001$), 3h; 0.05mM ($p < 0.001$), 3h; 0.1mM ($p < 0.01$) as determined by Bonferroni *post hoc*.

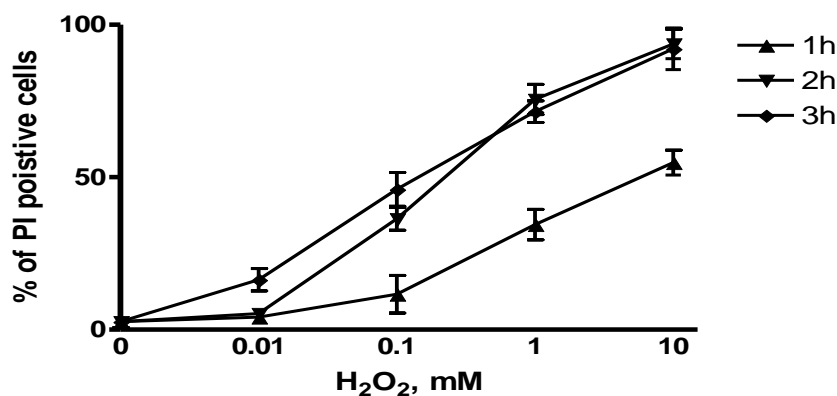


Figure 3.61: Time course study the effect of H₂O₂ on necrosis level of lymphocyte cells. Cells were incubated with a range of H₂O₂ concentrations (0-10mM) for 1, 2 and 3 hours. Then cells were stained with PI and analysed using flowcytometry and BD FACSDiva. Control cells were non-treated. The Data are means \pm SD $n=4$, $p < 0.001$ as determined by two-way ANOVA. Baseline (control) vs 1h; 1mM ($p < 0.001$), 1h; 10mM ($p < 0.001$), 2h; 0.1mM ($p < 0.001$), 2h; 1mM ($p < 0.001$), 2h; 10mM ($p < 0.001$), 3h; 0.1mM ($p < 0.001$), 3h; 1mM ($p < 0.001$), 3h; 10mM ($p < 0.001$) as determined by Bonferroni *post hoc*.

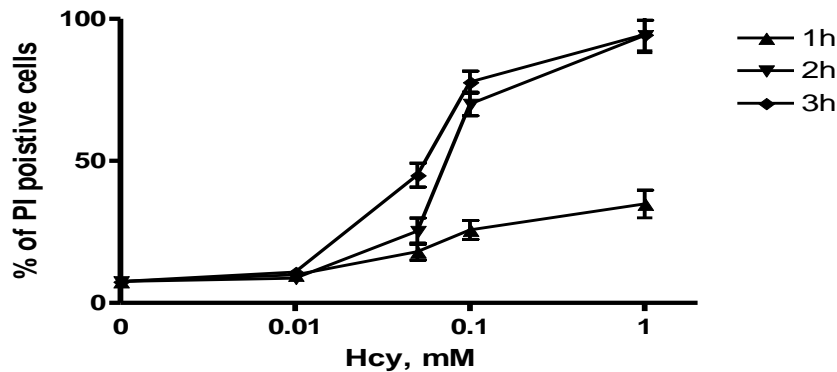


Figure 3.62: Time course study the effect of Hcy on necrosis level of lymphocyte cells.

Cells were incubated with a range of Hcy concentrations (0-1mM) for 1, 2 and 3 hours. Then cells were stained with PI and analysed using flowcytometry and BD FACSDiva. Control cells were non-treated. The Data are means \pm SD $n=4$, $p < 0.001$ as determined by two-way ANOVA. Baseline (control) vs 1h; 0.1mM ($p < 0.001$), 1h; 1mM ($p < 0.001$), 2h; 0.05mM ($p < 0.01$), 2h; 0.1mM ($p < 0.001$), 2h; 1mM ($p < 0.001$), 3h; 0.05mM ($p < 0.001$), 3h; 0.1mM ($p < 0.001$), 3h; 1mM ($p < 0.001$) as determined by Bonferroni *post hoc*.

The scatter plots in Figure 3.63, illustrates the distribution of the blood cells according to size and lymphocyte cells presented with red colour. The histogram present a significant increase of the fluorescence intensity of caspase-3 after 2 hours of exposing cells to 0.01mM Hcy, compared to control cells, and majority of cells were shifted to the annexin-v positive scatter. Also, majority of the cells were shifted to the necrotic/late apoptotic scatter after 2 hour exposing cells to 1mM Hcy compared to control cells. In order to induce mainly apoptosis once or necrosis once again, cells were exposed to a range of concentrations of H_2O_2 for 2 hours or Hcy for 2 hours and resulted in a significant effect in caspase-3 and necrosis activity ($P < 0.001$, as determined by one-way ANNOVA), (Figure 3.64). The Tukey pairwise analysis showed that a significant increase in caspase-3 activity which peaked at 0.01mM ($P < 0.001$), followed by a reduction in both of them with high concentrations of H_2O_2 or Hcy resulted in no significant increase in casapse-3 activity as

compared to control cells ($P > 0.05$). In contrast, necrosis has increased significantly at $\geq 0.1\text{mM H}_2\text{O}_2$ or $> 0.05\text{mM Hcy}$ ($P < 0.001$), which then reached 93% necrosis at $10\text{mM H}_2\text{O}_2$ or 1mM Hcy with no caspase-3 activity (Figure 3.64).

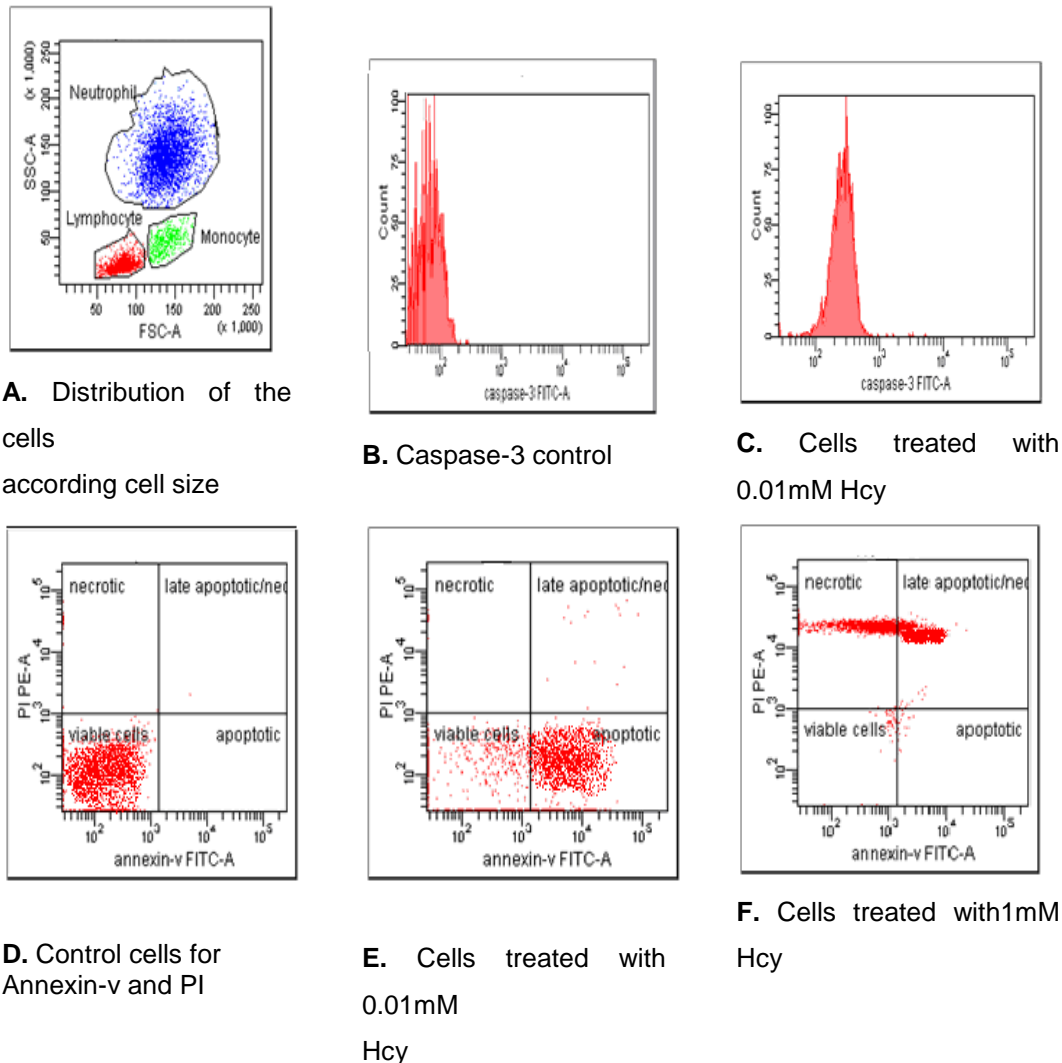
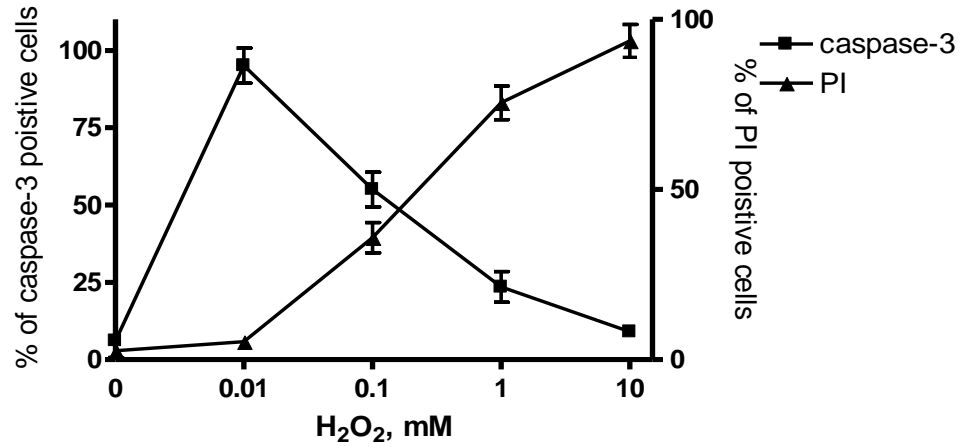


Figure 3.63: Induction of apoptosis and necrosis in lymphocyte cells. Cells were treated for 2 hours with 0.01mM Hcy for apoptosis induction and 1mM Hcy for necrosis induction. Then cells were stained with monoclonal anti-rabbit caspase-3 FITC labelled antibody for caspase activity measurement and doubled stain with Annexin-v and PI for early apoptosis and necrosis measurements using flowcytometry and BD FACSDiva software to analyse: **A.** distribution of the cells according cell size, **B.** Caspase-3 control, **C.** Cells treated with 0.01mM Hcy , **D.** control cells for Annexin-v and PI, **E.** Cells treated with 0.01mM Hcy and **F.** cells treated with 1mM Hcy .

A.



B.

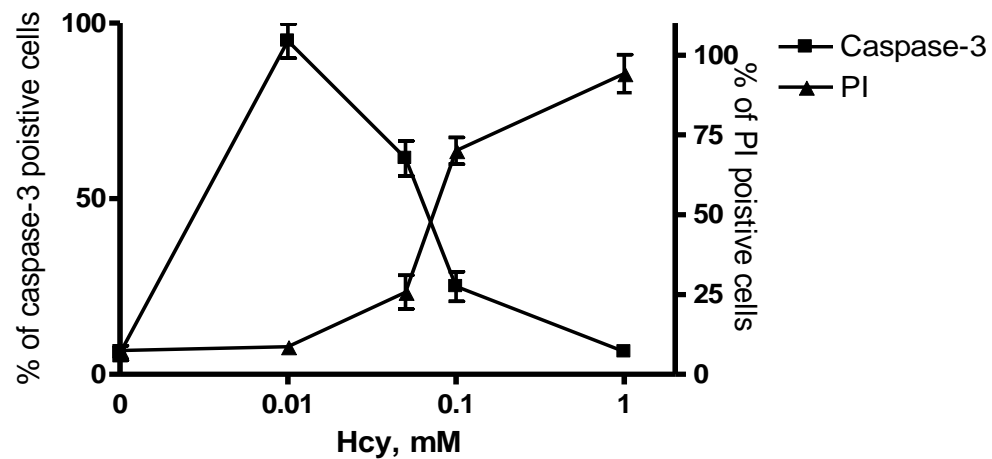


Figure 3.64: Mechanisms of lymphocyte cells death subjected to H_2O_2 or Hcy Cells were exposed to increasing concentrations of **A.** H_2O_2 (0-10mM) for 2 hours or **B.** of Hcy (0-1mM) for 2 hours. Then cells were stained with monoclonal anti-rabbit caspase-3 FITC labelled antibody for caspase activity measurement using flowcytometry and BD FACSDiva software to analyse. The present data are means \pm SD n=4, $p < 0.001$ as determined by two-way ANOVA.

3.4 Discussion:

The aims of this chapter were to investigate mechanisms of cells death under oxidative stress, and the protection role of folate and cobalamin that they can be provided against oxidative stress.

The results in this chapter present clearly the mechanisms of cell death under oxidative stress is dose-dependent hence, at 3.125 μ M Hcy or H₂O₂ Sk-Hep-1 cells were mostly apoptotic with high activity of caspase-3, and this activity reduced when cell death switched to the necrosis pathway. The PI assay showed significant increase in necrosis activity and cells were dying neurotically with 50 μ M Hcy or H₂O₂. Additionally, the same pattern of cell death pathways under oxidative stress observed in other cells types such as Jurkat cells, were mainly dying through apoptosis pathway with a significant increase in caspase-3 and translocation of PS to the surface of the cells at 0.01mM H₂O₂ or at 3.125 μ M Hcy after 6 hours. While the activity of apoptosis was reduced with higher concentrations when necrosis was induced and cell were dying through necrosis such at 10mM H₂O₂ or 100 μ M Hcy reached 100% necrosis. Furthermore, the normal peripheral blood (Neutrophil, Monocyte and lymphocyte) cells had a specific point where cells undergo apoptosis and another different point where cells undergo necrosis under oxidative stress.

These results indicate that cell death mechanisms under oxidative stress are apoptosis or necrosis depending on the dose and time. This data strengthen the previous results obtained by others studies, that low concentrations of oxidative stressor induce apoptosis and high concentrations induce necrosis in Jurkat cells (Hampton & Orrenius, 1997), endothelium cells (Liu *et al.*, 2005; Obeid & Herrmann, 2006), smooth muscle cells (Buemi *et al.*, 2001), primary human bone marrow stromal cells and the HS-5 cell line (Kim, *et al.*, 2006) It has been reported that when cells undergo apoptosis intracellular ATP increased while necrotic cells have no such ATP activity. However, when the loss of the intracellular ATP inhibited in the necrotic cell, cell death type switched to apoptosis (Saito *et al.*, 2006; Nicotera & Melino, 2004). This might suggest that cells undergo necrosis at higher concentration due to the loss of intracellular ATP.

The results presented in this chapter suggest that endothelial cells are more sensitive to oxidative stress than blood cells with 2 hours incubation of 3.125 μ M Hcy or H₂O₂ induce apoptosis in sk-hep1 cells, whereas 6 hours are required for inducing apoptosis in Jurkat cells by 3.125 μ M Hcy or 0.01mM H₂O₂. This sensitivity might be due to the fact that endothelial cells interface between the vessel wall and circulating bloods, so they act as a sensor and transducer of signals, and therefore they are sensitive to oxidative stress (Ryter *et al.*, 2007). On this basis Sk-hep1 was used as a suitable model for the further studies.

As it is known that peripheral blood cells function differently, interestingly their resistance against oxidative stress were also different. Previous researchers have shown that neutrophils are resistance to H₂O₂ (Pietarinen-Runtti *et al.*, 2000), also there was another study demonstrated the resistance of peripheral blood cells to H₂O₂ but this study was limited to investigating the PS exposure only (Nishioka *et al.*, 2003). However, there is no such study that showed the effect of the homocysteine. The result in this chapter demonstrates the resistance of peripheral blood cells against oxidative stress as such, monocyte cells were more resistance to hydrogen peroxide than neutrophils and lymphocyte cells since they required higher concentration and time to induce apoptosis and necrosis. The resistance of the monocyte cells to the oxidative agents might be due to the level of glutathione peroxidase (GPx) and glutathione activity, which were high in the monocyte cells GPx containing a selenocysteine moiety in its catalytic centre, which is an antioxidant enzymes that reduce lipid and hydrogen peroxide to their respective alcohols (Pietarinen-Runtti *et al.*, 2000). Moreover, peripheral blood cells were more sensitive to homocysteine compared to hydrogen peroxide as less incubation time and concentrations of Hcy were required to induce cell death either by apoptosis or necrosis and the same observation detected in other cell lines such as Jurkat. This sensitivity of cells to Hcy might be due to generating intracellular H₂O₂ by Hcy when Hcy-induced cell death (Malinow, 1990; Harker *et al.*, 1976).

After determining the mechanisms of cells death under oxidative stress in different cells type, the hypothesis of antioxidant and cobalamin provide protection from apoptosis or necrosis induced by oxidative stressor was examined. Since in the literature it has been reported that folate and cobalamin supplementations reduce

Hcy level in the plasma of hyperhomocysteinemia patient and protect cells from oxidative stress injury (Rosenberg, 2007; Kazerooni *et al.*, 2008; Nagaraja *et al.*, 2008). Folic acid supplementation could be a useful approach for reducing the risk and treatment of cardiovascular diseases associated with hyperhomocysteinemia (Woo *et al.*, 1999; Chambers *et al.*, 2000). The results in this chapter clearly demonstrated that folate provides protection to the cells from apoptosis and necrosis induced by oxidative stress. Moreover, cobalamin has a significant protection impact on apoptosis and necrosis induced by Hcy and H_2O_2 ; hence ~70% of cells were protected from apoptosis and necrosis which correlated with reduction in caspase-3 in the apoptosis condition or reduction in free penetration of PI in the necrosis condition, which indicates a novel role of cobalamin as antioxidant activity despite being a cofactor enzyme as recent studies confirm this finding (Birch *et al.*, 2009). The protection was not limited to the sk-hep1 cells but it was also found in Jurkat cells. At the same time, there was no toxicity effect on the cells observed from cobalamin and folate on sk-hep1 and Jurkat cells. This study showed clearly the protective role of folate and cobalamin which support other studies that suggested folate and cobalamin administration improve the severity of coronary heart disease and prevents endothelial dysfunction (Chamber *et al.*, 2000). Also, it has examined the protective effect of folate on U937 cells against apoptosis induced by 7-ketocholesterol (Huang *et al.*, 2004).

Furthermore, the result showed that cobalamin and folate have the ability to reduce ROS and superoxide activity. This finding agreed with previous research which suggested that folate have the ability to reduce ROS (Huang *et al.*, 2004).

To conclude, the result in this chapter clearly demonstrates that under oxidative stress apoptosis and necrosis occurred in a dose dependent manner in different cells types. Folate and cobalamin provide significant protection against apoptosis and necrosis. Also, the result indicates that cobalamin function is not only as a cofactor enzyme but it plays a vital role in anti-oxidative activity. The folate and cobalamin protection was associated with reduction in the ROS and super oxide which indicate that folate and cobalamin had a significant effect on the apoptosis signalling.

The mechanisms of cobalamin protection is still not clearly understood, and possibly the Hsps plays a vital role in this protection. This hypothesis will be investigated in the next chapter.

Chapter 4

Heat Shock Proteins Induction By Cobalamin

4.1 Introduction:

Heat shock proteins are up-regulated to protect against various physiological and environmental stress conditions (Binder *et al.*, 2004). It has been demonstrated *in vitro* and *in vivo* that over-expression of Hsps can prevent apoptosis induced by chemicals or non-lethal thermal stress (Musch *et al.*, 1996; Otani *et al.*, 1997; Ren *et al.*, 2001; Ropeleski *et al.*, 2003; Kojima *et al.*, 2003). Over-expression of Hsp27 protects hippocampal progenitor cells (Son *et al.*, 2005), HeLa cells (Tsuchiya *et al.*, 2005) and breast cancer cells (Casado *et al.*, 2007) from apoptosis.

Furthermore, Hsp27 over-expression protects cells from necrosis induced by oxidative stress (Mehlen *et al.*, 1995). The chaperone activity of Hsp27 reduces the toxic effect of oxidised proteins, and Hsp27 has the ability to induce glutathione thereby increasing the antioxidant defence of the cells (Arrigo *et al.*, 2005).

Several studies have shown previously that induction of HO-1 by different stimuli provides an important cellular defence mechanism against tissue injury (Motterlini. *et al.*, 1996, Tian. *et al.*, 2001; Amersi. *et al.*, 1999; Clark. *et al.*, 2000, Yet. *et al.*, 2001, Foresti. *et al.*, 1999). While, over-expression of HO-1 inhibits apoptosis in vascular smooth muscle cells (Liu. *et al.*, 2005).

Over-expression of Hsp72 provides protection against cell death induced by oxidative stress (Huot *et al.*, 1991; Mehlen *et al.*, 1993), hyperthermia (Landry, 1989), and anticancer drugs (Huot *et al.*, 1991; Garrido *et al.*, 1997). It has been reported that Hsp72 has the ability to protect cells from both apoptosis and necrosis induced by oxidative stress (Samali *et al.*, 1996; Lindquist, 1986; Creagh & Cotter, 1999; Creagh, 2000; Ohkawara *et al.*, 2006; Batelli *et al.*, 2008). Hsp90 is likely to play a role in the oxidative stress as it is induced in vascular smooth muscle cells during oxidative stress (Liao *et al.*, 2000).

The aim of this chapter is to investigate whether cobalamin and folate induce Hsps, and if Hsps are involved in the protection mechanism of cobalamin.

4.2 Methods

All preparations and cell culture experiments were carried out within a class II tissue culture hood.

4.2.1 Sk-hep1 cells preparation.

Cells were passage every 3 days as described in (section 2.4.1).

4.2.2 Jurkat cells preparation

Cells were passage every 3 days as described in (section 2.4.2)

4.2.3 Cells count and viability test by trypan blue exclusion:

For the flow cytometry assays, following treatment cells were re-suspend in to the media by pipetting. Cells were then counted and assessed by trypan blue exclusion (section 2.4.6)

4.2.4 Measurement of intracellular Hsps

Following test conditions, cells were processed for staining and analysis as described in (section 2.4.13)

The antibodies used were: Anti-Hsp27 mouse monoclonal FITC conjugated antibody, Anti-HO-1 mouse monoclonal FITC conjugated antibody, Anti-Hsp72 mouse monoclonal FITC conjugated antibody and Anti-Hsp90 mouse monoclonal R-Phycoerythrin conjugated antibody. The dilution was 1:100.

4.2.5 Inhibition of HO-1 and Hsp72

For inhibition of HO-1, cells were pre-treated with 12.5 μ M SN (IV) Protoporphyrin IX dichloride for 4 hours then subjected to the test compounds.

For inhibition of the Hsp72, cells were pre-treated with 200 μ M KNK437 for 1 hour, and then cells subjected to the test compounds.

4.2.6 Induction of HO-1 and Hsp72

In order to induce HO-1 prior to treatment with test compound, cells were subjected to 12 μ M Hemin for 2 hours.

For the induction of the Hsp72 prior treatment, cells were heat shocked at 42°C for 1 hour and then incubated at 37°C for 2 hours.

4.2.7 Determination of apoptosis

Cells were plated on to a black 96 well cell plate, treated under test conditions and then analysed for apoptosis by determination of caspase-3/7 activity (section 2.4.9).

4.2.8 Determination of necrosis:

Cells were plated on to a black 96 well cell plate, treated under test condition then analysed for necrosis by PI incorporation (section 2.4.11).

The treatment with Hcy+cobalamin or folate will be referred to as cobalamin-apoptosis protection or folate-apoptosis protection.

4.3 Result

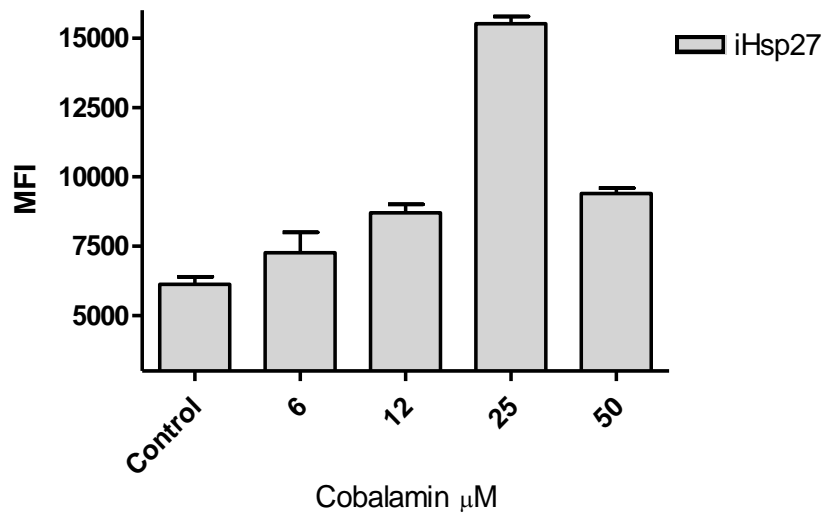
4.3.1 Induction of intracellular Hsps under apoptosis induced by oxidative stress and under apoptosis protection conditions:

4.3.1.1 Impact of cobalamin on intracellular Hsps:

In order to investigate the impact of cobalamin on intracellular Hsps, sk-hep1 cells were treated with a range of cobalamin concentrations (0-50 μ M) for 2 hours, which resulted in a significant effect ($P < 0.001$, as determined by one-way ANNOVA), (Figures 4.1& 4.2). The Post-hoc comparison showed that at $\geq 12\mu$ M of cobalamin there was a significant induction of iHsp27 ($P < 0.05$), iHO-1 ($P < 0.05$), iHsp72 ($P < 0.05$) and iHsp90 ($P < 0.01$) compared to control cells. The induction of the iHsps peaked at 25 μ M cobalamin ($P < 0.001$) followed by a significant reduction in iHsp27 ($P < 0.001$), iHO-1 ($P < 0.05$), iHsp72 ($P < 0.01$) and iHsp90 ($P < 0.01$) at higher concentrations (50 μ M) as compared to 25 μ M cobalamin treatment.

The histograms demonstrate the induction of iHsps when sk-hep1 exposed to 25 μ M cobalamin. The significant increase in the intensity fluoresces of iHsp27, iHO-1, iHsp72 and iHsp90 compared to control cells can be visualised clearly in the histograms (Figure 4.3).

A.



B.

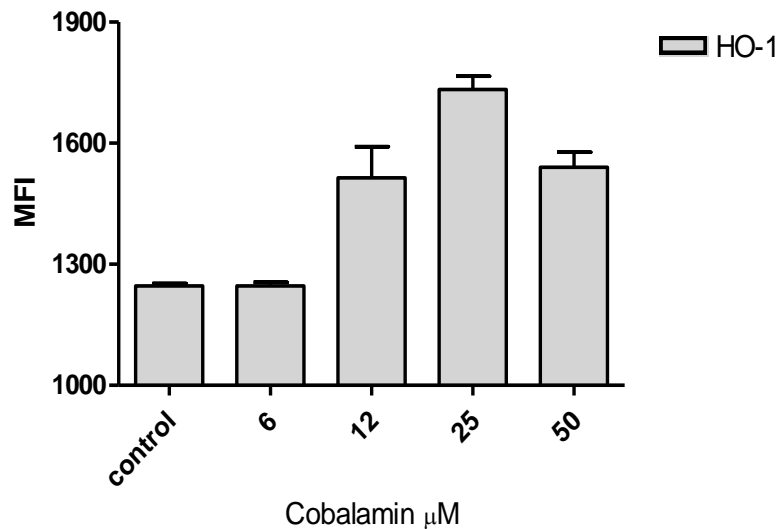
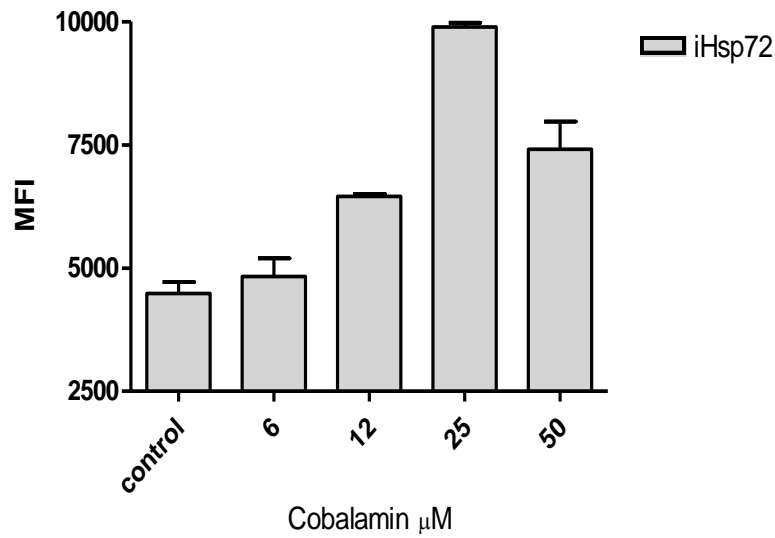


Figure 4.1: Effect of cobalamin on the iHsp27 and iHO-1 level. Sk-hep1 cells were treated with a range of cobalamin concentrations (0-50 μ M) for 2 hours, control cells were not treated. Cells were then stained with monoclonal mouse **A.** Anti-Hsp27 or **B.** Anti-HO-1 FITC labelled antibodies and analyzed using Flow cytometry and BD FACSDiva software. The Data are means \pm SD n=4, $p < 0.001$ as determined by one-way ANOVA. Baseline (control) vs 12 μ M ($p < 0.05$), 25 μ M ($p < 0.001$), 50 μ M ($p < 0.01$) as determined by Tukey *post hoc*.

A.



B.

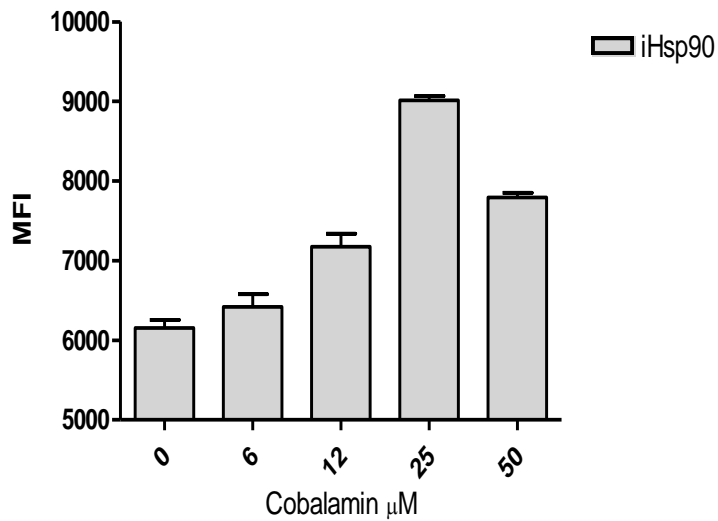
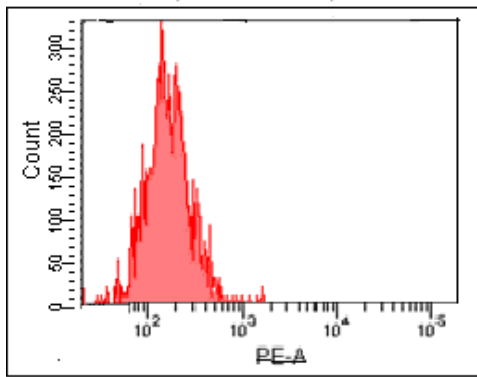
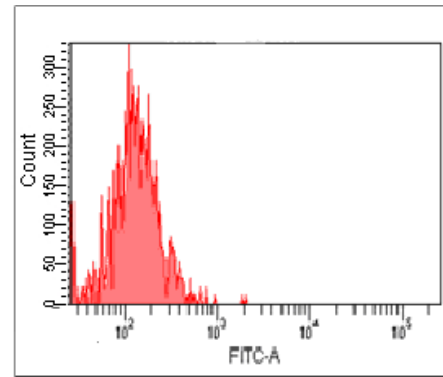


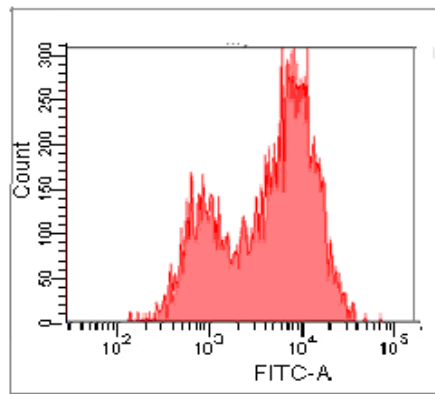
Figure 4.2: Effect of cobalamin on iHsp72 and iHsp90. Sk-hep1 cells were treated with a range of cobalamin concentrations (0-50 μM) for 2 hours, control cells were non-treated. Cells were then stained with monoclonal mouse **A.** Anti-Hsp72 FITC labelled or **B.** Anti-Hsp90 PE labelled antibodies and analyzed using Flow cytometry and BD FACSDiva software. The Data are means \pm SD $n=4$, $p < 0.001$ as determined by one-way ANOVA. Baseline (control) vs 12 μM ($p < 0.05$), 25 μM ($p < 0.001$), 50 μM ($p < 0.01$) as determined by Tukey *post hoc*.



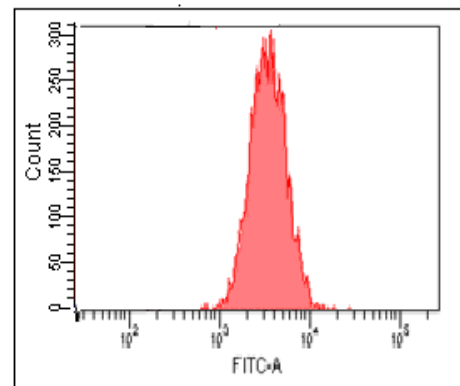
A. PE control cells



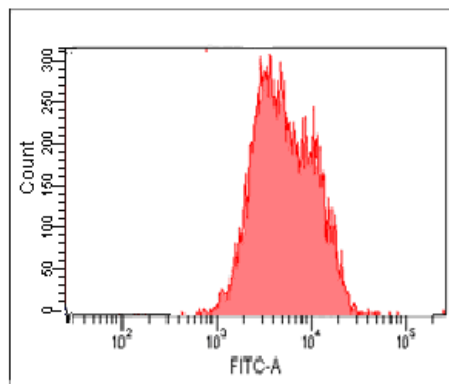
B. FITC control



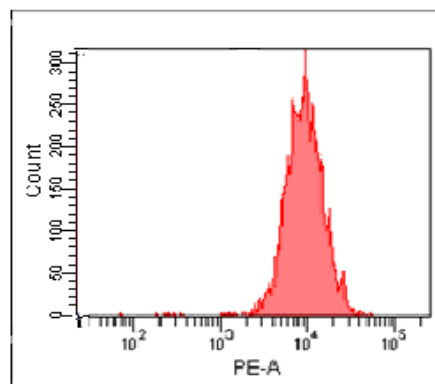
C. iHsp27



D. HO-1



E. iHsp72

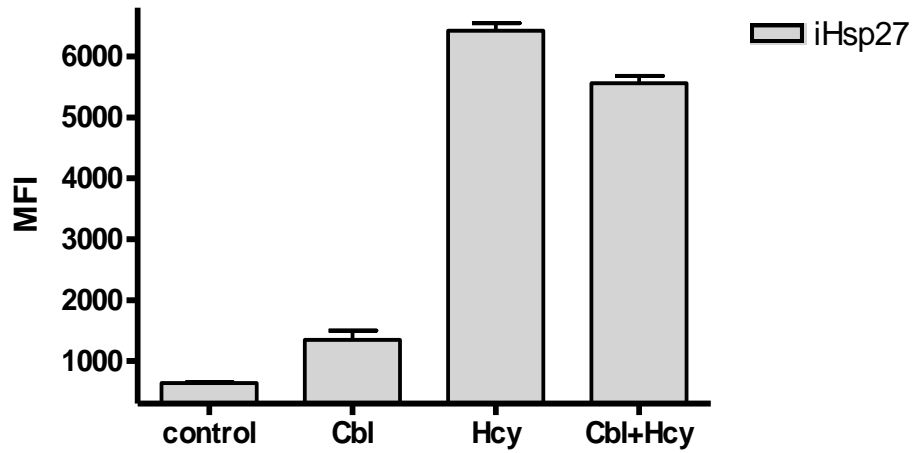


F. iHsp90

Figure 4.3: Effect of cobalamin on intracellular Hsps level. Sk-hep1 cells were treated with 25 μ M cobalamin for 2 hours then cells were stained with specific antibodies and analyzed using Flow cytometry BD FACSDiva. **A.** non treated cells PE control, **B.** non treated cells FITC control, **C.** iHsp27 **D.** iHO-1, **E.** iHsp72, and **F.** iHsp90.

In the previous chapter it had been demonstrated that 25 μ M cobalamin protects cells from apoptosis induced by 3.125 μ M Hcy. In this chapter, the intracellular Hsps under apoptosis and protection conditions were examined. There were significant effect on iHsps under apoptosis and protection condition ($p < 0.001$, as determined by one-way ANNOVA), (Figures 4.4& 4.5). Further analysis with Tukey pairwise showed that iHsp27 were increased significantly at 3.125 μ M Hcy and reached 97% ($p < 0.001$) as compared to control cells. However, pre-incubation with 25 μ M cobalamin for 2 hours followed by 2 hours incubation with 3.125 μ M Hcy, decreased iHsp27 by 20% in comparison to Hcy treatment only. On the other hand, at 3.125 μ M Hcy iHO-1, iHsp72, and iHsp90 elevated up to 70%, 53%, and 58% respectively ($p < 0.001$), while incubating cells with 25 μ M cobalamin prior to exposure to 3.125 μ M Hcy, the iHO-1, iHsp72 and iHsp90 reached 98% induction ($p < 0.001$).

A.



B.

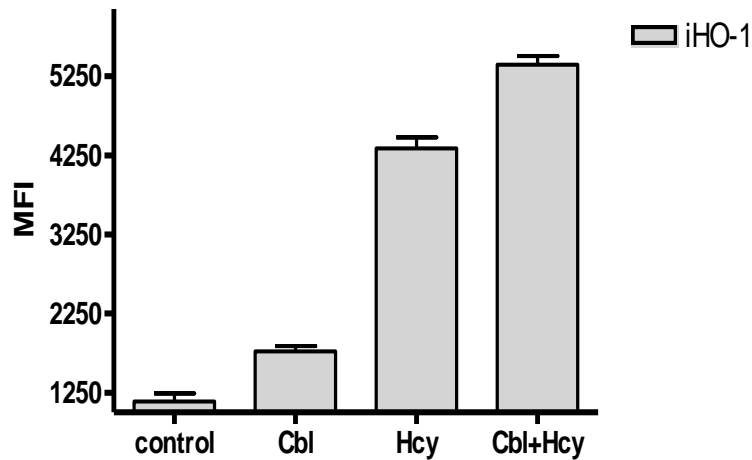
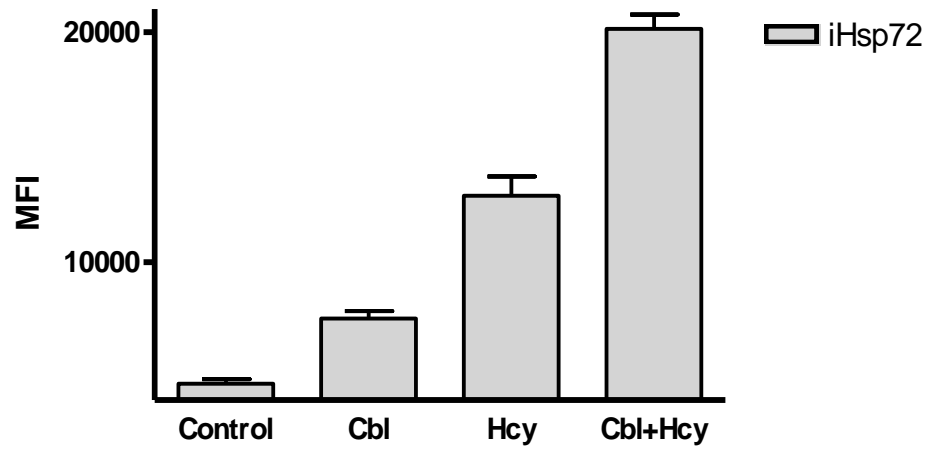


Figure 4.4: Intracellular Hsp27 and HO-1 during cobalamin apoptosis-protection. Sk-hep1 cells were pre-treated with 25 μ M cobalamin for 2 hours followed by 2hours treatments with 3.125 μ M Hcy, then cells were stained with monoclonal mouse **A.** Anti-Hsp27 or **B.** Anti-HO-1 FITC labelled and analyzed using Flow cytometry, Control cells were non-treated. The Data are means \pm SD n=4, $p < 0.001$ as determined by one-way ANOVA. Baseline (control) vs Cbl ($p < 0.05$), Hcy ($p < 0.001$), Cbl+Hcy ($p < 0.001$) as determined by Tukey *post hoc*.

A.



B.

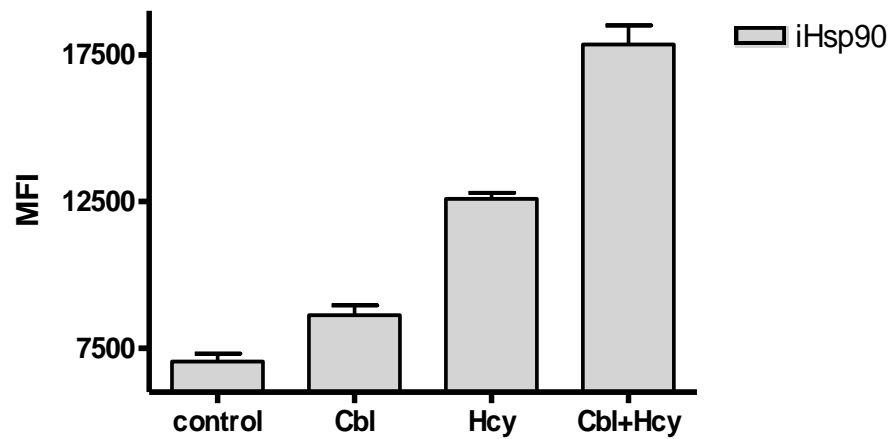


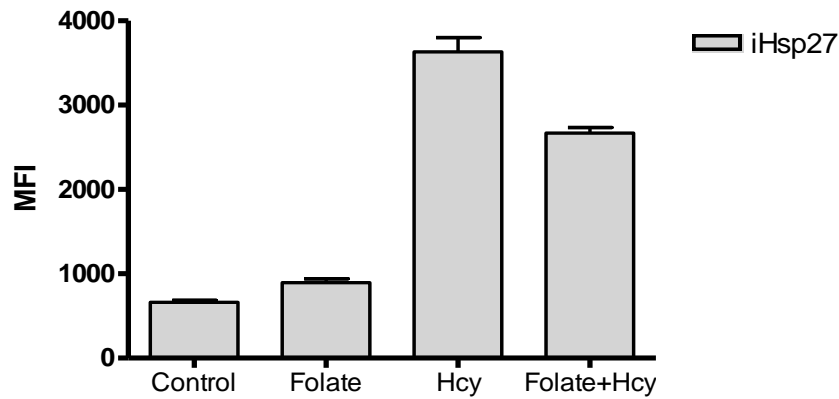
Figure 4.5: Intracellular Hsp72 and Hsp90 during cobalamin apoptosis-protection. Sk-hep1 cells were pre-treated with 25 μ M cobalamin for 2 hours followed by 2hours treatments with 3.125 μ M Hcy, then cells were stained with monoclonal mouse **A.** Anti-Hsp72 FITC labelled or **B.** Anti-Hsp90 PE labelled antibodies and analyzed using Flow cytometry, control cells were non-treated. The Data are means \pm SD n=4, $p < 0.001$ as determined by one-way ANOVA. Baseline (control) vs Cbl ($p < 0.05$), Hcy ($p < 0.01$), Cbl+Hcy ($p < 0.001$) as determined by Tukey *post hoc*.

4.3.1.2 Induction of intracellular Hsps under oxidative stress and under protection from apoptosis *via* folate in sk-hep1:

As previously demonstrated that cobalamin has a significant effect on intracellular Hsps under apoptosis protection conditions, so the aim is to investigate intracellular Hsps under folate-apoptosis protection conditions.

Folate treatment had a significant effect on iHsps ($P < 0.001$, as determined by one-way ANNOVA), (Figures 4.6 & 4.7). The Tukey comparison showed that exposing cells to 30 μ M folate had no significant effect on iHsp27 ($P > 0.05$) but it had induced iHO-1 significantly ($P < 0.05$). However, iHsp27 reached 98% at 3.125 μ M Hcy, while pre-incubation with folate reduced iHsp27 by 25%. In the same time 75% of HO-1 was induced by Hcy and reached 100% when cells were pre-incubated with folate (Figure 4.6). Additionally, folate treatment alone induced iHsp72 ($P < 0.05$) and iHsp90 ($P < 0.05$) significantly compared to control cells (non-treated). Moreover 51% of iHsp72 and 46% of iHsp90 increased at 3.125 μ M Hcy ($P < 0.001$) to reach 100% induction of iHsp72 and iHsp90 when cells were exposed to folate prior to treatment with Hcy (Figure 4.7).

A.



B.

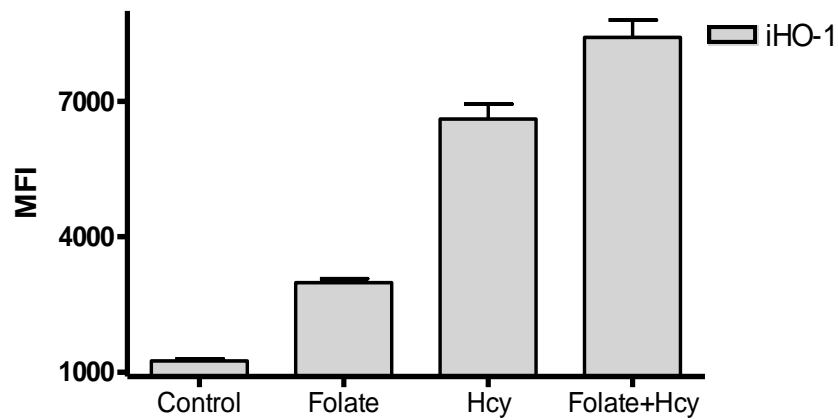
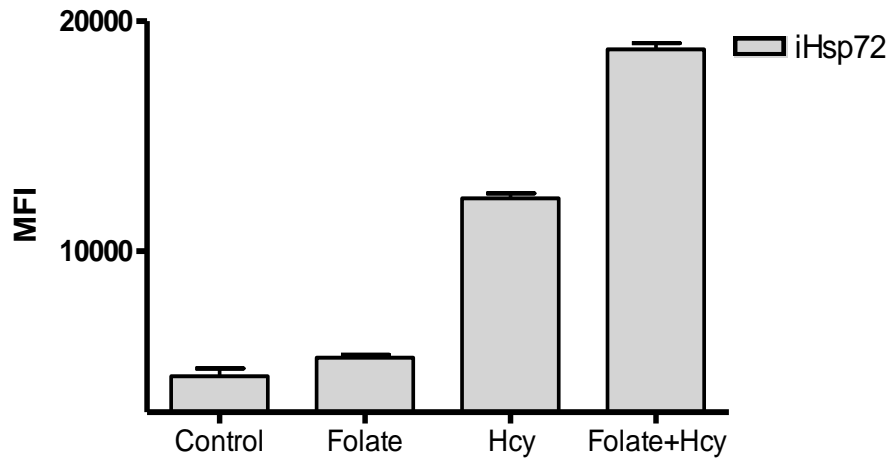


Figure 4.6: Effect of folate on iHsp27 and iHO-1 induction. Sk-hep1 cells were pre-treated with 30 μ M folate for 2 hours followed by 2hours treatments with 3.125 μ M Hcy, or 30 μ M folate alone or 3.125 μ M Hcy. Cells were then stained with monoclonal mouse **A.** Anti-Hsp27 or **B.** Anti-HO-1 FITC labelled antibodies and analyzed by flow cytometry, control cells were non-treated. The Data are means \pm SD n=4, $p < 0.001$ as determined by one-way ANOVA. Baseline (control) vs folate ($p < 0.05$)-HO-1, Hcy ($p < 0.001$), folate+Hcy ($p < 0.001$) as determined by Tukey *post hoc*.

A.



B.

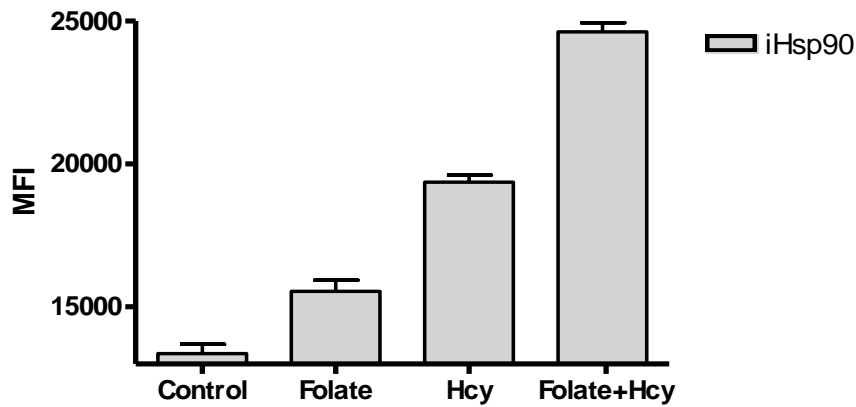


Figure 4.7: Effect of folate on iHsp72 and iHsp90 induction. Sk-hep1 cells were pre-treated with 30 μ M folate for 2 hours followed by 2hours treatments with 3.125 μ M Hcy 30 μ M folate alone or 3.125 μ M Hcy, Cells were then stained with monoclonal mouse **A.** Anti-Hsp72 FITC or **B.** Anti-Hsp90 PE labelled antibodies and analyzed by flow cytometry, control cells were non-treated. The Data are means \pm SD n=4, $p < 0.001$ as determined by one-way ANOVA. Baseline (control) vs Folate ($p < 0.05$)-HO-1, Hcy ($p < 0.001$), folate+Hcy ($p < 0.001$) as determined by Tukey *post hoc*.

4.3.2 The impact of overexpression and inhibition of Hsp72 on apoptosis induced by oxidative stress and protected by cobalamin:

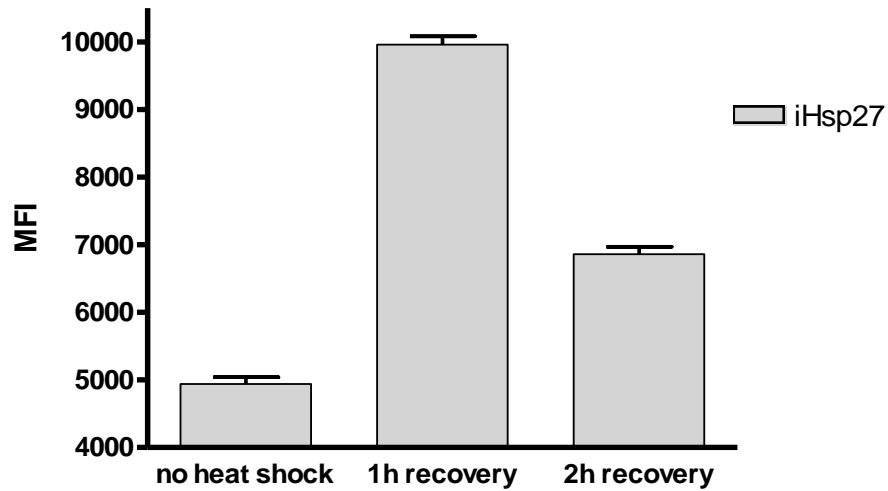
4.3.2.1 Induction of Hsp72 and oxidative stress.

Previously it had been demonstrated that iHsps were induced by cobalamin. So the potential involvement of these proteins in the cobalamin-apoptosis protection was investigated.

Sk-hep1 cells were heat shocked at 42°C for 1 hour followed by 2 hours recovery at 37°C which resulted in a significant effect on the iHsp27 and iHsp72 ($P<0.001$, as determined by one-way ANNOVA), (Figure 4.8). The post-hoc comparison showed significant increase in iHsp27 and iHsp72 after 1 hour ($P<0.001$) and 2 hours recovery ($P<0.001$) compared to control cells (non-treated). Although there was a significant reduction in both iHsp27 and iHsp72 after 2 hours recovery compared to 1 hour recovery ($P<0.001$), (Figure 4.8).

Interestingly, the overexpression of iHsp27 and iHsp72 had significant effect on caspase-3 ($P<0.001$, as determined by two-way ANNOVA), (Figures 4.9, 4.10 & 4.11). The post-hoc comparison showed that induction of iHsp27 and iHsp72 prior to treatment with 3.125 μ M Hcy or H₂O₂ for 2 hours (these concentrations previously proved to induce apoptosis), showed a significant reduction in caspase-3 after 1 and 2 hours recovery prior to treatment with Hcy ($P<0.001$) or H₂O₂ ($P<0.001$) compared to Hcy or H₂O₂ treatment alone (Figure 4.9). However, 1 hour recovery partially protected the cells from apoptosis induced by Hcy ($P<0.05$) or H₂O₂ ($P<0.001$) compared to control, whereas 2 hours recovery provided complete protection against apoptosis induced by Hcy ($P>0.05$) or H₂O₂ ($P>0.05$), (Figure 4.10). At the same time there was no significant detection of necrosis activity in the heat shocked and cells recovered for 1 hour or 2 hours as compared to non-treated cells ($P<0.05$), also cells recovered for 1 or 2 hours+Hcy showed no significant necrosis activity as compared to non-treated cells ($P<0.05$), (Figure 4.11).

A.



B.

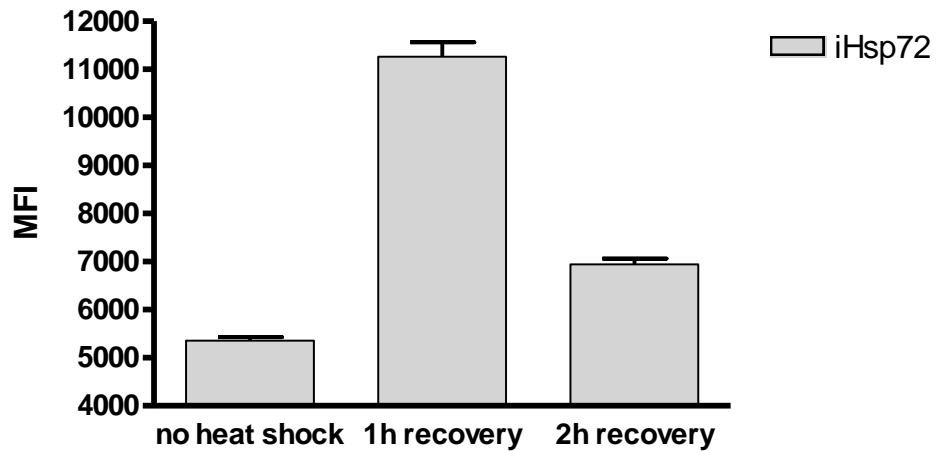
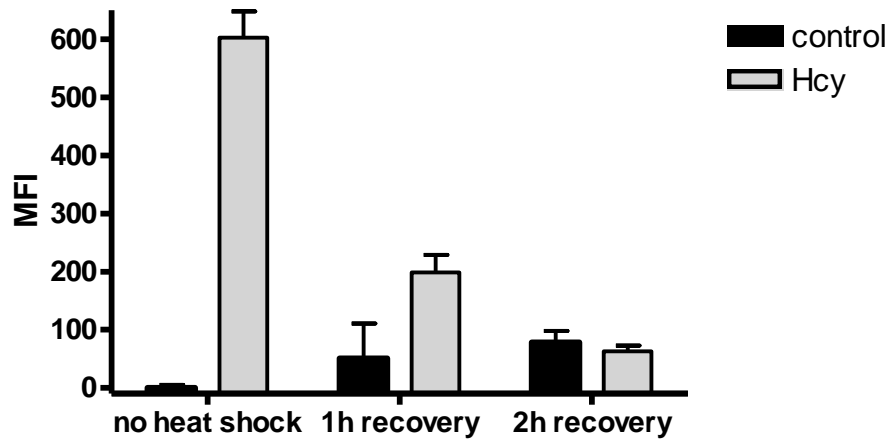


Figure 4.8: Induction of iHsp27 and iHsp72 in sk-hep1. Cells were heat shocked for 1hour at 42°C followed by 1hour and 2 hours recovery at 37°C prior treatments with 3.125µM Hcy for 2 hours. Cells were then stained with monoclonal mouse **A.** Anti-Hsp27 or **B.** Anti-Hsp72 FITC labelled antibodies and analyzed by flow cytometry, control cells were non-treated. The Data are means \pm SD n=4, $p < 0.001$ as determined by one-way ANOVA. Baseline (control) vs 1h recovery ($p < 0.001$), 2h recovery ($p < 0.001$) as determined by Tukey *post hoc*.

A.



B.

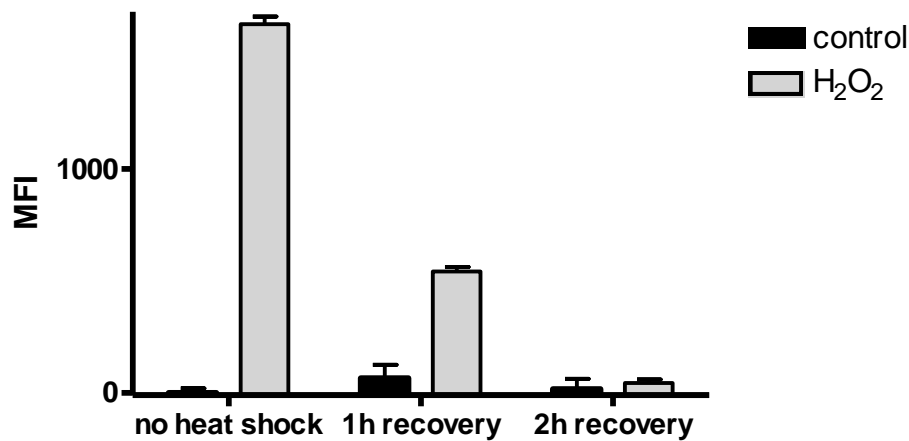


Figure 4.9: Effect induction of Hsp72 on caspase-3 activity induced by Hcy or H₂O₂. Sk-hep1 cells were heat shocked for 1hours at 42°C and followed by 1hour and 2 hours recovery at 37°C prior treatments with 3.125μM **A.** Hcy or **B.**H₂O₂ for 2 hours. Caspase-3 was measured after by staining the cells with monoclonal anti-caspase-3 FITC congregated antibodies and analyzed by flow cytometry, control cells were heat shocked for 2 hours at 42°C. The Data are means ± SD n=4, p< 0.001 as determined by two-way ANOVA. Baseline (control) vs 1h recovery+ H₂O₂ or Hcy (p<0.01), H₂O₂ or Hcy (p<0.001) as determined by Bonferroni *post hoc*.

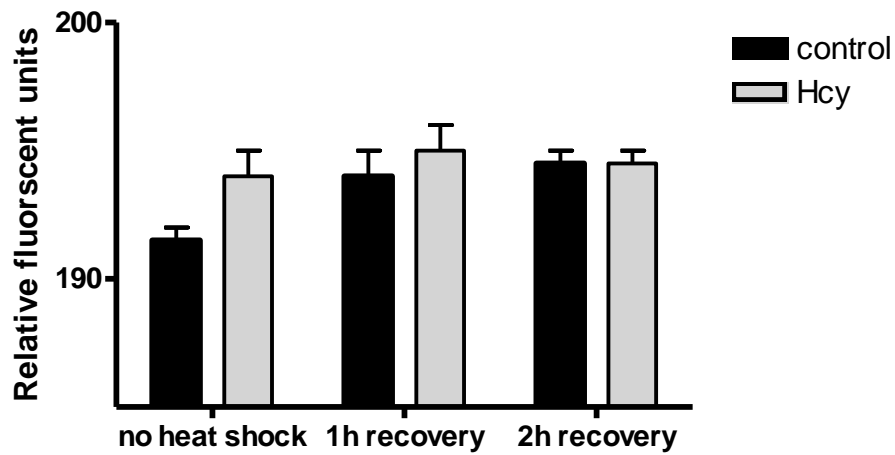
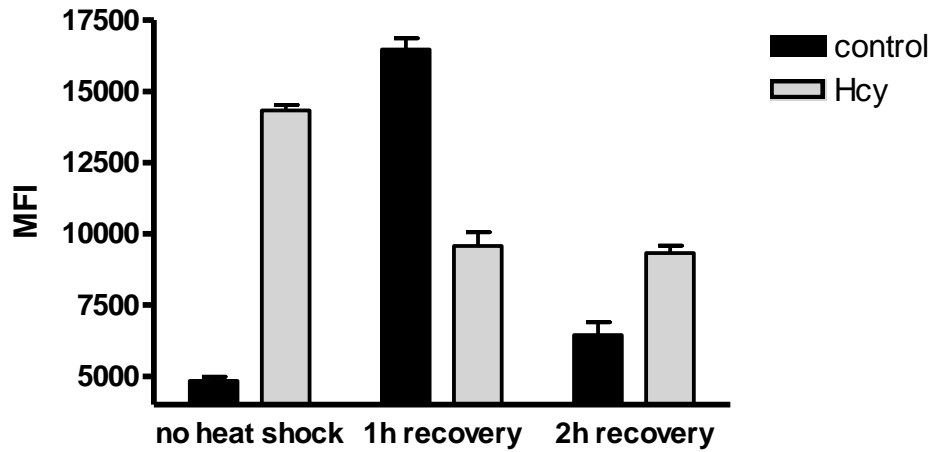


Figure 4.10: Effect of induction of the Hsp72 on necrosis activity under oxidative stress. Sk-hep1 cells were heat shocked for 1 hour at 42°C followed by 1hour and 2 hours recovery at 37°C prior treatments with 3.125 μ MHcy for 2 hours. Necrosis measured at EX=535/EM=617. , control cells were non-treated. The Data are means \pm SD n=4, $p>0.05$ as determined by two-way ANOVA.

The heat shock and recovery had significant effect on iHsps ($P < 0.001$, as determined by two-way ANNOVA), (Figures 4.11, 4.12, 4.13 & 4.14). Further analysis with Bonferroni pairwise showed that exposing cells for 1 hour at 42°C followed by 1 hour or 2 hours incubation at 37°C (when apoptosis reduced), showed a significant increase in iHsp27 ($P < 0.001$), iHsp72 ($P < 0.001$) and iHsp90 ($P < 0.001$) with no effect on iHO-1 ($P > 0.05$) as compared to control cells. Moreover, after 2 hours of recovery the iHsp27 showed significant induction under oxidative stress+ recovery more than under recovery only ($P < 0.001$). However, after 1 hour of recovery showed a significant induction of iHsp27 more than under 1 hour of recovery+oxidative recovery only ($P < 0.001$). During the same time, iHsp27 significantly increased at 3.125 μ M Hcy or H₂O₂ (under apoptosis condition) more than non-treated cells ($P < 0.001$) (Figure 4.11). Whereas after 1 or 2 hours recovered + oxidative stress treated cells, iHO-1 was significantly more than those in 1 or 2 hours recovered cells only ($P < 0.001$), (Figure 4.12). Additionally, cells subjected to 3.125 μ M Hcy or H₂O₂ (apoptosis condition) induced iHsp72 significantly when compared to control cells ($P < 0.001$). After 1 hour of recovery it showed a significant increase of iHsp72 more than 1 hour recovered+oxidative treated cells ($P < 0.001$), however, 2 hours recovered cells showed significant reduction of iHsp72 compared to 2 hours recovered+oxidative treated cells ($P < 0.001$) (Figure 4.13). Furthermore, iHsp90 induced at 3.125 μ M Hcy or H₂O₂ above control cells ($P < 0.001$). While 1 hour recovered cells resulted in significant increase in the iHsp90 more than 1 hour recovered+oxidative ($P < 0.001$), but there was no significant difference in the iHsp90 after 2 hours recovered cells compared to 2 hours recovered+ recovered+oxidative treated cells ($P > 0.05$), (Figure 4.13).

A.



B.

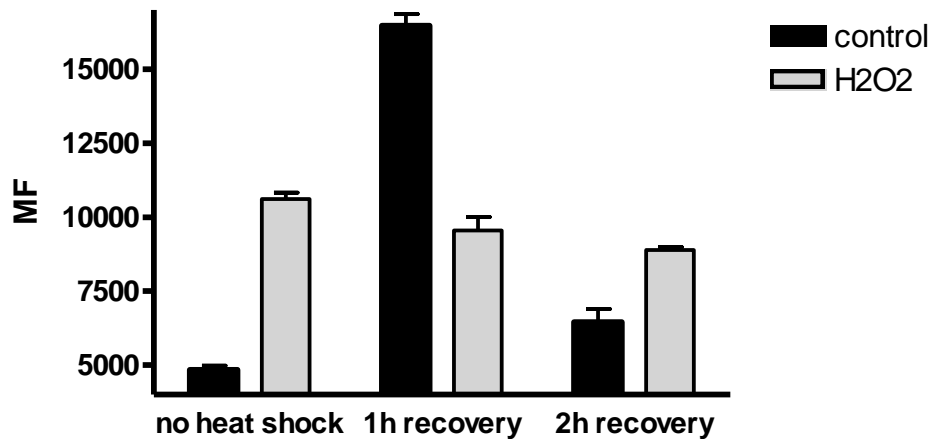
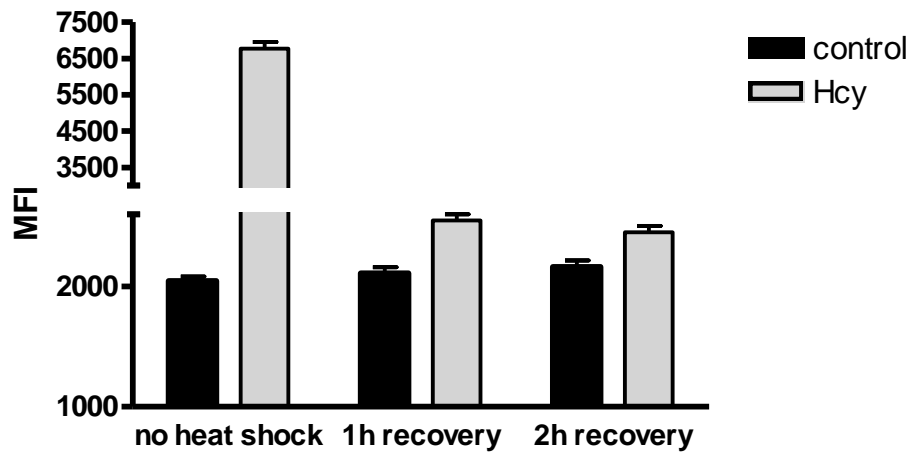


Figure 4.11: The intracellular Hsp27 after heat shock and apoptosis induction by oxidative stress. Sk-hep1 cells were incubated for 1 hour at 42°C followed by 1 hour and 2 hours recovery at 37°C prior treatments with **A.** 3.125 μM Hcy or **B.** 3.125 μM H₂O₂ for 2 hour. Cells were then stained with monoclonal mouse anti-Hsp27 FITC labelled antibodies and analyzed by flow cytometry and BD FACSDiva, control cells were heat shocked for 1 hour at 42°C. The Data are means ± SD n=4, p< 0.001 as determined by two-way ANOVA. Baseline (control) vs H₂O₂ or Hcy (p<0.01), 1h recovery+H₂O₂ or Hcy (p<0.001) 2h recovery+H₂O₂ or Hcy (p<0.01) as determined by Bonferroni *post hoc*.

A.



B.

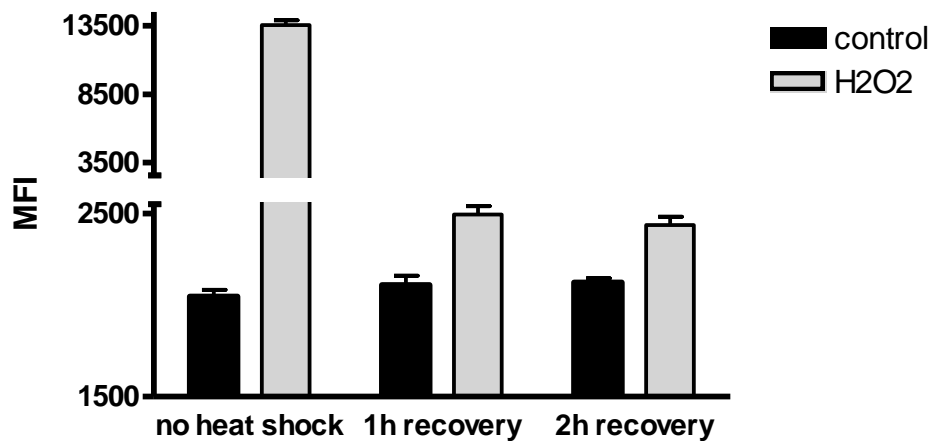
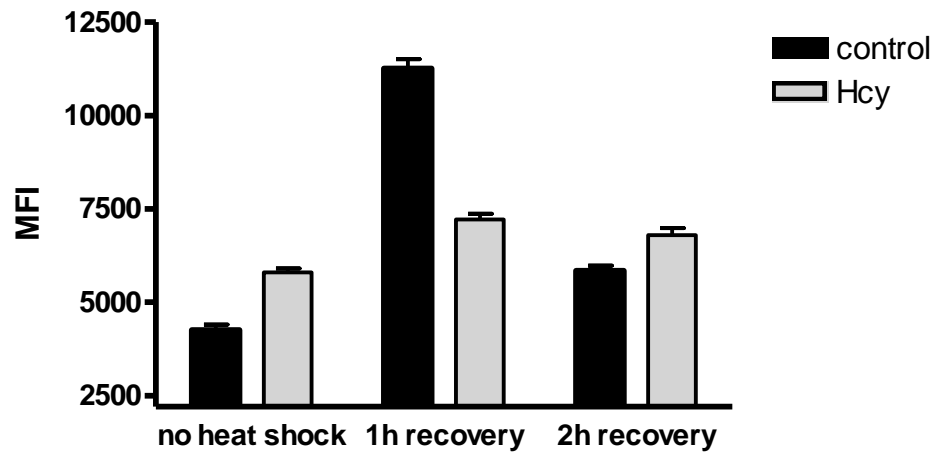


Figure 4.12: The intracellular HO-1 after heat shock and apoptosis induction by oxidative stress. Sk-hep1 cells were incubated for 1 hour at 42°C followed by 1hour and 2 hours recovery at 37°C prior treatments with **A.** 3.125μM Hcy or **B.** 3.125μM H₂O₂ for 2 hour. Cells then were stained with monoclonal mouse anti-HO-1 FITC labelled antibodies and analyzed by flow cytometry and BD FACSDiva, control cells were heat shocked for 1 hour at 42°C. The Data are means ± SD n=4, p< 0.001 as determined by two-way ANOVA. Baseline (control) vs H₂O₂ or Hcy (p<0.001), 1h recovery+H₂O₂ or Hcy (p<0.01) 2h recovery+H₂O₂ or Hcy (p<0.01) as determined by Bonferroni *post hoc*.

A.



B.

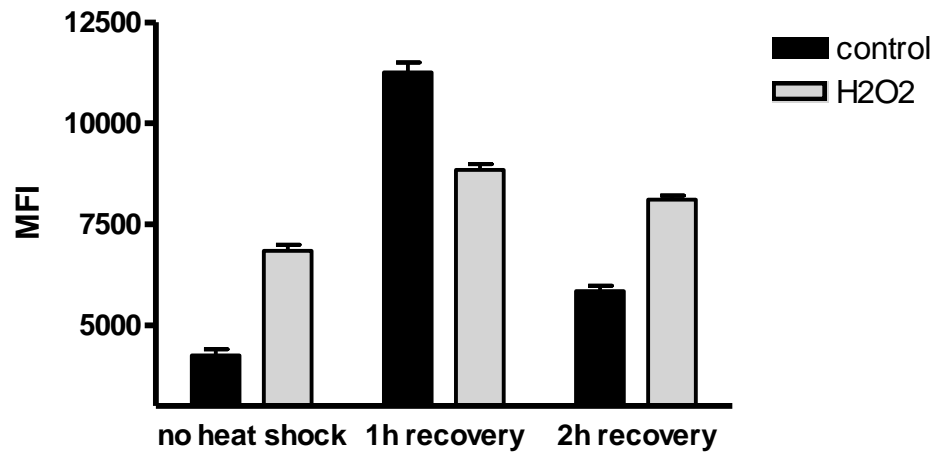
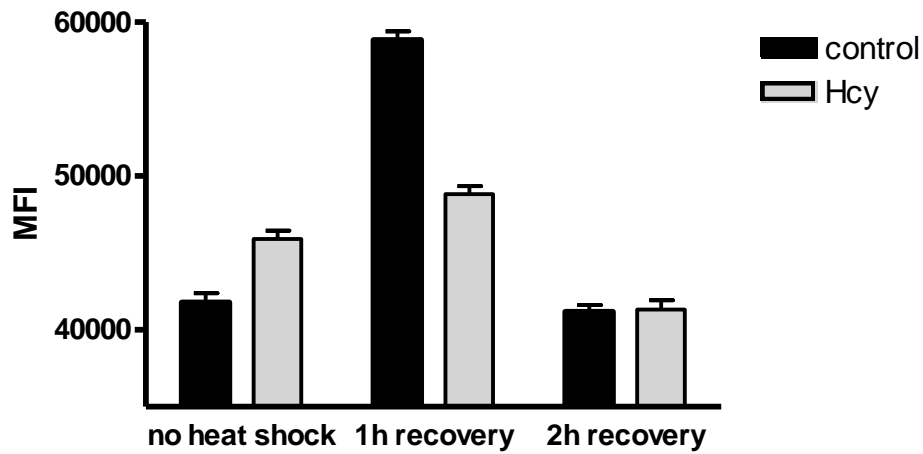


Figure 4.13: The intracellular Hsp72 after heat shock and apoptosis induction by oxidative stress. Sk-hep1 cells were incubated for 1 hour at 42°C followed by 1hour and 2 hours recovery at 37°C prior treatments with **A.** 3.125μM Hcy or **B.**3.125μM H₂O₂ for 2 hours. Cells then stained with monoclonal mouse anti-Hsp72 FITC labelled antibodies and analyzed by flow cytometry and BD FACSDiva, control cells were heat shocked for 1 hour at 42°C. The Data are means ± SD n=4, p< 0.001 as determined by two-way ANOVA. Baseline (control) vs H₂O₂ or Hcy (p<0.001), 1h recovery+H₂O₂ or Hcy (p<0.001) 2h recovery+H₂O₂ or Hcy (p<0.001) as determined by Bonferroni *post hoc*.

A.



B.

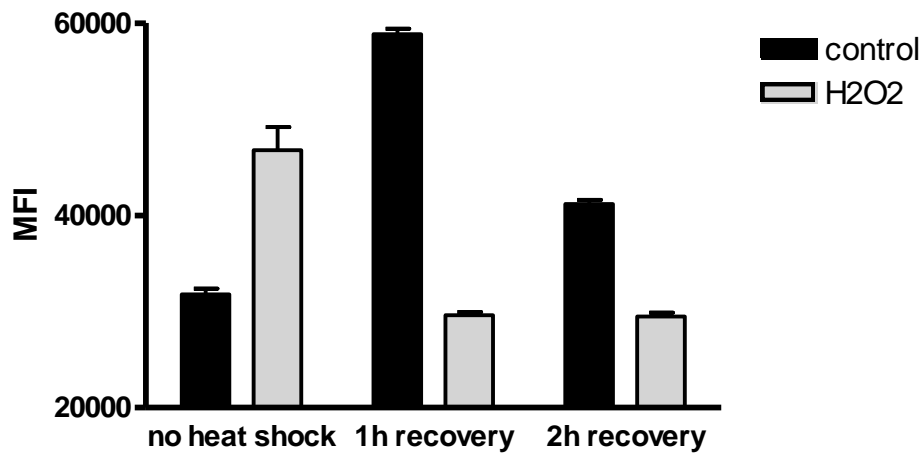


Figure 4.14: The intracellular Hsp90 after heat shock and apoptosis induction by oxidative stress. Sk-hep1 cells were incubated for 1 hour at 42°C followed by 1hour and 2 hours recovery at 37°C prior treatments with **A.** 3.125μM Hcy or **B.** H₂O₂ for 2 hours. Cells then were stained with monoclonal mouse anti-Hsp90 PE labelled antibodies and analyzed by flow cytometry and BD FACSDiva. Control cells were heat shocked for 1 hour at 42°C. The Data are means ± SD n=4, p< 0.001 as determined by two-way ANOVA. Baseline (control) vs H₂O₂ or Hcy (p<0.001), 1h recovery+H₂O₂ or Hcy (p<0.001) 2h recovery+H₂O₂ or Hcy (p<0.001) as determined by Bonferroni *post hoc*.

4.3.2.2 Effect of Hsp72 inhibition by KNK437 on cobalamin protection.

In order to inhibit iHsp72, cells subjected to 200 μ M KNK437 for 1 hour prior heat shock at 42°C for 1 hour and recovered for 1 hour at 37°C, resulted in significant inhibition of iHsps72 ($P<0.001$, as determined by one-way ANNOVA), (Figure 4.15). Moreover Tukey pairwise showed there was significant reduction of iHsp72 as compared to heat shocked and recovered cells ($P<0.001$). Also the inhibition of Hsp72 has no significant effect on necrosis activity in the cells treated with Hcy as compared to control cells ($P>0.05$, as determined by two-way ANNOVA), (Figure 4.16).

The inhibition of iHsp72 prevented cobalamin protecting cells from apoptosis induced by oxidative stress significantly ($P<0.001$, as determined by two-way ANNOVA), (Figures 4.17 & 4.18). The post-hoc comparison showed that when cells were treated with 200 μ M KNK437 for 1 hour, followed by 25 μ M cobalamin and 3.125 μ M Hcy or H₂O₂, the protection against Hcy or H₂O₂ induced apoptosis was lost ($P<0.001$), (Figure 4.17). Caspase activity was not significantly different from Hcy treated cells ($P>0.05$), (Figure 4.17). Similarly folate protection against Hcy or H₂O₂ induced apoptosis was lost following treatment with 200 μ M KNK437 for 1 hour ($P<0.001$), (Figure 4.18).

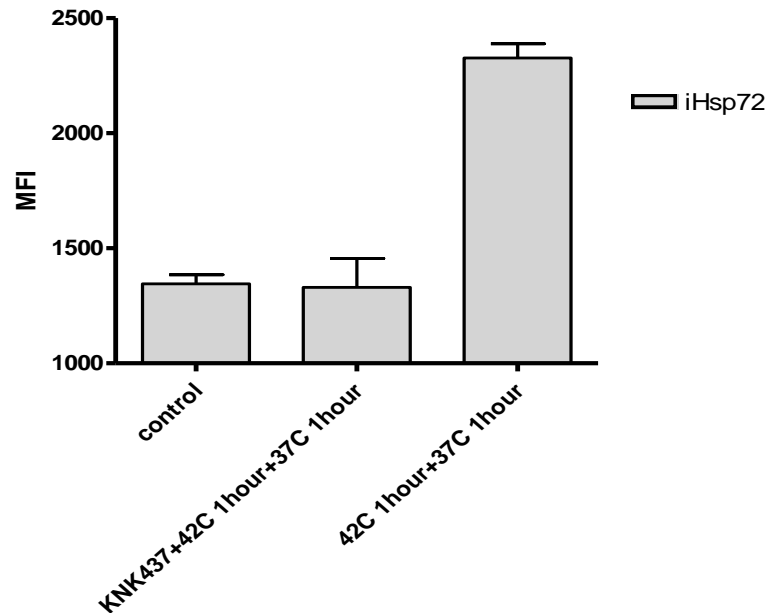


Figure 4.15: inhibition of Hsp72 by KNK437 in sk-hep1 cells. Sk-hep1 cells were pre-treated with 200 μ M KNK437 for 1hours followed by 1 hour exposure to 42°C and 1 hour at 37°C, control cells were non-treated cells. Cells were then stained with monoclonal anti-hsp72 FITC congegated and analyzed by flow cytometry and BD FACSDiva. The Data are means \pm SD n=4, $p < 0.001$ as determined by one-way ANOVA. 1h 42°C+1h at 37°C vs 1h 42°C+1h at 37°C+KNK437 ($p < 0.001$), as determined by Tukey *post hoc*.

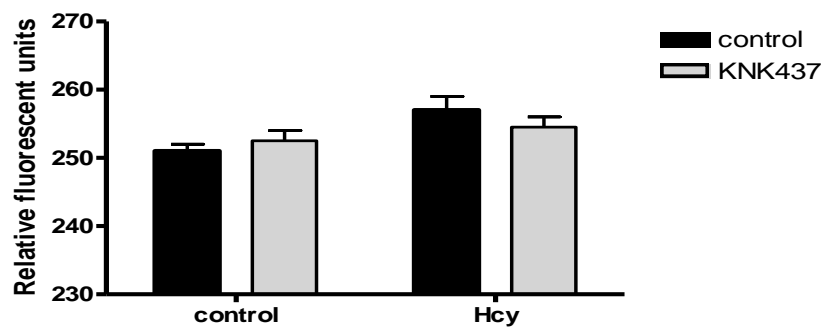
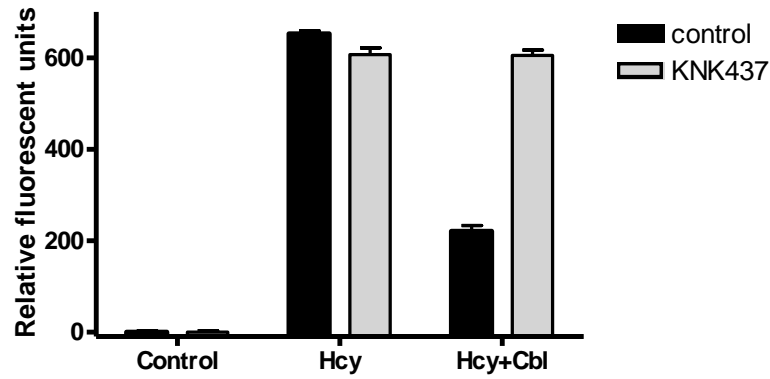


Figure 4.16: Effect of Hsp72 inhibition on necrosis activity under oxidative stress. Sk-hep1 cells were pre-treated with 200 μ M KNK437 for 1 hours followed by 2 hours treatment with 3.125 μ M Hcy. Control cells were non-treated with inhibitor. Necrosis activity measured at EX=535/EM=617. The Data are means \pm SD n=4, $p > 0.05$ as determined by two-way ANOVA.

A.



B.

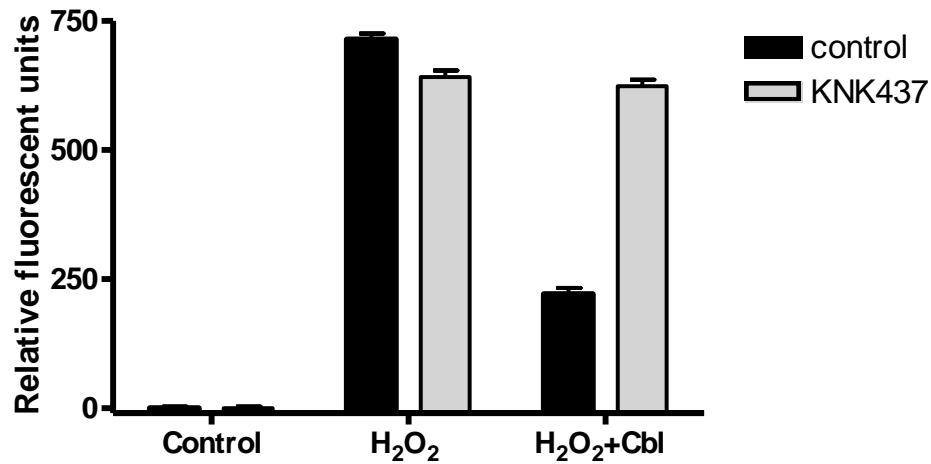
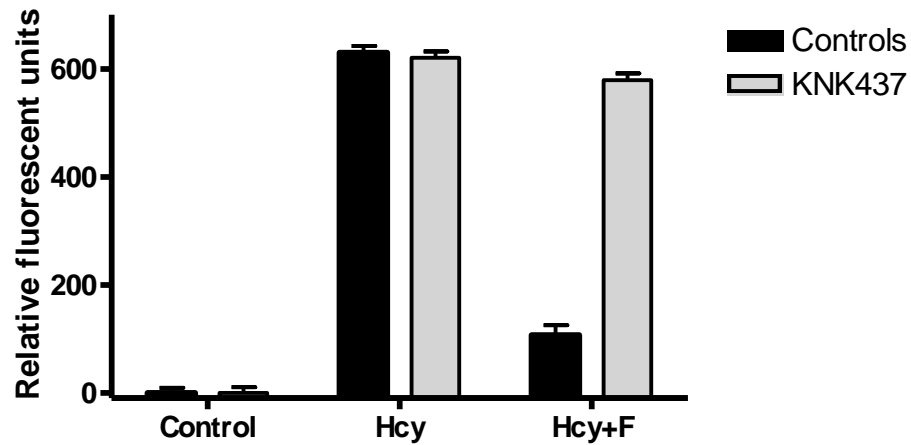


Figure 4.17: Effect of Hsp72 inhibition on cobalamin apoptosis-protection. Sk-hep1 cells were pre-treated with 200 μ M KNK437 for 1 hour followed by 2 hours treatment with 25 μ M cobalamin and 2 hours treatment with **A.** 3.125 μ M Hcy or **B.** H₂O₂. Cells were stained with monoclonal anti-caspase-3 FITC conjugated antibodies and analyzed by flow cytometry, control cells were non-treated with the inhibitor. The Data are means \pm SD n=4, $p < 0.001$ as determined by two-way ANOVA. H₂O₂ or Hcy+cbl vs H₂O₂ or Hcy+Cbl+KNK437 ($p < 0.001$), as determined by Bonferroni *post hoc*.

A.



B.

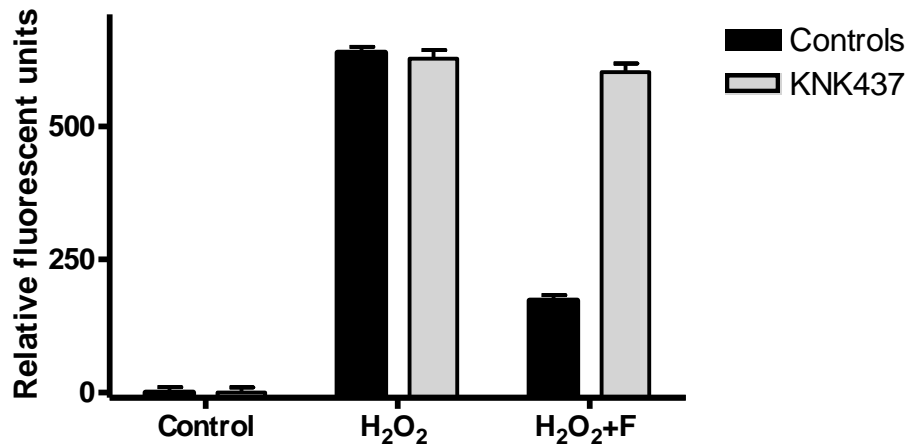


Figure 4.18: Effect of Hsp72 inhibition on folate apoptosis-protection. Sk-hep1 cells were pre-treated with KNK437 for 1 hour followed by 2 hours treatment with 25 μ M cobalamin or 30 μ M folate and 2 hours treatment with **A.** 3.125 μ M Hcy or **B.** 3.125 μ M H₂O₂. Cells stained with monoclonal anti-caspase-3 FITC conjugated antibodies and analyzed by flow cytometry, control cells were non-treated with the inhibitor. The Data are means \pm SD n=4, $p < 0.001$ as determined by two-way ANOVA. H₂O₂ or Hcy+Folate vs H₂O₂ or Hcy+Folate+KNK437 ($p < 0.001$), as determined by Bonferroni *post hoc*.

4.3.3 Impact of inhibition and induction of HO-1 on cobalamin and folate apoptosis-protection:

4.3.3.1 The effect of iHO-1 induction by hemin on apoptosis induced by oxidative stress:

In order to induce iHO-1, Sk-hep1 cells which were subjected to 12 μ M Hemin for 2 hours had a significant effect on Ho-1 induction and caspase-3 level under apoptosis condition ($P < 0.001$, as determined by two-way ANNOVA), (Figures 4.19 & 4.20). Further post-hoc comparison showed that hemin treatment had a significant increase of iHO-1 when compared to control cells ($P < 0.001$), (Figure 4.19) and a reduction in Hcy induced caspase-3 activation ($P < 0.001$), (Figure 4.20). Also, there was no significant necrosis activity detected in cells treated with hemin prior Hcy as compared to control cells ($P > 0.05$, as determined by two way ANNOVA), (Figure 4.21).

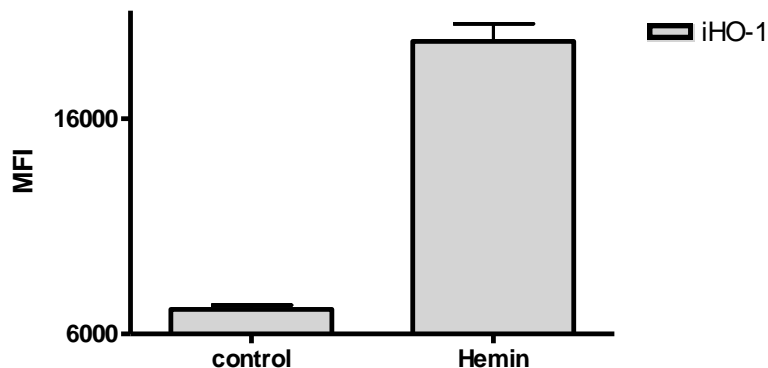


Figure 4.19: The induction of iHO-1 by Hemin. Sk-hep1 cells were pre-treated with 12 μ M Hemin for 2 hours followed by 2 hours treatment with of 3.125 μ M Hcy. Control cells were non-treated cells. Cells were then stained with specific monoclonal HO-1 FITC labelled antibody and analyses by flow cytometry and BD FACSDiva software. The Data are means \pm SD $n=4$, $p < 0.001$ as determined by one-way ANOVA. Baseline (control) vs Hemin ($p < 0.001$), as determined by Tukey *post hoc*.

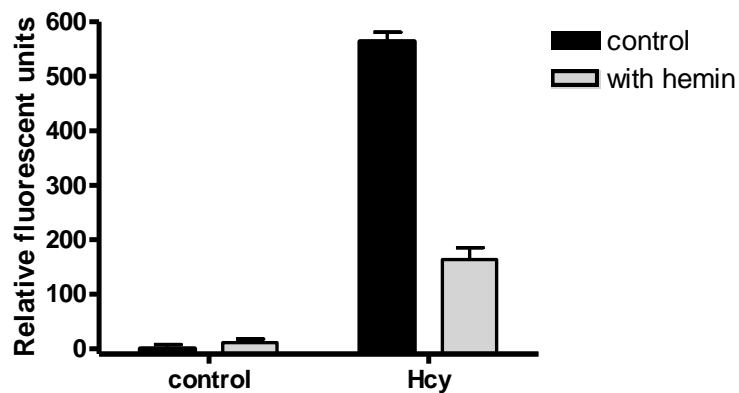


Figure 4.20: Effect of iHO-1 induction on caspase-3 under oxidative stress. Sk-hep1 cells were pre-treated with 12 μ M Hemin for 2 hours and followed by 2 hours treatment with 3.125 μ M Hcy. Caspase-3 was measured after at EX=496/EM=520. Control cells were non-treated with hemin cells. The Data are means \pm SD n=4, $p < 0.001$ as determined by two-way ANOVA. Baseline (control) vs Hcy+Hemin ($p < 0.001$), as determined by Bonferroni *post hoc*.

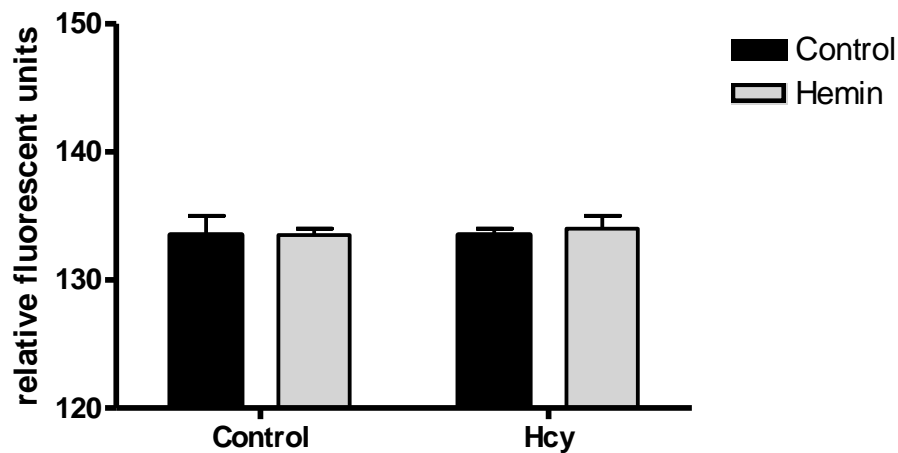


Figure 4.21: Effect of HO-1 induction on necrosis activity under oxidative stress induces. Sk-hep1 cells were pre-treated with 12 μ M Hemin for 2 hours followed by 2 hours treatment with 3.125 μ M Hcy. Necrosis was measured after at EX=535/EM=617. Control cells were non-treated with hemin. The Data are means \pm SD n=4, $p > 0.05$ as determined by two-way ANOVA.

4.3.3.2 The impact of iHO-1 inhibition by Sn(IV) Protoporphyrin IX dichloride on cobalamin-apoptosis protection:

Treatment cells were induced with 12.5 μ M Sn(IV) Protoporphyrin IX dichloride for 4 hours prior to exposure to 3.125 μ M Hcy for another 2 hours, which resulted in significant inhibition of iHO-1 compared to Hcy alone ($P < 0.001$, as determined by one-way ANNOVA), (Figure 4.22). Also inhibition of HO-1 had a significant effect on caspase-3 activity under protection ($P < 0.001$, as determined by two-way ANNOVA), (Figures 4.23 & 4.24). Further analysis with Bonferroni pairwise showed that when the Sn(IV) Protoporphyrin IX dichloride was applied prior to incubation with 25 μ M cobalamin followed by 3.125 μ M Hcy or H₂O₂ there was a significant increase in the caspase-3 activity by 54% or 43%, respectively, more than cells treated with cobalamin+Hcy or H₂O₂ alone ($P < 0.001$), (Figure 4.23). There was no significant effect of HO-1 inhibition on caspase-3 induced by Hcy or H₂O₂ alone ($P > 0.05$), (Figure 4.23). Similarly, inhibition of HO-1 with Sn(IV) Protoporphyrin IX dichloride had a significant effect on caspase-3 activity in cells treated with folate+Hcy or H₂O₂ such caspase-3 increased by 35% or 30% above cells treated with folate+Hcy or H₂O₂ alone ($P < 0.001$), (Figure 4.24). However, there was no significant activity of necrosis detected in the cells treated with Hcy after inhibition of HO-1 ($P > 0.05$, as determined by two-way ANNOVA), (Figure 4.25).

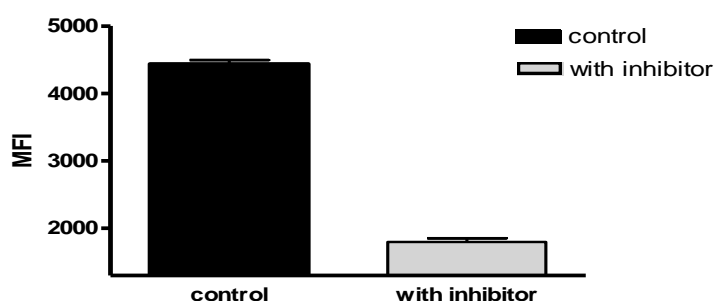
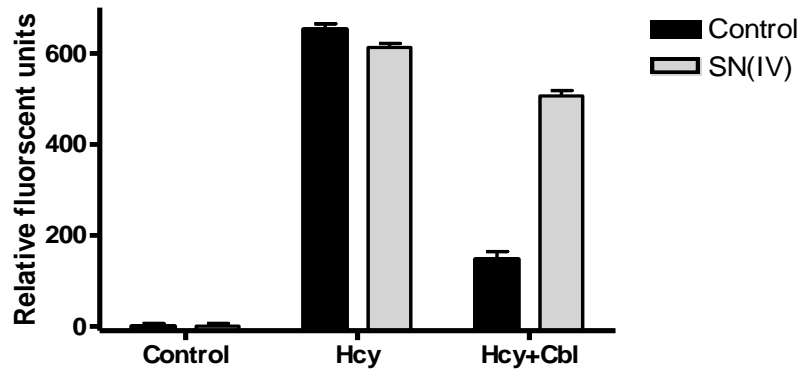


Figure 4.22: Inhibition of iHO-1 with SN (IV) Protoporphyrin IX dichloride in sk-hep1.

Cells were treated with 12.5 μ M SN (IV) Protoporphyrin IX dichloride for 4 hours. iHO-1 measured after using Flow cytometry and BD FACSDiva software. Control cells were treated with 3.125 μ M Hcy for 2 hours. The Data are means \pm SD $n=4$, $P < 0.001$ as determined by one-way ANOVA. Baseline (Hcy) vs Hcy+SN(IV) ($p < 0.001$) as determined by tukey *post hoc*

A.



B.

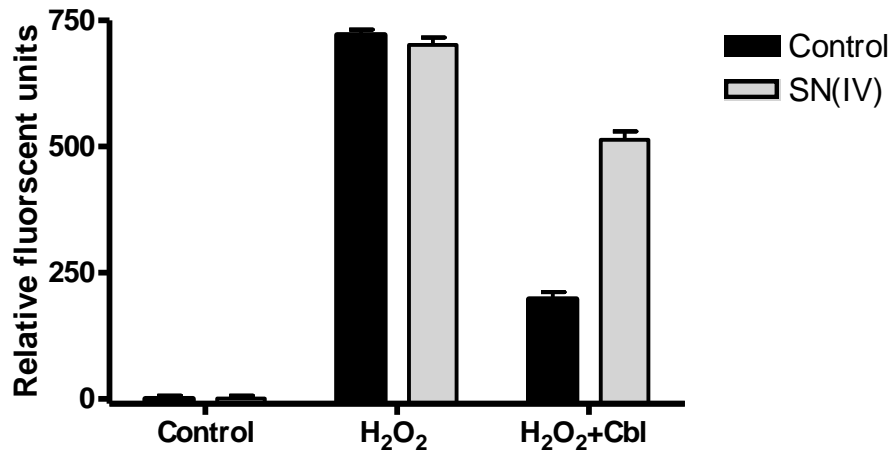
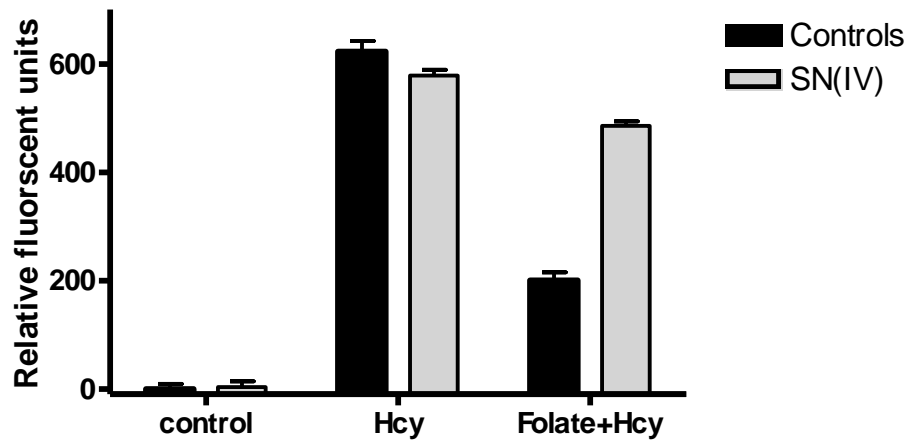


Figure 4.23: Effect of iHO-1 inhibition on Cobalamin–apoptosis protection in sk-hep1 cells. Cells were treated with 12.5 μ M SN (IV) Protoporphyrin IX dichloride for 4 hours followed by 2 hours treatment with 25 μ M of cobalamin and 2 hours of **A.** 3.125 μ M Hcy or **B.** 3.125 μ M H₂O₂. Caspase-3 was measured at EX=496/EM=520. Control cells were treated with 3.125 μ M Hcy for 2hours. The Data are means \pm SD n=4, $p < 0.001$ as determined by two-way ANOVA. Baseline (H₂O₂ or Hcy+Cbl) vs H₂O₂+Hcy+Cbl+SN(IV) ($p < 0.001$), as determined by Bonferroni *post hoc*.

A.



B.

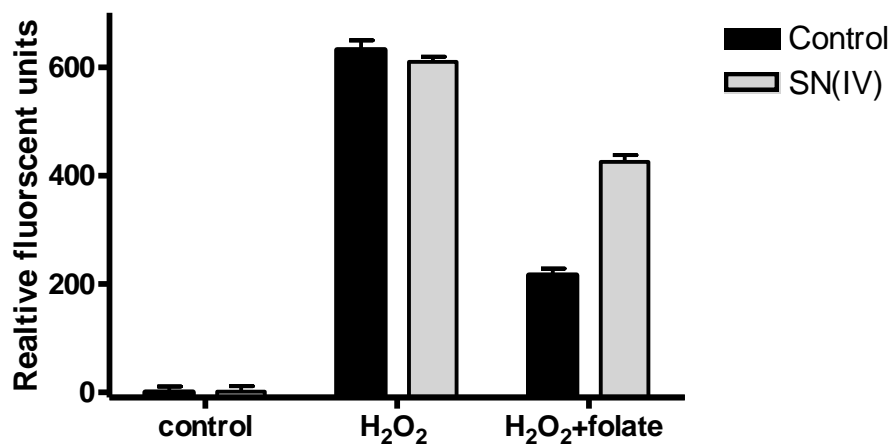


Figure 4.24: Effect of iHO-1 inhibition on folate–apoptosis protection in sk-hep1 cells.

Cells were treated with 12.5 μ M SN (IV) Protoporphyrin IX dichloride for 4 hours followed by 2 hours treatment with 30 μ M of folate and 2 hours of 3.125 μ M **A.** Hcy or **B.** H₂O₂. Caspase-3 was measured after at EX=496/EM=520. Control cells were treated with 3.125 μ M Hcy for 2hours. The Data are means \pm SD n=4, $p < 0.001$ as determined by two-way ANOVA. Baseline (H₂O₂ or Hcy+folate) vs H₂O₂+Hcy+folate+SN(IV) ($p < 0.001$), as determined by Bonferroni *post hoc*.

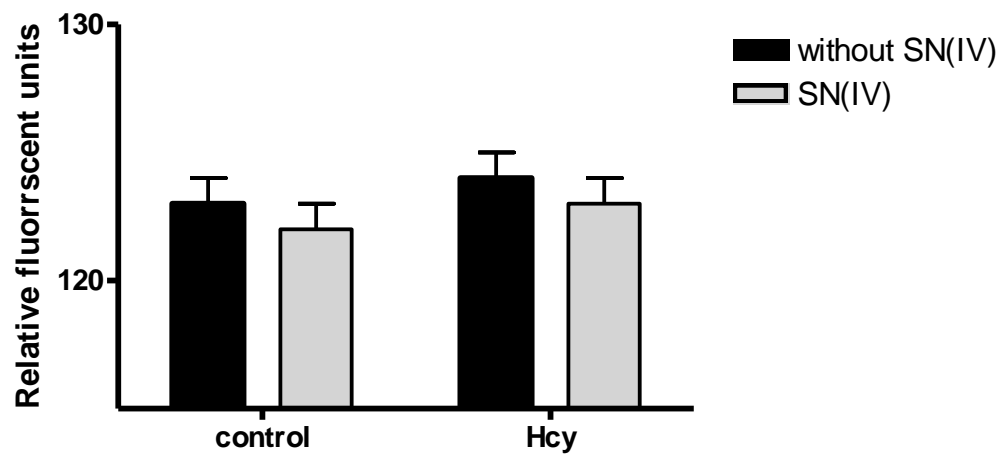
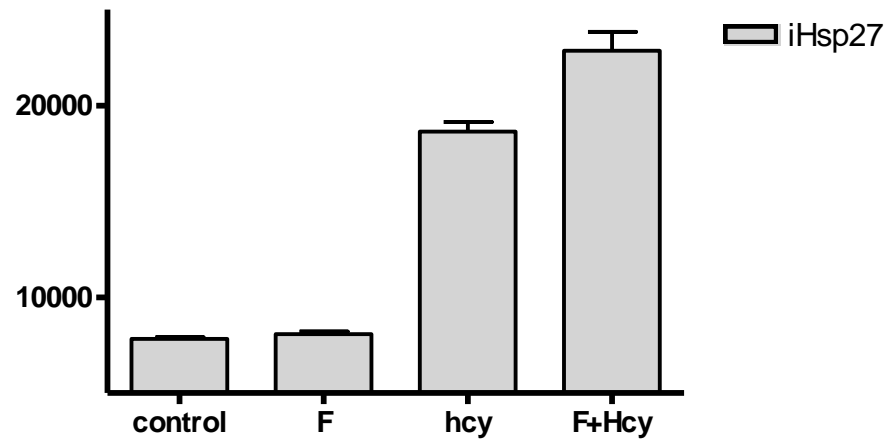


Figure 4.25: Effect of iHO-1 inhibition on necrosis activity under oxidative stress. Sk-hep1 cells were treated with 12.5 μ M SN (IV) Protoporphyrin IX dichloride for 4 hour followed by 2 hours treatment and 2 hours of 3.125 μ M Hcy. Necrosis was measured after at ex=535/em=617. Control cells were treated with 3.125 μ M Hcy for 2 hours. The Data are means \pm SD n=4, $p>0.05$ as determined by two-way ANOVA.

4.3.4 Intracellular Hsps under antioxidant protection in Jurkat:

In Jurkat cells, folate had a significant effect on the iHsps ($P < 0.001$, as determined by one-way ANNOVA), (Figures 4.25 & 4.26). However, Post-hoc comparison showed folate did not have significant effect on iHsp27 or iHO-1 induction more than in control cells ($P > 0.05$). However, pre-incubation cells with folate, followed by treatment with Hcy showed a significant increase of iHsp27 and iHO-1 by 24% and 27% respectively ($P < 0.001$), (Figure 4.25). Furthermore, folate has a significant effect on iHsp72 ($P < 0.001$) and iHsp90 ($P < 0.05$) induction in comparison to control cells. Also, exposing cells to folate prior to Hcy treatment resulted in significant induction of iHsp72 and iHsp90, by 58% and 49% more than Hcy treatment alone ($P < 0.001$), (Figure 4.26).

A.



B.

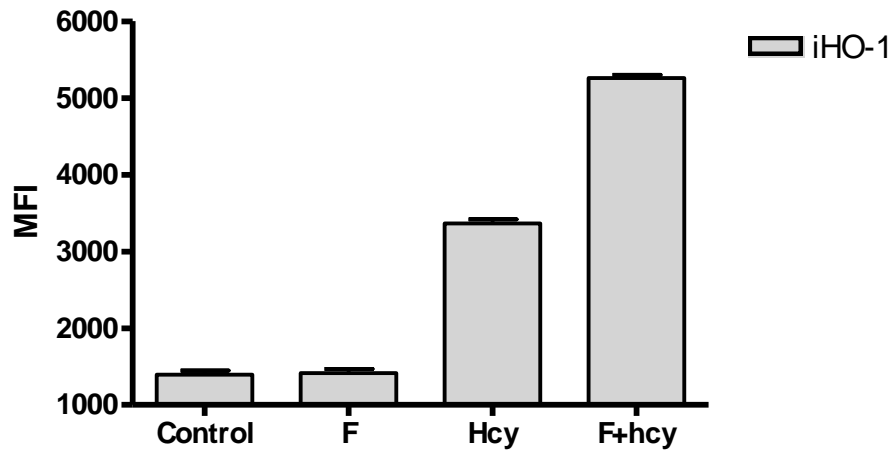
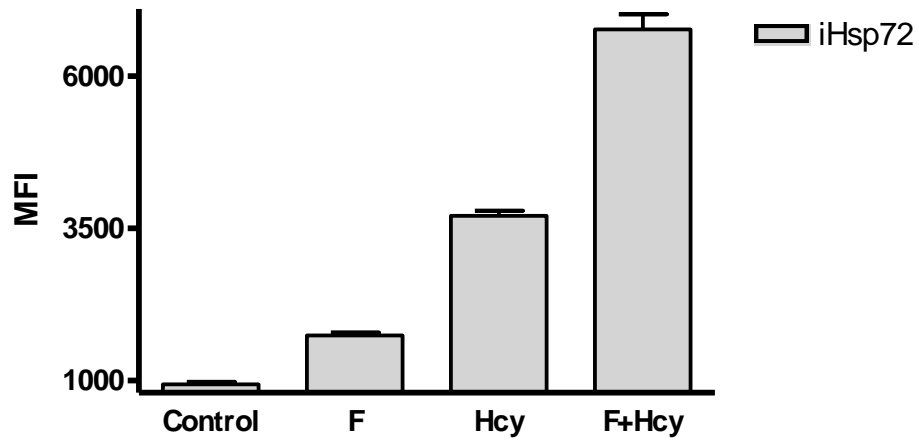


Figure 4.26: Effect of folate on iHsp27 and iHO-1 level in Jurkat cells. Cells were pre-treated with 30 μ M Folate for 2 hours followed by 6 hours treatments with 3.125 μ M Hcy then cells were stained with monoclonal mouse **A.** Anti-Hsp27 **B.** Anti-HO-1 FITC labelled antibodies and analyzed using Flow cytometry and BD FACSDiva software. Control cells were non-treated. The Data are means \pm SD n=4, $p < 0.001$ as determined by two-way ANOVA. Baseline (control) vs Hcy ($p < 0.001$), folate+Hcy ($p < 0.001$), as determined by Bonferroni *post hoc*.

A.



B.

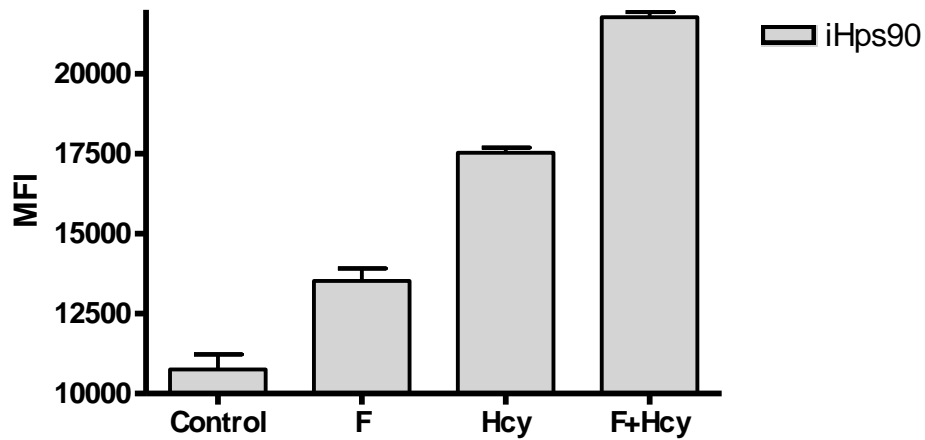


Figure 4.27: Effect of folate on iHsp72 and iHsp90 level in Jurkat cells. Cells were pre-treated with 30 μ M Folate for 2 hours followed by 6 hours treatments with 3.125 μ M Hcy then cells were stained with monoclonal mouse **A.** Anti-Hsp72 FITC **B.** Anti-Hsp90 PE labelled antibodies and analyzed using Flow cytometry and BD FACSDiva software. Control cells were non-treated. The Data are means \pm SD n=4, $p < 0.001$ as determined by two-way ANOVA. Baseline (control) vs Folate ($p < 0.05$), Hcy ($p < 0.001$), folate+Hcy ($p < 0.001$), as determined by Bonferroni post hoc.

4.4 Discussion:

The aim of this chapter was to investigate the impact of cobalamin on iHsps and the involvement of the Hsps in the apoptosis protection mechanism.

Previous work has shown that oxidative stress induces the production of Hsp27, HO-1, Hsp72 and Hsp90 (Liu *et al.*, 2007; Musch *et al.*, 1996, Musch *et al.*, 1999; Liao *et al.*, 2000). HSP production is known to be induced by a wide range of treatments (Landry *et al.*, 1989; Huot *et al.*, 1991; Mehlen *et al.*, 1993; Garrido *et al.*, 1996; Garrido *et al.*, 1997). Interestingly, the results in this chapter demonstrated that cobalamin to be a novel inducer of HSP production. Subjecting cells to cobalamin resulted in significant increase of iHsp27, iHO-1, iHsp72 and iHsp90. This result was not expected and the mechanisms by which cobalamin have antiapoptotic effects will be explored further in the next chapter.

Moreover, when cobalamin is protecting cells from apoptosis, iHO-1, iHsp72 and iHsp90 were higher than their level with Hcy alone. The same was observed with folate-apoptosis protection. Folate treatment alone induced iHsp72 and iHsp90 and under folate apoptosis protection there was a further induction of iHsp27, iHO-1, iHsp72 and iHsp90 in both Sk-hep1 and Jurkat cells. This suggests that one of the properties of protective molecules such as cobalamin and folate is to prime the cells to produce HSPs. When challenged with Hcy, the cells then responded with a more rapid response in terms of HSP production.

HSPs are known to have antiapoptotic properties (Mosser *et al.*, 1997; Samali *et al.*, 2001). In the literature it has been reported that overexpression of Hsps protects cells from oxidative injury and other stressors (Huot *et al.*, 1991; Mehlen *et al.*, 1993; Ohkawara *et al.*, 2006). More over, it has been reported that overexpression of Hsp72 through heat shock in prostate cancer cells prevents apoptosis induction by chemical and radiation (Gibbson *et al.*, 2000). Also, increased expressions of Hsp72 in breast cancer cells by heat shock provided protection against chemotherapy (Fuqua *et al.*, 1994), and the inhibition of Hsp72 resulted in losing the protection (Gibbson *et al.*, 2000). The results of this chapter were in agreement with the previous investigations of cytoprotective role of Hsps, hence over-expression of

Hsp72 or HO-1 by heat shock or hemin, have protected cells from apoptosis induced by oxidative stress.

In order to investigate the role of Hsps in the cobalamin protection mechanism, Hsp72 inhibited by KNK437 and HO-1 by Sn (VI) Protoporphyrin IX dichloride respectively as they are known as Hsp72 and HO-1 inhibitors (Brich, PhD 2007). Inhibition of Hsp72 prevented the protection provided by cobalamin and folate against apoptosis induced by oxidative stress. Also inhibition of HO-1 partially prevents protection of cobalamin and folate. This was not a general inhibition of apoptosis or necrosis because neither inhibitor had any effect on caspase 3 activity or PI incorporation in control cells.

Several studies have demonstrated the antiapoptotic effect of Hsps through their ability to regulate pro-caspases and release of cytochrome c. The protection of cobalamin was associated with induction of Hsps, and this was essential for the protection from apoptosis induced by oxidative stress. It has been reported that the induction of Hsp27 blocks cytochrome c release and reduces ROS generation under oxidative stress. (Garrido *et al.*, 1999; Bruey *et al.*, 2000; Pandey *et al.*, 2000; Concannon *et al.*, 2001; Samali *et al.*, 2001; Liu *et al.*, 2007) At the same time Hsp72 prevents formation of apoptosomal and prevent caspases activation which leads to protect cells from apoptosis (Samali *et al.*, 2001; Beere *et al.*, 2000; Saleh *et al.*, 2000).

Furthermore overexpression of HO-1 induces antioxidant and antiapoptotic proteins (Brouard *et al.*, 2000; Lee *et al.*, 2002; Choi *et al.*, 2002). HO-1 also produces bilirubin, which is an antioxidant molecule that has the ability to protect cells from oxidative stress (Stocker *et al.*, 1990). It is obvious that the induction of Hsps is essential for the cobalamin protection mechanism.

To conclude, the results in this chapter clearly demonstrated a novel impact of cobalamin and folate on iHsps. Moreover, the induction of Hsps that is associated with cobalamin or folate protection was essential in the protection mechanism. This conclusion leads to the next questions: how does cobalamin turn on the Hsp genes?

And which signal transduction pathway does lead to cobalamin induced HSP production? These questions shall be investigated further in the next chapter.

Chapter 5

Cobalamin Protection Mechanism

5.1 Introduction

Signal transduction pathways regulate survival and death signalling of the cells under different stimuli (Xia *et al.*, 1995; Matsuzaki *et al.*, 1999; Uchiyama *et al.*, 2004; Wang *et al.*, 1998; Qin & Chock., 2003). The signalling pathways regulate essential processes of the cells such as gene transcription, protein translation, cytoskeletal remodelling, endocytosis, cell metabolism, cell proliferation and survival. Recently, it has been reported that oxidative stress activates the JNK and P38 pathways, and they act as death signalling pathways (Xia *et al.*, 1995; Harper & LoGrasso, 2001; Crossthwaite *et al.*, 2002). Inhibition of these pathways by specific inhibitors suppressed apoptosis induced by oxidative stress. On the other hand, oxidative stress also activated the Nf_κB , ERK1/2 and PI3/AKT pathways and these act as antiapoptotic pathways (Junttila *et al.*, 2008; Kurland *et al.*, 2003; Johnson & Lapadat, 2002).

Nf_κB plays a vital role in cell protection from apoptosis by regulating antiapoptotic protein induction (Lin & Karin., 2003; Wang *et al.*, 1998). It has been reported that activation of Nf_κB leads to reduce ROS and protects cells from apoptosis induced by oxidative stress (Kim *et al.*, 2008; Kiningham *et al.*, 2008; Nakano *et al.*, 2006; Pham *et al.*, 2004; Zanotto-Filho *et al.*, 2009) and the inhibition of Nf_κB by Bay-117082, increased the induction of ROS and cells became apoptotic (Zanotto-Filho *et al.*, 2009). Also it is known that Nf_κB regulates iNOS, which is an important anti-inflammatory factor (Guoping *et al.*, 2001; Zeng *et al.*, 2005).

At the same time, The MAPK family is activated under oxidative stress (wang *et al.*, 1998; Qin & chock, 2003). ERK1/2 has been suggested to be a survival signal (Junttila *et al.*, 2008) and this role has been demonstrated in several cell line under oxidative stress for example; in neuroblastoma cells (Ruffel *et al.*, 2004) and osteoblastic cells (Yung *et al.*, 2007), PC12 cells and primary cortical neurons (Guyton *et al.*, 1996; Crossthwaite *et al.*, 2002) in which the activation of ERK1/2 protects

cells from apoptosis induced by oxidative stress. Moreover, the inhibition of ERK1/2 by U0126 enhanced apoptosis (Seo *et al.*, 2005).

In contrast, other members of the MAPK family JNK and P38 act as cell death signals (Xia *et al.*, 1995; Matsuzaki *et al.*, 1999; Uchiyama *et al.*, 2004) and the inhibition of these pathways suppressed cell death induced by oxidative stress.

Furthermore, the third main signal transduction pathway is the AKT/PI3 pathway, which is known to be activated under oxidative stress and is believed to act as antiapoptotic pathway (Crossthwaite *et al.*, 2002). Also it is known that the activation of AKT/PI3 pathway leads to upregulation of Nrf2. Recent studies have showed that Nrf2 is involved in the oxidative stress protection *via* binding and activating the ARE (Nguyen *et al.*, 2003). Many genes important to the response to oxidative stress include ARE in their promoter, such as HO-1, glutathione transferases and SOD-1 (Lee *et al.*, 2003). Furthermore, several studies have demonstrated ERK1/2 involvement in the activation of Nrf2; when cells were protected from apoptosis induced by oxidative stress Nrf2 is upregulated through AKT/ERK1/2 signals transduction pathways and leads to induction of the HO-1 (Kim *et al.*, 2008; Chen *et al.*, 2004; Kong *et al.*, 2001; Nakaso *et al.*, 2003; Zhang *et al.*, 2006). Inhibition of AKT/ERK1/2 prevents the protection of oxidative stress and prevents HO-1 induction.

From this context it is obvious that NF- κ B, ERK1/2 and AKT/PI3 pathways are antiapoptotic pathways while JNK and P38 enhanced cell death. In the previous chapters it has been demonstrated that cobalamin provided protection against oxidative stress induced apoptosis. And this protection correlated with induction of the Hsps which is essential in the protection mechanism.

The aim of this chapter is to investigate the mechanism of cobalamin apoptosis protection *via* the possible involvement of the signal transduction pathways.

5.2 Methods

All preparations and cell culture experiments were carried out within a class II tissue culture hood and the Sk-hep1 cell was the main cell line.

5.2.1 The inhibitory study:

Cells were plated on to a black 96 well cell plate over night. Cells then were pre-incubated with the inhibitors for 2 hours followed by treatment with 25 μ M cobalamin for 2 hours and 3.125 μ M Hcy for another 2 hours, different analysis was carried out after.

Actinomycin was used as gene transcription inhibitor. A stock of 2mg/ml actinomycin was prepared by dissolving it in acetonitrile and stored at 2-5°C. On the day of the experiment, the required concentration was prepared by diluting the stock in media.

Bay11-7082 was used to inhibit the Nf κ B activation. A stock of 10mM Bay11-7082 was prepared by dissolving it in dimethyl sulfoxide and stored at 2-5°C. On the day of the experiment, the required concentration was prepared by diluting the stock in media.

U0126 was used to inhibit the ERK1/2 activation. A stock of 1mM U0126 was prepared by dissolving in dimethyl sulfoxide and stored at 2-5°C. On the day of the experiment, the required concentration was prepared by diluting the stock in media.

LY-294 was used to inhibit the AKT/PI3 activation. A stock of 1mM LY-294 was prepared by dissolving it in ethanol acetate and stored at 2-5°C. On the day of the experiment, the required concentration was prepared by diluting the stock in media.

Wortmanin was used to inhibit the Nrf2 activation. A stock of 1mM wortmanin was prepared by dissolving it in ethanol acetate and stored at 2-5°C. On the day of the experiment, the required concentration was prepared by diluting the stock in media.

SP600125 was used to inhibit the JNK activation. A stock of 1mM SP600125 was prepared by dissolving it in dimethyl sulfoxide and stored at 2-5°C. On the day of the experiment, the required concentration was prepared by diluting the stock in media.

SB202190 was used to inhibit the P38 activation. A stock of 1mM U0126 was prepared by dissolving it in dimethyl sulfoxide and stored at 2-5°C. On the day of the experiment, the required concentration was prepared by diluting the stock in media.

5.2.2 Cells count and viability test by trypan blue exclusion:

For the flow cytometry assays, the following treatment cells were re-suspend into the media by pipetting. Cells were then counted and assessed by trypan blue exclusion as described in (section 2.4.6)

5.2.3 Measurement of intracellular Hsps

The antibodies used were: Anti-Hsp27 mouse monoclonal FITC conjugated antibody, Anti-HO-1 mouse monoclonal FITC conjugated antibody, Anti-Hsp72 mouse monoclonal FITC conjugated antibody and Anti-Hsp90 mouse monoclonal R-PHYcoerythrin conjugated antibody. The dilution was 1:100.

Cells were treated under test condition. , Once incubation time was over, cells were processed for staining and analysis as described in (section 2.4.13)

5.2.4 Measurement of pNf κ B induction:

Cells were treated under test condition and then processed as in (section 2.4.13). Polyclonal anti-pNf κ B Rabbit IgG antibody was diluted to 1:100 and used as first antibody and anti- rabbit IgG-FITC conjugated antibody was diluted to 1:100 and used as second antibody.

5.2.5 Measurement of pERK1/2 induction:

Cells were treated under test condition and then processed as in (section 2.4.13). Polyclonal anti-pERK1/2 Rabbit IgG antibody was diluted to 1:100 and used as first antibody and anti- rabbit IgG-FITC conjugated antibody was diluted to 1:100 and used as second antibody.

5.2.6 Measurement of pAKT induction:

Cells were treated under test condition and then processed as in (section 2.4.13). Polyclonal anti-pAKT Rabbit IgG antibody was diluted to 1:100 and used as first antibody and anti- rabbit IgG-FITC conjugated antibody was diluted to 1:100 and used as second antibody.

5.2.7 Measurement of Nrf2 induction:

Cells were treated under test condition and then processed as in (section 2.4.13). Polyclonal anti-NRF2 goat IgG antibody was diluted to 1:100 and used as first antibody and anti- goat IgG-FITC conjugated antibody was diluted to 1:100 and used as second antibody.

5.2.8 Measurement iNOS induction:

Cells were treated under test condition and then processed as in (section 2.4.13). Polyclonal anti-iNOS Rabbit IgG antibody was diluted to 1:100 and used as first antibody and anti-rabbit IgG-FITC conjugated antibody was diluted to 1:100 and used as second antibody.

5.2.9 Measurement of super oxide generation

Cells were plated onto a black 96 well cell plate and treated under test condition then analysed for generation of super oxide by Lucigenin assay as described in (section 2.4.15).

5.2.10 Measurement of ROS generation

Cells were plated onto a black 96 well cell plate and treated under test condition then analysed for generation of reactive oxygen species by the fluorescence redox active probe 2', 7'-dichlorofluorescein-diacetate detection as described in (section 2.4.16).

5.2.11 Determination of apoptosis

Cells were plated on to a black 96 well cell plate and treated under test condition then analyzed for apoptosis by caspase-3/7 detection as described in (section 2.4.9).

5.3 Result

5.3.1 Impact of signal transduction pathways on cobalamin apoptosis-protection:

To investigate the mechanisms of the cobalamin protection, the effect of gene transcription on the cobalamin's protection was first determined. Cells were pre-treated with 1 and 5 $\mu\text{g/ml}$ of actinomycin for 2 hours, prior to incubation with 25 μM cobalamin for 2 hours followed by 2 hours exposure to 3.125 μM Hcy showed significant effect on caspase-3 ($P < 0.001$, as determined by two-way ANNOVA), (Figure 5.1). Further analysis with Bonferroni pairwise has resulted in a significant increase of caspase-3 at 1 and 5 $\mu\text{g/ml}$ actinomycin compared to control cells treated with cobalamin and Hcy only ($P < 0.001$). At the same time actinomycin had no significant effect on caspase-3 under apoptosis induction ($P > 0.05$) and there was no significant induction of caspase-3 with actinomycin treatment only ($P > 0.05$) as compared to control cells (non-treated) (Figure 5.1).

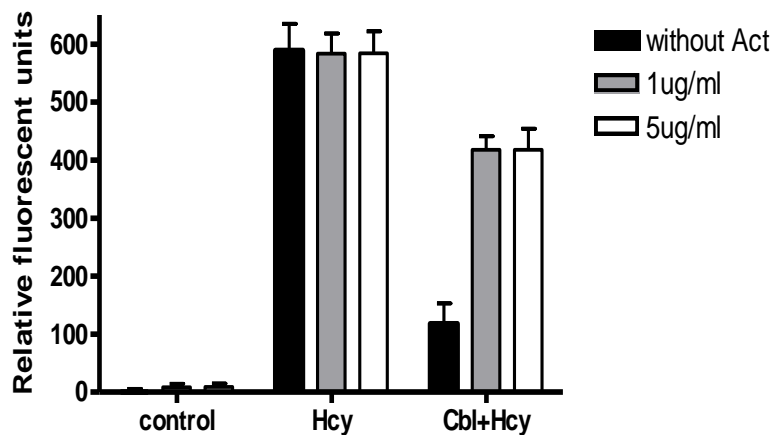


Figure 5.1: Effect of gene transcription inhibitor on cobalamin apoptosis protection.

Sk-hep1 cells were pre-treated with 1 and 5 $\mu\text{g/ml}$ of actinomycin for 2 hours followed by 2 hours treatment with 25 μM cobalamin and 2 hours of 3.125 μM Hcy. Control cells were not treated with actinomycin. Caspase-3 was measured after at EX=496/EM=520. The Data are means \pm SD $n=4$, $p < 0.001$ as determined by two-way ANOVA. Baseline (Hcy+Cbl) vs Cbl+Hcy+ACt ($p < 0.001$), as determined by Bonferroni *post hoc*.

Following determining the regulation level of the cobalamin-apoptosis protection, we investigated the effect of signal transduction pathways on the apoptosis protection provided by cobalamin. Cells were subjected to 5 μ M Bay-117082 for 2 hours prior to treatments with 25 μ M cobalamin for 2 hours followed by 3.125 μ M Hcy for another 2 hours. This treatment had significant effect on caspase-3 ($P<0.001$, as determined by two-way ANNOVA), (Figure 5.2). The post-hoc comparison resulted in a significant increase in caspase-3 level up to 62% more than cells treated with 25 μ M cobalamin for 2 hours and Hcy for 2 hours more ($P<0.001$). Inhibition of pNf $_{\kappa}$ B by Bay-117082 had no significant effect on caspase-3 induced by Hcy compared to cells treated with Hcy only ($P>0.05$) and the Bay-117082 alone had no significant activity of caspase-3 as compared to control cells (Figure 5.2).

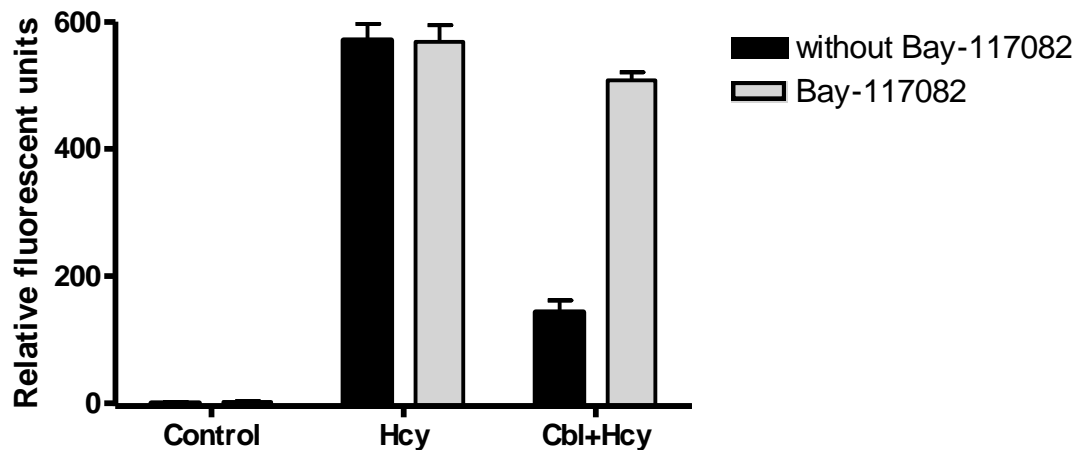


Figure 5.2: Effect of Bay-117082 on cobalamin apoptosis-protection. Sk-hep1 cells were pre-treated with 5 μ M Bay-117082 for 2 hours followed by 2 hours treatment with 25 μ M cobalamin and 2 hours of 3.125 μ M Hcy. Control cells were not treated with Bay-117082. Caspase-3 was measured after at EX=496/EM=520. The Data are means \pm SD $n=4$, $p<0.001$ as determined by two-way ANOVA. Baseline (Hcy+Cbl) vs Cbl+Hcy+Bay-117082 ($p<0.001$), as determined by Bonferroni *post hoc*.

Inhibition of pERK1/2 had a significant effect on the protection of apoptosis by cobalamin ($P<0.001$, as determined by two-way ANNOVA), (Figure 5.3). The Bonferroni pairwise showed that when cells were subjected to $1\mu\text{M}$ U0126 for 1 hour followed by incubation for 2 hours with $25\mu\text{M}$ cobalamin and 2 hours incubation with $3.125\mu\text{M}$ Hcy, they showed a significant increase of caspase-3 up to 60% above cobalamin+Hcy treatment ($P<0.001$). Inhibition of pERK1/2 had no significant effect on caspase-3 level at $3.125\mu\text{M}$ Hcy as compared to Hcy treatment alone ($P>0.05$). The U0126 had no significant activity of caspase-3 ($P>0.05$) as compared to control cells (non-treated) (Figure 5.3).

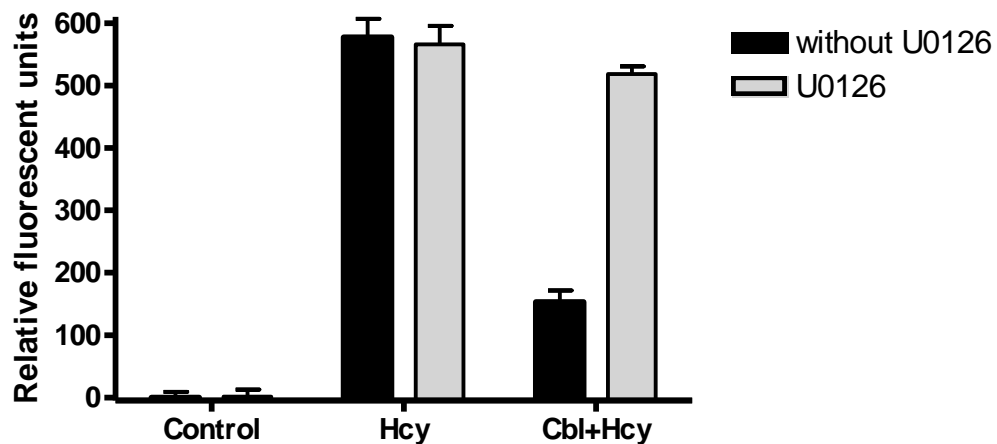


Figure 5.3: Effect of U0126 on cobalamin apoptosis-protection. Sk-hep1 cells were pre-treated with $1\mu\text{M}$ U0126 for 1 hour followed by 2 hours treatment with $25\mu\text{M}$ cobalamin and 2 hours of $3.125\mu\text{M}$ Hcy. Control cells were not treated with U0126. Caspase-3 was measured at EX=496/EM=520. The Data are means \pm SD $n=4$, $p<0.001$ as determined by two-way ANOVA. Baseline (Hcy+Cbl) vs Cbl+Hcy+U0126 ($p<0.001$), as determined by Bonferroni *post hoc*.

Inhibition of PI3/AKT with 10 μ M of LY294002 inhibitor for 1 hour prior to treatment with 25 μ M cobalamin for 2 hours and 3.125 μ M Hcy for 2 hours had a significant effect on caspase-3 ($P<0.001$, as determined by two-way ANNOVA), (Figure 5.4). Moreover, analysis with Bonferroni pairwise resulted in a significant increase of caspase-3 up to 61% above cobalamin+ Hcy treatment only ($P<0.001$). The LY294002 inhibitor had no significant effect on the caspase-3 level at 3.125 μ M Hcy as compared to Hcy treatment only ($P>0.05$). Also the inhibition of PI3/AKT didn't induce caspase-3 ($P>0.05$) as compared to control cells (non-treated) (Figure 5.4).

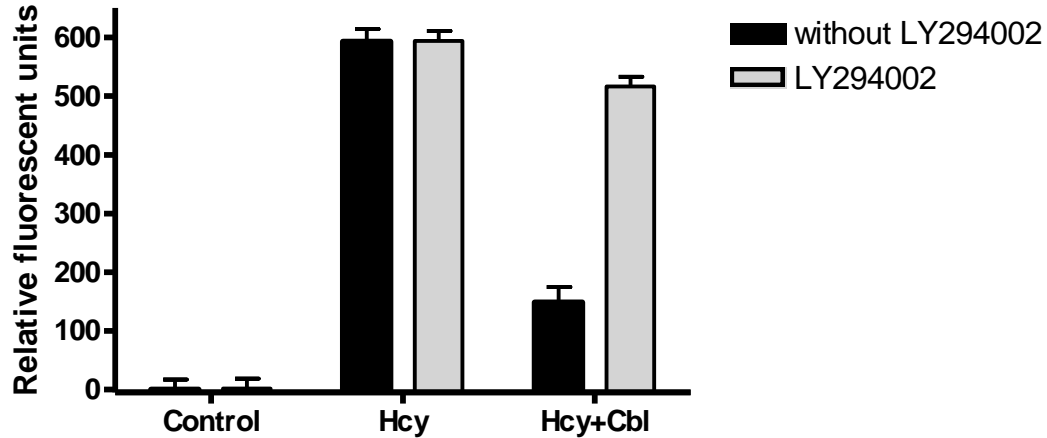


Figure 5.4: Effect of LY294002 cobalamin apoptosis-protection. Sk-hep1 cells were pre-treated with 10 μ M LY294002 for 1 hour followed by 2 hours treatment with 25 μ M cobalamin and 2 hours of 3.125 μ M Hcy. Control cells were not treated with LY294002. Caspase-3 was measured after at EX=496/EM=520. The Data are means \pm SD $n=4$, $p<0.001$ as determined by two-way ANOVA. Baseline (Hcy+Cbl) vs Cbl+Hcy+ LY294002 ($p<0.001$), as determined by Bonferroni *post hoc*.

Nrf2 was also inhibited with 1 μ M Wortmanin for 1 hour prior to treatment with 25 μ M cobalamin for 2 hours followed by 3.125 μ M Hcy for 2 hours of incubation. This inhibition had significant effect on caspase-3 activity ($P<0.001$, two-way ANNOVA), (Figure 5.5). Also post-hoc comparison showed a significant increase in caspase-3 up to 61% above 25 μ M cobalamin+Hcy treatment without the inhibitor ($P<0.001$). While there was no significant effect on caspase-3 in cells treated with 1 μ M Wortmanin for 1 hour prior treatment with 3.125 μ M Hcy for 2 hours as compared to cells treated with Hcy only ($P>0.05$). Also cells were subjected to 1 μ M Wortmanin had no caspase-3 activity ($P>0.05$) as compared to control cells (non-treated) (Figure 5.5).

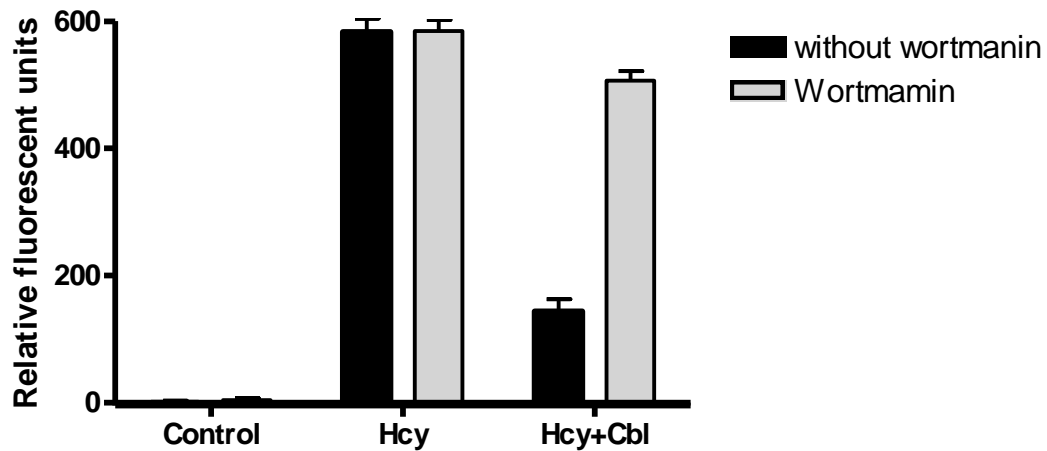


Figure 5.5: Effect of wortmanin cobalamin apoptosis-protection. Sk-hep1 cells were pre-treated with 1 μ M wortmanin for 1 hour followed by 2 hours treatment with 25 μ M cobalamin and 2 hours of 3.125 μ M Hcy. Control cells were not treated with wortmanin. Caspase-3 was measured at EX=496/EM=520. The Data are means \pm SD n=4, $p<0.001$ as determined by two-way ANOVA. Baseline (Hcy+Cbl) vs Cbl+Hcy+ wortmanin ($p<0.001$), as determined by Bonferroni *post hoc*.

In order to determine effect of P38 pathway on the cobalamin apoptosis protection, cells were treated with 12 μ M SB202190 for 1 hour prior to exposing the cells to 25 μ M cobalamin for 2 hours and another 2 hours for 3.125 μ M Hcy, resulted in significant effect on caspase-3 activity ($P<0.001$, as determined by two-way ANNOVA), (Figure 5.6). The Bonferroni pairwise analysis showed there was a significant increase in caspase-3 by 10% above cobalamin+Hcy treatment alone ($P<0.001$). Although the inhibition of P38 showed a significant reduction in the caspase-3 level up to 25% less than Hcy treatment alone ($P<0.001$). There was no significant activity of caspase-3 at 12 μ M SB202190 treatment alone ($P>0.05$) as compared to control cells (non-treated) (Figure 5.6).

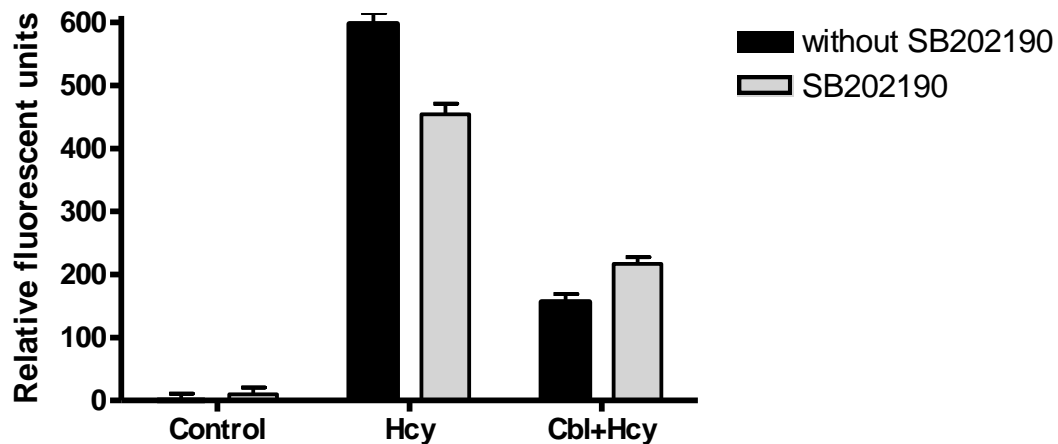


Figure 5.6: Effect of SB202190 cobalamin apoptosis-protection. Sk-hep1 cells were pre-treated with 12 μ M SB202190 for 1 hour followed by 2 hours treatment with 25 μ M cobalamin and 2 hours of 3.125 μ M Hcy. Control cells were not treated with SB202190. Caspase-3 was measured at EX=496/EM=520. The Data are means \pm SD $n=4$, $p<0.001$ as determined by two-way ANOVA. Baseline (Hcy) vs Hcy+ SB202190 ($p<0.001$), Baseline (Hcy+Cbl) vs Cbl+Hcy+ SB202190 ($p<0.001$), as determined by Bonferroni *post hoc*.

JNK was inhibited by treating cells with 5 μ M SP600125 for 2 hours followed by 2 hours treatment with 25 μ M cobalamin and 2 hours of 3.125 μ M Hcy. This inhibition had significant effect on caspase-3 ($P<0.001$, as determined by two-way ANNOVA), (Figure 5.7). However, the post-hoc comparison showed no significant difference in caspase-3 as compared to cells treated with cobalamin+Hcy alone ($P>0.05$). However, the SP600125 had a significant effect on the caspase-3 level of such at 3.125 μ M Hcy showed a significant reduction of caspase-3 by 38% less than Hcy alone ($P<0.001$) The JNK inhibitor treatment alone had no significant caspase-3 activity ($P>0.05$) as compared to control cells (non-treated(Figure 5.7).

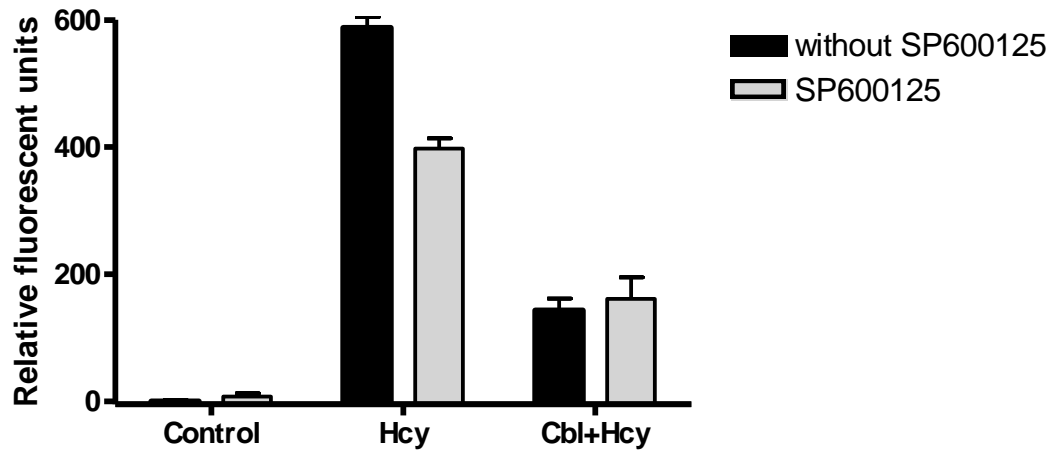
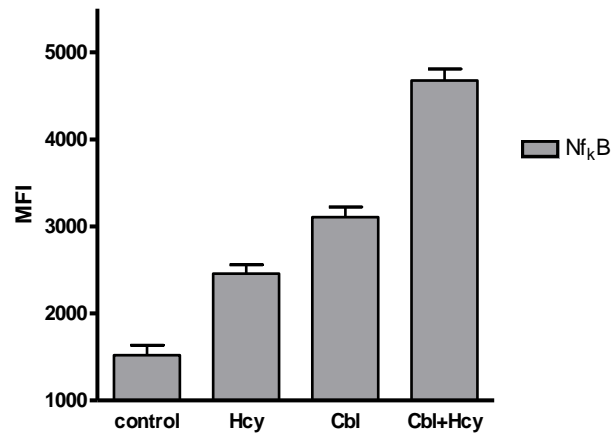


Figure 5.7: Effect of SP600125 on cobalamin apoptosis-protection. Sk-hep1 cells were pre-treated with 5 μ M SP600125 for 2 hours followed by 2 hours treatment with 25 μ M cobalamin and 2 hours of 3.125 μ M Hcy. Control cells were not -treated with SP600125. Caspase-3 was measured at EX=496/EM=520. The Data are means \pm SD $n=4$, $p<0.001$ as determined by two-way ANOVA. Baseline (Hcy) vs Hcy+ SP600125 ($p<0.001$), as determined by Bonferroni *post hoc*.

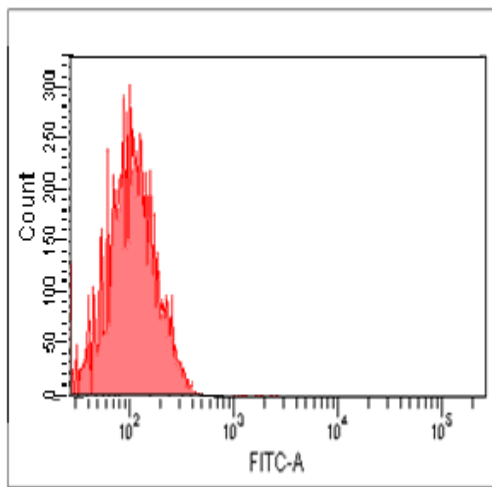
5.3.2 Impact of cobalamin on phosphorelated level of signal transduction pathways:

In order to determine the impact of signal transduction pathways on cobalamin protection mechanism, we investigated the effect of cobalamin on phosphorelated Nf_κB (p Nf_κB), phosphorelated ERK1/2 (pERK1/2) and phosphorelated (pAKT) which identified by flowcytometry. Resulted in cobalamin had significant effect on p Nf_κB ($P < 0.001$, as determined by one-way ANNOVA), (Figure 5.8A). Further analysis with Tukey pairwise showed there was a significant increase in p Nf_κB induction at 3.125 μM Hcy as compared to control cells (non-treated) ($P < 0.001$). Although there was a significant increase in the intracellular level of p Nf_κB at 25 μM cobalamin as compared to the apoptotic cells ($P < 0.01$). Furthermore, co-treatments of 25 μM cobalamin and 3.125 μM Hcy, induced p Nf_κB significantly more than Hcy or cobalamin treatments alone ($P < 0.001$).

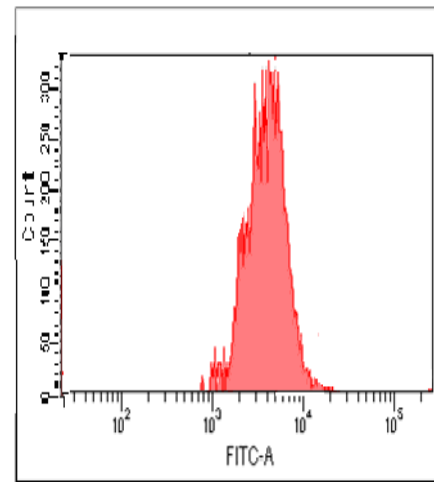
The histogram (Figure 5.8 B&C) illustrates the significant increase in the fluorescent intensity of p Nf_κB at 25 μM cobalamin as compared to control cells (non-treated).



A. Intracellular level of pNf $_{\kappa}$ B via flowcytometry



B. Control cells

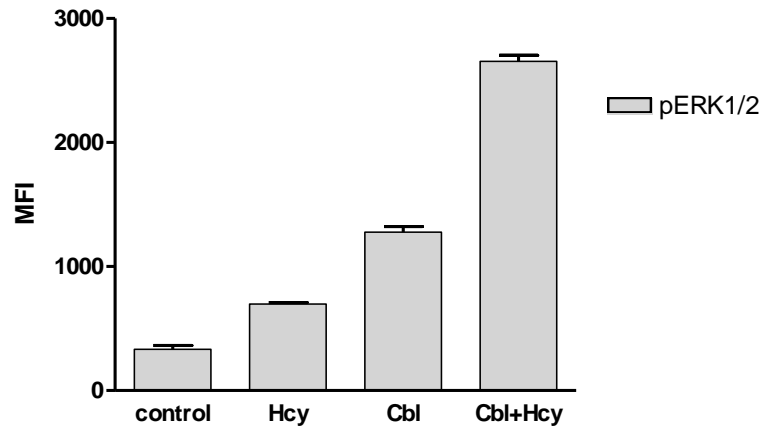


C. Cells treated with 25μMCbl

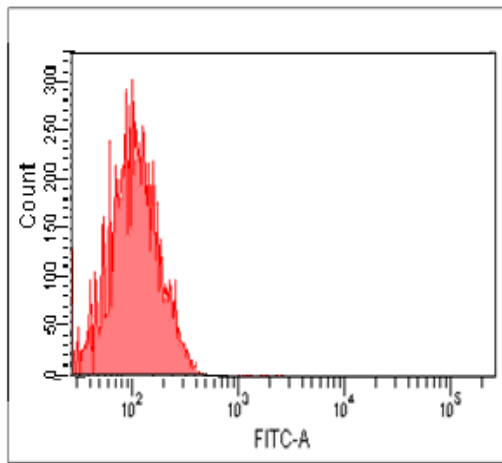
Figure 5.8: induction of pNf $_{\kappa}$ B by cobalamin. **A)** sk-hep1 cells were pre-treated with 25μMCbl for 2 hours followed by 2 hour treatment with 3.125μM Hcy, then cells were stained with a specific antibody and analysed by Flowcytometry FACSDiva. Control cells were not treated. The Data are means \pm SD n=4, $p < 0.001$ as determined by one-way ANOVA. Baseline (control) vs Hcy ($p < 0.001$), Cbl ($p < 0.001$), Cbl+Hcy ($p < 0.001$), as determined by Tukey t *post hoc*. **B)** Control cells (non-treated). **C)** Cells treated with 25μMCbl.

Furthermore, cobalamin had significant effect on the pERK1/2 ($P < 0.001$, as determined by one-way ANNOVA), (Figure 5.9A). Also the post-hoc comparison showed that there was a significant induction of pERK1/2 at $3.125\mu\text{M}$ Hcy ($P < 0.05$) as compared to control cells (non-treated), while cobalamin treatment alone resulted in significant induction of pERK1/2 more than Hcy treatment alone ($P < 0.001$). And cells subjected to $25\mu\text{M}$ cobalamin for 2 hours prior treatment with $3.125\mu\text{M}$ Hcy for another 2 hours had a significant induction of pERK1/2, higher than cobalamin or Hcy treatment alone ($P < 0.001$), (Figure 5.9A).

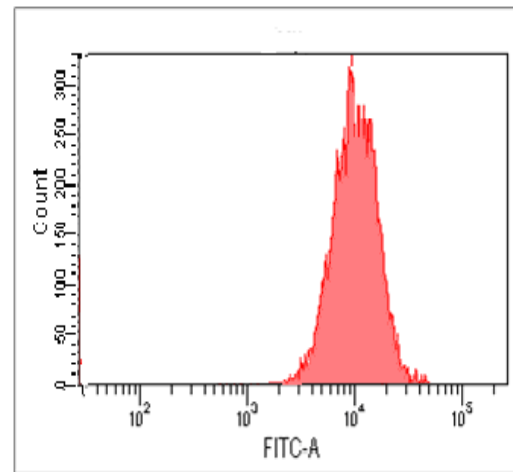
The histogram in Figure 5.9 B & C, illustrated the induction of pERK1/2 by cobalamin, since there was a significant increase in the fluorescent intensity of pERK1/2 at $25\mu\text{M}$ cobalamin as compared to control cells (non-treated).



A. Intracellular level of pERK1/2 by flowcytometry.



B. Control cells

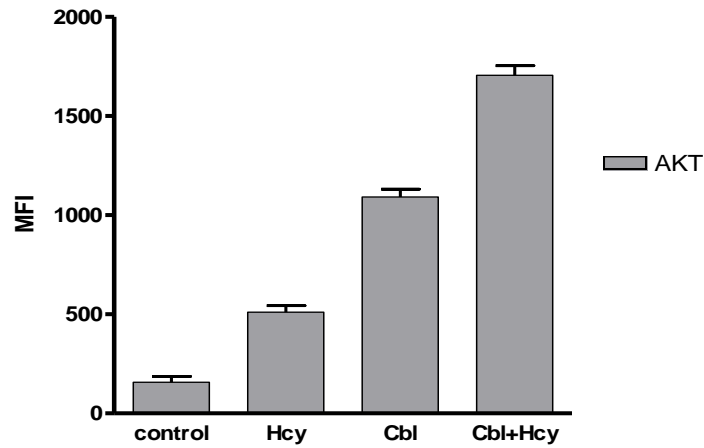


C. Cells treated with 25μMCbl

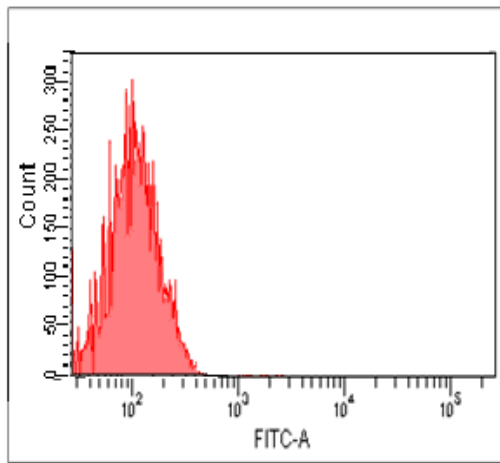
Figure 5.9: Induction of pERK1/2 by cobalamin. **A)** Cells were pre-treated with 25μMCbl for 2 hours followed by 2 hour treatment with 3.125μM Hcy. Cells were then stained with a specific antibody and analysed by Flowcytometry FACSDiva. Control cells were not treated. The Data are means \pm SD $n=4$, $p < 0.001$ as determined by one-way ANOVA. Baseline (control) vs Hcy ($p < 0.05$), Cbl ($p < 0.001$), Cbl+Hcy ($p < 0.001$), as determined by Tukey test *post hoc*. **B)** Control cells (non-treated). **C)** Cells treated with 25μMCbl.

The cobalamin also had a significant effect on the pAKT level ($P < 0.001$, as determined by one-way ANNOVA), (Figure 5.10A). Additionally, Tukey pairwise showed that cells treated with $3.125\mu\text{M}$ Hcy showed a significant induction of pAKT as compared to control cells (non-treated) ($P < 0.01$). The pAKT induction was increased significantly more at $25\mu\text{M}$ cobalamin than Hcy alone ($P < 0.01$). Also cells subjected to $25\mu\text{M}$ cobalamin prior treatment with Hcy showed a significant induction of pAKT ($P < 0.001$) as compared to cobalamin treatment or Hcy treatment alone (Figure 5.10A).

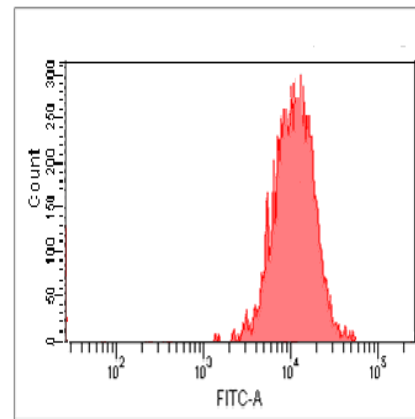
The histogram demonstrated the induction of pAKT since there was a significant increase in the fluorescent intensity at $25\mu\text{M}$ cobalamin as compared to control cells (non-treated) (Figure 5.10 B & C).



A. Intracellular level of pAKT *via* flowcytometry.



B. Control cells



C. Cells treated with 25μMCbl

Figure 5.10: induction of pAKT by cobalamin. **A)** Cells were pre-treated with 25μMCbl for 2 hours followed by 2 hour treatment with 3.125μM Hcy, then cells were stained with a specific antibody and analyzed by Flowcytometry FACSDiva. Control cells were not treated. The Data are means \pm SD $n=4$, $p < 0.001$ as determined by one-way ANOVA. Baseline (control) vs Hcy ($p < 0.001$), Cbl ($p < 0.001$), Cbl+Hcy ($p < 0.001$), as determined by Tukey test *post hoc*. **A)** Intracellular pNf κ B by flowcytometry. **B)** Control cells (non-treated). **C)** Cells treated with 25μMCbl.

5.3.3 Effect of cobalamin protection on Nrf2

Cobalamin and folate had significant effect on the Nrf2 level in sk-hep1 cells ($P < 0.001$, as determined by one-way ANNOVA), (Figures 5.11&5.12). The post-hoc comparison showed that at $\geq 25\mu\text{M}$ cobalamin induce Nrf2 significantly and peaked at $50\mu\text{M}$ cobalamin as compared to control cells (non-treated) ($P < 0.001$), and Nrf2 induction decreased at higher concentration ($100\mu\text{M}$) of cobalamin (Figure 5.11). Moreover, cells subjected to $3.125\mu\text{M}$ Hcy showed a significant increase in the Nrf2 induction as compared to control cells (non-treated) ($P < 0.001$). And there was a further induction of Nrf2 when cells were subjected to $25\mu\text{M}$ cobalamin prior Hcy treatment as compared to Hcy alone ($P < 0.001$). Furthermore, cells were pre-treated with folate showed a significant induction of Nrf2 as compared to Hcy treatment alone ($P < 0.001$), (Figure 5.12).

The histograms in Figure 5.13, present the induction of Nrf2, such at $3.125\mu\text{M}$ Hcy showed a significant increase in the fluorescent intensity. Also when cells were pre-incubated with folate or cobalamin, it resulted in a significant shift in the fluorescent intensity.

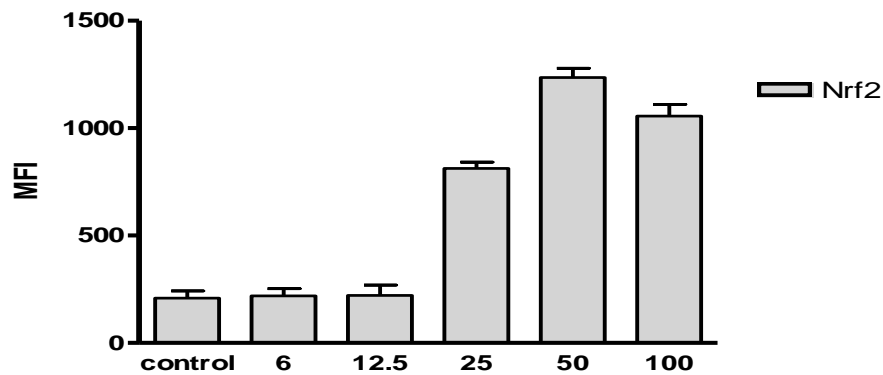


Figure 5.11: Effect of cobalamin on Nrf2 induction. Sk-hep1 cells were treated with a range of cobalamin concentrations (0-100μM) for 2 hours, control cells were not treated. Cells then were stained with Nrf2 specific antibody and analyzed using flow cytometry FACSDiva. The Data are means \pm SD n=4, $p < 0.001$ as determined by one-way ANOVA. Baseline (control) vs 25μM ($p < 0.001$), 50μM ($p < 0.001$), 100μM ($p < 0.001$), as determined by Tukey *post hoc*.

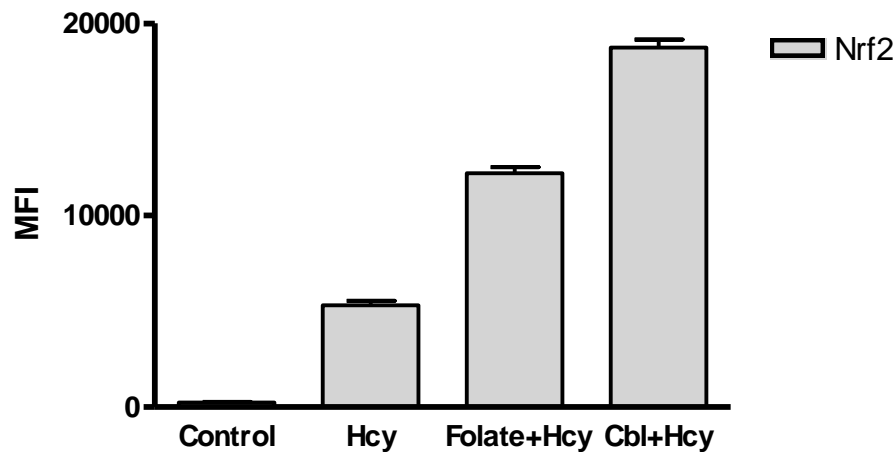
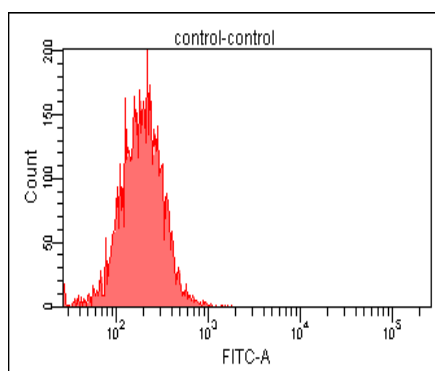
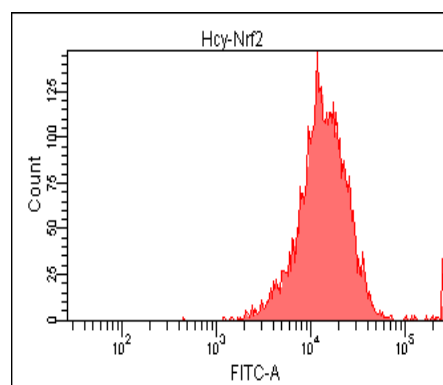


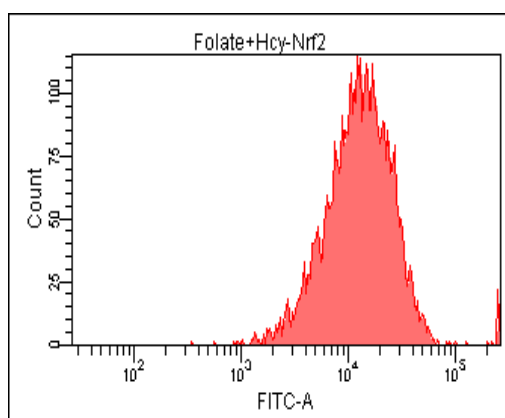
Figure 5.12: Induction of Nrf2 under cobalamin apoptosis protection. Sk-hep1 cells were pre-treated with 25μM cobalamin for 2 hours followed by treatment with 3.125μM Hcy for another 2 hours, control cells were not treated. Cells then were stained with specific antibody and analyzed using flow cytometry and BD FACSDiva software. The Data are means \pm SD n=4, $p < 0.001$ as determined by one-way ANOVA. Baseline (control) vs Hcy ($p < 0.001$), Folate+Hcy ($p < 0.001$), Cbl+Hcy ($p < 0.001$), as determined by Tukey *post hoc*.



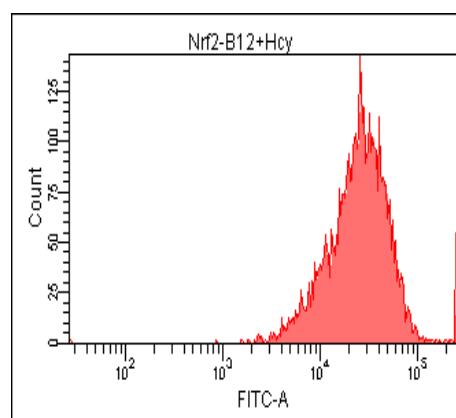
A. Control cells



B. 3.125 μ M Hcy



C. 30 μ M folate 2hours + 3.125 μ M Hcy



D. 25 μ MCbl + 3.125 μ M Hcy

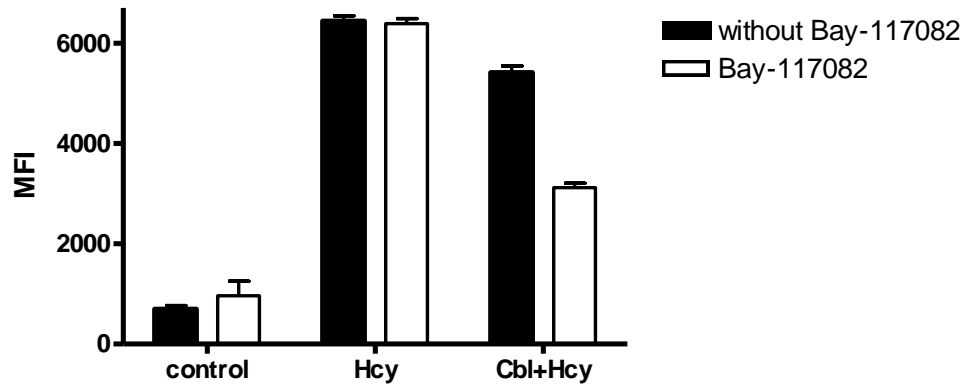
Figure 5.13: Induction of Nrf2 under oxidative stress and apoptosis protection conditions. After the indicated treatments and incubation time Sk-hep1 cells were stained with Nrf2 antibody and analyzed using flow cytometry. The Histograms are; **A.** control cells (non-treated), **B.** 3.125 μ M Hcy for 2 hours, **C.** 30 μ M folate 2hours followed by 3.125 μ M Hcy for 2 hours, **D.** 25 μ MCbl for 2 hours and 3.125 μ M Hcy for 2 hours.

5.3.4 Effect of signals transduction inhibitors on intracellular Hsps:

5.3.4.1 Effect of NfκB inhibition on intracellular Hsps:

As previously demonstrated, signals transduction pathways had a significant effect on cobalamin apoptosis protection; we further investigated the effect of these pathways on the intracellular Hsps under cobalamin apoptosis protection. Cells were sequentially treated with 5μM Bay-117082 for 2 hours, 25μM cobalamin for 2 hours and 3.125μM Hcy for another 2 hours. The result showed a significant effect on the intracellular Hsps under cobalamin protection condition ($P<0.001$, as determined by two-way ANNOVA), (Figures 5.14 & 5.15). Further analysis with Bonferroni pairwise showed that there were significant reductions in iHsp27, iHO-1 and iHsp72 by 20%, 40% and 75% respectively ($P<0.001$), while Bay-117082 had no significant effect on iHsp90. Moreover, when cells were treated with Bay-117082 and Hcy showed no significant effect iHsp27, iHO-1, iHsp72 and iHsp90 compared to control cells (Hcy alone) ($P>0.05$), (Figures 5.14 & 5.15), and treatment with Bay-117082 alone had no significant effect on iHsps induction as compared to control cells (non-treated) ($P>0.05$) .

A.



B.

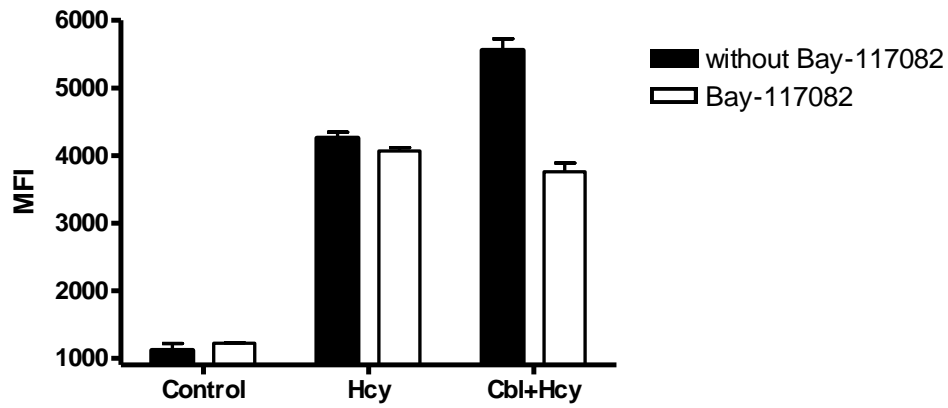
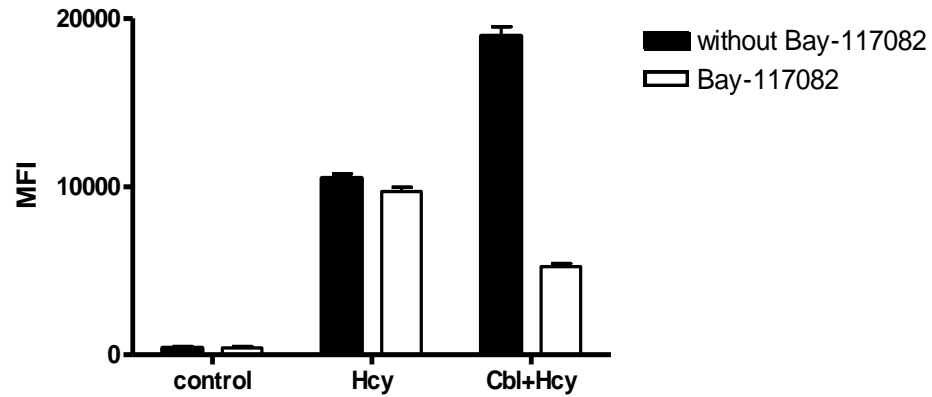


Figure 5.14: Effect of Bay-117082 on intracellular Hsp27 and HO-1 under cobalamin apoptosis-protection. Sk-hep-1 cells were pre-treated with 5 μ M Bay-117082 for 2 hour followed by 2 hours treatment with 25 μ M cobalamin and 2 hours of 3.125 μ M Hcy, control cells were not treated with bay-117082. Cells were then stained with monoclonal **A.** anti-Hsp27 or **B.** anti-HO-1 FITC was labelled and analyzed using flowcytometry FACSDiva. The Data are means \pm SD n=4, $p < 0.001$ as determined by two-way ANOVA. Baseline (Cbl+Hcy) vs Cbl+Hcy+Bay-117082 ($p < 0.001$), as determined by Bonferroni *post hoc*.

A.



B.

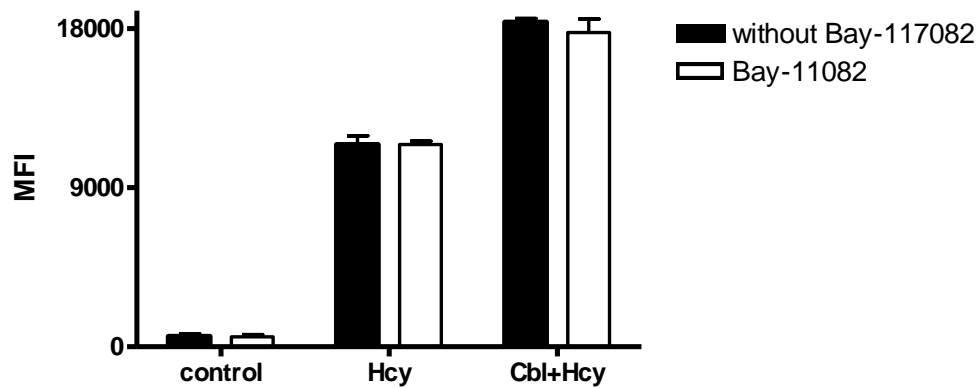


Figure 5.15: Effect of Bay-117082 on intracellular Hsp72 and Hsp90 under cobalamin apoptosis-protection. Sk-hep1 cells were pre-treated with 5 μ M Bay-117082 for 2 hours followed by 2 hours treatment with 25 μ M cobalamin and 2 hours of 3.125 μ M Hcy, control cells were not treated with bay-117082. Cells were then stained with monoclonal **A.** anti-Hsp72 FITC labelled or **B.** anti-Hsp90 PE was labelled and analyzed using flowcytometry FACSDiva. The Data are means \pm SD n=4, $p < 0.001$ as determined by two-way ANOVA. Baseline (Cbl+Hcy) vs Cbl+Hcy+Bay-117082 ($p < 0.001$)-Hsp72, as determined by Bonferroni *post hoc*.

5.3.4.2 Effect of ERK1/2 inhibition on intracellular Hsps:

Cells were subjected to 1 μ M U0126 for 1 hour prior exposure to 25 μ M cobalamin for 2 hours and 3.125 μ M Hcy for another 2 hours resulted in a significant effect on the iHsps ($p < 0.001$, as determined by two-way ANNOVA), (Figures 5.16 & 5.17). further analysis with Bonferroni pairwise showed significant reduction in the iHsp27 ($P < 0.01$), iHO-1 ($P < 0.001$), iHsp72 ($P < 0.001$) and iHsp90 ($P < 0.05$), by 25%, %61, %64 and %17 respectively less than cobalamin+Hcy treatment alone. However, U0126 had no significant effect on iHsps at Hcy treatment compared to Hcy treatment alone ($P > 0.05$). Also the iHsps had not been affected by treatment with U0126 alone as compared to control cells (non-treated) ($P > 0.05$), (Figures 5.16 & 5.17).

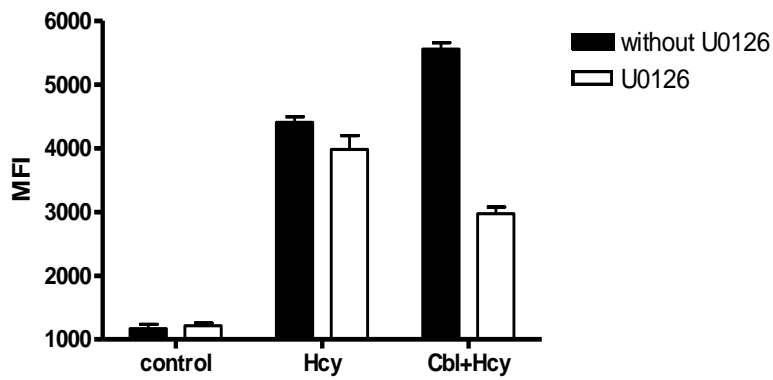
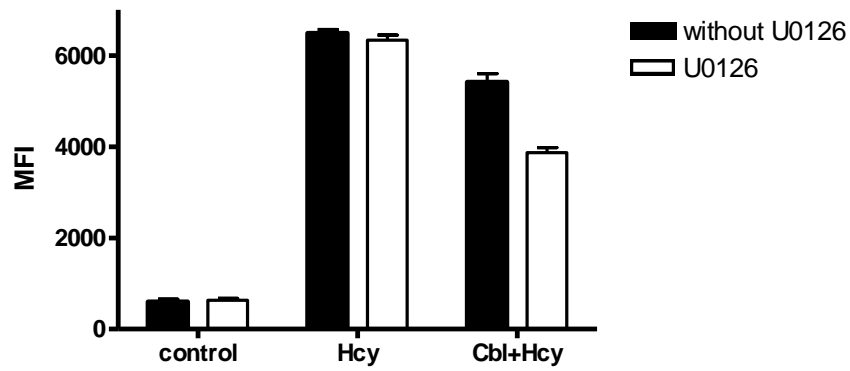


Figure 5.16: Effect of U0126 on intracellular Hsp27 and HO-1 under cobalamin apoptosis-protection. Sk-hep1 cells were pre-treated with 1 μ M U0126 for 2 hour followed by 2 hours treatment with 25 μ M cobalamin and 2 hours of 3.125 μ M Hcy. Control cells were non-treated with U0126. Cells were then stained with monoclonal **A.** anti-Hsp27 or **B.** anti-HO-1 FITC was labelled and analyzed using flowcytometry FACSDiva. The Data are means \pm SD n=4, $p < 0.001$ as determined by two-way ANOVA. Baseline (Cbl+Hcy) vs Cbl+Hcy+U0126 ($p < 0.001$), as determined by Bonferroni *post hoc*.

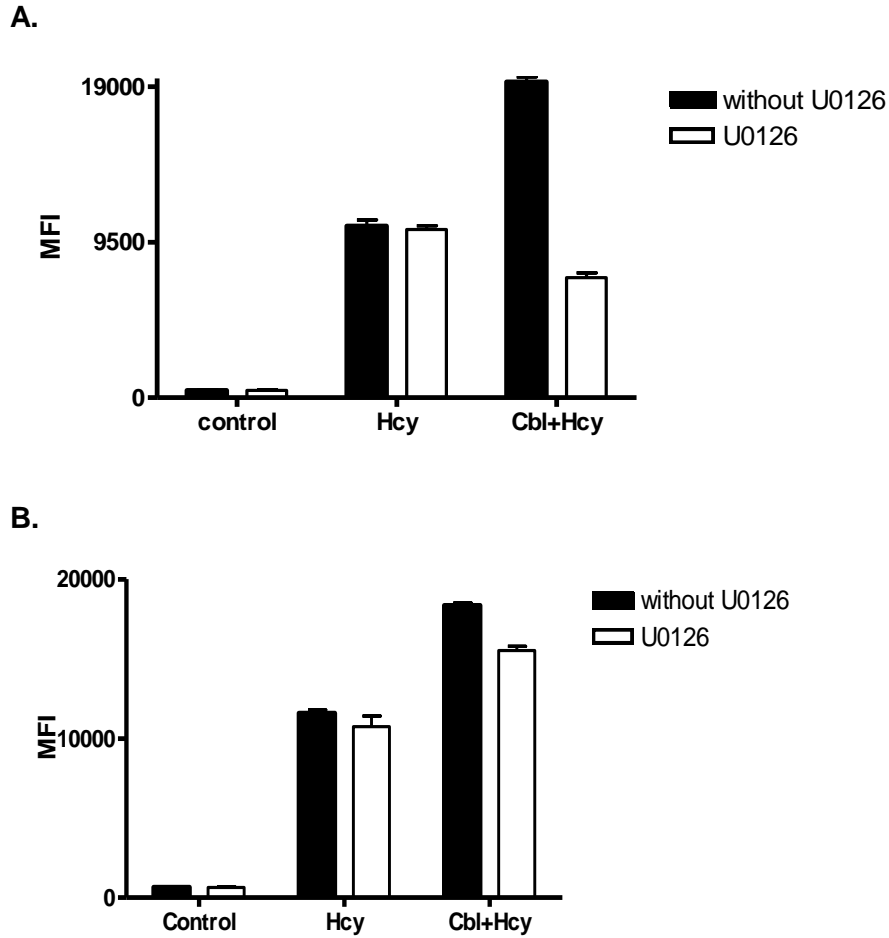
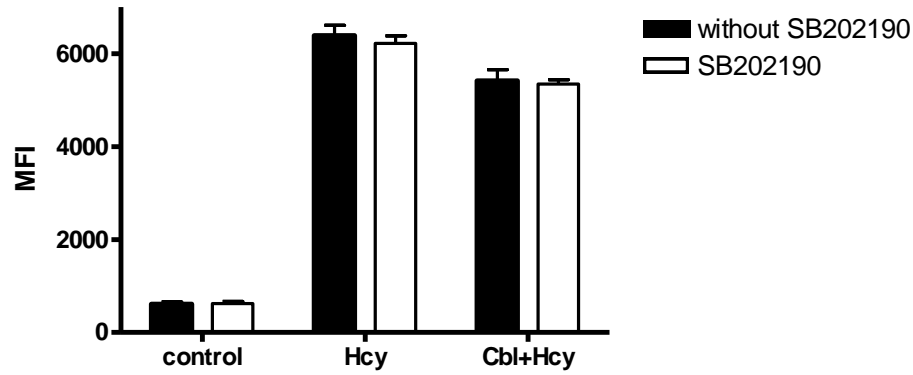


Figure 5.17: Effect of U0126 on intracellular Hsp72 and Hsp90 under cobalamin apoptosis-protection. Sk-hep1 cells were pre-treated with 1 μ M U0126 for 2 hour followed by 2 hours treatment with 25 μ M cobalamin and 2 hours of 3.125 μ M Hcy, control cells were not treated with U0126. Cells were then stained with monoclonal **A.** anti-Hsp72 FITC labelled or **B.** anti-Hsp90 PE was labelled and analyzed using flowcytometry FACSDiva. The Data are means \pm SD n=4, $p < 0.001$ as determined by two-way ANOVA. Baseline (Cbl+Hcy) vs Cbl+Hcy+ U0126 ($p < 0.001$), as determined by Bonferroni *post hoc*.

5.3.4.3 Effect of P38 inhibition on intracellular Hsps:

Cells were subjected to 12 μ M SB202190 for 2 hours prior to 25 μ M cobalamin for 2 hours and Hcy treatment resulted in no significant difference in the iHsp27 as compared to cobalamin+Hcy treatment alone ($P>0.05$, as determined by two-way ANNOVA). However, inhibition of P38 had a significant effect on iHO-1, iHsp72 and iHsp90 ($P<0.001$, as determined by two-way ANNOVA), (Figures 5.18 & 5.19). Also the post-hoc comparison showed that there was a significant reduction in the iHO-1 ($P<0.001$), iHsp72 ($P<0.001$), iHsp90 ($P<0.001$) by 20%, 22% and 23% respectively less than cobalamin+Hcy treatment alone. Moreover, the inhibition of P38 had no significant effect on iHsps at 3.125 μ M Hcy, compared to Hcy treatment alone ($P>0.05$). In the same time, SB202190 treatment alone had no significant effect on the intracellular Hsps as compared to control cells (non-treated) ($P>0.05$), (Figures 5.18 & 5.19).

A.



B.

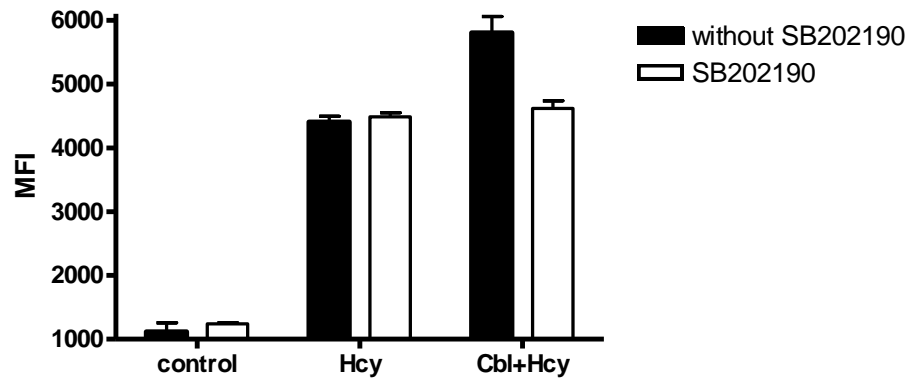


Figure 5.18: Effect of SB202190 on intracellular Hsp27 and HO-1 under cobalamin apoptosis-protection. Sk-hep1 cells were pre-treated with 12 μ M SB202190 for 2 hours followed by 2 hours treatment with 25 μ M cobalamin and 2 hours of 3.125 μ M Hcy, control cells were not treated with SB202190. Cells were then stained with monoclonal A. anti-Hsp27 or B. anti-HO-1 FITC was labelled and analyzed using flowcytometry FACSDiva. The Data are means \pm SD n=4, $p < 0.001$ as determined by two-way ANOVA. Baseline (Cbl+Hcy) vs Cbl+Hcy+ SB202190 ($p < 0.001$)-HO-1, as determined by Bonferroni *post hoc*.

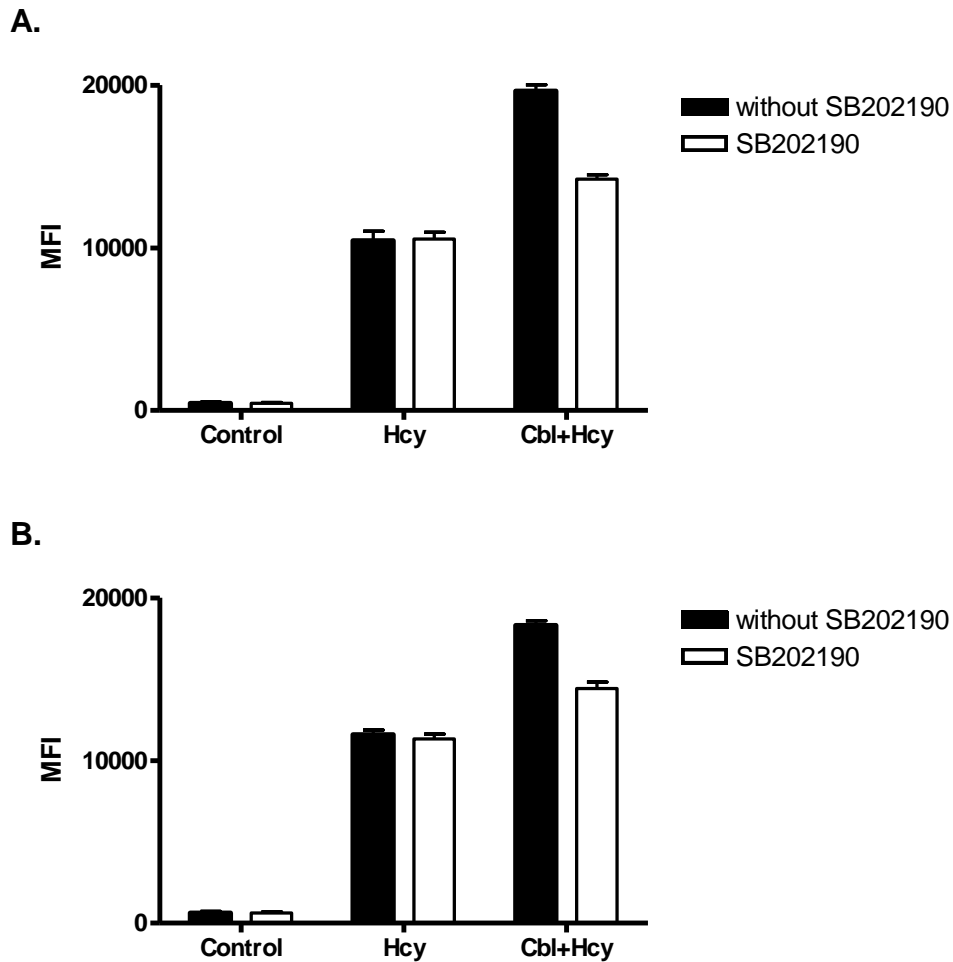
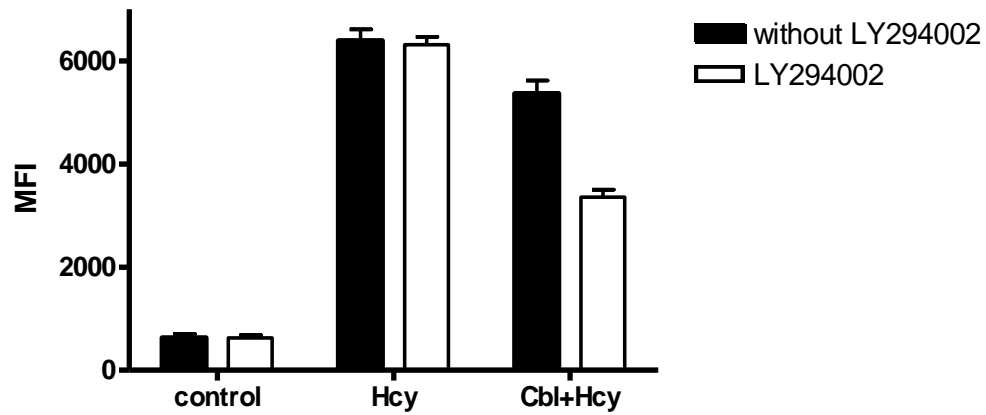


Figure 5.19: Effect of SB202190 on intracellular Hsp72 and Hsp90 under cobalamin apoptosis-protection. Sk-hep1 cells were pre-treated with 12 μ M SB202190 for 2 hours followed by 2 hours treatment with 25 μ M cobalamin and 2 hours of 3.125 μ M Hcy. Control cells were not treated with SB202190. Cells were then stained with monoclonal **A.** anti-Hsp72 FITC labelled or **B.** anti-Hsp90 PE was labelled and analyzed using flowcytometry FACSDiva. The Data are means \pm SD n=4, $p < 0.001$ as determined by two-way ANOVA. Baseline (Cbl+Hcy) vs Cbl+Hcy+ SB202190 ($p < 0.001$), as determined by Bonferroni *post hoc*.

5.3.4.4 Effect of (PI3 /AKT) inhibition on intracellular Hsps:

As previously showed PI3/AKT had a significant effect on cobalamin protection, also it seems had a significant effect on intracellular Hsps ($P < 0.001$, as determined by two-way ANNOVA), (Figures 5.20& 5.21). Further analysis with Bonferroni pairwise showed that when cells were treated with $10\mu\text{M}$ LY294002 for 1 hour followed by 2 hours treatment with $25\mu\text{M}$ cobalamin and 2 hours of $3.125\mu\text{M}$ Hcy, they showed a significant reduction in the iHsp27, iHO-1, iHsp72 and iHsp90 by 43%, 88%, 51% and 40% respectively less than cobalamin+Hcy alone ($P < 0.001$). However, cells exposed to LY294002 and Hcy showed no significant difference in iHsp27, iHO-1, iHsp72 and iHsp90 as compared to Hcy alone ($P > 0.05$). The LY294002 treatment only showed no significant difference in the intracellular Hsps compared to control cells (non-treated) ($P > 0.05$), (Figures 5.20& 5.21).

A.



B.

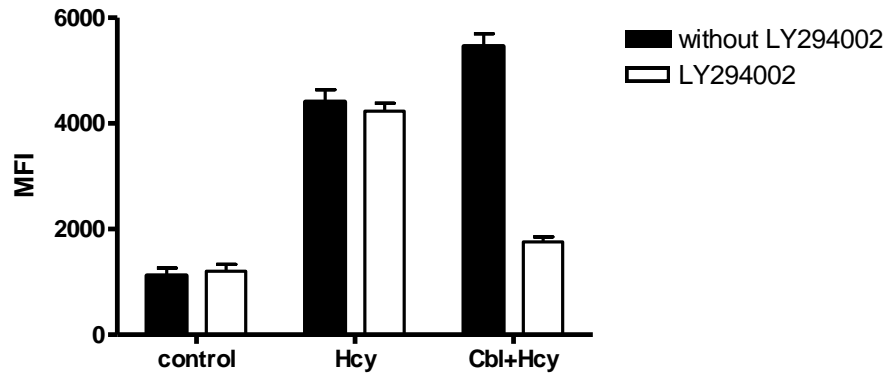
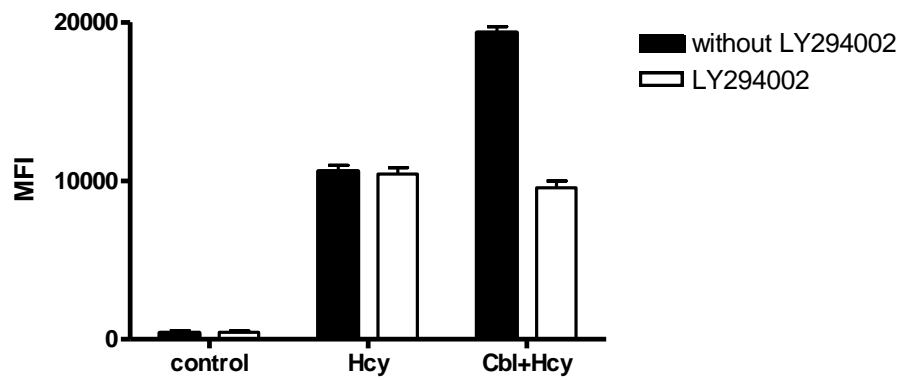


Figure 5.20: Effect of LY294002 on intracellular Hsp27 and HO-1 under cobalamin apoptosis-protection. Sk-hep1 cells were pre-treated with 10 μ M LY294002 for 2 hours followed by 2 hours treatment with 25 μ M cobalamin and 2 hours of 3.125 μ M Hcy. Control cells were non-treated with LY294002. Cells were then stained with monoclonal **A.** anti-Hsp27 or **B.** anti-HO-1 FITC was labelled and analyzed using flowcytometry FACSDiva. The Data are means \pm SD n=4, $p < 0.001$ as determined by two-way ANOVA. Baseline (Cbl+Hcy) vs Cbl+Hcy+ LY294002 ($p < 0.001$), as determined by Bonferroni *post hoc*.

A.



B.

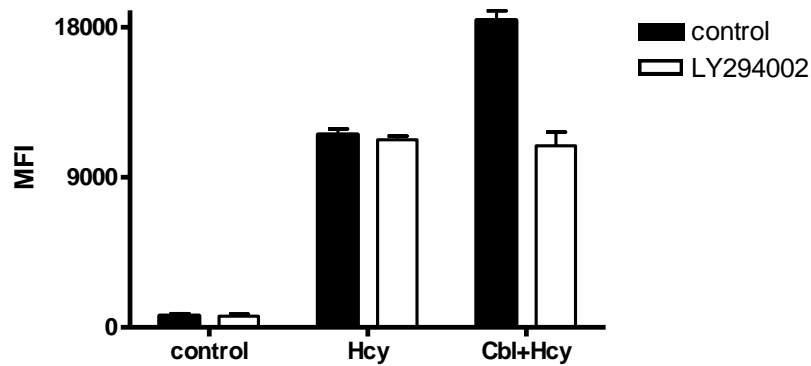
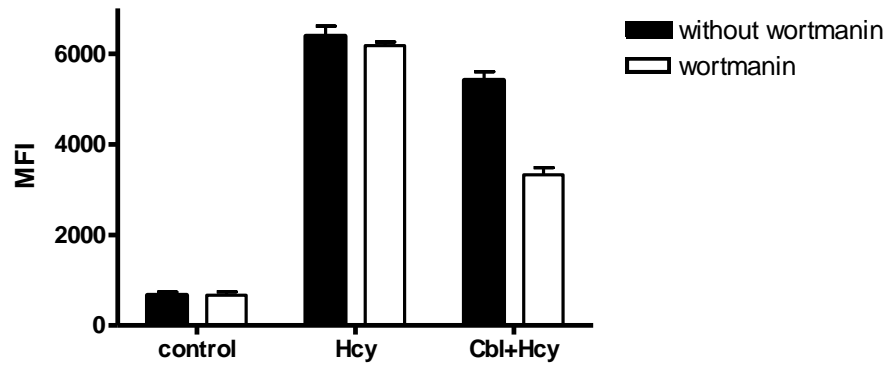


Figure 5.21: Effect of LY294002 on intracellular Hsp72 and Hsp90 under cobalamin apoptosis-protection. Sk-hep1 cells were pre-treated with 10 μ M LY294002 for 2 hours followed by 2 hours treatment with 25 μ M cobalamin and 2 hours of 3.125 μ M Hcy. Control cells were not treated with LY294002. Cells were then stained with monoclonal **A.** anti-Hsp72 FITC labelled or **B.** anti-Hsp90 PE was labelled and analyzed using flowcytometry FACSDiva. The Data are means \pm SD n=4, $p < 0.001$ as determined by two-way ANOVA. Baseline (Cbl+Hcy) vs Cbl+Hcy+ LY294002 ($p < 0.001$), as determined by Bonferroni *post hoc*.

5.3.4.5 Effect of Nrf2 inhibitor (Wortmanin) on intracellular Hsps under cobalamin apoptosis protection:

Nrf2 was involved in the protection mechanism of cobalamin as had been showed previously. Following this, cells were treated with 1 μ M Wortmanin for 1 hour prior treatments with 25 μ M cobalamin for 2hours and 3.125 μ M Hcy for another 2 hours, showed a significant effect on the iHsps ($P<0.001$, as determined by two-way ANNOVA), (Figures 5.22& 5.23). moreover, the post-hoc comparison showed significant differences in the iHsp27, iHO-1, iHsp72 and iHsp90 by 30%, 76%, 42% and 61% respectively less than cobalamin+Hcy alone ($P<0.001$). On the other hand, cells subjected to wortmanin prior Hcy treatment had no significant effect on iHsps as compared to Hcy alone ($P>0.05$). In the same time, the inhibition of Nrf2 didn't effect the intracellular Hsps significantly as compared to control cells (non-treated) ($P>0.05$), (Figures 5.22& 5.23).

A.



B.

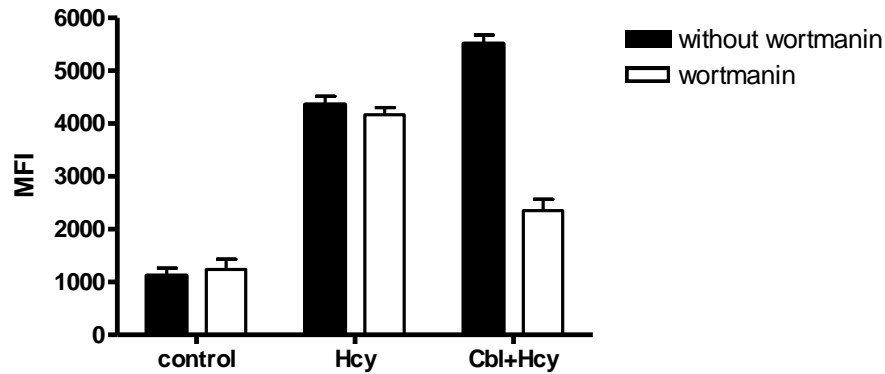


Figure 5.22: Effect of wortmanin on intracellular Hsp27 and HO-1 after cobalamin apoptosis-protection. Sk-hep1 cells were pre-treated with 1 μ M wortmanin for 2 hour followed by 2 hours treatment with 25 μ M cobalamin and 2 hours of 3.125 μ M Hcy. Control cells were not treated with wortmanin. Cells were then stained with monoclonal **A.** anti-Hsp27 or **B.** anti-HO-1 FITC was labelled and analyzed using flowcytometry FACSDiva. The Data are means \pm SD n=4, $p < 0.001$ as determined by two-way ANOVA. Baseline (Cbl+Hcy) vs Cbl+Hcy+ wortmanin ($p < 0.001$), as determined by Bonferroni *post hoc*.

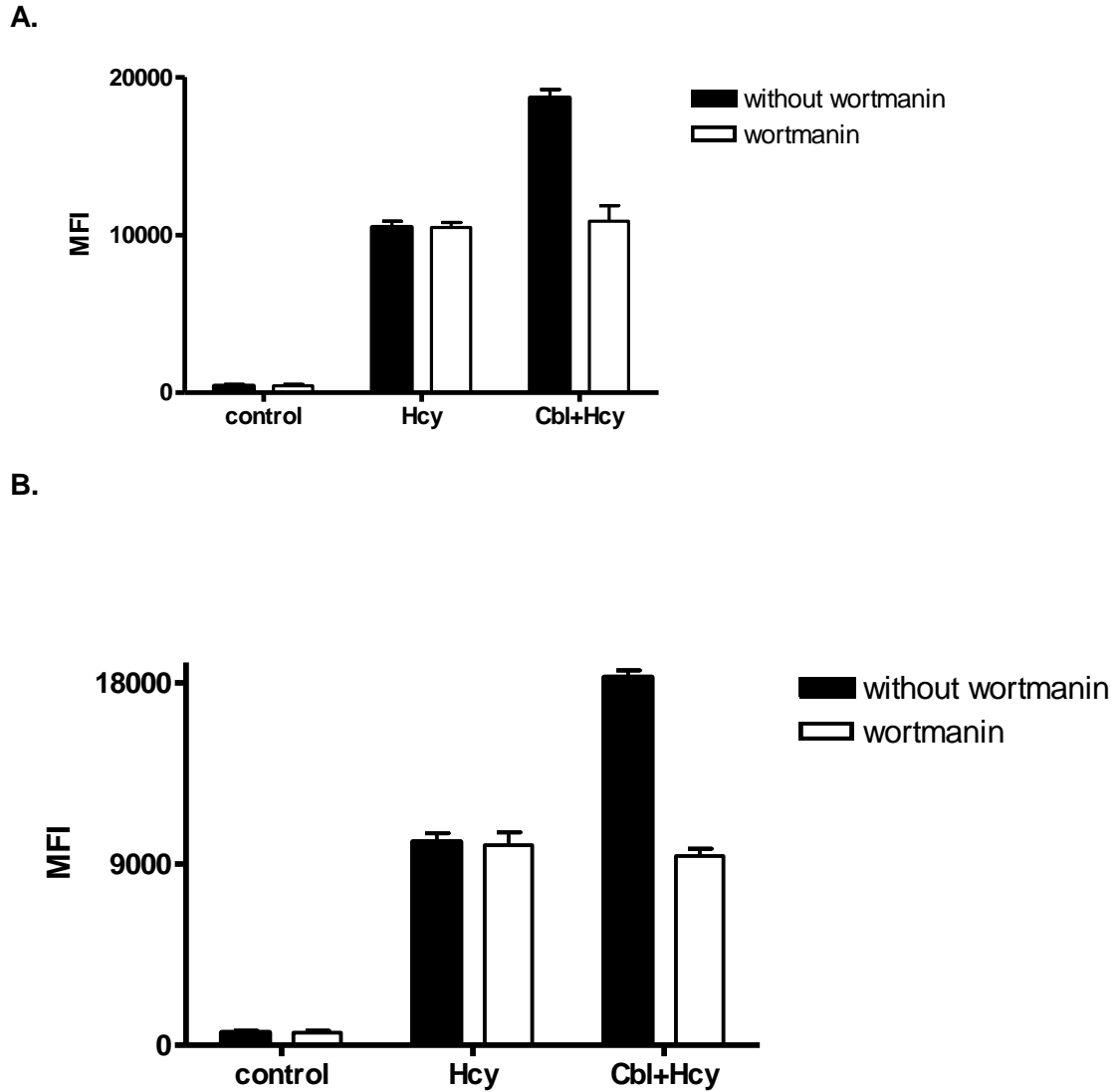


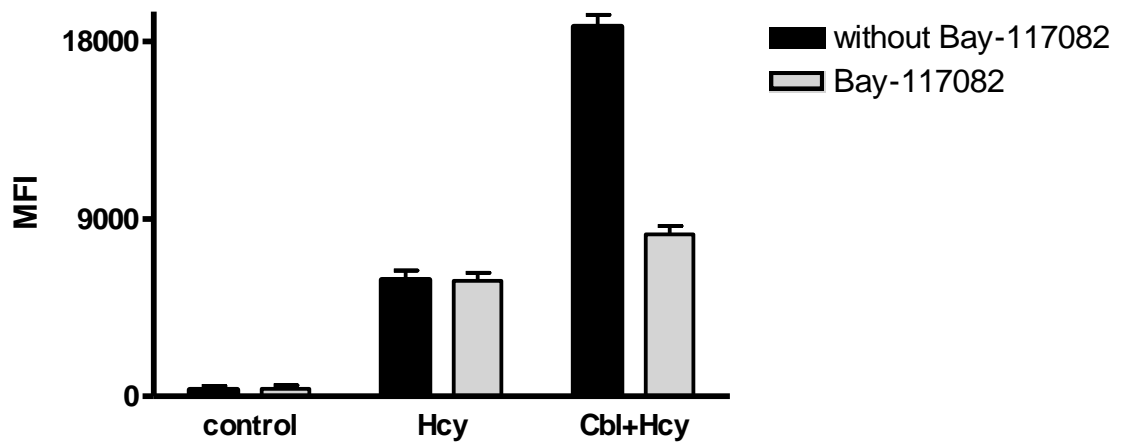
Figure 5.23: Effect of wortmanin on intracellular Hsp72 and Hsp90 under cobalamin apoptosis-protection. Sk-hep1 cells were pre-treated with 1 μ M wortmanin for 2 hours followed by 2 hours treatment with 25 μ M cobalamin and 2 hours of 3.125 μ M Hcy. Control cells were not treated with wortmanin. Cells were then stained with monoclonal **A.** anti-Hsp72 FITC labelled or **B.** anti-Hsp90 PE was labelled, and analyzed using flowcytometry FACSDiva. The Data are means \pm SD n=4, $p < 0.001$ as determined by two-way ANOVA. Baseline (Cbl+Hcy) vs Cbl+Hcy+ wortmanin ($p < 0.001$), as determined by Bonferroni *post hoc*.

5.3.5 Impact of signal transduction pathways on Nrf2 induction:

In order to investigate if the Nf_κB , ERK1/2, AKT/PI3, P38 and JNK regulate the Nrf2 induction, cells were subjected to 5 μM Bay-117082 or 1 μM U0126 or 10 μM LY294002 for 2 hours prior to exposure to 25 μM cobalamin for 2 hours and 3.125 μM Hcy for another 2 hours. Resulted in; Nrf2 significantly effected by this treatments ($P<0.001$, as determined by two-way ANNOVA), (Figures 5.23, 5.24, 5.24 & 5.25). Further more Bonferroni pairwise showed significant differences, by 60%, 70% and 94% at Bay-117082, U0126 and LY294002 prior cobalamin+Hcy respectively as compared to cobalamin+Hcy alone ($P<0.001$) (Figures 5.23 & 5.24). In the same time Bay-117082 and U0126 had no significant effect on Nrf2 induction at 3.125 μM Hcy as compared to Hcy alone ($P>0.05$), except pre-treatment of LY294002 reduced Nrf2 by 50% at 3.125 μM Hcy as compared to Hcy alone ($P<0.01$). Bay-117082, U0126 and LY294002 alone had no effect on Nrf2 induction significantly as compared to control cells (non-treated) ($P>0.05$) (Figures 5.24 & 5.25).

On the other hand, cells were treated with 12 μM SB202190 or 5 μM SP600125 for 2 hours prior to exposure to 25 μM cobalamin for 2 hours and 3.125 μM Hcy for another 2 hours showed, no significant difference in the Nrf2 induction as compared to control cells (Hcy+Cbl) ($P>0.05$, as determined by two-way ANNOVA), (Figure 5.26).

A.



B.

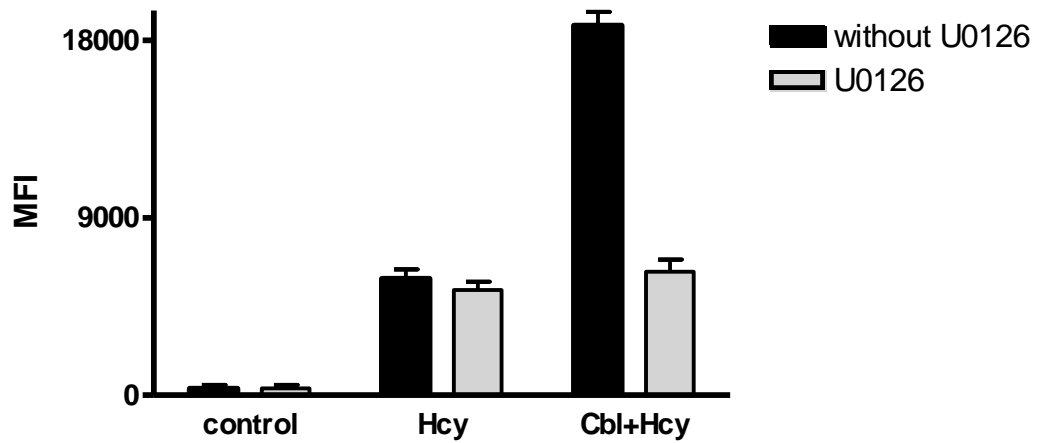


Figure 5.24: effect of Bay-117082 and U0126 on Nrf2 induction under cobalamin-apoptosis protection. Sk-hep1 cells were pre-treated with **A.** 5 μ M Bay-117082 or **B.** 1 μ M U0126 for 2 hours followed by treatments with 25 μ M cobalamin 2 hours and with 3.125 μ M Hcy. Control cells were not treated with U0126 or bay-117082. Then cells were stained with Nrf2 antibody and analyzed using flow cytometry FACSDiva. The Data are means \pm SD n=4, $p < 0.001$ as determined by two-way ANOVA. Baseline (Cbl+Hcy) vs Cbl+Hcy+ Bay-117082 ($p < 0.001$), Cbl+Hcy+ U0126 ($p < 0.001$), as determined by Bonferroni *post hoc*.

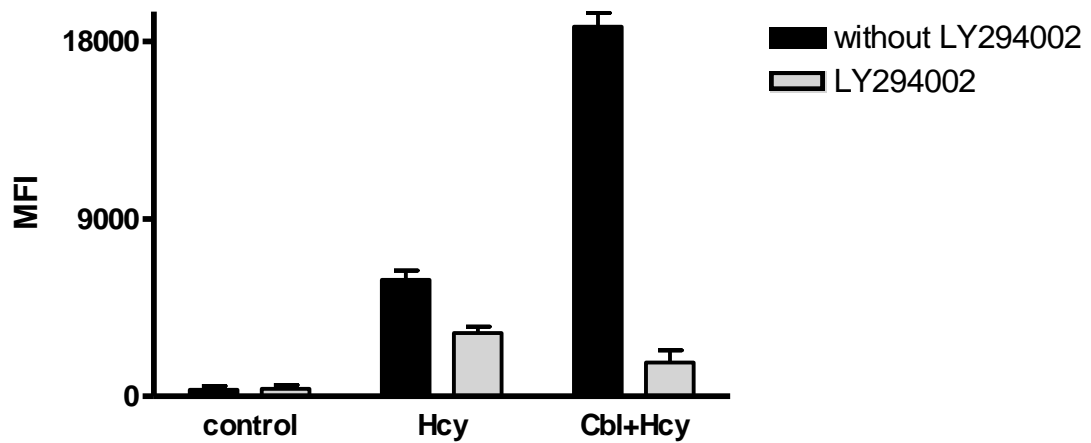
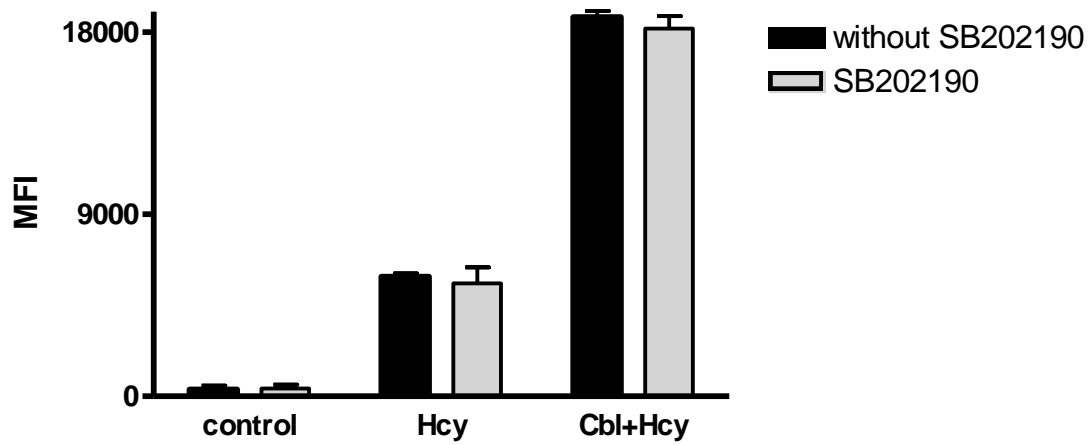


Figure 5.25: Effect of LY294002 on Nrf2 induction under cobalamin-apoptosis protection. Sk-hep1 cells were pre-treated with 10 μ M LY294002 for 2 hours followed by treatments with 25 μ M cobalamin 2 hours and with 3.125 μ M Hcy for another 2 hours. Control cells were not treated with LY294002. Then cells were stained with Nrf2 antibody and analyzed using flow cytometry FACSDiva. The Data are means \pm SD n=4, $p < 0.001$ as determined by two-way ANOVA. Baseline (Cbl+Hcy) vs Cbl+Hcy+ LY294002 ($p < 0.001$), Baseline (Hcy) vs Hcy+ LY294002 ($p < 0.001$), as determined by Bonferroni *post hoc*.

A.



B.

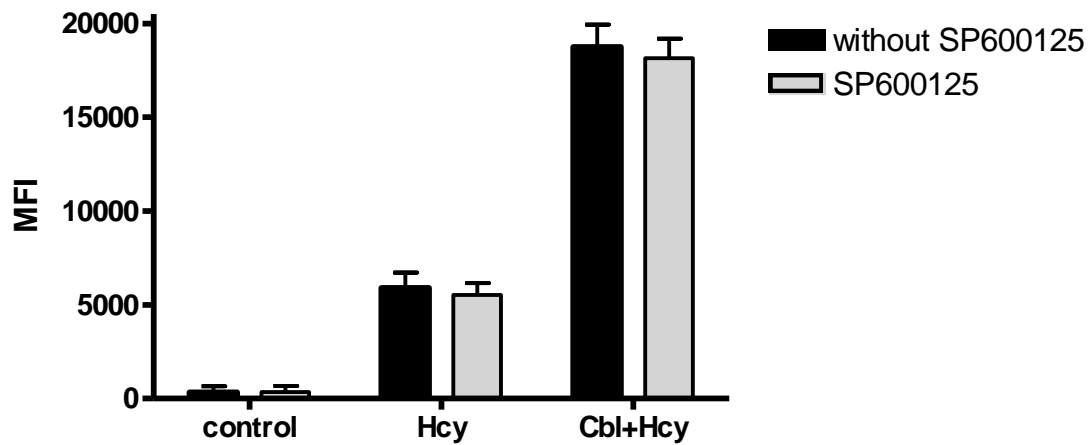
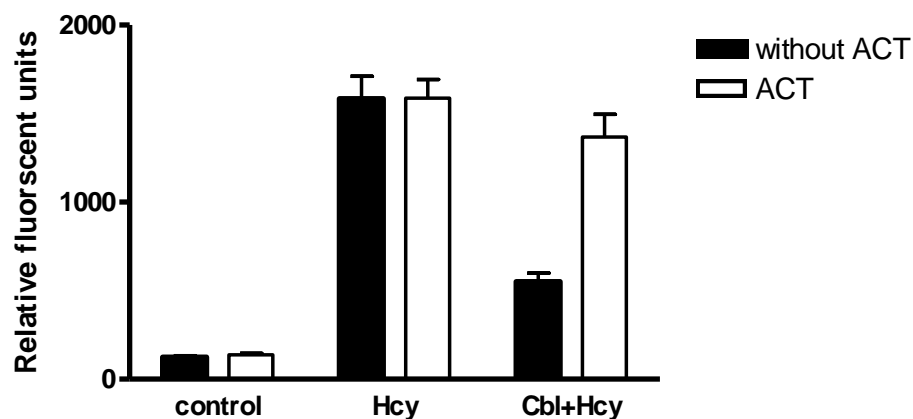


Figure 5.26: Effect of SB202190 or SP600125 on Nrf2 induction under cobalamin-apoptosis protection. Cells were pre-treated with **A.** 12 μ M SB202190 or **B.** 5 μ M SP600125 for 2 hours followed by treatments with 25 μ M cobalamin for 2 hours and with 3.125 μ M Hcy for another 2 hours. Control cells were not treated with SB202190 or SP600125. Cells then were stained with Nrf2 antibody and analyzed using flow cytometry FACSDiva. The Data are means \pm SD n=4, p> 0.05 as determined by two-way ANOVA.

5.3.6 Effect of signal transduction pathways on ROS reduction by cobalamin.

In order to study the effect of signal transduction pathways on ROS generation, cells were pre-treated with 5 μ M Actinomycin, 5 μ M Bay-117082, 1 μ M ERK1/2, 10 μ M LY294002, 12 μ M SB202190 or 5 μ M SP600125 for 2 hours followed by treatment with 25 μ M cobalamin and 3.125 μ M Hcy. The result showed that there was a significant effect on the ROS generation ($P < 0.001$, as determined by two-way ANNOVA), (Figures 5.27, 5.28, 5.29 & 5.30). The post-hoc comparison showed significant increase in the fluorescence intensity of DCFH-AC reached 45%, 56%, 60% and 66% respectively ($P < 0.001$). However, pre-treatment with Actinomycin, Bay-117082, ERK1/2 and LY294002 had no significant effect on Hcy fluorescence intensity of DCFH-AC as compared to Hcy alone ($P > 0.05$). The treatment of Actinomycin, Bay-117082, ERK1/2 or LY294002 alone didn't effect ROS generation as compared to control cells ($P > 0.05$), (Figures 5.27& 5.28). On the other hand, the treatment of SB202190 or SP600125 had no significant effect on the fluorescence intensity of DCFH-AC above cobalamin+Hcy alone ($P > 0.05$). Whereas cells exposed to SB202190 or SP600125 prior to Hcy showed a significant reduction of the fluorescence intensity of DCFH-AC by 42% and 40% respectively as compared to Hcy alone ($P < 0.001$). However, the fluorescence intensity of DCFH-AC doesn't had effect by the SB202190 or SP600125 treatment alone as compared to control cells ($P > 0.05$), (Figures 5.29 & 5.30).

A.



B.

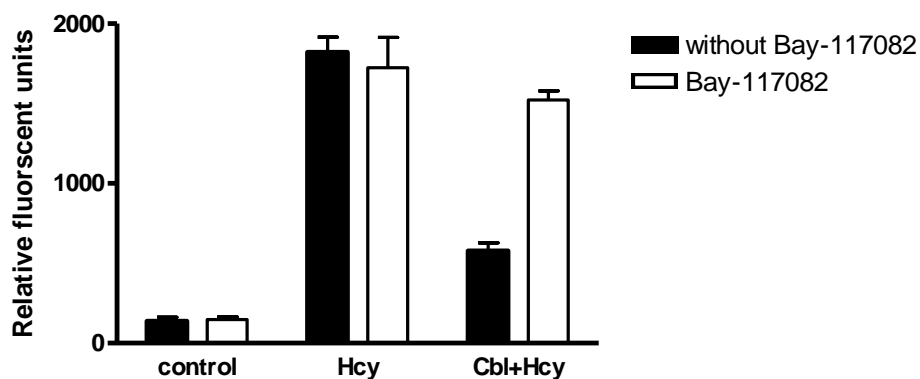
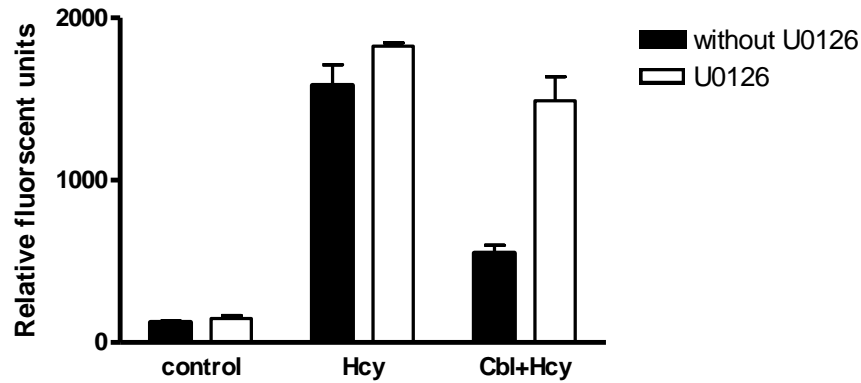


Figure 5.27: Effect of Actinomycin and Bay-110782 on generation of ROS. Sk-hep1 cells were pre-incubated in black 96-well plate with 10mM DCFH-diacetate, and then cells were treated with **A.** 5 μ M Actinomycin for 1 hour or **B.** 5 μ M Bay-117082 for 2 hours and with 25 μ M cobalamin for 2 hours followed by 2 hours treatments with 3.125 μ M Hcy. Control cells were not treated with Actinomycine or Bay-110782. Cells then were solubilised in 0.1N NaOH. DCFH-DA activity was measured at $\lambda_{Ex}485/\lambda_{Em}530$ nm following incubation. The Data are means \pm SD n=4, $p < 0.001$ as determined by two-way ANOVA. Baseline (Cbl+Hcy) vs Cbl+Hcy+ actinomycine ($p < 0.001$), Cbl+Hcy+ Bay-110782 ($p < 0.001$), as determined by Bonferroni *post hoc*.

A.



B.

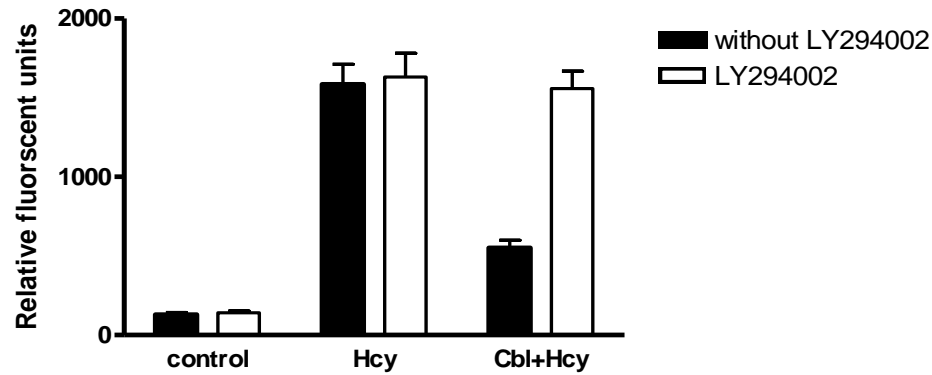
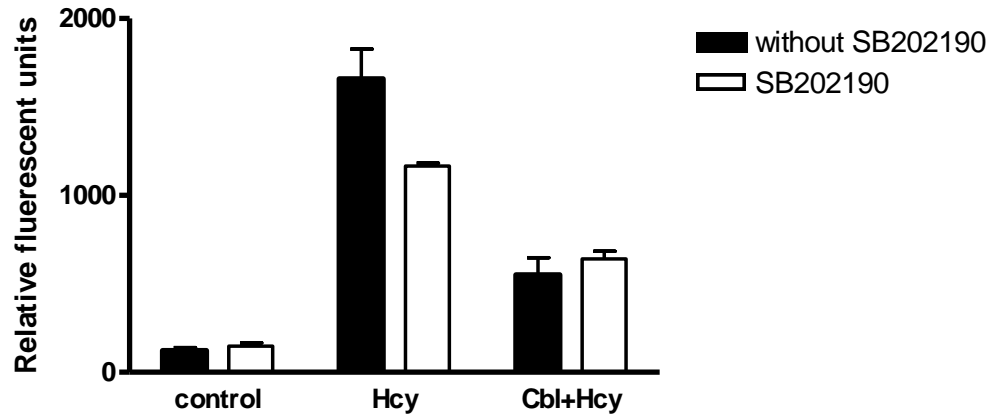


Figure 5.28: Effect of U0126 and LY294002 on generation of ROS. Sk-hep1 cells were pre-incubated in black 96-well plate with 10mM DCFH-diacetate, and then cells treated with **A.** 1 μ M U0126 for 1 hour or **B.** 10 μ M LY294002 for 2 hours and with 25 μ M cobalamin for 2 hours followed by 2 hours treatments with 3.125 μ M Hcy. Control cells were not treated with LY294002 or U0126. Then cells were solubilised in 0.1N NaOH. DCFH-DA activity was measured at EX=485/EM=530nm following incubation. The Data are means \pm SD n=4, $p < 0.001$ as determined by two-way ANOVA. Baseline (Cbl+Hcy) vs Cbl+Hcy+ LY294002 ($p < 0.001$), Cbl+Hcy+ U0126 ($p < 0.001$), as determined by Bonferroni *post hoc*.

A.



B.

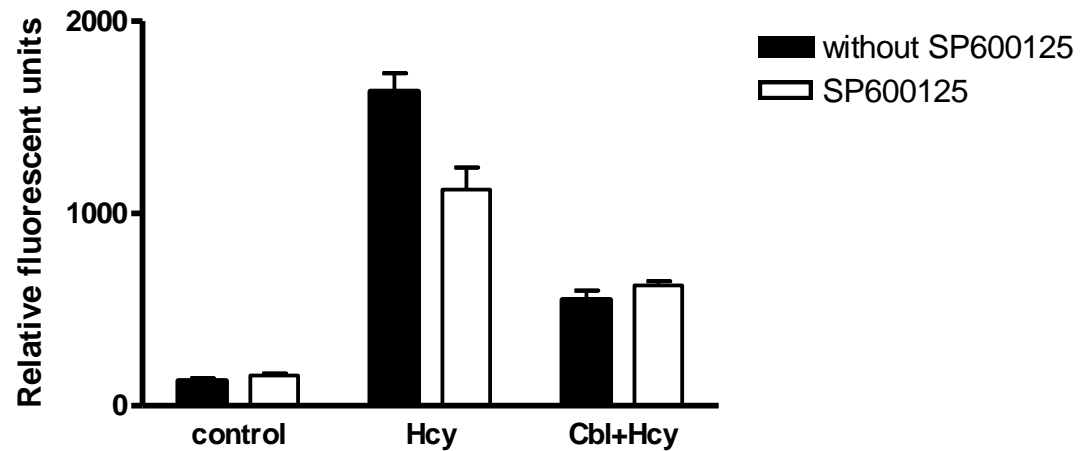
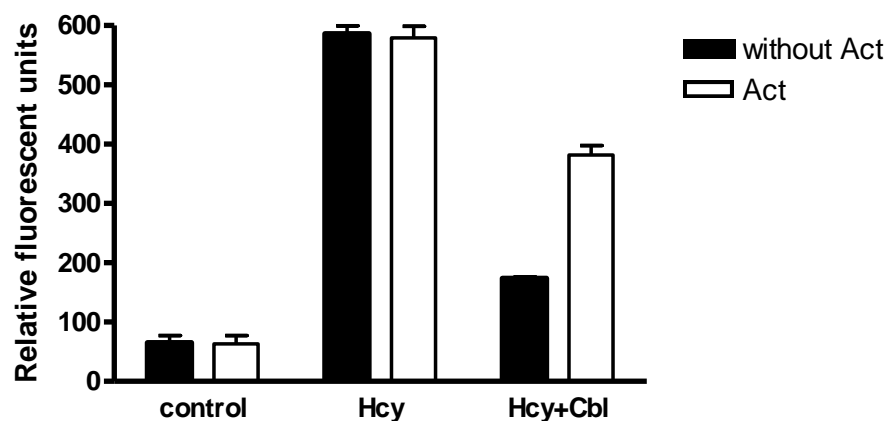


Figure 5.29: Effect of SB202190 and SP600125 on generation of ROS. Sk-hep1 cells were pre-incubated in black 96-well plate with 10mM DCFH-diacetate, and then cells were treated with **A.** 12 μ M SB202190 for 1 hour or **B.** 5 μ M SP600125 for 2 hours and with 25 μ M cobalamin for 2 hours followed by 2 hours treatments with 3.125 μ M Hcy. Control cells were not treated with SB202190 or SP600125. Cells were then solubilised in 0.1N NaOH. DCFH-DA activity was measured at EX=485/EM=530nm following incubation. The Data are means \pm SD n=4, $p < 0.001$ as determined by two-way ANOVA. Baseline (Hcy) vs Hcy+ SB202190 ($p < 0.001$), Hcy+ SP600125 ($p < 0.001$), as determined by Bonferroni *post hoc*.

5.3.7 Effect of signal transduction pathways on super oxide reduction by cobalamin

The inhibitors of signal transduction had a significant effect on the superoxide generation ($P < 0.001$, as determined by two-way ANNOVA), (Figures 5.30, 5.31 & 5.32). The post-hoc comparison showed that when cells were exposed to Actinomycin, Bay-117082, U0126 and LY294002 alone, they had no significant effect on the super oxide generation more than control cells ($P > 0.05$). However, When cells were exposed to the inhibitors (Actinomycin, Bay-117082, U0126 and LY294002 before 25 μ M cobalamin and 3.125 μ M Hcy treatment, that resulted insignificant increase in O_2^- generation which reached 45%, 64%, 63% and 68% above cobalamin+ Hcy treatment alone ($P < 0.001$). On the other hand, inhibitors had no significant effect on O_2^- generation at 3.125 μ M Hcy as compared to Hcy alone ($P > 0.05$), (Figures 5.30 & 5.31). Also, treatment with SB202190 and SP600125 prior to cobalamin and Hcy showed no significant difference on the O_2^- generation above cobalamin+Hcy alone ($P > 0.05$). However, inhibition of P38 and JNK reduced generation of O_2^- significantly at 3.125 μ M Hcy by 44% and 48% respectively less than Hcy alone ($P < 0.001$). The SB202190 and SP600125 alone had no significant effect on O_2^- generation as compared to control cells ($P > 0.05$), (Figure 5.32).

A.



B.

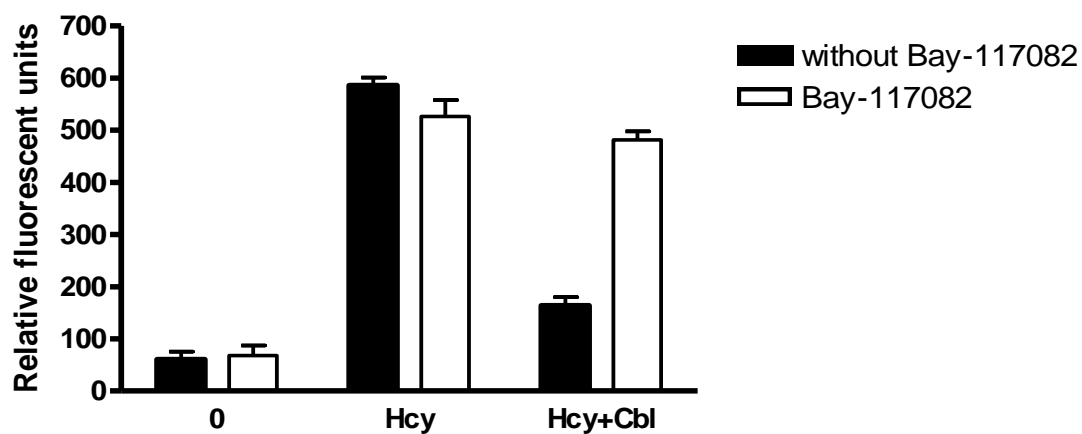
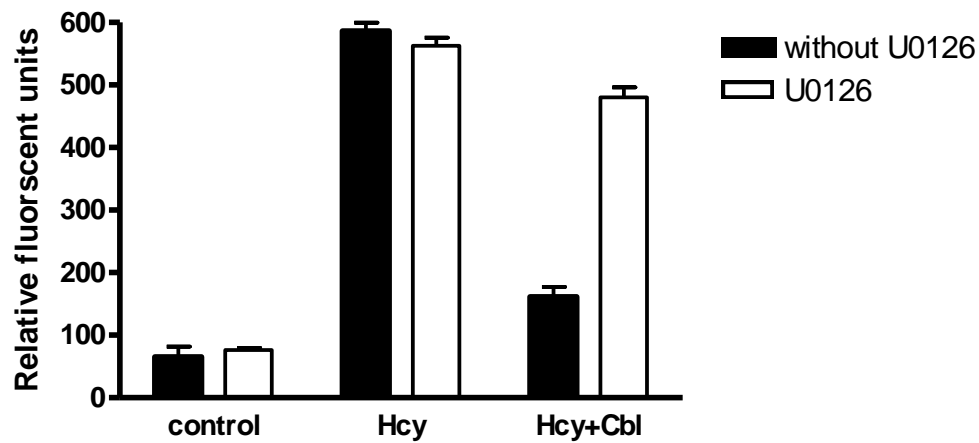


Figure 5.30: Effect of Actinomycin or Bay-11 on the superoxide generation. Sk-hep1 cells were pre-treated in 96-well plate with Lucigenin (5 μ M), and then cells were treated with **A.** 5 μ M actinomycin for 1 hour or **B.** 5 μ M Bay-117082 for 2 hours prior to treatment with 25 μ M cobalamin for 2 hours followed by 2 hours with 3.125 μ M Hcy. Control cells were not treated with actinomycin or Bay-11. Lucigenin chemiluminescence was measured at 550nm following incubation. The Data are means \pm SD n=4, $p < 0.001$ as determined by two-way ANOVA. Baseline (Cbl+Hcy) vs Cbl+Hcy+actinomycin ($p < 0.001$), Cbl+Hcy+Bay-117082 ($p < 0.001$), as determined by Bonferroni *post hoc*.

A.



B.

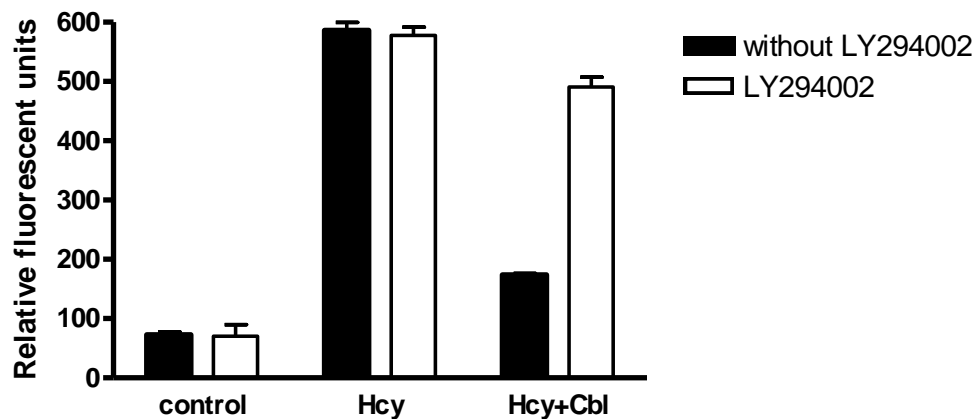
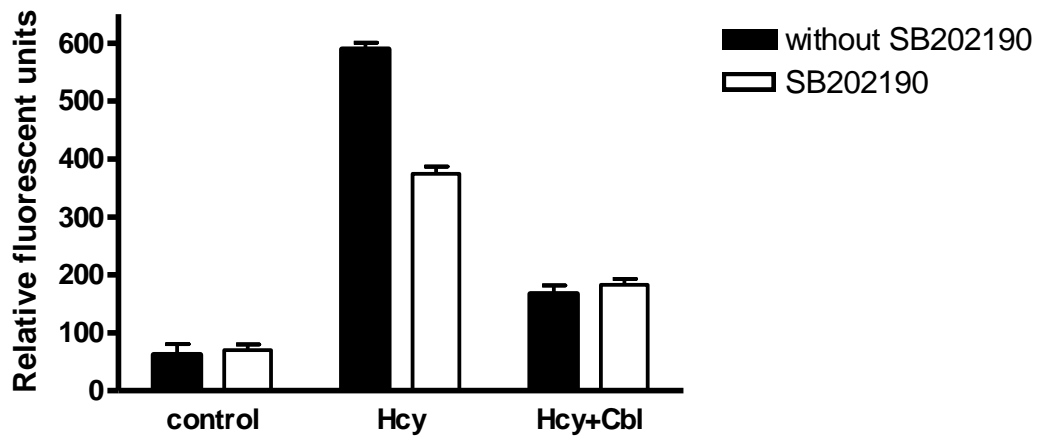


Figure 5.31: Effect of U0126 or LY294002 on the superoxide generation. Sk-hep1 cells were pre-treated in 96-well plate with Lucigenin (5 μ M), and then cells were treated with **A.** 1 μ M U0126 for 1 hour or **B.** 10 μ M LY294002 for 2 hours prior to treatment with 25 μ M cobalamin for 2 hours followed by 2 hours with 3.125 μ M Hcy. Control cells were not treated with U0126 or LY294002. Lucigenin chemiluminescence was measured at 550nm following incubation. The Data are means \pm SD n=4, $p < 0.001$ as determined by two-way ANOVA. Baseline (Cbl+Hcy) vs Cbl+Hcy+U0126 ($p < 0.001$), Cbl+Hcy+LY294002 ($p < 0.001$), as determined by Bonferroni *post hoc*.

A.



B.

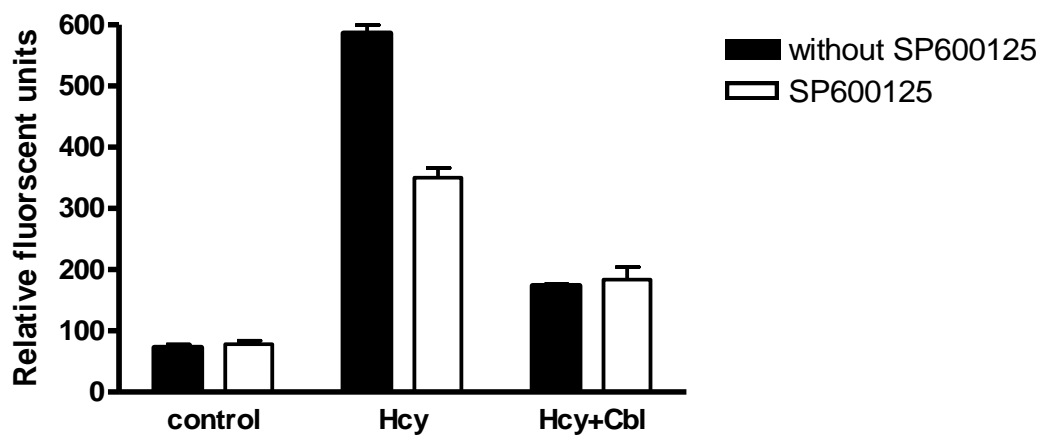


Figure 5.32: Effect of SB202190 or SP600125 on the superoxide generation. Sk-hep1 cells were pre-treated in 96-well plate with Lucigenin (5 μ M), and then cells were treated with **A.** 12 μ M SB202190 for 1 hour or **B.** 5 μ M SP600125 for 2 hours prior to treatment with 25 μ M cobalamin for 2 hours followed by 2 hours with 3.125 μ M Hcy. Control cells were not treated with SB202190 or SP600125. Lucigenin chemiluminescence was measured at 550nm following incubation. The Data are means \pm SD n=4, $p < 0.001$ as determined by two-way ANOVA. Baseline (Hcy) vs Hcy+ SB202190 ($p < 0.001$), Hcy+ SP600125 ($p < 0.001$), as determined by Bonferroni *post hoc*.

5.3.8 Impact cobalamin on iNOS induction:

To investigate the effect cobalamin on iNOS induction, cells which were exposed to 25 μ M cobalamin for 2 hours showed a significant increase in the fluorescent intensity of the iNOS as shown in Figure 5.33A-B.

Also cobalamin had a significant effect on the iNOS induction ($P < 0.001$, as determined by one-way ANNOVA), (Figure 5.34). The post-hoc comparison showed that under cobalamin, apoptosis protection condition iNOS has significantly increased as compared to control cells ($P < 0.001$), while Hcy treatment showed no significant effect on the iNOS induction ($P > 0.05$), however cobalamin treatment alone showed a significant increase in the iNOS fluorescent intensity ($p > 0.001$), (Figure 5.34).

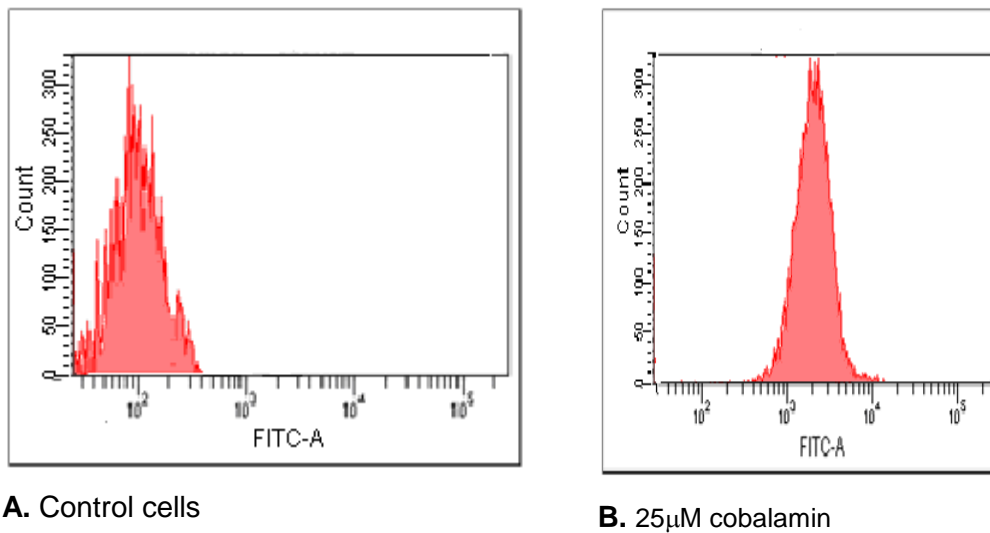


Figure 5.33: Effect of cobalamin on iNOS induction. Sk-hep1 cells were subjected to 25 μ M cobalamin for 2 hours. Following incubation, cells were stained with specific monoclonal iNOS antibody and analyzed by flowcytometry using FACSDiva software; **A.** non-treated cells, **B.** cells treated with 25 μ M cobalamin.

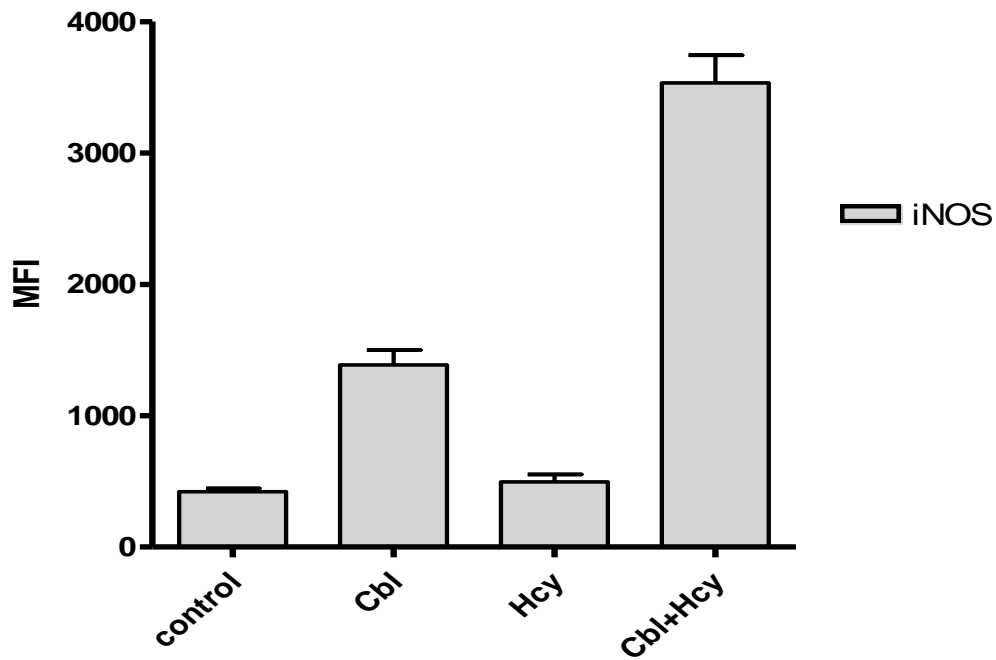


Figure 5.34: Effect cobalamin apoptosis protection on iNOS induction. Sk-hep1 cells were subjected to 25 μ M cobalamin for 2 hours. Following incubation, cells were stained with specific monoclonal iNOS antibody and analyzed by flowcytometry using FACSDiva software. Control cells were not treated. The Data are means \pm SD n=4, $p < 0.001$ as determined by one-way ANOVA. Baseline (control) vs Cbl+Hcy ($p < 0.001$), Cbl ($p < 0.001$), as determined by Tukey *post hoc*.

5.3.9 Impact of signals transduction pathways on iNOS induction:

In order to investigate the effect of signal transduction inhibitors, cells were pre-incubated with 5 μ M Bay-117082 or 1 μ M U0126 or 10 μ M LY294002 for 2 hours followed by 2 hours incubation with 25 μ M cobalamin and another 2 hours with 3.125 μ M Hcy. This treatment had a significant effect on the iNOS induction ($P < 0.001$, as determined by one-way ANNOVA), (Figures 5.35, 5.36 & 5.37). The tukey pairwise showed there was a significant reduction of iNOS induction by 85%, 65% and 52% at 5 μ M Bay-117082, 1 μ M U0126, 10 μ M LY294002 respectively less than cobalamin+Hcy alone ($P < 0.001$).

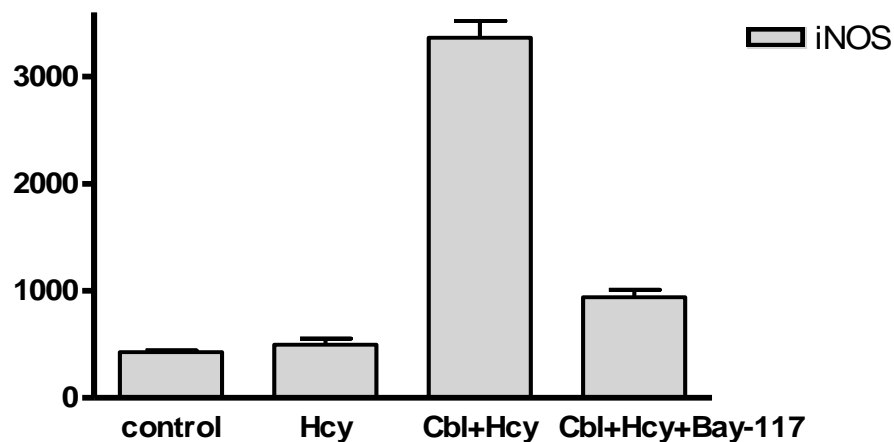


Figure 5.35: Effect of Bay-117082 on iNOS induction. Sk-hep1 cells were subjected to 5 μ M Bay-117082 for 2 hours prior to treatment with 25 μ M cobalamin for 2 hours followed by 2 hours with 3.125 μ M Hcy. Following incubation, cells were stained with specific monoclonal iNOS antibody and analyzed by flowcytometry using FACSDiva software. Control cells were not treated with Bay-11082. The Data are means \pm SD $n=4$, $p < 0.001$ as determined by one-way ANOVA. Baseline (cbl+hcy) vs Cbl+Hcy+Bay-117082 ($p < 0.001$), as determined by Tukey *post hoc*.

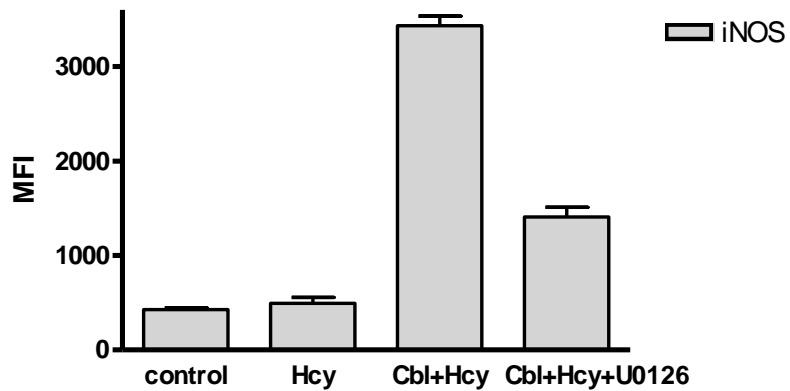


Figure 5.36: Effect of U0126 on iNOS induction. Sk-hep1 cells were subjected to $1\mu\text{M}$ U0126 for 2 hours prior to treatment with $25\mu\text{M}$ cobalamin for 2 hours followed by 2 hours with $3.125\mu\text{M}$ Hcy. Following incubation, cells were stained with specific monoclonal iNOS antibody and analyzed by flowcytometry using FACSDiva software. Control cells were not treated with U0126. The Data are means \pm SD $n=4$, $p < 0.001$ as determined by one-way ANOVA. Baseline (cbl+Hcy) vs Cbl+Hcy+U0126 ($p < 0.001$), as determined by Tukey *post hoc*.

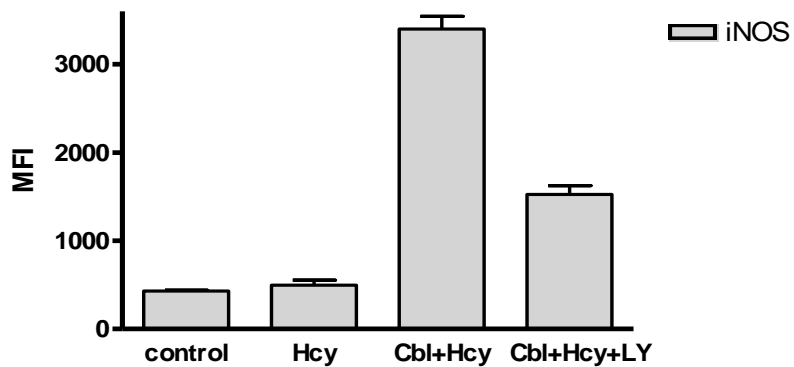


Figure 5.37: Effect of LY294002 on iNOS induction. Sk-hep1 cells were subjected to $10\mu\text{M}$ LY294002 for 2 hours prior to treatment with $25\mu\text{M}$ cobalamin for 2 hours followed by 2 hours with $3.125\mu\text{M}$ Hcy. Following incubation cells were stained with specific monoclonal iNOS antibody and analyzed by flowcytometry using FACSDiva software. Control cells were not treated with LY294002. The Data are means \pm SD $n=4$, $p < 0.001$ as determined by one-way ANOVA. Baseline (cbl+Hcy) vs Cbl+Hcy+ LY294002 ($p < 0.001$), as determined by Tukey *post hoc*.

5.4 Discussion:

The aim of this chapter is to investigate the mechanism of cobalamin-apoptosis protection and the involvement of the signal transduction pathways in this mechanism.

We first determined that cobalamin-apoptosis protection involves gene activation, regulated at gene transcription level, since the protection of cobalamin was prevented by pre-incubation with actinomycin which is known to inhibit gene transcription activity (Kvale & Holme, 1996).

Cobalamin is not known to directly affect signal transduction pathways, but it is known to influence TNF α production (Veber *et al.*, 2008). Nf κ B, ERK1/2 and AKT are induced by oxidative stress and act as a survival signals (Luo *et al.*, 2005; Xia *et al.*, 1995; brunet *et al.*, 2001; Harper & LoGrasso, 2001). The result in this chapter demonstrated a novel impact of cobalamin on the signal transduction pathways; hence there was a significant induction of pNf κ B, pERK1/2 and pAKT at 25 μ M cobalamin alone, although there was a further increase of pNf κ B, pERK1/2 and pAKT during cobalamin apoptosis protection, more than their level under apoptosis and cobalamin alone.

Moreover, Nrf2 was significantly induced by 25 μ M cobalamin and higher concentrations. Also, under cobalamin apoptosis protection Nrf2 induction increased more than their level under apoptosis. We can say that cobalamin induced the survival signals of transduction pathways and activities the Nrf2 which in turn regulate the activity of the antioxidant proteins.

We investigated further if these pathways are essential for the cobalamin-apoptosis protection. The result in this chapter showed that cobalamin protection was prevented when the pNf κ B inhibited by Bay-117082 or pERK1/2 inhibited by U01267 or pAKT/PI3 inhibited by LY294002 or Nrf2 inhibited by wortmanin. The inhibition of these proteins had no significant effect on the apoptosis induced by Hcy. Also the inhibition of these pathways increased superoxide and reactive oxygen species generation under cobalamin apoptosis protection. At the same time inhibition of pNf κ B

or pERK1/2 or pAKT had no significant effect on superoxide and reactive oxygen species generation under apoptosis induction. So we can confirm that Nf_κB, ERK1/2 and AKT are antiapoptosis signals and they are essential for cobalamin apoptosis protection.

On the other hand, the JNK and P38 are known as death signal pathways (Xia *et al.*, 1995; Brunet *et al.*, 2001; Harper & LoGrasso, 2001; Luo *et al.*, 2005), this statement supports the results of this chapter, which showed that the inhibition of these pathways had no significant effect on the cobalamin apoptosis protection. However, there was a significant reduction on apoptosis induction when JNK or P38 were inhibited, and this did not result in any increase in necrosis. At the same time the inhibition of JNK by SP600125 or P38 by SB202190 had no significant effect on superoxide and reactive oxygen species generation under cobalamin apoptosis protection, whereas there was a significant reduction in the superoxide and reactive oxygen species generation under apoptosis induction. It therefore has been demonstrated that JNK and P38 pathways are not essential in the cobalamin apoptosis protection.

The possible explanation of the antiapoptotic effect of the ERK1/2 might be due to their ability to suppress the expression of apoptotic genes and reduce ROS generation which leads to prevention of apoptotic cell death (Kurland *et al.*, 2003; Monick *et al.*, 2008). And moreover it has been suggested to regulate the induction of Nrf2 as the results in this chapter confirm (Chen *et al.*, 2004; Balogun *et al.*, 2003; Gong *et al.*, 2004). Furthermore, it has been demonstrated that AKT/PI3 regulate Nrf2 induction which controls ARE transcription that as a result regulates HO-1 and other antioxidant enzyme (Zhang & Gordon, 2004). Our result confirms that Nrf2 is mainly regulated by AKT/PI3, also by ERK1/2 and Nf_κB since there was a significant reduction of Nrf2 induction under cobalamin-apoptosis protection when ERK1/2 and Nf_κB inhibited. However, JNK and p38 had no significant effect on the Nrf2 activation as they are not essential for the protection.

Moreover, as it is shown in this chapter that Nf_κB plays a vital role in the cobalamin-apoptosis protection which might be due to Nf_κB ability to regulate the antiapoptotic proteins (Lin & Karin, 2003; Luo *et al.*, 2005). And also it confirmed that Nf_κB

regulates iNOS induction (Guoping *et al.*, 2001; Zeng *et al.*, 2005; Li *et al.*, 2006). Adding to the previous finding, the result showed that cobalamin had a novel impact on iNOS activity, since iNOS was induced by cobalamin and there was a further increase under cobalamin apoptosis protection as been hypothesised by Wheatley in 2007.

Recently it has been reported that Nf κ B/iNOS is regulated through ERK1/2 (Chun-Han, 2009). This statement supports our results and suggests the Nf κ B/iNOS signalling pathways is regulated through ERK1/2 and AKT pathways cobalamin-apoptosis protection system. As the inhibition of Nf κ B reduced iNOS induction by 85%, while ERK1/2 or AKT decreased iNOS induction by 65% and 52% respectively. So the iNOS mainly regulated by Nf κ B through ERK1/2 and AKT pathways.

In the previous chapter, we showed that cobalamin induced iHsps and also that HO-1 and Hsp72 are essential for cobalamin apoptosis protection. The results in this chapter showed that under cobalamin apoptosis protection; Nf κ B had a significant impact on Hsp72 induction, also the ERK1/2 regulates the HO-1 and Hsp72, and the AKT regulate HO-1 induction. These findings are consistent with other studies demonstrating the regulation of HO-1 through AKT-ERK1/2/Nrf2 (Balogum *et al.*, 2003; Zipper & Mulcuhy, 2003; Chen *et al.*, 2004; Gong *et al.*, 2004; Shen *et al.*, 2004) and the induction of Hsp72 through ERK1/2 pathway (Chen *et al.*, 2001). Hsp72 has been proposed to be regulated through ERK1/2, due to the ability of the ERK1/2 to phosphorelate Hsf1 which is a transcription factor of Hsp72 (Hung *et al.*, 1998). The inhibition of ERK1/2 leading to reduce Hsp72 expression as been demonstrated in this chapter confirm data from other laboratories (Chen *et al.*, 2001; Yang *et al.*, 2004; Seo *et al.*, 2005; Taylor *et al.*, 2007).

So the mechanism of cobalamin apoptosis protection involves three signal transduction pathways: Nf κ B, ERK/12 and AKT, These signals regulate Nrf2 and iNOS induction which leads to activation of HO-1 and Hsp72 and other antioxidant proteins to provide cell protection from apoptosis.

Chapter 6

Novel Cobalamin Protection Mechanism

6.1 Introduction

There are several forms of cobalamin, such as methylcobalamin, hydroxycobalamin, cyanocobalamin and adenosylcobalamin, GSCbl is one of the cobalamin derivatives which, is synthesised in the presence of glutathione, methylcobalamin and adenosylcobalamin. The GSCbl synthesis reaction required cobalamin dependent enzymes; MS and methylmalonyl-CoA mutase (MCM) (Pezacka 1993). GSCbl is proposed to be more effective than other cobalamin derivatives, due to its superior ability to promote methionine synthase activity (Pezacka *et al.*, 1990). Therefore, GSCbl might play a central role in the treatment of oxidative stress related diseases such as Alzheimer's disease.

Although GSCbl is a natural product and suggested to provide a protection against oxidative stress, also NACCbl proposed to provide a significant protection against oxidative stress (Birch *et al* 2009).

In the previous chapter it had been demonstrated that cobalamin has the ability to protect cells from oxidative stress. Also it had been proposed a mechanism of this protection that includes signals transduction and Hsps induction.

The aim of this chapter is to examine the protective role of the GSCbl and NACCbl and suggest a mechanism of their protection.

6.2 Methods

All preparations and cell culture experiments were carried out within a class II tissue culture hood.

6.2.1 The inhibitory study:

Cells were plated onto a black 96 well cell plate over night. Cells then were pre-incubated with the inhibitors for 2 hours followed by treatment with 25 μ M cobalamin for 2 hours and 3.125 μ M Hcy for another 2 hours, different analysis carried out after.

Actinomycin used as gene transcription inhibitor. A stock of 2mg/ml actinomycin was prepared by dissolving with acetonitrile and stored at 2-5°C. On the day of the experiment, the required concentration was prepared by diluting the stock with media.

Bay11-7082 was used to inhibit the Nf κ B activation. A stock of 10mM Bay11-7082 was prepared by dissolving with dimethyl sulfoxide and stored at 2-5°C. On the day of the experiment, the required concentration was prepared by diluting the stock with media.

U0126 was used to inhibit the ERK1/2 activation. A stock of 1mM U0126 was prepared by dissolving with dimethyl sulfoxide and stored at 2-5°C. On the day of the experiment, the required concentration was prepared by diluting the stock with media.

LY-294 was used to inhibit the AKT/PI3 activation. A stock of 1mM LY-294 was prepared by dissolving with ethanol acetate and stored at 2-5°C. On the day of the experiment, the required concentration was prepared by diluting the stock with media.

Wortmanin was used to inhibit the Nrf2 activation. A stock of 1mM wortmanin was prepared by dissolving with ethanol acetate and stored at 2-5°C. On the day of the experiment, the required concentration was prepared by diluting the stock with media.

SP600125 was used to inhibit the JNK activation. A stock of 1mM SP600125 was prepared by dissolving with dimethyl sulfoxide and stored at 2-5°C. On the day of the experiment, the required concentration was prepared by diluting the stock with media.

SB202190 was used to inhibit the P38 activation. A stock of 1mM U0126 was prepared by dissolving with dimethyl sulfoxide and stored at 2-5°C. On the day of the experiment, the required concentration was prepared by diluting the stock with media.

6.2.2 Cells count and viability test by trypan blue exclusion:

For the flow cytometry assays, following treatment, cells were re-suspended into the media by pipetting. Cells were then counted and assessed by trypan blue exclusion as described in (section 2.4.6)

6.2.3 Measurement of intracellular Hsps

The antibodies used were Anti-Hsp27 mouse monoclonal FITC conjugated antibody, Anti-HO-1 mouse monoclonal FITC conjugated antibody, Anti-Hsp72 mouse monoclonal FITC conjugated antibody and Anti-Hsp90 mouse monoclonal R-PHycoerythrin conjugated antibody. The dilution was 1:100.

Cells were treated under test conditions, once incubation time was over, cells were processed for staining and analysis as described in (section 2.4.13)

6.2.4 Measurement of pNf κ B induction:

Cells were treated under test condition and then processed as in (section 2.4.13). Polyclonal anti-pNf κ B Rabbit IgG antibody were diluted to 1:100 and used as first antibody and anti- rabbit IgG-FITC conjugated antibody were diluted to 1:100 and used as second antibody.

6.2.5 Measurement of pERK1/2 induction:

Cells were treated under test condition and then processed as in (section 2.4.13). Polyclonal anti-pERK1/2 Rabbit IgG antibody were diluted to 1:100 and used as first antibody and anti- rabbit IgG-FITC conjugated antibody were diluted to 1:100 and used as second antibody.

6.2.6 Measurement of pAKT induction:

Cells were treated under test condition and then processed as in (section 2.4.13). Polyclonal anti-pAKT Rabbit IgG antibody were diluted to 1:100 and used as first

antibody and anti- rabbit IgG-FITC conjugated antibody were diluted to 1:100 and used as second antibody.

6.2.7 Measurement of Nrf2 induction:

Cells were treated under test condition and then processed as in (section 2.4.13). Polyclonal anti-NRf2 goat IgG antibody were diluted to 1:100 and used as first antibody and anti- goat IgG-FITC conjugated antibody were diluted to 1:100 and used as second antibody.

6.2.8 Measurement iNOS induction:

Cells were treated under test condition and then processed as in (section 2.4.13). Polyclonal anti-iNOS Rabbit IgG antibody were diluted to 1:100 and used as first antibody and anti-rabbit IgG-FITC conjugated antibody were diluted to 1:100 and used as second antibody.

6.2.9 Measurement of super oxide generation

Cells were plated on to a black 96 well cell plate and treated under test condition then analysed for generation of super oxide by Lucigenin assay as described in (section 2.4.15).

6.2.10 Measurement of ROS generation

Cells were plated on to a black 96 well cell plate and treated under test condition then analysed for generation of reactive oxygen species by the fluorescence redox active probe 2', 7'-dichlorofluorescein-diacetate detection as described in (section 2.4.16).

6.2.11 Determination of apoptosis

Cells were plated on to a black 96 well cell plate and treated under test condition then analyzed for apoptosis by caspase-3/7 detection as described in (section 2.4.9).

6.3 Results

6.3.1 Effect of GSCbl and NACCbl on the apoptosis, necrosis induced by oxidative stress:

In chapter 3, it was demonstrated that folate and cobalamin provided a significant protection against apoptosis and necrosis induced by oxidative stress. However, in this chapter, NACCbl and GSCbl were more effective in terms of protection from apoptosis and necrosis induced by Hcy ($P<0.001$, as determined by two-way ANNOVA), (Figures 6.3& 6.4). Further analysis with Bonferroni pairwise showed that pre-treatment of cells for 2 hours with 30 μ M NACCbl and GSCbl followed by 2 hours exposing to range of Hcy concentrations (0-50 μ M), resulted in a significant protection provided at low concentration(1.325 μ M) of Hcy ($P<0.001$). Protection increased up to 80% and 82% at 3.125 μ M Hcy with pre-treatment with NACCbl and GSCbl respectively compared to control cells ($P<0.001$), followed by a significant protection with increasing concentration, compared to control cells ($P<0.001$), (Figures 6.1 & 6.2). More over, NACCbl and GSCbl both provided significant protection against necrosis at $\geq 12.5\mu$ M Hcy ($P<0.001$). Necrosis activity reached less than 25% or 20% with pre-incubation of NACCbl and GSCbl respectively compared to control cells (non-treated) ($P<0.001$), (Figures 6.3& 6.4).

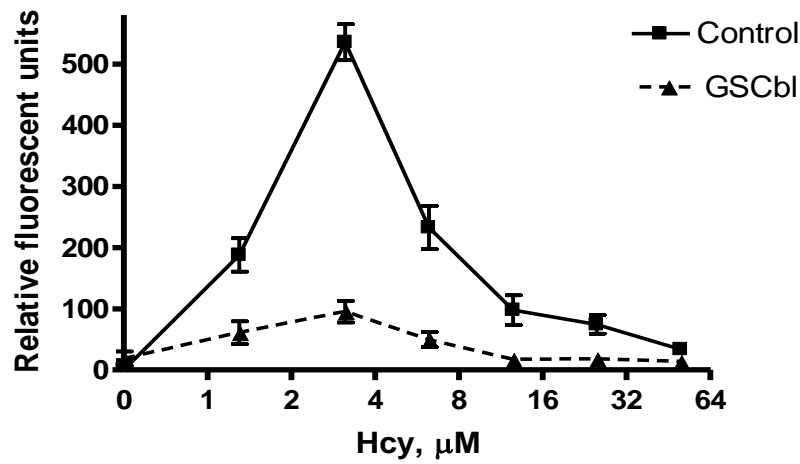


Figure 6.1: The effect of GSCbl pre-treatment on the caspase-3 activity. Sk-hep1 cells were pre-incubated with 30 μM GSCbl for 2 hours and treated with range of Hcy concentrations for 2 hours and control cells were treated with range of Hcy concentrations for 2 hours; Caspase-3 measured at EX=496nm/EM=520nm. The Data are means \pm SD n=4, $p < 0.001$ as determined by two-way ANOVA. Baseline (Hcy) vs GSCbl +1.325 μM Hcy ($p < 0.001$), GSCbl+3.125 μM Hcy ($p < 0.001$), GSCbl+6.25 μM Hcy ($p < 0.001$), GSCbl+12.5 μM Hcy ($p < 0.01$), as determined by Bonferroni *post hoc*.

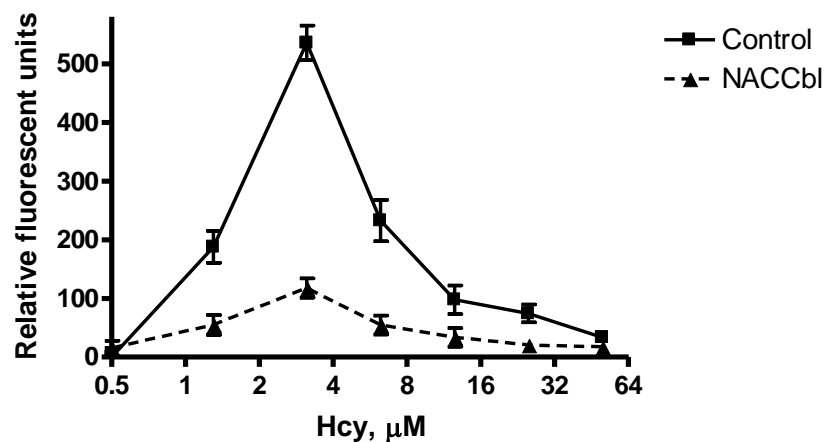


Figure 6.2: The effect of NACCbl pre-treatment on the caspase-3 activity. Sk-hep1 cells were pre-incubated with 30 μM NACCbl for 2 hours and treated with a range of concentrations of Hcy for 2 hours and the control cells were treated with a range of Hcy concentrations for 2 hours; Caspase-3 measured at EX=496nm/EM=520nm. The Data are means \pm SD n=4, $p < 0.001$ as determined by two-way ANOVA. Baseline (Hcy) vs NACCbl 1.325 μMHcy ($p < 0.001$), NACCbl+3.125 μMHcy ($p < 0.001$), NACCbl +6.25 μMHcy ($p < 0.001$), NACCbl+12.5 μMHcy ($p < 0.01$), as determined by Bonferroni *post hoc*.

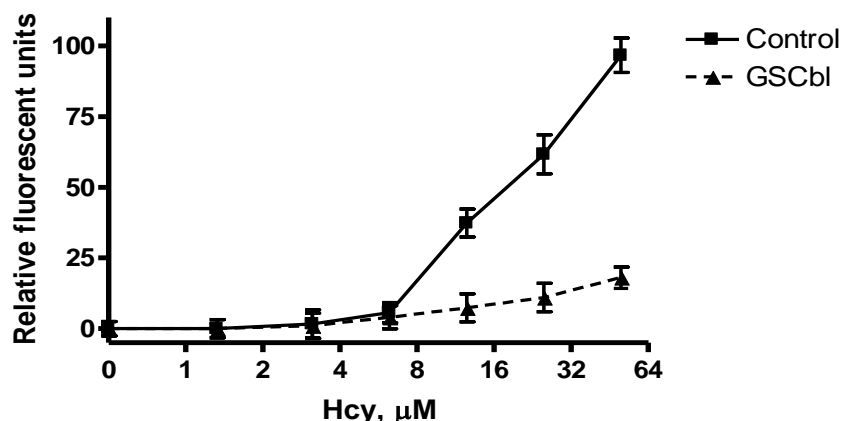


Figure 6.3: The effect of GSCbl pre-treatment on necrosis. Sk-hep1 cells were pre-incubated with 30 μM GSCbl for 2 hours and treated with a range of Hcy concentrations for 2 hours and the control cells were treated with a range of Hcy concentrations for 2 hours; PI penetration assay was measured after at EX=535/EM=617. The Data are means \pm SD n=4, $p < 0.001$ as determined by two-way ANOVA. Baseline (Hcy) vs GSCbl +12.5 μM Hcy ($p < 0.001$), GSCbl+25 μM Hcy ($p < 0.001$), GSCbl+50 μM Hcy ($p < 0.001$), GSCbl+12.5 μM Hcy ($p < 0.01$), as determined by Bonferroni *post hoc*.

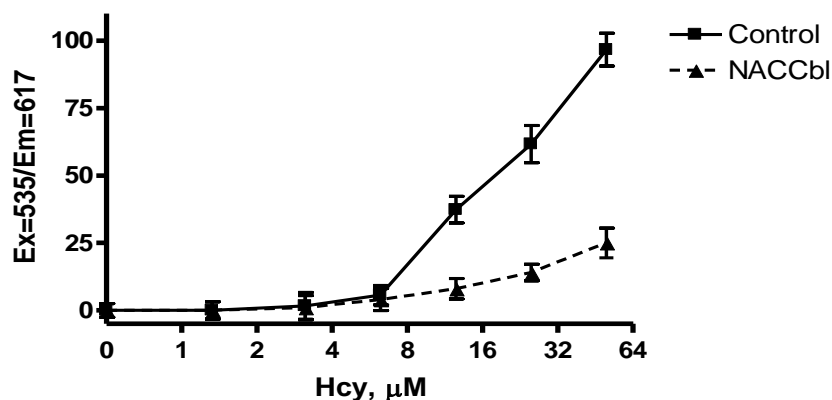


Figure 6.4: The effect of NACCbl pre-treatment on necrosis. Sk-hep1 cells were pre-incubated with 30 μM NACCbl for 2 hours and treated with a range of Hcy concentrations for 2 hours while control cells were treated with a range of Hcy concentrations for 2 hours; PI penetration was measured after at EX=535/EM=617. The Data are means \pm SD n=4, $p < 0.001$ as determined by two-way ANOVA. Baseline (Hcy) vs NACCbl 12.5 μM Hcy ($p < 0.001$), NACCbl+25 μM Hcy ($p < 0.001$), NACCbl+50 μM Hcy ($p < 0.001$), as determined by Bonferroni *post hoc*.

6.3.2 The impact of GSCbl and NACCbl on ROS and super oxide generation:

In chapter 3, it had been showed that cobalamin reduce superoxide and ROS significantly, so in order to determine the effect of GSCbl and NACCbl on ROS and O_2^- generation and compare it to cobalamin, cells were subjected to 30 μ M GSCbl, 30 μ M NACCbl and 25 μ M cobalamin for 2 hours prior 3.125 μ M Hcy for another 2 hours. This resulted in a significant effect on the ROS and super oxide generation ($P < 0.001$, as determined by one-way ANNOVA), (Figures 6.5& 6.6). The post hoc comparison showed that the DCFH-AC fluorescence intensity decreased significantly at 30 μ M GSCbl ($P < 0.001$), 30 μ M NACCbl ($P < 0.01$) as compared to cobalamin+Hcy, in the same time GSCbl, NACCbl and cobalamin treatment alone had no significant effect on the DCFH-AC fluorescence intensity as compared to control cells ($P > 0.05$), (Figure 6.5). Additionally, there was a significant decrease in the O_2^- generation at 30 μ M GSCbl ($P < 0.001$), 30 μ M NACCbl ($P < 0.001$) as compared to cobalamin+Hcy. Also there was no detectable difference in O_2^- generation in GSCbl and NACCbl treatment alone compared to control cells ($P > 0.05$), (Figure 6.6).

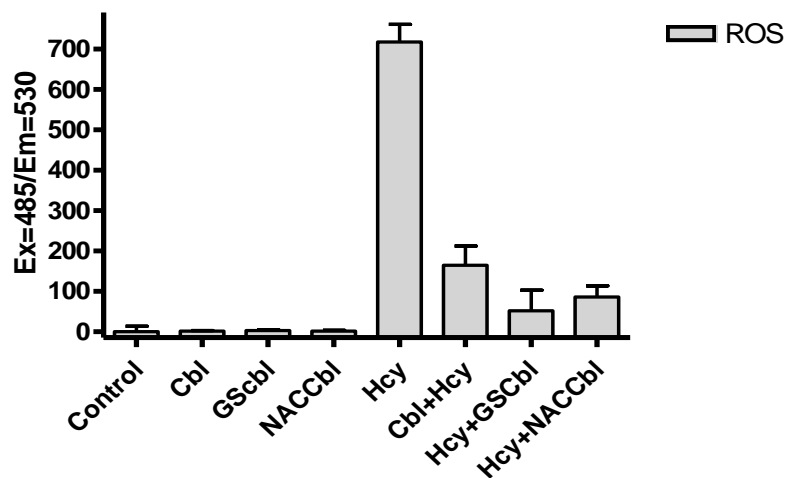


Figure 6.5: Effect of GSCbl and NACCbl on generation of reactive oxygen species. Sk-hep1 cells were pre-incubated in black 96-well plate with 10mM DCFH-diacetate, then 25 μ M cobalamin for 2 hours followed by 2 hours treatments with 3.125 μ M Hcy, control cells were not treated and then all cells were solubilised in 0.1N NaOH. DCFH-DA activity was measured at EX=485/EM=530nm following incubation. The Data are means \pm SD n=4, $p < 0.001$ as determined by one-way ANOVA. Baseline (Hcy) vs Cbl+Hcy ($p < 0.001$), GSCbl+Hcy ($p < 0.001$), NACCbl+Hcy ($p < 0.001$), as determined by Tukey *post hoc*.

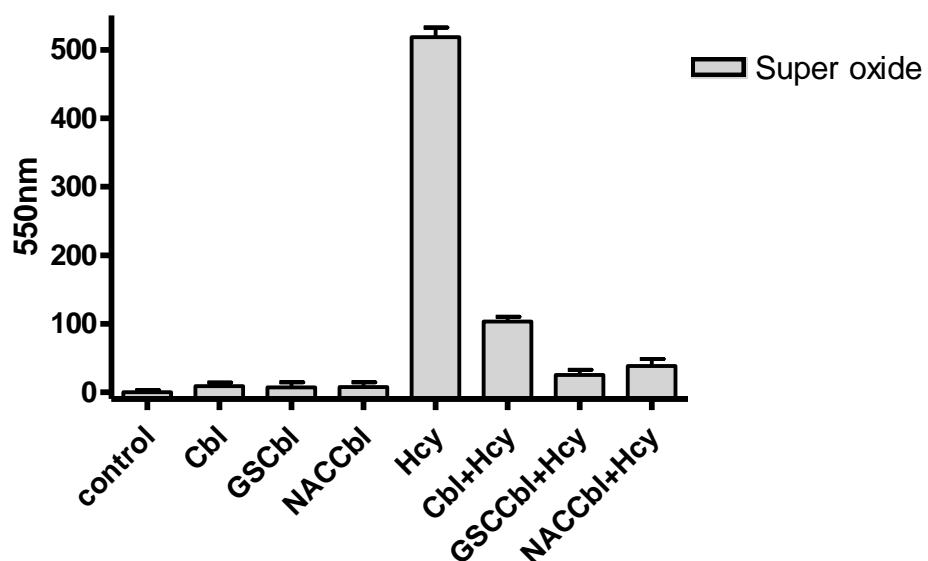
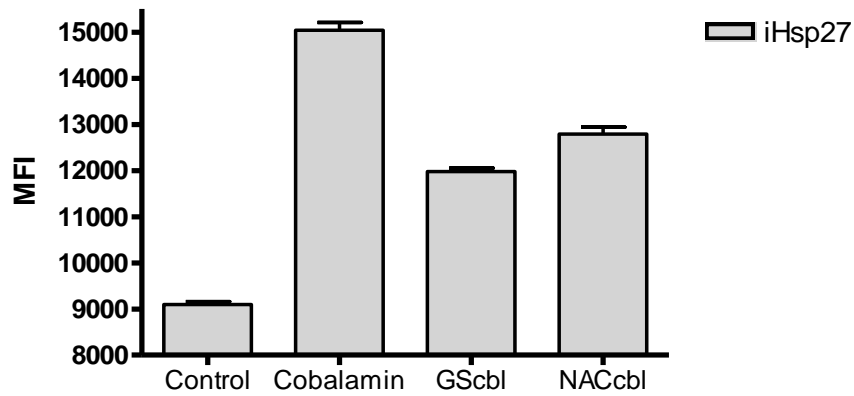


Figure 6.6: Effect of GSCbl and NACCbl on the superoxide generation. Sk-hep1 cells were pre-treated in 96-well plate with Lucigenin (5 μ M), and then treated with 30 μ M GSCbl, 30 μ M NACCbl or 25 μ M cobalamin for 2 hours followed by 2 hours treatments with 3.125 μ M Hcy, control cells were not treated. Lucigenin chemiluminescence was measured at 550nm following incubation. The Data are means \pm SD n=4, $p < 0.001$ as determined by one-way ANOVA. Baseline (Hcy) vs Cbl+Hcy ($p < 0.001$), GSCbl+Hcy ($p < 0.001$), NACCbl+Hcy ($p < 0.001$), as determined by Tukey *post hoc*.

6.3.3 Induction of Hsps by novel cobalamin NACCbl and GSCbl

Previously it had been demonstrated in chapter 4, that treatment with 25 μ M cobalamin induces the iHsps significantly. The result in this chapter showed that 30 μ M GSCbl or 30 μ M NACCbl has significantly induced iHsps compared to control cells ($P<0.001$, as determined by one-way ANNOVA), (Figures 6.7 & 6.8). However, Tukey pairwise showed that induction of iHsp27 by cobalamin was significantly more than GSCbl ($P<0.001$) and NACCbl ($P<0.001$), although GSCbl induced iHsp27 significantly more than NACCbl ($P<0.001$). The iHO-1 was highly induced by GSCbl compared to cobalamin ($P<0.01$) and NACCbl ($P<0.001$). Moreover, NACCbl induced iHO-1 significantly less than cobalamin ($P<0.001$); (Figure 6.7). The iHsp72 was induced significantly more by GSCbl than cobalamin ($P<0.001$), whereas there was no significant difference to NACCbl ($P>0.05$). Finally GSCbl induced iHsp90 significantly more than NACCbl ($P<0.01$) and cobalamin ($P<0.01$), however, there was no significant difference in the iHsp90 induction between NACCbl and cobalamin ($P>0.05$), (Figure 6.8).

A.



B.

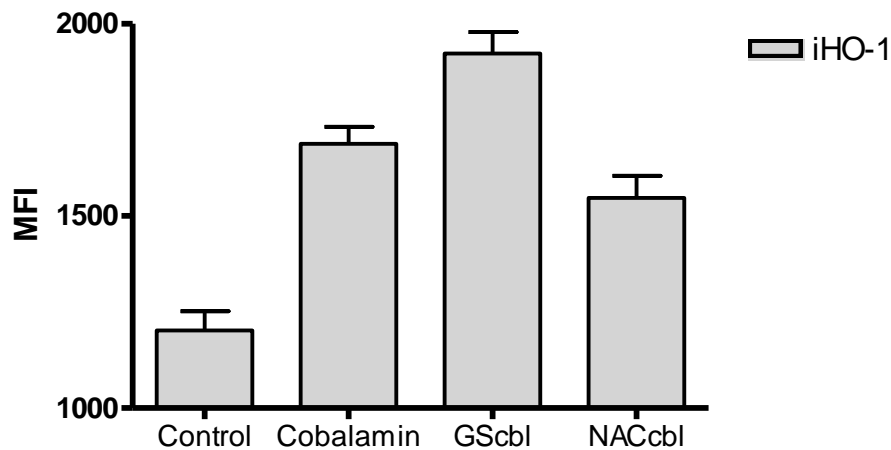
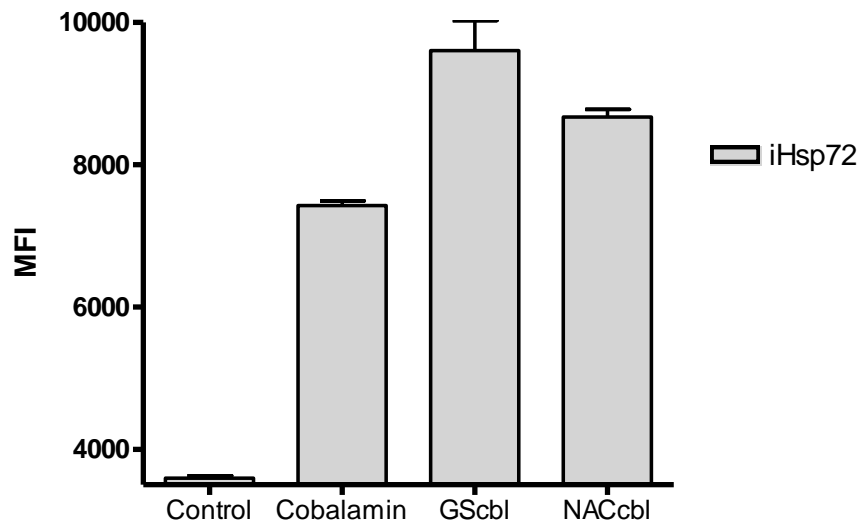


Figure 6.7: Effect of cobalamin, NACCbl and GSCbl on iHsps level. Sk-hep1 cells were pre-treated with 25 μ M cobalamin or 30 μ M NACCbl and GSCbl for 2 hours, control cells were non-treated. Then cells were stained with monoclonal mouse **A.** Anti-Hsp27 or **B.** Anti-HO-1 FITC lantibodies were abelled and analyzed using Flow cytometry. The Data are means \pm SD n=4, $p < 0.001$ as determined by one-way ANOVA. Baseline (control) vs Cbl ($p < 0.001$), GSCbl ($p < 0.001$), NACCbl ($p < 0.001$), as determined by Tukey *post hoc*.

A.



B.

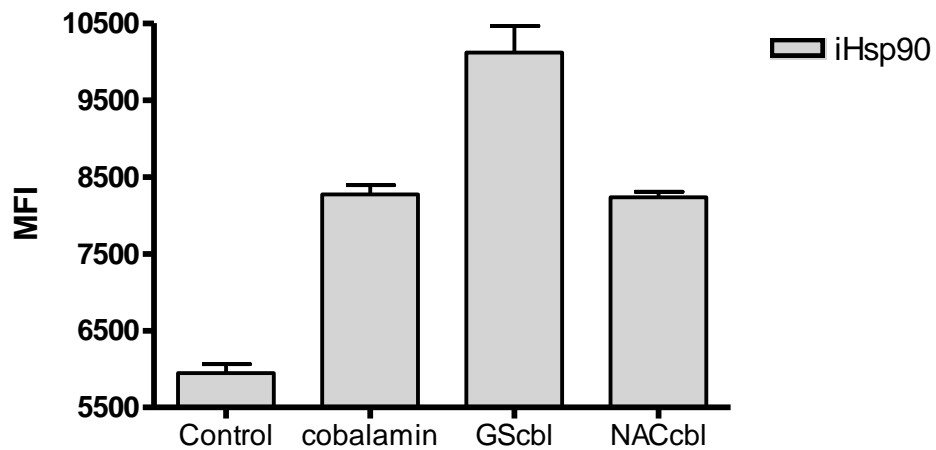


Figure 6.8: Effect of cobalamin, NACCbl and GSCbl on intracellular Hsps. SK-hep1 cells were pre-treated with 25 μ M cobalamin or 30 μ M NACCbl and GSCbl for 2 hours, control cells were not treated. Cells were then stained with monoclonal mouse anti-Hsp72 FITC or anti-Hsp90 PE labelled antibodies and analyzed using Flow cytometry. The Data are means \pm SD n=4, $p < 0.001$ as determined by one-way ANOVA. Baseline (control) vs Cbl ($p < 0.001$), GSCbl ($p < 0.001$), NACCbl ($p < 0.001$), as determined by Tukey *post hoc*.

6.3.4 The NACCbl and GSCbl and signal transduction pathways:

6.3.4.1 The impact of signal transduction inhibitor on NACCbl and GSCbl-apoptosis protection:

In the previous chapter, it was demonstrated that cobalamin apoptosis protection prevented by signal transduction pathways inhibitors. In order to examine the effect of signal transduction inhibitors, cells were incubated with 5 μ M Bay-117082 for 2 hours prior to treatments with 25 μ M cobalamin or 30 μ M NACCbl or GSCbl for 2 hours followed by 3.125 μ M Hcy for another 2 hours. Resulted in a significant effect on the caspase-3 activity ($P < 0.001$, as determined by two-way ANNOVA), (Figure 6.9). The post-hoc comparison showed a significant increase in casapase-3 with bay-110782 compared to cobalamin+Hcy or NACCbl+Hcy or GSCbl+Hcy alone ($P < 0.001$). However there was no significant effect on caspase-3 at Hcy treatment with the inhibitor compared to Hcy alone ($P > 0.05$),

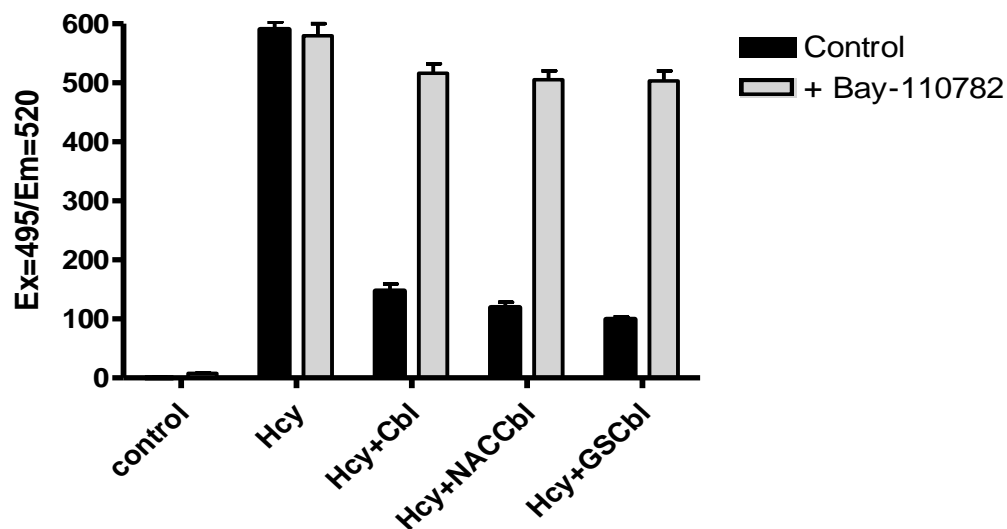


Figure 6.9: Effect of Bay-117082 on NACCbl or GSCbl-apoptosis-protection. Sk-hep1 cells were pre-treated with 5 μ M Bay-117082 for 2 hours followed by 2 hours treatment with 25 μ M cobalamin or 30 μ M NACCbl or GSCbl and 2 hours of 3.125 μ M Hcy. Control cells were not treated with Bay-117082. Caspase-3 was measured at EX=496/EM=520. The Data are means \pm SD n=4, $p < 0.001$ as determined by two-way ANOVA. Baseline (control) vs Cbl+Hcy ($p < 0.001$), GSCbl+Hcy ($p < 0.001$), NACCbl+Hcy ($p < 0.001$), as determined by Bonferroni *post hoc*.

Moreover, The U0126 had a significant effect on protection provided by cobalamin, GSCbl and NACCbl ($P<0.001$, as determined by two-way ANNOVA), (Figure 6.10). The Bonferroni pairwise showed that inhibition of pERK1/2 by $1\mu\text{M}$ U0126 for 1 hour followed by 2 hours incubation with $25\mu\text{M}$ cobalamin or $30\mu\text{M}$ NACCbl or GSCbl and 2 hours incubation with $3.125\mu\text{M}$ Hcy, resulting in a significant increase in caspase-3 compared to cobalamin+Hcy or NACCbl+Hcy or GSCbl+Hcy alone ($P<0.001$). The $1\mu\text{M}$ U0126 had no significant effect on caspase-3 at Hcy treatment as compared to Hcy alone ($P>0.05$).

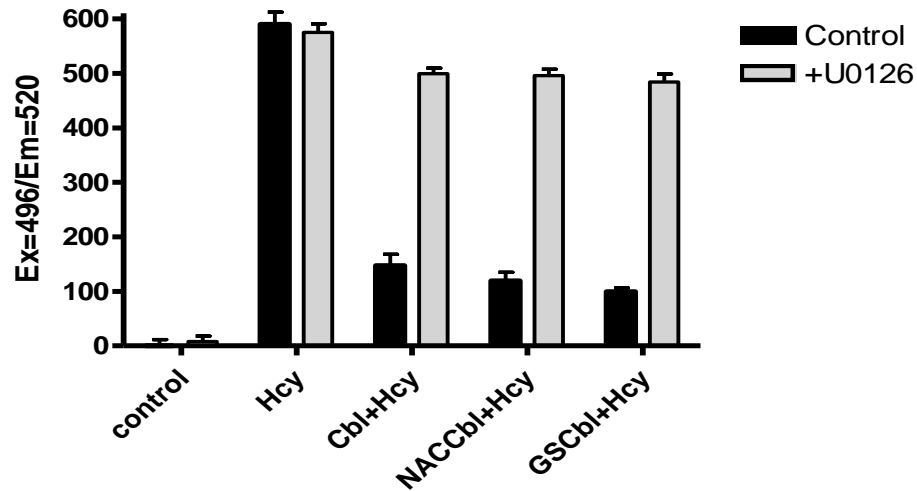


Figure 6.10: Effect of U0126 on NACCbl or GSCbl-apoptosis protection. Sk-hep1 cells were pre-treated with $1\mu\text{M}$ U0126 for 1 hour followed by 2 hours treatment with $25\mu\text{M}$ cobalamin or $30\mu\text{M}$ NACCbl or GSCbl and 2 hours of $3.125\mu\text{M}$ Hcy. Control cells were not treated with U0126. Caspase-3 was measured at EX=496/EM=520. The Data are means \pm SD $n=4$, $p<0.001$ as determined by two-way ANOVA. Baseline (control) vs Cbl+Hcy ($p<0.001$), GSCbl+Hcy ($p<0.001$), NACCbl+Hcy ($p<0.001$), as determined by Bonferroni *post hoc*.

Also, the Inhibition of AKT had a significant effect on the protection provided by cobalamin, GSCbl and NACCbl ($P < 0.001$, as determined by two-way ANNOVA), (Figure 6.11). The pos-hoc comparison showed that when cells were treated with $10\mu\text{M}$ of LY294002 inhibitor for 1 hour prior treatment with $25\mu\text{M}$ cobalamin or $30\mu\text{M}$ NACCbl or GSCbl for 2 hours and $3.125\mu\text{M}$ Hcy for 2 hours resulted in a significant increase in caspase-3 compared to cobalamin+Hcy or NACCbl+Hcy or GSCbl+Hcy alone ($P < 0.001$). There was no significant difference to Hcy treatment as compared to Hcy alone ($P > 0.05$).

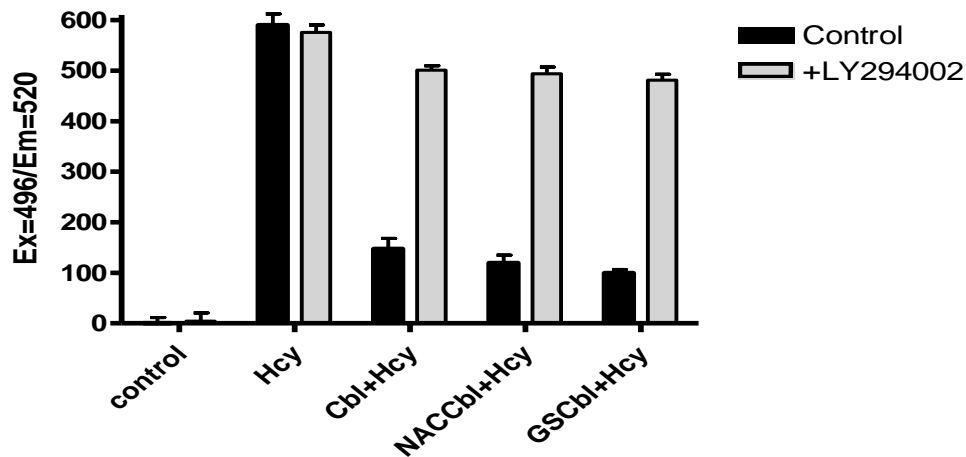


Figure 6.11: Effect of LY294002 NACCbl or GSCbl-apoptosis protection. Sk-hep1 cells were pre-treated with $10\mu\text{M}$ LY294002 for 1 hour followed by 2 hours treatment with $25\mu\text{M}$ cobalamin or $30\mu\text{M}$ NACCbl or GSCbl and 2 hours of $3.125\mu\text{M}$ Hcy. Control cells were non-treated with LY294002. Caspase-3 was measured at EX=496/EM=520. The Data are means \pm SD $n=4$, $p < 0.001$ as determined by two-way ANOVA. Baseline (control) vs Cbl+Hcy ($p < 0.001$), GSCbl+Hcy ($p < 0.001$), NACCbl+Hcy ($p < 0.001$), as determined by Bonferroni *post hoc*.

The inhibition of Nrf2 by 1 μ M Wortmanin had a significant effect on NACCbl or GSCbl-apoptosis protection ($P<0.001$, as determined by two-way ANNOVA), (Figure 6.12). The post-hoc analysis showed that the inhibition of Nrf2 led to increase in caspase-3 significantly as compared to NACCbl+Hcy or GSCbl+Hcy alone ($P<0.001$). The wortmanin had no significant effect on caspase-3 at 3.125 μ M Hcy as compared to Hcy alone ($P>0.05$).

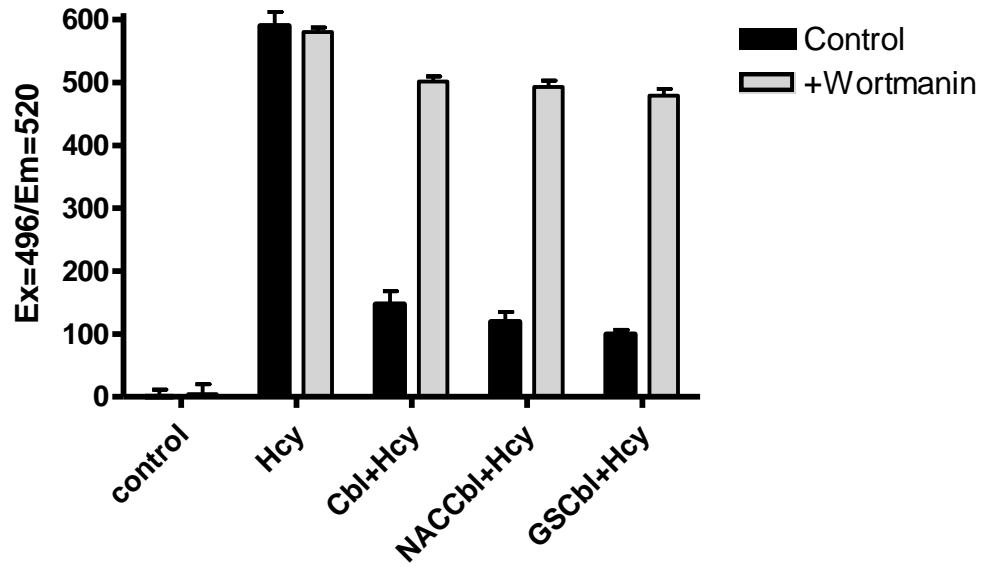


Figure 6.12: Effect of wortmanin NACCbl or GSCbl-apoptosis protection. Sk-hep1 cells were pre-treated with 1 μ M wortmanin for 1 hour followed by 2 hours treatment with 25 μ M cobalamin or 30 μ M NACCbl or GSCbl and 2 hours of 3.125 μ M Hcy. Control cells were not treated with wortmanin. Caspase-3 was measured after at EX=496/EM=520. The Data are means \pm SD $n=4$, $p<0.001$ as determined by two-way ANOVA. Baseline (control) vs Cbl+Hcy ($p<0.001$), GSCbl+Hcy ($p<0.001$), NACCbl+Hcy ($p<0.001$), as determined by Bonferroni *post hoc*.

The P38 had a significant effect on the protection provided by the NACCbl and GSCbl ($P < 0.001$, as determined by two-way ANNOVA), (Figure 6.13). Moreover, the Bonferroni pairwise showed that cells were pre-incubated with $12\mu\text{M}$ SB202190 for 1 hour prior treatment with $25\mu\text{M}$ cobalamin or $30\mu\text{M}$ NACCbl or GSCbl for 2 hours and 2 hours of $3.125\mu\text{M}$ Hcy had a significant increase on caspase-3 as compared to NACCbl+Hcy or GSCbl+Hcy alone ($P < 0.001$). Also SB202190 had a significant effect on Hcy treatment, since there was a significant reduction on caspase-3 as compared to Hcy alone ($P < 0.001$).

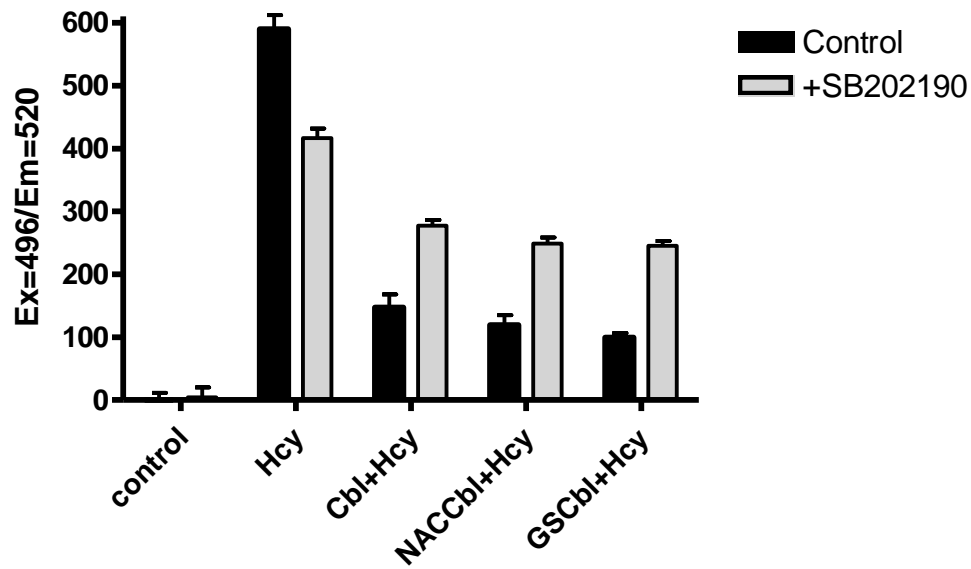


Figure 6.13: Effect of SB202190 on NACCbl or GSCbl-apoptosis protection. Sk-hep1 cells were pre-treated with $12\mu\text{M}$ SB202190 for 1 hour followed by 2 hours treatment with $25\mu\text{M}$ cobalamin or $30\mu\text{M}$ NACCbl or GSCbl and 2 hours of $3.125\mu\text{M}$ Hcy. Control cells were not treated with SB202190. Caspase-3 was measured at EX=496/EM=520. The Data are means \pm SD $n=4$, $p < 0.001$ as determined by two-way ANOVA. Baseline (control) vs Hcy ($p < 0.001$), Cbl+Hcy ($p < 0.001$), GSCbl+Hcy ($p < 0.001$), NACCbl+Hcy ($p < 0.001$), as determined by Bonferroni *post hoc*.

The SP600125 effect on caspase-3 activity ($P < 0.001$, as determined by two-way ANNOVA), (Figure 6.14). However, the inhibition of JNK had no significant effect on caspase-3 as compared to NACCbl+Hcy or GSCbl+Hcy alone ($P > 0.05$). In the same time the inhibition of JNK had a significant effect on caspase-3 at Hcy treatment as compared to Hcy alone ($P < 0.001$).

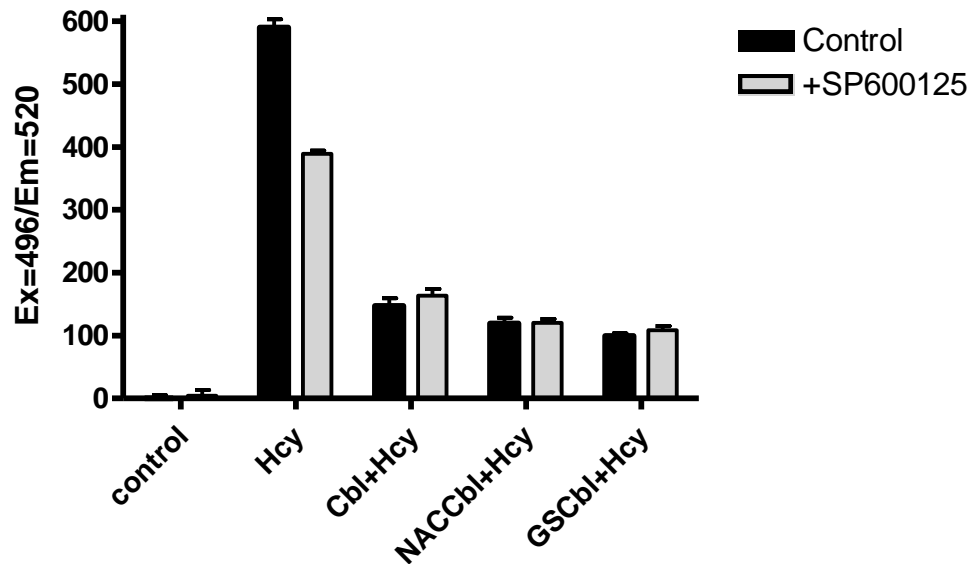


Figure 6.14: Effect of SP600125 on NACCbl or GSCbl-apoptosis-protection. Sk-hep1 cells were pre-treated with 5 μ M SP600125 for 2 hours followed by 2 hours treatment with 25 μ M cobalamin or 30 μ M NACCbl or GSCbl and 2 hours of 3.125 μ M Hcy. Control cells were not treated with SB202190. Caspase-3 was measured at EX=496/EM=520. The Data are means \pm SD $n=4$, $p < 0.001$ as determined by two-way ANOVA. Baseline (control) vs Hcy ($p < 0.001$), as determined by Bonferroni *post hoc*.

6.3.4.2 Impact of NACCbl and GSCbl on pNf κ B, pERK1/2 and pAKT induction:

In order to determine the effect of GSCbl and NACCbl on the pNf κ B, pERK1/2 and pAKT induction, cells were subjected to 30 μ M GSCbl, 30 μ M NACCbl or 25 μ M cobalamin for 2 hours. This resulted in a significant effect on the level of the pNf κ B, pERK1/2 and pAKT induction ($P < 0.001$, as determined by one-way ANNOVA), (Figures 6.15, 6.16 & 6.17). The Tukey comparison showed that there was a significant increase of Nf κ B at 30 μ M NACCbl more than GSCbl and cobalamin ($P < 0.001$), and GSCbl induced Nf κ B more than cobalamin ($P < 0.001$), (Figure 6.15). On the other hand, the pERK1/2 was significantly more induced by GSCbl than NACCbl ($P < 0.001$) and cobalamin ($P < 0.01$). Also cobalamin induced pERK1/2 significantly more than NACCbl ($P < 0.01$), (Figure 6.16). Additionally, GSCbl induced pAKT significantly more than NACCbl and cobalamin ($P < 0.001$). And the cobalamin treatment induced pAKT significantly more than NACCbl ($P < 0.001$), (Figure 6.17).

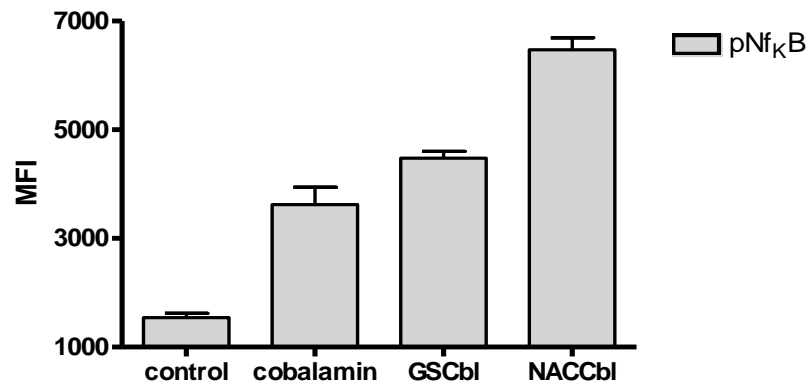


Figure 6.15: Effect of GSCbl, NACCbl and cobalamin on pNf κ B induction. Sk-hep1 cells were subjected to 25 μ M cobalamin, 30 μ M GSCbl and 30 μ M NACCbl for 2 hours, control cells were not treated. Following incubation, cells were stained with specific monoclonal pNf κ B antibody and analyzed by flowcytometry using FACSDiva software. The Data are means \pm SD $n=4$, $p < 0.001$ as determined by one-way ANOVA. Baseline (control) vs Cobalamin ($p < 0.001$), GSCbl ($p < 0.001$), NACCbl ($p < 0.001$), as determined by Tukey *post hoc*.

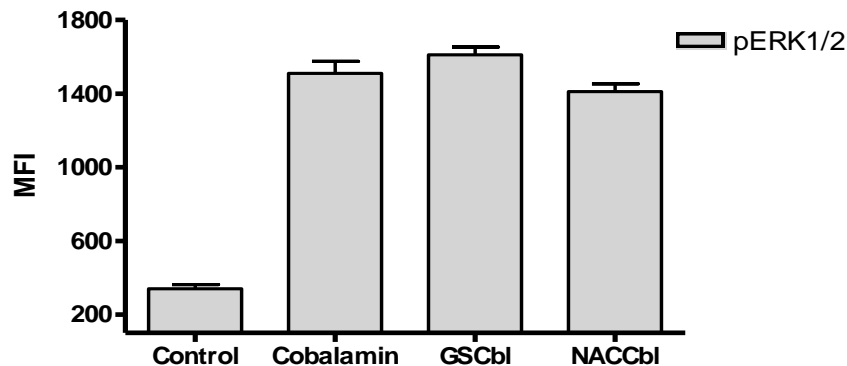


Figure 6.16: Effect of GSCbl, NACCbl and cobalamin on pERK1/2 induction. Sk-hep1 cells were subjected to 25 μ M cobalamin, 30 μ M GSCbl and 30 μ MNACCbl for 2 hours, control cells were not treated. Following incubation, cells were stained with specific monoclonal pERK1/2 antibody and analyzed by flowcytometry using FACSDiva software. The Data are means \pm SD n=4, $p < 0.001$ as determined by one-way ANOVA. Baseline (control) vs Cobalamin ($p < 0.001$), GSCbl ($p < 0.001$), NACCbl ($p < 0.001$), as determined by Tukey *post hoc*.

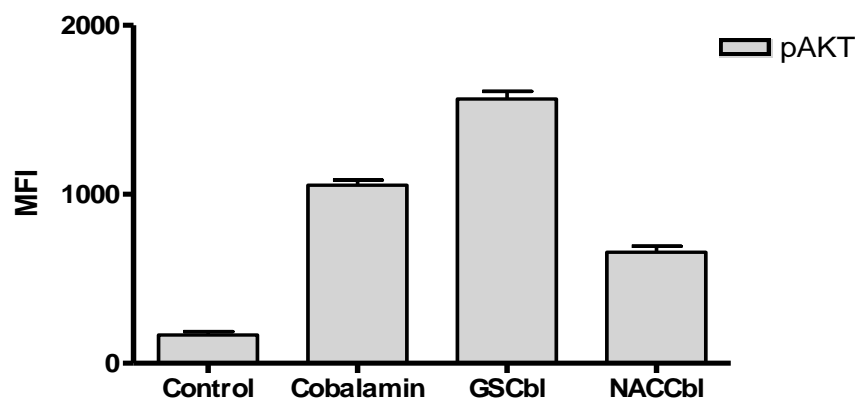


Figure 6.17: Effect of GSCbl, NACCbl and cobalamin on pAKT induction. Sk-hep1 cells were subjected to 25 μ M cobalamin, 30 μ M GSCbl and 30 μ MNACCbl for 2 hours, control cells were not treated. Following incubation, cells were stained with specific monoclonal pAKT antibody and analyzed by flowcytometry using FACSDiva software. The Data are means \pm SD n=4, $p < 0.001$ as determined by one-way ANOVA. Baseline (control) vs Cobalamin ($p < 0.001$), GSCbl ($p < 0.001$), NACCbl ($p < 0.001$), as determined by Tukey *post hoc*.

6.3.4.3 Impact of NACCbl and GSCbl on Nrf2 induction:

Previously, we showed that GSCbl and NACCbl had significantly induced pNf κ B, pERK1/2 and pAKT, so further investigation was carried out on their effect on Nrf2 induction, which resulted in a significant effect ($P < 0.001$, as determined by one-way ANNOVA), (Figure 6.18). The pos-hoc analysis showed that cells were subjected to 30 μ M GSCbl, 30 μ M NACCbl or 25 μ M cobalamin for 2 hours, which resulted in significantly inducing Nrf2 at 30 μ M GSCbl, 30 μ M NACCbl but the Nrf2 induction at 30 μ M GSCbl was higher than at cobalamin and NACCbl ($P < 0.001$). Also cobalamin induced Nrf2 significantly more than NACCbl ($P < 0.001$).

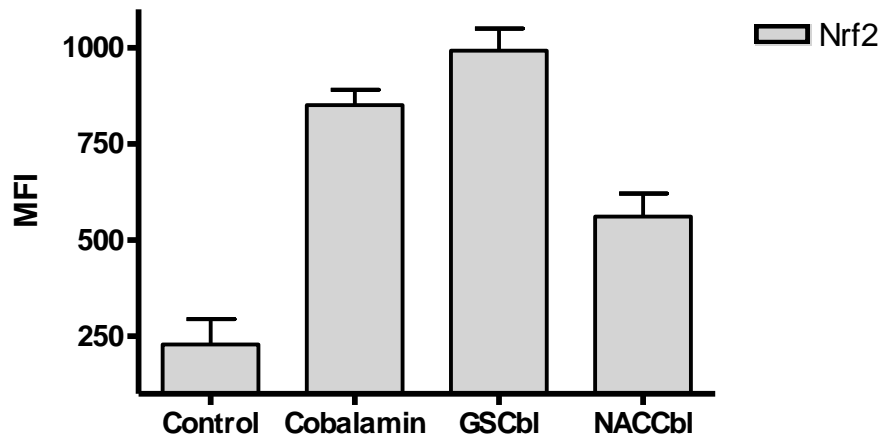


Figure 6.18: Effect of GSCbl, NACCbl on Nrf2 induction. Sk-hep1 cells were subjected to 25 μ M cobalamin, 30 μ M GSCbl and 30 μ M NACCbl for 2 hours, control cells were not treated. Following incubation, cells were stained with specific monoclonal Nrf2 antibody and analyzed by flowcytometry using FACSDiva software. The Data are means \pm SD $n=4$, $p < 0.001$ as determined by one-way ANOVA. Baseline (control) vs Cobalamin ($p < 0.001$), GSCbl ($p < 0.001$), NACCbl ($p < 0.001$), as determined by Tukey *post hoc*.

6.3.4.4 Impact of GSCbl and NACCbl on iNOS induction:

In order to investigate the effect of GSCbl, NACCbl and cobalamin on iNOS induction, cells were exposed to 30 μ M GSCbl, 30 μ M NACCbl or 25 μ M cobalamin for 2 hours. The result in Figure 6.19 showed that iNOS was significantly induced by GSCbl, NACCbl and cobalamin compared to control cells ($P < 0.001$, as determined by one-way ANNOVA). However, post-hoc comparison showed that NACCbl induced iNOS more significantly than GSCbl and cobalamin, and that iNOS was significantly higher at 30 μ M GSCbl than cobalamin ($P < 0.001$). Moreover, under protection condition there was a further induction of the iNOS as compared to cobalamin, GSCbl and NACCbl alone ($P < 0.001$). The histogram in Figure 6.20 demonstrated the significant increase in the fluorescent intensity of iNOS at 30 μ M GSCbl, 30 μ M NACCbl or 25 μ M cobalamin.

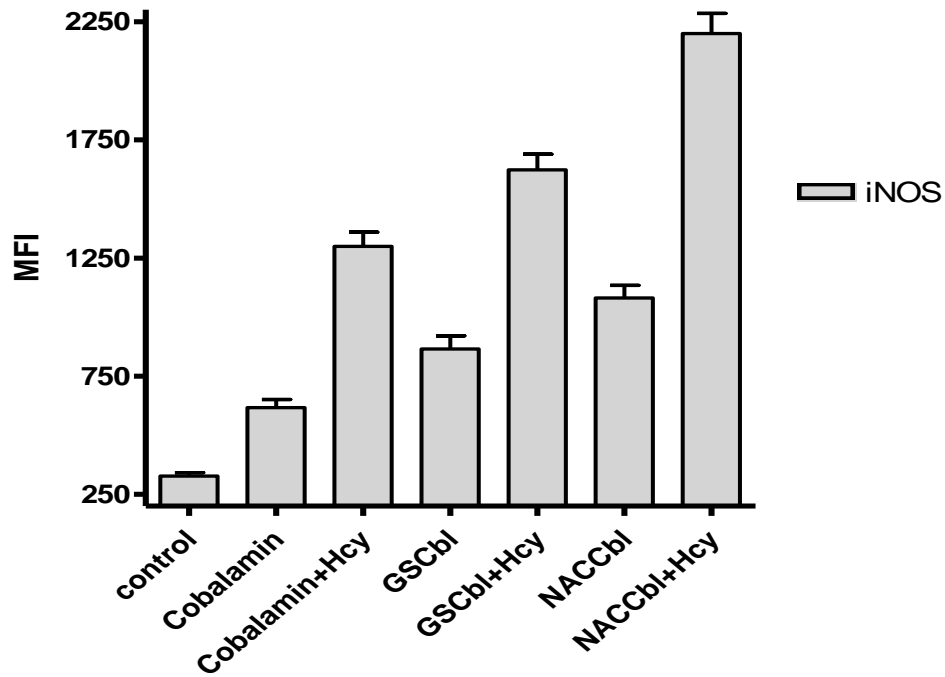
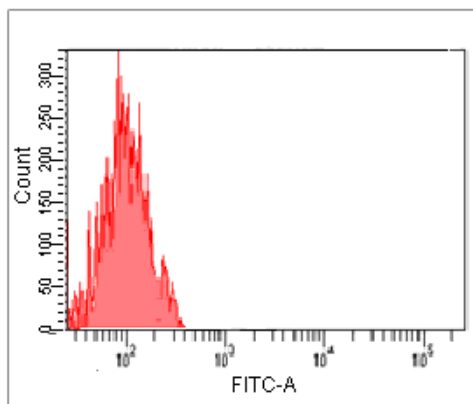
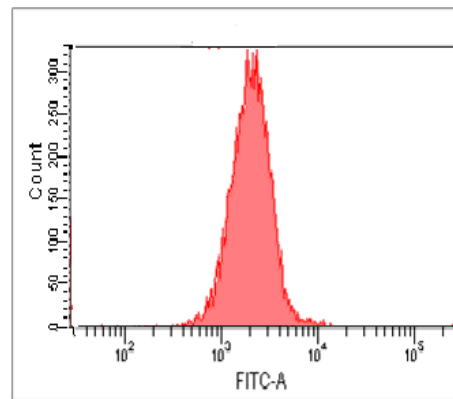


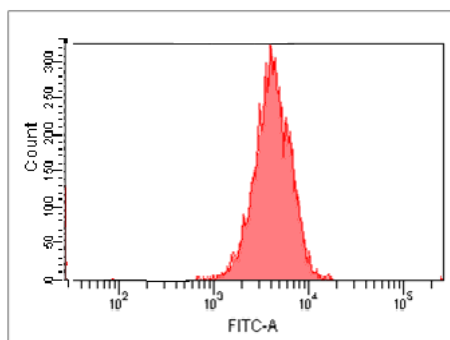
Figure 6.19: Effect of GSCbl, NACCbl on iNOS induction. Sk-hep1 cells were subjected to 25 μ M cobalamin, 30 μ M GSCbl and 30 μ M NACCbl for 2 hours. Following incubation, cells were stained with specific monoclonal iNOS antibody and analyzed by flowcytometry using FACSDiva software. The Data are means \pm SD n=4, $p < 0.001$ as determined by one-way ANOVA. Baseline (control) vs Cobalamin ($p < 0.001$), GSCbl ($p < 0.001$), NACCbl ($p < 0.001$), Hcy+Cobalamin ($p < 0.001$), Hcy+GSCbl ($p < 0.001$), Hcy+NACCbl ($p < 0.001$), as determined by Tukey *post hoc*.



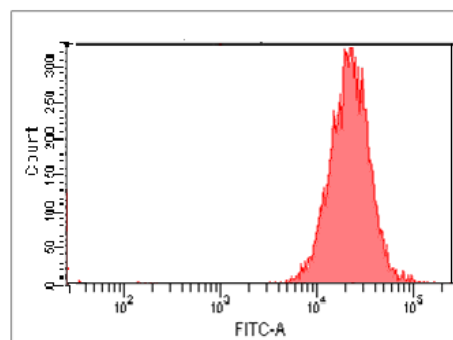
A. Control cells



B. 25 μ M cobalamin



C. 30 μ M GSCbl



D. 30 μ M NACCbl

Figure 6.20: Effect of GSCbl, NACCbl on iNOS induction. Sk-hep1 cells were subjected to 25 μ M cobalamin, 30 μ M GSCbl and 30 μ MNACCbl for 2 hours. Control cells were not treated. Following incubation, cells were stained with specific monoclonal iNOS antibody and A-D were analyzed by flowcytometry using FACSDiva software.

6.4 Discussion:

The aim of this chapter was to evaluate the efficiency of the GSCbl and NACCbl oxidative stress protection, and compare the mechanisms to those identified in the previous chapter.

Recently, it was reported that GS and NAC partially protect Sk-hep1 from oxidative stress, while the GSCbl and NACCbl provided a significant protection from oxidative stress injury (Birch *et al.*, 2009). These findings are consistent with the results in this chapter, since there was a significant protection from apoptosis and necrosis induced by Hcy. Moreover, the GSCbl and NACCbl have the ability to scavenge the superoxide and ROS generation more than cobalamin.

It has been suggested that the antioxidant role of cobalamin might be due to the ability to stimulate the methionine synthase activity (McCaddon *et al.*, 2002) and their direct interaction with reactive oxygen and nitrogen species (Ling & Chow, 1953). Also, it has been suggested that cobalamin might stimulate signalling molecules such as Nf_κB to mediate the gene expression of the antiapoptotic proteins (Veber *et al.*, 2008). These suggestions are in line with the previous result in chapter 5, which showed that cobalamin-apoptosis protection involved induction of signal transduction pathways. In this chapter GSCbl or NACCbl- apoptosis protection condition was associated with a significant induction of $\text{pNf}_\kappa\text{B}$, pERK1/2 and pAKT . However, pERK and pAKT were more significantly induced with GSCbl pre-treatment when compared to cobalamin or NACCbl pre-treatments. Furthermore, GSCbl pre-treatment induced Nrf2 to a greater degree, while NACCbl induced iNOS more significantly. Additionally the induction of the $\text{pNf}_\kappa\text{B}$, pERK1/2 and pAKT are essential for the apoptosis protection. Since the inhibition of these proteins by their specific inhibitors lead to loss of the protection and cells were apoptotic. On the other hand, the inhibition of P38 prevents the protection partially but it had a significant effect on apoptosis induced by Hcy. Also the inhibition of JNK had an effect on apoptosis induced by Hcy but JNK is not essential for the NACCbl or GSCbl apoptosis-protection.

As cobalamin treatment showed a significant induction of the Hsps, GSCbl or NACCbl-apoptosis protection has also induced iHsps significantly. More specifically, GSCbl induced iHO-1, iHsp72 and iHps90 more than cobalamin and NACCbl. Also NACCbl induce iHsp72 more than cobalamin.

It is clear that cobalamins are utilising the same pathways but they vary in the effect on these pathways to provide an efficient protection. For instance, GSCbl induced pERK1/2 and pAKT and those pathways lead to activate the Nrf2 which in turn, induced the expression of the antioxidant genes, HO-1 and Hsp72. In this way GSCbl protects the cells from the oxidative stress induced. In contrast, NACCbl induces Nf_κB which in turn leads to induction of the iNOS and several antiapoptotic proteins, resulting in apoptosis protection.

The conclusion of this chapter is that GSCbl and NACCbl provide a better protection from apoptosis induced by oxidative stress, due to their ability to induce the anti-apoptotic proteins more than the cobalamin in two different pathways. NACCbl protect cells from apoptosis mainly through Nf_κB /iNOS pathway, while GSCbl take the ERK1/2-AKT/Nrf2 pathway to provide apoptosis protection.

Chapter 7

General Discussion

Oxidative stress is a result of the imbalance between the oxidant and the antioxidant production (Sies, 1999). It has been proposed that oxidative stress induces damage to cells and that might lead to cardiovascular disease and neurodegenerative disease (Refsum *et al.*, 1998; Diaz-Arrastia, 2000). The high level of Hcy, generation of ROS and superoxide are three important factors associated with oxidative damage and all can lead to cell death. The first objective of this thesis was to characterise cell death caused by oxidative stress (Chapter 3). At the same time, several studies have demonstrated the mechanism of oxidative stress cell death in different cell lines such as; Jurkat cells (Hampton & Orrenius, 1997), endothelium cells (Liu *et al.*, 2005; Obeid & Herrmann, 2006), smooth muscle cells (Buemi *et al.*, 2001), primary human bone marrow stromal cells and the HS-5 cell line (Duk *et al.*, 2006). The mode of cell death induced by oxidative stress is dose dependent and varies from cell to cell. For example, Sk-hep1 cells were apoptotic when treated 3.125 μ M Hcy or H₂O₂ and were necrotic at 50 μ M of either compound (chapter 3). These data were obtained following 2 hours of treatment, whereas Jurkat cells died by apoptosis at 3.125 μ M Hcy or 0.01mM H₂O₂ and by necrosis with 100 μ M Hcy or 10mM H₂O₂ in experiments that required 6 hours treatment.

Due to the different in the content of the antioxidant enzymes in the peripheral blood cells (Pietarinen-Runtti *et al.*, 2000), so they had different sensitivity to the oxidative stress. For example, monocyte cells required higher concentrations of H₂O₂ to induce apoptosis and necrosis compared to the concentrations required for neutrophils and lymphocytes. Similar to Jurkat cells the peripheral blood cells were more sensitive to Hcy than H₂O₂ in terms of apoptosis or necrosis. These differences might be due to the ability of Hcy to generate intracellular H₂O₂ (Harker *et al.*, 1976; Malinow, 1990).

The results of chapter 3 reflect other studies findings that, low concentrations of oxidative stress induce apoptosis while high concentrations induce necrosis (Saito *et al.*, 2006), a finding consistent with other stressors such as temperature (Lione PhD thesis, 2009).

The second objective of this thesis was to examine if the cells protect themselves from apoptosis and necrosis induced by oxidative stress as it is known that the generation of ROS is a natural cellular process. However, cells prevent the accumulation of the ROS *via* production of antioxidants (Chen & Kunsch, 2004), such as glutathione peroxidase and glutathione that reduces accumulated H_2O_2 (Pietarinen-Runtti *et al.*, 2000). In recent years research strategies of antioxidant against oxidative stress have received great intentions, since folate is an antioxidant molecule and cobalamin is co-factor enzyme in Hcy metabolism (Figure 1.3). In 2006 McNulty and colleagues suggested that riboflavin, which in its coenzymatic form (flavin adenine dinucleotide) required as a cofactor for the MTHFR enzyme, reduce Hcy level significantly in individuals with homozygous for the *MTHFR* 677C3T polymorphism. Accumulated evidence has shown that folate treatment reduces hyperhomocysteinemia that is associated with several diseases such as cardiovascular diseases (Woo *et al.*, 1999; Ward, 2001; McNulty *et al.*, 2008). It has been suggested that folate can reduce the risk of neural tube defects (McNulty *et al.*, 2000). Also, folate treatment provides a protection against cell death induced by oxidative stress in smooth muscle and endothelial cells (Buemi *et al.*, 2001). The results in chapter 3 confirmed this protective role of folate against both apoptosis and necrosis.

In the literature, cobalamin has been suggested to provide indirect protection from apoptosis and necrosis induced by oxidative stress due to its classical function as a cofactor to the methionine synthase enzyme in Hcy metabolism cycle (Figure 1.3). However, it has been reported recently that cobalamin had the ability to scavenge super oxide directly and provide protection against chronic inflammation (Suarez-Moreir *et al.*, 2006). Also cobalamin deficiency increases the synthesis of tumor necrosis factor (TNF)- α (Scalabrino, 2005). Interestingly the results in chapter 3 demonstrate a novel role of cobalamin as an antioxidant molecule, which provided a significant protection against apoptosis and necrosis induced by Hcy and H_2O_2 in Sk-hep1 and Jurkat cells. Cobalamin-apoptosis protection correlated with a significant reduction in the superoxide and ROS generation as demonstrated by another study (Birch *et al.*, 2009).

Moreover, the novel thiolatocobalamins GSCbl and NACCbl provided superior protection against apoptosis and necrosis induced by oxidative stress when compared to protection provided by cobalamin (chapter 6).

Folate and cobalamin have been suggested to reduce hyperhomocysteinemia in oxidative stress associated diseases, and as discussed above they protect cells from apoptosis and necrosis induced by oxidative stress. However the mechanism is not known. So the third objective of the thesis was to determine the mechanism of cobalamin apoptosis protection. Knowing the mechanism of cobalamin protection could be a useful tool for clinical application.

It is known that amongst the natural processes, cells have to provide protection from any stressor by the activation of Hsps. It has been demonstrated that Hsp27, HO-1 and Hsp72 are induced under oxidative stress (Mehlen *et al* 1993; Oesterreich *et al.*, 1993; Arrigo, 2001). The overexpression of Hsp72 and HO-1 protected cells from apoptosis induced by Hcy (chapter 4) is consistent with previous studies (Huot *et al.*, 1991; Mehlen *et al.*, 1993; Ohkawara *et al.*, 2006). However, whether cobalamin induces the Hsps was not investigated previously.

The novel induction of Hsps by cobalamin was presented in Chapter 4. Also, under apoptosis-cobalamin protection, the level of Hsps increased further (chapter 4). The induction of Hsps was essential for the cobalamin-apoptosis protection, since inhibition of Hsp72 or HO-1 prevented cobalamin-apoptosis protection. These observations indicated that Hsp72 and HO-1 are involved in the mechanism of cobalamin protection. The suppression of apoptosis by the Hsps is in agreement with other studies that investigated the protective potential role of Hsps in cells overexpressing these proteins (Mosser, *et al.*, 1997).

The important question leading on from this work is how cobalamin induces Hsps, which was the fourth objective in this thesis. It is important to identify at what level cobalamin regulates the induction of the Hsps and whether this alone is responsible for the protection mechanism.

It has been proposed that cobalamin treatment decrease synthesis of TNF- α and increase synthesis of epidermal growth factor (Buccellato *et al.*, 1999; Scalabrino *et al.*, 1999) but the understanding of the mechanisms was limited. Also recently Surez-Moreira *et al* (2006) suggested that the direct interaction of cobalamin with the superoxide can be the molecular mechanism that activates the signals transduction to provide the protection. Interestingly, the cobalamin-apoptosis protection was prevented when gene transcription inhibited by actinomycin (chapter 5). This suggested that cobalamin-apoptosis protection mechanism involves signal transduction pathways to induce the Hsps. The inhibition of the Nf κ B, ERK1/2 and AKT, anti-apoptosis signal pathways prevented cobalamin-apoptosis protection by increasing the caspase-3 level, ROS and superoxide (Chapter 5). Moreover, activation of pNf κ B, pERK1/2 and pAKT was induced significantly by cobalamin, and this level increased further under cobalamin-apoptosis protection. Conversely, the inhibition of the apoptosis signal transduction pathway (JNK and P38), had no significant impact on the cobalamin apoptosis protection. While the results confirmed their apoptosis induction role, since the inhibition of JNK and P38 reduced apoptosis significantly (Chapter 5). It is obvious that the anti-apoptosis signal transduction pathways and the Hsps are essential for the cobalamin apoptosis protection (chapter 4 &5). So, there are three pathways that involved in the cobalamin-apoptosis protection.

In the literature it has been suggested that Nf κ B regulates the transcription of HO-1 (Maines, 1997; Choi *et al.*, 2004). Interestingly Nf κ B has a significant impact on the induction of the Hsp72 and HO-1 under cobalamin-apoptosis protection. There was no significant effect on the Hsp72 and HO-1 level under apoptosis level (chapter 5). This indicates that induction of the Hsp72 and HO-1 under cobalamin apoptosis-protection is regulated by Nf κ B.

Also, it was observed that cobalamin induced iNOS and the level increased further under cobalamin-apoptosis protection (chapter 5). It is known that Nf κ B regulates the induction of iNOS, and the result in chapter 5 showed that inhibition of Nf κ B has a significant impact on the iNOS induction. Nf κ B inhibition also had a significant effect on the Nrf2 induction under cobalamin-apoptosis protection (chapter 5). Therefore under apoptosis protection conditions; cobalamin induces the activation of Nf κ B. In

turn, NF_κB induces mainly iNOS also effect on the expression of Hsp72, HO-1, and Nrf2 expression as illustrated in (Figure 7.1).

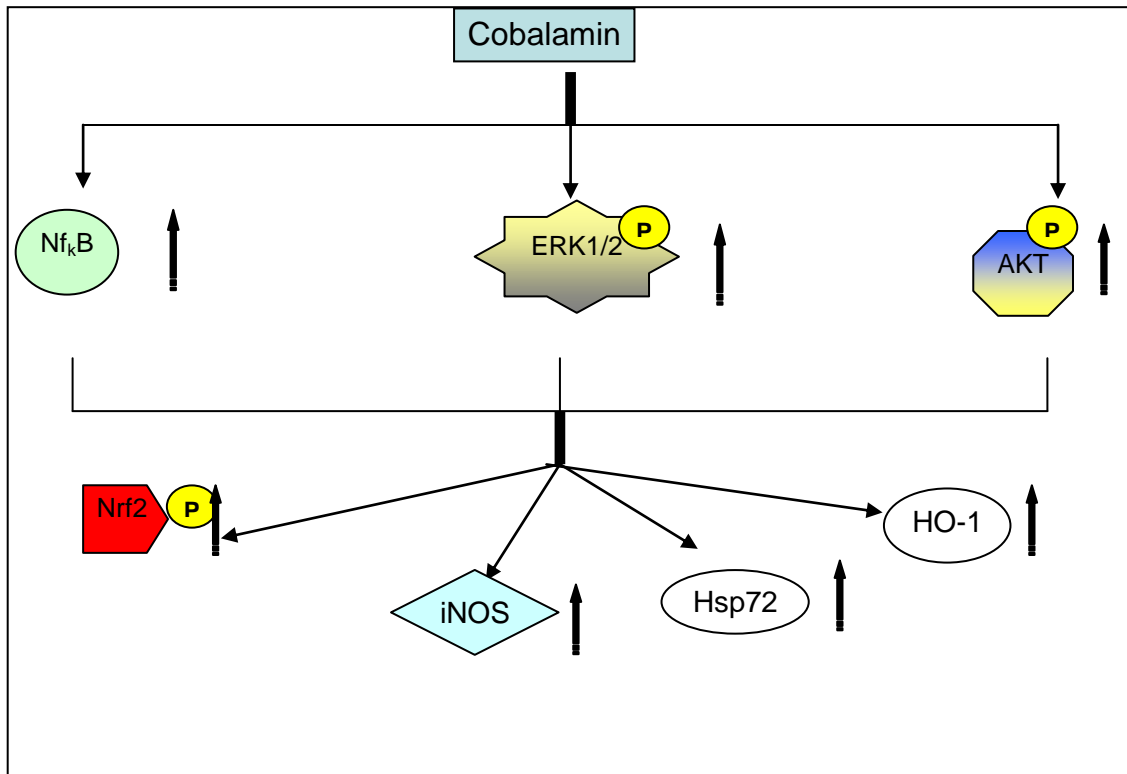


Figure 7.1: The mechanism of cobalamin-apoptosis protection. Cobalamin treatment leads to activate NF_κB and phosphorylation of ERK1/2 and AKT. This leads to induce the Nrf2, iNOS, Hsp72 and Hsp27, which provides protection against oxidative stress.

The second signal transduction pathway that is involved in the cobalamin apoptosis protection is ERK12. Previously it was shown that cobalamin activated ERK1/2 and that ERK1/2 is essential for the cobalamin apoptosis protection. Furthermore,

inhibition of ERK1/2 has a significant impact on the induction of the Hsp72 and HO-1 under cobalamin apoptosis protection, But ERK1/2 mostly effects the Hsp72 expression. There was no significant effect on the induction of the Hsp72 and HO-1 under apoptosis condition (chapter 5). These observations mean that induction of the Hsp72 and HO-1 under cobalamin-apoptosis protection is regulated by ERK1/2 activation which is induced by cobalamin. These results are consistent with pervious studies which reported that the induction of the Hsp72 by ERK1/2 signalling pathways (Chen *et al.*, 2001) and that inhibition of ERK1/2 decreased Hsp72 induction under different stress conditions (Chen *et al.*, 2001; Yang *et al.*, 2004). It has been suggested by Huang *et al.*, 1998, that ERK1/2 acts on the phosphorylation of HSF1 to increase the expression of the Hsp72. Also it has been reported that ERK1/2 might regulate the expression of Nrf2 (Chen *et al.*, 2001; Yang *et al.*, 2004). Inhibition of ERK1/2 has an impact on iNOS and Nrf2 level under cobalamin-apoptosis protection. So the ERK1/2 signal pathway, which is activated by cobalamin, induces Hsp72, HO-1, Nrf2, and iNOS expression and through this provides protection against apoptosis induced by oxidative stress (Figure 7.1).

The third signal transduction pathway involved in the cobalamin-apoptosis protection is AKT as demonstrated previously. The role of AKT in upregulation of Nrf2 in response to different stimuli is well investigated in rat hepatoma cells and human neuroblastoma cells (Kang *et al.*, 2001; Lee *et al.*, 2001). Also the upregulation of HO-1 *via* AKT has been demonstrated in several studies (Chung *et al.*, 2005; Martin *et al.*, 2003; Pischke *et al.*, 2005; Salina *et al.*, 2003). In the cobalamin-apoptosis protection, AKT regulated mainly the expression of the Nrf2 and HO-1 (chapter 5). Additionally, AKT was also involved in the regulation of the expression of Hsp72 and iNOS as the inhibition of the AKT leads to lose the protection. So activation of the AKT signal pathway by cobalamin leads to upregulation of the expression of the Nrf2, HO-1, Hsp72 and iNOS. The upregulation of these proteins provides the protection against apoptosis induced by oxidative stress (Figure 7.1).

Taken together the above findings suggest that cobalamin has a novel impact on the signal transduction pathways (Figure 7.1). Consequently, Nf κ B, ERK1/2 and AKT together mediate the upregulation of Nrf2, HO-1 Hsp72 and iNOS which provide protection against apoptosis induced by oxidative stress. More specifically first Nf κ B mainly upregulate the iNOS, this finding is supported by pervious study suggest that

Nf κ B regulate the iNOS (Xia *et al.*, 2001). Secondly Erk1/2 mainly increases the expression of the Hsp72. Finally, AKT mostly up regulates HO-1 through Nrf2. As it has been well document that AKT can mediate the expression of the HO-1 *via* Nrf2 providing protection against oxidative stress (Park *et al.*, 2007). Moreover, it has been recently reported that Nrf2 is activated *via* AKT/ERK1/2, thus increasing the expression of the HO-1 and antioxidant enzymes (Kim *et al.*, 2008).

Together the induction of the Nrf2, HO-1, Hsp72 and iNOS provide a significant protection against apoptosis induced by oxidative stress and each one has its own pathway to provide the protection.

The activation of Nrf2 and translocation to the nucleus leads to bind with the ARE. The common function of the ARE is to regulate the expression of proteins that mediate the cellular ROS level, detoxification reaction and cell protection against oxidative stress (Alam & Cook, 2003; Lee & Surh, 2005; Nguyen *et al.*, 2003; Jaiswal, 2004). Nrf2 induce several antioxidant proteins to provide protection such as glutathione, glutathioneperoxidase, superoxide dismutase (Alam & Cook, 2003; Lee & Surh, 2005; Lee *et al.*, 2003; Kwak *et al.* 2001; McMahon *et al.*, 2001).

The protective role of HO-1 against oxidative stress has been reported in the literature (Chio *et al.*, 2002; Brouard *et al.*, 2000). The ability of HO-1 to provide protection from oxidative stress is possibly due to the generation of CO and bilirubin, since there is a direct link between scavenging of ROS and the activity of bilirubin and CO (Choi *et al.*, 2002; Morse *et al.*, 2002; Ryter *et al.*, 2002; Kim *et al.*, 2006).

Earlier it was demonstrated that induction of the Hsp27 and Hsp72, has a vital role in cobalamin-apoptosis protection. It also showed that the anti-apoptosis signalling transduction pathways are involved in upregulation of these proteins. The protective role of the Hsp27 and Hsp72 is suggested to be due to the ability of the Hsp72 to prevent formation of the apoptosome, and to block caspase activation (Beere *et al.*, 2005; Saleh *et al.*, 2000). The overexpression of the Hsp27 protects cells from oxidative stress by reducing ROS generation and increasing glutathione induction (Mehlen *et al.*, 1995; Ito *et al.*, 1998; Concannon *et al.*, 2001; Liu *et al.*, 2007; Preville *et al.*, 1999). It is believed that protection activity of Hsp27 is glutathione dependent

(Mehlen *et al.*, 1996) in addition to its ability to suppress the cytochrome c (Garrido *et al.*, 1997; Samali *et al.*, 1996). In the same time the inhibition of the Hsp27 decrease the glutathione level and increase apoptosis (Aloy *et al.*, 2008). The overexpression of Hsp27 is associated with the induction of the glucose-6-phosphate dehydrogenase and increase in the reduced form of the glutathione in murine L929 fibroblast cells, HeLa cells, C6 rat glioma cells and NIH 3T3-ras cells (Mehlen *et al.*, 1996; Ito *et al.*, 1998; Perville *et al.*, 1999). So Arrigo in 2001 suggested that the expressed glucose-6-phosphate dehydrogenase *via* Hsp27 increased the upholding of reduce glutathione and that leads to reduced level of the ROS which forms as a result of the oxidative stress.

Further more, as been demonstrated in chapter 4, the heat shock increases expression of Hsp72. Also, it is believed that heat shock induces glutathione (Li & webb, 1982) and the suppresser of the glutathione induction leads to prevent the Hsp72 protection role (Mitchell & Russo, 1983). Also under oxidative stress, Hsp72 is believed to bind to dihydrofolate reductase and prevent the thiol oxidation of dihydrofolate reductase to function normally in one carbon cycle (Mark *et al.*, 2004).

The iNOS is also observed to be upregulated by cobalamin and under cobalamin-apoptosis protection. Adding to this, Nf κ B, ERK1/2 and AKT are involved in mediating the expression of the iNOS under cobalamin-apoptosis protection as been mentioned before. The iNOS is commonly regulated by the Nf κ B and believes to have pro-inflammatory responses (Kleinwort *et al.*, 2003). The iNOS induction leads to production of NO. The induction of NO provides protection against cell death (Pinsky *et al.*, 1997). There is negative feedback mechanism that controls the level of iNOS expression through NO/I κ B to avoid the accumulation of NO. Thus the recent NO synthesis might acts with the recent I κ B synthesis to suppress the DNA binding activity of Nf κ B and inhibit the transcription of the iNOS gene (Peng *et al.*, 1995b). However it was recently reported that hydroxycobalamin and dicyanocobinamide inhibit the enzyme activity of the iNOS where cyanocobalamin, methylcobalamin, and adenosylcobalamin have less effect (Weinberg *et al.*, 2009)

In the addition to the objectives to determine the mechanism of cobalamin novel antioxidant role, the last objective of this thesis was to examine the protection role of

GSCbl and NACCbl and the possible mechanism they acts on. The work in chapter 6 showed that the superior protection GSCbl and NACCbl provide against apoptosis induced by oxidative stress. These findings support the recent finding present the proactive role of GSCbl and NACCbl from cell death induced by oxidative stress (Birch *et al.*, 2009). Moreover, GSCbl and NACCbl significantly induced the Nf_κB , ERK1/2 and AKT and there were further induction of these proteins at apoptosis protection condition. Also these signal transduction pathways were essential for the protection, as the inhibition of Nf_κB , ERK1/2 and AKT leads to lose the protection (chapter 6). Since, Under GSCbl-apoptosis protection the expression of AKT/ERK1/2 increased more than under cobalamin or NACCbl-apoptosis protection (chapter 6), so the superior protection provided by GSCbl against apoptosis induced by oxidative stress might be due to the ability of GSCbl to upregulate the Nrf2, HO-1 and Hsp72 through AKT/ERK1/2 signalling pathway. The pharmaceutical available form of cobalamins are required to be converted to GSCbl otherwise it wont be utilized by the neurons under oxidative stress, so GSCbl can be used in treatment of neuropsychiatric disorders oxidative stress related such as Alzheimer's disease (McCaddon & Cobalz Limited, 2001)

On the other hand, Nf_κB was significantly activated under NACCbl-apoptosis protection more than its level at cobalamin or GSCbl-apoptosis protection (chapter 6). As a result, iNOS expression increased significantly more than at GSCbl-apoptosis protection. And also the Hsp72 induction was induced by NACCbl more than at cobalamin treatments. Interestingly, cobalamins acts on the three suggested protection pathways but their effect were different which explain the superior protection provided.

The ability of cobalamin to induce the signal transduction cascades can be applied to be used in the drug development of related diseases. Muslin in 2008 reported that signal transduction might have an effective role in cardiovascular diseases. Since the cardiomyocytes growth increased by the activation of ERK1/2, while the activation of JNK and P38 led to increased cardiomyocytes dysfunction (Muslin, 2008). Moreover the induction of the Hsps can be used to reduce the severity of the diseases. Such as the overexpression of Hsp72 in transfect heart cells reduced the mitochondrial dysfunction after ischemia reperfusion injury (Jayakumar *et al.*, 2001). Most of

elderly diseases are associated with hyperhomocysteinemia and cobalamin deficiency such as Alzheimer's disease, Parkinson's disease, Huntington's disease, active multiple sclerosis and cardiovascular disease (Mattson *et al.*, 2001; Memet, 2006, Ward, 2001) knowing the molecular mechanism by which cobalamins provides protection against oxidative stress can be a useful tool to be applied in the drug development to reduce the severity and treat these diseases.

In conclusion, the ideas presented in this discussion are summarised in Figure 7.1. Cobalamin provides a protection against oxidative stress. Cobalamin does this by multiple pathways which include direct antioxidant stimulation and induction of signal transduction pathways. Different cobalamins derivatives have superior protections and they can be useful for clinical implication for most of oxidative stress related diseases. These findings can act as a base for further studies such as per-clinical researches applying the antioxidant properties of cobalamin on oxidative related diseases such as Alzheimer and cardiovascular diseases. Since several studies referred to the ability of cobalamin to reduce Hcy, our findings may support the on going researches in this field in order to reduce the risk of these diseases. Furthermore, it might be important to determine the cause of cobalamin deficiency. i.e. to determine whether the deficiency is due to lack of cobalamin, the lack of the cobalamin transport protein, an imputation in the receptor of the cells, or just a genetic mutation. These further studies will have an impact on the treatment of oxidative related disease.

Chapter 8

References:

- Abdella. N.A., Mojiminiyi O.A., Akanji, A.O., Moussa M.A., (2002). Associations of plasma homocysteine concentration in subjects with type 2 diabetes mellitus. *Acta Diabetol.*, 39,(4):183-90.
- Abraham, N. G., & Kappas, A.,(2005). Heme oxugenase and the cardiovascular-renal system, *Free Radical Biology & Medicine*, 39, (2):161-170.
- Agarwal, A. & Nick, H. S., (2000). Renal Response to tissue injury: Lessons from heme oxygenase-1 gene ablation and expression, *J. Amiriacan Society Nephrology*, 11, 965-973.
- Ahn, S.-G., & Thiele (2003). Redoxregulation of mammalian heat shock factor-1 is essential for Hsp gene activation and protection from stress, *Gene and Development*, 17, 516-528.
- Aikawa, R., Komuro, I., Yamazaki, T., Zou, Y., Kudoh, S., Tanaka, M., Shiojima, I., Hiroi, Y.,Yazaki, Y., (1997). Oxidative stress activates extracellular signal-regulated kinases through Src and Ras in cultured cardiac myocytes of neonatal rats, *J. Clin. Invest*,100, 1813–1821.
- Aktan, F., (2004). iNOS-mediated nitric oxide production and its regulation, *Life Sciences*, 75 639–653.
- Alderton, W.K., Cooper, C.E., Knowles, R.G., 2001. Nitric oxide synthases: structure, function and inhibition. *Biochemical Journal*, 357, 593–615.
- Alam, J. and Cook, J. L., (2003). Trascriptional regulation of the heme oxygenase-1 gene via the stress response element pathway, *Current Pharmaceutical Design*, 9, 2499-2511.
- Alderton, W.K., Cooper, C.E., & Knowles, R.G., (2001). Nitric oxide synthases: structure, function and inhibition. *Biochemical Journal* , 357, 593–615.
- Alexandrova, M. L., & Bocev, P.G., (2005). Oxidative stress during the chronic phase after stroke, *Free Radical Biology and Medicine*, 39, (3):297-316.
- Alnemri, E. S., Livingston, D. J., Nicholson, D. W., Salvesen, G., Thornberry, N. A., Wong, W. W., Yuan, J., (1996). Human ICE/CED-3 protease nomenclature. *Cell*, 87(2):171.
- Aloy MT, Hadchity E, Bionda C, Diaz-Latoud C, Claude L, Rousson R, Arrigo AP, Rodriguez-Lafrasse C.. (2008) Protective role of Hsp27 protein against gamma radiation-induced apoptosis and radiosensitization effects of Hsp27 gene silencing in different human tumor cells. *Int J Radiat Oncol Biol Phys* 1;70(2):543-53.

Allen, L. H., (2004). Folate and vitamin B12 status in Americas, *Nutrition Reviews*, 62(6): S29.

Amersi, F., Buelow, R., Kato, H., Ke, B., Coito, A. J., Shen, X. D., Zhao, D., Zaky, J., Melineck, J., Lassman, C. R., Kolls, J. K., Alam, J., Ritter, T., Volk, H. D., Farmer, D. G., Ghobrial, R. M., Bussutil, R. W., and Kupiek-Weglienski, J. W., (1999). *J. Clin. Investig.* 104, 1631–1639.

Anes, J. M., Beck, R. A., Brink, J. J. & Goldberg, R. J. (1994). *J. Chromatogr., B: Biomed. Appl.*, 660, 180–185.

Antoniades, C., Shirodaria, C., Warrick, N., Cai, S., De Bono, J. P., Lee, J. C., Leeson, P., Neubauer, S., Ratnatunga, C., Pillai, R., Refsum, H., & Channon K.M., (2006). 5-MTHF rapidly improves endothelial function and decreases superoxide production in human vessel: effects on vascular tetrahydrobiopterin availability and endothelial nitric oxide synthase coupling, *Circulation*, 114, (11):1193-1201.

Arrigo, A. P., (2001). Hsp27: novel regulator of intracellular redox state. *IUBMB Life*, 52, (6):303-7.

Arrigo, A. P., Firdaus, W. J., Mellier, G., Moulin, M., Paul, C., Diaz-latoud, C., Kretz-remy, C., (2005). Cytotoxic effects induced by oxidative stress in cultured mammalian cells and protection provided by Hsp27 expression, *Methods*, 35, (2): 126-38.

Arrigo, A. P., Viot, S., Chaufour, S., Firdaus, W., Kretz-Remy, C., Diaz-Latoud, C., (2005). Hsp27 consolidates intracellular redox homeostasis by upholding glutathione in its reduced form and by decreasing iron intracellular levels, *Antioxid Redox Signal*, 7, 414-422.

Ashfield-Watt, P. A. L., Moat, S. J., Doshi, S. N., & McFowell, I. F. W., (2001). Folate homocysteine, endothelial function and cardiovascular disease. What is the link? *Biomedicine & Pharmacotherapy*, 55, (8);425-433.

Atarod, E. B., Kehrer, J. P., (2004). Dissociation of oxidant production by peroxisome proliferator-activated receptor ligands from cell death in human cell lines, *Free Radical Biology and Medicine*, 37, (1);36-47.

Avogaro, A., de Kreutzenberg, S. V., Fadini, G. P., (2008). Oxidative stress and vascular disease in diabetes: is the dichotomization of insulin signaling still valid? *Free Radic. Biol. Med*, 44,1209–1215.

Au-Yeung, K. K., Yip, J. C., Siow, Y.L., O. K., (2006). Folic acid inhibits homocysteine-induced superoxide anion production and nuclear factor kappa B activation in macrophages. *J Physiol Pharmacol*, 84, (1):141-7.

Bach, F. H., (2005). Heme oxygenase-1, a therapeutic amplification funnel, 19, 1216-1219.

Baeuerle, P.A., (1998). I κ B and Nf κ B structures: at the interface of inflammation control, *Cell*, 95, 729–731.

Bailey, L.B., (2003). Folate and vitamin b12 recommended intakes and status in USA, *Nutrition reviews*, 56, (10):294.

Bailey, L.B., (2005). Dietary reference intake for folate: the debut of dietary folate equivalents, *Nutrition Reviews*, 51, (11): 263.

Balla, G., Jacob, H. S., Balla, J., Rosenberg, M., Nath, K., Apple, F., Eaton J. W., Vercellotti, G. M., (1992). Ferritin: A cytoprotective antioxidant stratagem of endothelium, *J. Biological chemistry*, 267(5): 18148-18153.

Banki, K. Huntter, E., Gonchoroff, N. J., and Perl, A., (1999). Elevation of mitochondrial transmembrane potential and reactive oxygen intermediate levels are early event and occur independently from activation of caspases in fas signaling, *J. Immunol*, 162(3): 1466-1479.

Barja, G., (2004). Free radicals and aging, *Trends in Neurosciences*, 27(10):595-600.

Batelli, S., Albani, D., Rametta, R., Polito, L., Prato, F., Pesaresi, M., Negro, A., Forloni, G., (2008). DJ-1 modulates alpha-synuclein aggregation state in a cellular model of oxidative stress: relevance for Parkinson's disease and involvement of HSP70, *PLoS One*, 3(4):e1884

Beere, H. M., (2005). Death versus survival: functional interaction between the apoptotic and stress-inducible heat shock protein pathways. *J. Clin. Invest*, 115(10):2633-2639.

Behrendt, D. & Ganz, P., (2002). Endothelial function: From vascular biology to clinical application, *The American Journal of Cardiology*, 90(10, Supplement 3): L40-L48.

Berger, A. B., Witte, M. D., Denault, J.-B., Sadaghiani A. M., Sexton, K. M. B., Salvesen, G. S., & Bogoy, M., (2006). Identification of early intermediates of caspase activation using selective inhibition and activity-Based probes, *Molecular Cell*, 23(4): 509-521.

Bitar, M.S., Wahid, S., Mustafa, S., Al-saleh, E., Dhaunsi, G. S., & AlMulla, F., (2005). Nitric oxide dynamics & endothelial dysfunction in type II model of genetic diabetes, *European Journal of pharmacology*, 511(1):53-64.

Binder, R. J., Vatner, R., Srivastava, P., (2004). The heat-shock protein receptors: some answers and more questions, *Tissue Antigens*, 64, 442-451.

Birch, C., Brasch, N. E., McCaddon, A., Williams, J. H. H., (2009). A novel role for vitamin B12: cobalamins are intracellular antioxidant in vitro. *Free Radical Biology and Medicine*, 47(2):184-8

Brich, C., PhD thesis (2007). University of chester.

Blandini, F., Fancellu, R., Martignoni, E., Mangiagalli, A., Pacchetti, C., Samuele, A. & Nappi, G., (2001). Comorbid disorders and hospitalisation in Parkinson's disease: a prospective study. *Neurological Sciences*, 47, 1102–1104.

Blatter, L. A., Taha, Z., Mesaros, S., Shacklock, P.S., Wier, W.G., and Malinski, T., (1995). Simultaneous measurements of Ca²⁺ and nitric oxide in bradykinin-stimulated vascular endothelial cells, *Circ Res* 76, 922–924.

Blennow, K., De Leon, M. J., Zetterberg, H., (2006). Alzheimer's disease, *The Lancet*, 368(9533): 387-403.

Bogdan, C., Roßlinghoff, M., Diefenbach A., (2000). Reactive oxygen and reactive nitrogen intermediates in innate and specific immunity, *Curr Opin Immunol*, 12, 64–76.

Bogdan, C., (2001). Nitric oxide and the immune response. *Nature Immunology*, 2(10): 907–916.

Bonetti, B., Stegagno, C., Cannella, B., Rizzuto, N., Moretto, G., Raine, C. S., (1999). Activation of NF-kappaB and c-jun transcription factors in multiple sclerosis lesions. Implications for oligodendrocyte pathology, *Am J Pathol*, 155(5):1433-8.

Bostantjopolou, S., Katsarou, Z., Frangia, T., Hatzizisi, O., Papazisis, K., Kyriazis, G., Kiosseoglou, G., & Kazis, A., (2005). Endothelial function markers in parkinsonian patients with hyperhomocysteinemia, *J. of Clinical Neuroscience*, 12(6): 669-672.

Bousser, M. G., Ferro, J. M., (2007). Cerebral venous thrombosis: an update. *Lancet Neurol*, 6(2):162-70.

Brouard, S., Otterbein, L. E.; Anrather, J.; Tobiasch, E.; Bach, F. H.; Choi, A. M.; Soares, M. P., (2000). Carbon monoxide generated by heme oxygenase 1 suppresses endothelial cell apoptosis, *J. Exp. Med*, 192, 1015– 1025.

Bruey, J. M., Ducasse, C., Bonniaud, P., (2000). HSP27 negatively regulates cell death by interacting with cytochrome c, *Nat Cell Biol*, 2, 645–652.

Brunet, A., Datta, S.R., Greenberg, M. E., (2001). Transcription-dependent and -independent control of neuronal survival by the PI-3K-Akt signaling pathway, *Curr. Opin. Neurobiol*, 11, 297–305.

Buemi, M., Marino, D., Di Pasquale, G., Floccari, F., Ruello, A., Aloisi, C., Corica, F., M., Senatore, Romeo, A., and Frisina, N., (2001). Effects of Homocysteine on Proliferation, Necrosis, and Apoptosis of Vascular Smooth Muscle Cells in Culture and Influence of Folic Acid, *Thrombosis Research*, 104 , 207–213

Buccellato, F., (1999). Myelinolytic lesions in spinal cord of cobalamin-deficient rats are TNF- α -mediated, *FASEB J.* 13, 297–304.

Bukau, B., & Horwich, A. L., (1998). The Hsp70 and Hsp60 chaperone machines, *Cell*, 92(3): 351-366.

- Cano, E., Hazzalin, C. A., Mahadevan, L. C., (1994). Anisomycin-activated protein kinases p45 and p55 but not mitogen-activated protein kinases ERK-1 and -2 are implicated in the induction of c-fos and c-jun, *Mol Cell Biol* 14, 7352–7362.
- Carmel, R., Green, R., Rosenblatt, D. S., & Watkins, D., (2003). Update on cobalamin, Folate, and Homocysteine, *Hematology*, (1): 62-81.
- Casado, P., Zuazua-Villar, P., Valle, E. D., Martinez-Campa, C., (2007). Vincristine regulates the phosphorylation of the antiapoptotic protein HSP27 in breast cancer cells, *Chinese Medical Journal*, 120(24):2271-2277 2277.
- Cattaneo, M., (1999) Hyperhomocysteinemia, atherosclerosis and thrombosis. *Thromb, Haemost.* 81, 165–176.
- Ceriello, A., and Motz, E., (2004). Is oxidative stress the pathogenic mechanism underlying insulin resistance, diabetes, and cardiovascular disease? The common soil hypothesis revisited, *Arterioscler Thromb Vasc Biol*, 24, 816-823.
- Chambers, J. C., Obeid, O. A., Kooner, J. S., (1999). *Vasc Biol*, 19(12): 2922–7.
- Chan, J. Y., Kwong, M., (2000). Impaired expression of glutathione synthetic enzyme genes in mice with targeted deletion of the Nrf2 basic-leucine zipper protein, *Biochim Biophys Acta*, 1517(1):19–26.
- Chan, K., Kan, Y.W., (1999). NRF2 is essential for protection against acute pulmonary injury in mice, *Proc. Natl. Acad. Sci. USA*, 96, 12731–12736.
- Chan, K., Han, X. D., Kan, Y.W., (2001). An important function of NRF2 in combating oxidative stress: detoxification of acetaminophen, *Proc. Natl. Acad. Sci. USA*, 98, 4611–4616.
- Chandra, J., Samali, A., Orrenius, S., (2000). Triggering and modulation of apoptosis by oxidative stress, *Free Radic. Biol. Med*, 29, 323– 333.
- Chen, W., Martindale, J. L., Holbrook, N. J., Liu, Y., (1998). Tumor promoter arsenite activates extracellular signal-regulated kinase through a signaling pathway mediated by epidermal growth factor receptor and Shc. *Mol. Cell. Biol.*, 18, 5178–5188.
- Chen, L. F., Greene, W. C., (2004). Shaping the nuclear action of NF-kB. *Nat Rev Mol Cell Biol*, 5, 392–401
- Cho, H. Y., Jedlicka, A. E., Reddy, S. P., Kensler, T. W., Yamamoto, M., Zhang, L. Y., (2002). Role of NRF2 in protection against hyperoxic lung injury in mice, *Am J Respir Cell Mol Biol*, 26(2): 175–182.
- Choi, B.-M., Pea, H. -O., Jeong, Y.-R., Oh, G.-S., Jun, C.-D., Kim, B.-R., Kim, Y.-M., & Chung H.-T., (2004). Overexpression of heme oxygenase-1 renders Jurkat T cells resistant to Fas-mediated apoptosis: involvement of iron released by HO-1, *Free Radical Biology and medicine*, 36(7):858-871.

Choi, Y., Kang, J., & Perk, J. H. Y., (2003). Polyphenolic flavonoids differ in their antiapoptotic efficacy in hydrogen peroxide treated human vascular endothelial cells, *J. Nutr.* 133, 985-991.

Choi, B. M., Kim, H. J., Oh, G. S., Pae, H. O., Oh, H., Jeong, S., Kwon, T. O., Im, M., Chung, H. T., (2002). 1,2,3,4,6-Penta-O-galloyl-beta-D-glucose protects rat neuronal cells (Neuro 2A) from hydrogen peroxide-mediated cell death via the induction of heme oxygenase-1, *Neurosci. Lett.*, 328, 185–189.

Christians, E. X., Yan, L.-J., & Benjamin I. J., (2001). Heat shock factor-1 and heat shock proteins: Critical partners in protection against acute cell injury, *Crit Care Med*, 30, S43-S50.

Chung, S. W., Chen, Y. H., and Perrella, M. A., Role of Ets-2 in the regulation of heme oxygenase-1 by endotoxin, *J Biol Chem*, 280, 4578–4584, 2005.

Chun-Han, H., Jinn, L., Shier-Chieh, H., Sheng-Mou H., Chih-Hsin, T., (2009). Ultrasound Stimulates NF- κ B Activation and iNOS Expression Via the Ras/Raf/MEK/ERK Signaling Pathway in Cultured Preosteoblasts, *Journal of Cellular Physiology*, 220, (1): 196-203.

Clarke, R., Smith, A. D., Jobst, K. A., Refsum, H., Sutton, L. & Ueland, P. M., (1998) Folate, vitamin B12, and serum total homocysteine levels in confirmed Alzheimer disease, *Arch. Neurol*, 55, 1449–1455.

Clark, J. E., Foresti, R., Sarathchandra, P., Kaur, H., Green, C. J., and Motterlini, R., (2000). *Am. J. Physiol. Heart Circ. Physiol.*, 278, H643-H651.

Ciriolo, M. R., (2005). Redox control of apoptosis, *Antioxidants & Redox Signaling*, &, (3-4): 432-435.

Cosentino, F., Patton, S., d'Uscio, L. V., Werner, E. R., Werner-Felmayer, G., Moreau, P., Malinski T., and Luscher, T. F., (1998). Tetrahydrobiopterin alters superoxide and nitric oxide release in prehypertensive rats, *J Clin Invest*, 101(7):1530–1537.

Concannon, C. G., Orrenius, S., Samali, A., (2001). Hsp27 inhibits cytochrome c-mediated caspase activation by sequestering both pro-caspase-3 and cytochrome c. *Gene Expr*, 9, 195-201.

Creagh, E. M., and Cotter, T. G., (1999). Selective protection by hsp70 against cytotoxic drug-, but not Fas-induced T-cell apoptosis. *Immunology* 97, 36–44.

Crossthwaite, A. J., Hasan, S., Williams, R. J., (2002). Hydrogen peroxide-mediated phosphorylation of ERK1/2, Akt/PKB and JNK in cortical neurones: dependence on Ca²⁺ and PI3-kinase, *J. Neurochem*, 80, 24– 35.

Cullinan, S. B., Gordan, J. D., Jin, J., Harper, J. W., Diehl, J. A., (2004). The Keap1-BTB protein is an adaptor that bridges Nrf2 to a Cul3-based E3 ligase: oxidative stress sensing by a Cul3-Keap1 ligase, *Mol Cell Biol*, 24, (19):8477–8486.

Danial, N. N., & Korsmeyer, S. J., (2004). Cell death: critical control points, *Cell*, 116, 205-219.

Davies K. J., (1999). The broad spectrum of responses to oxidants in proliferating cells: A new paradigm for oxidative stress. *IUBMB Life*, 48, 41–47.

Davis, R. J., (1994). MAPKs: new JNK expands the group, *Trends Biochem Sci* 19, 470–473.

Dawn, B., Bolli, R., (2002). Role of nitric oxide in myocardial preconditioning, *Annals of the New York Academy of Sciences*, 962, 18–41.

De Lau, L. M. L., Koudstaal, P. J., Witteman, J. C. M., Hofman, A., Breterler, M. M. B., (2006). Dietary folate vitamin B12, and vitamin B6 and the risk of Parkinson disease, *Neurology*, 67(2): 315-318.

DeMaio, A. (1999). Heat shock proteins: facts, thoughts and dreams. *Shock*, 11, 1-12.

De´rijard, B., Hibi, M., Wu IH, Barrett, T., Su, B., Deng, T., (1994). JNK1: a protein kinase stimulated by UV light and Ha-Ras that binds and phosphorylates the c-Jun activation domain, *Cell*, 76, 1025–1037.

Deshane, J., Wrght, M., & Agarwal, A., (2005). Heme oxygenase-1 expression indisease states. *Acta Biochimica Polonica*, 52(2): 273-284.

Dhanasekaran, N., Reddy, E. P., (1998). Signaling by dual specificity kinases, *Oncogene*, 17, 1447–1755

Dhanasekaran, D. N., Kashef, K., Lee, C. M., Xu, H., and Reddy, E. P., (2007). Scaffold proteins of MAP-kinase modules, *Oncogene*, 26, 3185–3202.

Diaz-Latoud, C., Buache, E., Javouhey, E., Arrigo, A. P., (2005). Substitution of the unique cysteine residue of murine Hsp25 interferes with the protective activity of this stress protein through inhibition of dimer formation, *Antioxid Redox Signal*, 7, 436-45.

Diaz-Arrastia, R., (2000). Homocysteine and neurologic disease. *Arch. Neurol.* 57,1422–1427.

Diller, K. R., (2006). Stress protein expression kinetics. *Ann. Rev. Biomed. Eng*, 8, 403-424.

Dinkova-Kostova, A.T., Massiah, M.A., Bozak, R.E., Hicks, R.J., Talalay, P., (2001). Potency of Michael reaction acceptors as inducers of enzymes that protect against carcinogenesis depends on their reactivity with sulfhydryl groups, *Proc. Natl. Acad. Sci. USA*, 98, 3404–3409.

Dringen, R., Pawlowski, P. G., Hirrlinger, J., (2005). Peroxide detoxification by brain cells, *J. Neurosci Res*, 79,157–165.

Duan, W., Ladenheim, B., Cutler, R. G., Kruman, I. I., Cadet, J. L. & Mattson, M. P., (2002). Dietary folate deficiency and elevated homocysteine levels endanger dopaminergic neurons in models of Parkinson's disease, *J. Neurochem*, 80, 101–110.

Doulias, P.-T., Kotoglou, P., Tenopoulou, M., Keramisanou, D., Tzavarras, T., Galaris, B. U. D., & Angelidis, C., (2007). Involvement of heat shock protein-70 in the mechanism of hydrogen peroxide induced DNA damage: The role of lysosomes and iron. *Free Radical Biology and medicine*, 42, 567-577.

Duan-Fang, L., Zheng-Gen, J., Arnold, S., Baas, Guenter, D., Steven, P., Gygi, Ruedi, A., and Bradford, C., Berk., (2000) Purification and Identification of Secreted Oxidative Stress-induced Factors from Vascular Smooth Muscle Cells, *The Journal of biological chemistry*, 275, (7) 189–196.

Dypbukt, J. M., Ankarcrona, M., Burkitt, M., Sjöholm, Å., Ström, K., Orrenius, S. and Nicotera, P., (1994). Different prooxidant levels stimulate cell growth, activate apoptosis, or produce necrosis in insulin-secreting RINm5F cells, *J. Biol. Chem.*, 269, 30553-30560.

Earnshaw, W. C., Martins, L. M., Kaufmann, S. H., (1999). Mammalian caspases: structure, activation, substrates and functions during apoptosis, *Annu. Rev. Biochem.* 68, 383– 424.

Ehrnsperger, M., Grabel, S., Gaestel, M., and Buchner, J., (1997). Binding of non-native protein to Hsp25 during heat shock creates a reservoir of folding intermediates for reactivation, *EMBO J*, 16, 221–229.

Facchinetti, F., Furegato, S., Terrazzino, S., Leon, A., (2002). H₂O₂ induces up-regulation of Fas and Fas ligand in NGF-differentiated PC12 cells: modulation by cAMP, *J. Neurosci. Res*, 69, 178– 188.

Fenech, M., (1999). Micronucleus frequency in human lymphocytes is related to plasma vitamin B12 and homocysteine, *Mutat Res*, 428, 299–304.

Fenech, M., (2001). The role of folic acid and vitamin B12 in genomic stability of human cells. *Mutation research/fundamental and molecular mechanisms of mutagenesis, Micronutrients and genomic stability*, 475(1-2):57-67.

Fink A. L., (1999). Chaperone- mediated protein folding. *Physiol. Rev.*, 79, 425-449.

Finkelstein, J. D., & Martin J. J., (2000). Homocysteine . *The international journal of biochemistry & cell biology*, 32(4):385-389.

Foresti, R., Sarathchandra, P., Clark, J. E., Green, C. J., and Motterlini, R., (1999) *Biochem. J.*, 339, 729–736

Forouhi, N. G., & Sattar, N., (2006). CVD risk factors and ethnicity-A homogeneous relationship? *Atherosclerosis Supplements*, 7(1):11-19.

Frosst P, Blom HJ, Milos R, Goyette P, Sheppard CA, Matthews RG, Boers GJH, den Heijer M, Kluijtmans LAJ, van den Heuvel LP, Rozen R. A candidate genetic risk

factor for vascular disease: a common mutation in methylenetetrahydrofolate reductase. *Nat Genet.* 1995;10:111–113.

Frank, G., Eguchi, S., & Motly, E., (2005). The role of reactive oxygen species in insulin signaling in the vasculature. *Antioxidant & redox Signaling*, 7(5-6): 1053-1061.

Frank R. N., (2002). Potential new medical therapies for diabetic retinopathy: protein C inhibitors. *American J. of ophthalmology*, 133(5): 693-698.

Fiers, W., Beyaert, R., Declercq, W. and Vandenabeele, P. (1999). More than one way to die: apoptosis, necrosis and reactive oxygen damage. *Oncogene* 18, 7719-7730.

Furukawa, M, Xiong, Y., (2005). BTB protein Keap1 targets antioxidant transcription factor Nrf2 for ubiquitination by the Cullin 3-Roc1 ligase, *Mol Cell Biol*, 25(1):162–171.

Fuqua, S. A., Oesterreich, S., Hilsenbeck, S. G., Von Hoff, D. D., Eckardt, J, Osborne C. K., (1994). Heat shock proteins and drug resistance, *Breast Cancer Res Treat*, 32-67–71.

Garrido, C., Ottavi, P., Fromentin, A., Hammann, A., Arrigo, A. P., Chauffert, B., and Mehlen, P., (1997). Hsp27 as a mediator of confluence-dependent resistance to cell death induced by anticancer drugs, *Cancer Res*, 57, 2661–2667.

Gardner A. M., Xu F. H., Fady, C., Jacoby, F. J., Duffey, D. C., Tu, Y., Lichtenstein, A., (1997). Apoptotic vs. nonapoptotic cytotoxicity induced by hydrogen peroxide, *Free Radic Biol Med*, 22(1-2):73–83.

Ghosh, G., VanDuyne, G., Ghosh, S. and Sigler, P.B., (1995). Structure of NF-kappa B p50 homodimer bound to a kappa B site, *Nature*, 373, 303–310.

Ghosh, S., Karin, M., (2002). Missing pieces in the NF-kappaB puzzle. *Cell*, 109, S81–S96.

Gimsing, P., and E. Nexø. (1983). The forms of cobalamin in biological materials. in *Methods in Hematology: The Cobalamins*. 7–30.

Gibbons NB, Watson RW, Coffey RN, Brady HP, Fitzpatrick JM. Heat-shock proteins inhibit induction of prostate cancer cell apoptosis. *Prostate*. 2000 Sep 15;45(1):58-65.

Griendlin, K. K., & Ushio-Fukai, M., (1997). NADH/NADPH oxidase and vascular function. *Trends in cardiovascular medicine*, 7(8): 301-307.

Grosser, N., Abate, A., Oberle, S., Vreman, H. J., Dennery, P. A., Becker, J. C., Pohle, T., Seidman, D. S., Schroder, H., (2003). Heme oxygenase-1 induction may explain the antioxidant profile of aspirin. *Biochemical & Biophysical research comm.*, 308, 956-960.

Guyton, K.Z., Liu, Y., Gorospe, M., Xu, Q., Holbrook, N.J., (1996). Activation of mitogen-activated protein kinase by H₂O₂: role in cell survival following oxidant injury, *J. Biol. Chem*, 271, 4138–4142.

Hail, N. H., Carter, B. Z., Konopleva, M., Andreeff, M., (2006). Apoptosis effector mechanisms: a requiem performed in different ways. *Apoptosis*, 11, 889-904.

Hampton, M. B., & Orrenius, S., (1997). Dual regulation of caspase activity by hydrogen peroxide: implications for apoptosis, *FEBS Letters*, 414, 552-556.

Harm, H., Kampinga, & Hageman, J., & Michel, J., Vos & Kubota, H., & Robert, Tanguay, M., & Elspeth, Bruford, A., & Michael, E., Cheetham, & Chen, B. & Lawrence, Hightower, E., (2009). Guidelines for the nomenclature of the human heat shock proteins. *Cell Stress and Chaperones*, 14, 105–111.

Harlt, F. U., (1996). Molecular chaperone in cellular protein folding, *Nature*, 381, 571-580.

Harlt, F. U., & Hayer-Harlt, M., (2002). Protein folding-Molecular chaperone in the cytosol: from nascent chain to folded protein. *Science*, 295(5561): 1852-1858.

Harker, L. A., Ross, R., Slichter, S. J., Scott, C. R., (1976). Homocystine-induced arteriosclerosis. The role of endothelial cell injury and platelet response in its genesis. *J Clin Invest*, 58(3):731-41.

Harper, S. J., LoGrasso, P. (2001). Signalling for survival and death in neurones: the role of stress-activated kinases, JNK and p38, *Cell Signal*, 13:299–310.

Hatano, E., and Brenner, D., (2001). Akt protects mouse hepatocytes from TNF- α and Fas-mediated apoptosis through NF- κ B activation, *Am J Physiol Gastrointest Liver Physiol*, 282, G1357–G1368.

Hayashi, T., Ueno, Y., and Okamoto, T., (1993). Identification of a new serine kinase that activates NF kappa B by direct phosphorylation, *J. Biol. Chem.*, 268, 11380–11388.

Hayden, M. S., Ghosh, S., (2004). Signaling to NF-kB, *Genes Dev*, 18, 2195–2224.

Hayden, M. S., West, A. P., Ghosh, S., (2006). SnapShot: NF-kappaB signaling pathways. *Cell*, 127, 1286–1287.

Hayes, J. D., Chanas, S. A., Henderson, C. J., McMahon, M., Sun, C., Moffat, G. J., Wolf, C. R., Yamamoto, M., (2000). The NRF2 transcription factor contributes both to the basal expression of glutathione S-transferases in mouse liver and to their induction by the chemopreventive synthetic antioxidants, butylated hydroxyanisole and ethoxyquin, *Biochem. Soc. Trans.* 28, 33–41.

Hengartner, M. O., (2000). The Biochemistry of apoptosis. *Nature*, 407, 770-776.

Herrmann, W., Quast, S., Ullrich, H., Schultze, H., Bodis, M. and Geisel, J. (1999) Hyperhomocysteinemia in high-aged subjects: relation of B-vitamins, folic acid, renal function and the methylenetetrahydrofolate reductase mutation. *Atherosclerosis* 144, 91-101.

Hibi M, Lin A, Smeal T, Minden A, Karin M., (1993). Identification of an oncoprotein- and UV-responsive protein kinase that binds and potentiates the c-Jun activation domain, *Genes Dev*, 7, 2135–2148.

Hoffmann, A., Natoli, G., Ghosh, G., (2006). Transcriptional regulation via the NF- κ B signaling module, *Oncogene*, 25, 6706–6716.

Hommes, D. W., Peppelenbosch, M. P., Van Deventer, S. J., (2003). Mitogen activated protein (MAP) kinase signal transduction pathways and novel anti-inflammatory targets, *Gut*, 52,144–151.

Hosokawa, Y., Tanigawa, Y., (2000). Phorbol ester synergistically increases interferon regulatory factor-1 and inducible nitric oxide synthase induction in interferongamma-treated RAW 264.7, cells. *Biochimica et Biophysica Acta*, 1498(1) 19–31.

Hout, J., Houle, F., Spitz, D. R., and Landry, J., (1996). HSP27 phosphorylation-mediated resistance against actin fragmentation and cell death induced by oxidative stress, *Cancer Res.*, 56,273–279.

Huang, H. C., Nguyen, T., Pickett, C. B., (2000). Regulation of the antioxidant response element by protein kinase C-mediated phosphorylation of NFE2- related factor 2, *Proc. Natl. Acad. Sci. USA*, 97, 12475–12480.

Huang, K. T., Kuo, L., Liao, J. C., (1998). Lipopolysaccharide activates endothelial nitric oxide synthase through protein tyrosine kinase. *Biochemical and Biophysical Research Communications*, 245(1): 33–37.

Huang R. F. S, Yaong HC, Chen SC & Lu YF (2004) In vitro folate supplementation alleviates oxidative stress, mitochondria-associated death signalling and apoptosis induced by 7-ketocholesterol. *Br J Nutr* 92, 887–894.

Huot, J., Roy, G., Lambert, H., Chre'tien, P., and Landry, J., (1991). Increased survival after treatments with anticancer agents of Chinese hamster cells expressing the human Mr 27,000 heat shock protein, *Cancer Res.*, 51, 5245–5252.

Huk, I., Nanobashvili, J., Punz, A., Neumayer, C., Gassner, R., Fuegl, A., Polterauer, P., Brovkovich, V., Patton S., and Malinski, T., (1998). Ischemia/reperfusion injury: Nitric oxide superoxide and peroxynitrite changes, effect of prostaglandin E-1 treatment, *Journal of Vascular Research*, 35, 70.

Itoh, K., Tong, K. I., Yamamoto, M., (2004). Molecular mechanism activating Nrf2-Keap1 pathway in regulation of adaptive response to electrophiles. *Free Radic Biol. Med*, 36, 1208–1213.

- Ireland, H. E., Harding, S. J., Bonwick, G. A., Jones, M., Smith, C. J., & Williams, J. H. H., (2004). Evaluation of heat shock protein 70 as a biomarker of environmental stress in *Fucus serratus* and *lemna minor*, *Biomarkers*, 9(2):139-155.
- Ito, H., Okamoto, K., Kato, K., (1998). Enhancement of expression of stress proteins by agents that lower the levels of glutathione in cells. *Biochim Biophys Acta*, 1397: 223-230.
- Jaffrey, S. R., Snyder, S. H., (1995). Nitric oxide: A neural messenger, *Annu Rev Cell Dev Biol*, 11, 417–440.
- Jaiswal, A. K., (2004). Nrf2 signaling in coordinated activation of antioxidant gene expression, *Free Radic Biol Med*, 36(10):1199-207.
- Jacobson, M. D., (1996). Reactive oxygen species and programmed cell death, *Trends Biochem. Sci*, 21, 83-86.
- Jackson, A. L., Loeb, L. A., (2000). Microsatellite instability induced by hydrogen peroxide in *Escherichia coli*, *Mutat. Res.* 447,187–198.
- Jacobsen D. W., (1998). Homocysteine and vitamins in cardiovascular disease. *Clin Chem*, 44(8):1833-1843.
- James, S. J., Basnakian, A. G., Miller, B. J., (1994). In vitro folate deficiency induces deoxynucleotide pool imbalance, apoptosis, and mutagenesis in Chinese hamster ovary cells, *Cancer Res*, 54(19):5075-80.
- Jiang, Y., Sun, T., Xiong, J., Cao, J., Li, G., Wang, S., (2007). *Acta Biochim Biophys Sin*, 39(9): 657-67.
- Johnson, G. L., Lapadat, R., (2002). Mitogen-activated protein kinase pathways mediated by ERK, JNK, and p38 protein kinases. *Science*, 298:1911–1912.
- Junttila, M. R., Li, S. P., Westermarck, J., (2008). Phosphatase-mediated crosstalk between MAPK signaling pathways in the regulation of cell survival, *FASEB J.* 22:954–965.
- Kaltschmidt, B., Widera, D., Kaltschmidt, C., (2005). Signaling via NF-kappaB in the nervous system. *Biochim Biophys Acta*, 1745(3):287-99.
- Kang, K. W., Lee, S. J., Park, J. W., and Kim, S. G., (2002). Phosphatidylinositol 3-kinase regulates nuclear translocation of NF-E2-related factor 2 through actin rearrangement in response to oxidative stress, *Mol Pharmacol*, 62, 1001–1010.
- Kang, K. W., Cho, M. K., Lee, C. H., and Kim, S. G., Activation of phosphatidylinositol 3-kinase and Akt by *tert*-butylhydroquinone is responsible for antioxidant response element-mediated rGSTA2 induction in H4IIE cells, *Mol Pharmacol* 59, 1147–1156, 2001.

- Kazerooni, T., Asadi, N., Dehbashi, S., Zolghadri, J., (2008). Effect of folic acid in women with and without insulin resistance who have hyperhomocysteinemic polycystic ovary syndrome. *J. Clin. Endocrinol. Metab.* 101(2):156-60
- Kerr, J. F. R., Wyllie, A. H., Currie, A. R., (1972). Apoptosis: a basic biological phenomenon with widespread implications in tissue kinetics. *Br. J. Cancer*, 26, 239–257.
- Kebodraava, T. M., (2002). How cells protect themselves against stress? *Russian j. of Genetics*, 38(4):345-358.
- Kim, D. J., Jung-Min, K., Lee, O., Kim, N. J., Young-Sun, L., Kim, Y. S., Joong-Yeol, P., Ki-Up L., Kim, G. S., (2006). Homocysteine enhances apoptosis in human bone marrow stromal cells, *Bone*, 39, 582–590.
- Kim, H. P., Wang, X., Zhang, J., Suh, G. Y., Benjamin, I. J., Ryter, S. W., & Choi, A. M., (2005). Heat shock protein-70 mediates the cytoprotective effect of carbon monoxide: involvement of p38 beta MAPK and heat shock factor-1. *J. Immunol*, 175(4):2622-2629.
- Kim, J. S., Cho, H. W., Chung and Kim, I. G., (2006). Effect of trion, 4,5-dihydroxy-1,3-benzene disulfonic acid, on human promyelotic HL-60 leukemia cell differentiation and death. *Toxicology*, 223(1-2):36-45.
- Kim-Han, J. S., & Dugan, L. L., (2005). Mitochondrial uncoupling proteins in central nervous system. *Antioxidant & redox signaling*, 7(9-10): 1173-1181.
- Kim, J. W., Mei-Hua, L., Jung-Hee, J., Hye-Kyung, N., Na-Young S., Chan, L., Jeffrey, A., Johnson, Young-Joon, Surh, (2008). 15-Deoxy-D12,14-prostaglandin J2 rescues PC12 cells from H₂O₂-induced apoptosis through Nrf2-mediated upregulation of heme oxygenase-1: Potential roles of Akt and ERK1/2. *Biochemical pharmacology*, 76, 1577– 589.
- Kim, Y.-C., Masutani, H., Yamaguchi, Y., Itoh, K., Yamamoto, M., (2001). Hemin induced activation of the thioredoxin gene by Nrf2, *J. Biol.Chem*, 276, 18399–18406.
- Kiningham, K. K., Cardozo, Z. A., Cook, C., Cole, M. P., Stewart, J. C., Tassone, M., Coleman, M. C., Spitz, D. R., (2008). All-trans-retinoic acid induces manganese superoxide dismutase in human neuroblastoma through NF-kappaB. *Free Radic Biol Med*, 44(8)1610-6.
- Kirkeboen, K. A., Strand, O. A., (1999). The role of nitric oxide in sepsis—an overview. *Acta Anaesthesiol Scand*, 43, 275–288.
- Kleinwort, H., Schwarz, P. M. and Frstermann, U. (2003) Regulation of the expression of inducible nitric oxide synthase. *J Biol Chem* 278, pp. 1343-1364.
- Kobayashi, M., Yamamoto, M., (2005). Molecular mechanisms activating the Nrf2-Keap1 pathway of antioxidant gene expression, *Antioxid. Redox Signal*, 382–394.

- Kojima, K., Musch, M. W., Ren, H., Boone, D. L., Hendrickson, B. A., Ma, A., Chang E. B., (2003). Enteric flora and lymphocyte-derived cytokines determine expression of heat shock proteins in mouse colonic epithelial cells, *Gastroenterology*, 124, 1395-1407.
- Komatsuda, A., Wakui, H., Oyama, Y., Imai, H., Miura, A. B., Itoh, H., and Tashima, Y., (1999). Overexpression of the human 72 kDa heat shock protein in renal tubular cells confers resistance against oxidative injury and cisplatin toxicity, *Nephrol Dial Transplant* 14, 1385–1390.
- Kong, A. N., Owuor, E., Yu, R., Hebbar, V., Chen, C., Hu, R., Mandlekar, S., (2001). Induction of xenobiotic enzymes by the MAP kinase pathway and the antioxidant or electrophile response element (ARE/EpRE), *Drug Metab. Rev.* 33, 255–271.
- Koury, M. J., Park, D. J., Martincic, D., Horne, D. W., Kravtsov, V., Whitlock, J. A., del Pilar Aguinaga, M., Kopsombut, P., (1997). Folate deficiency delays the onset but increases the incidence of leukemia in Friend virus-infected mice. *Blood*, 90(10): 4054-61
- Kovacic, P., Pozos, R. S., Somantan, R., Shangari, N., O'Brien (2005). Mechanism of mitochondrial uncouplers, inhibitors and toxins: Focus on electron transfer, free radicals and structure- activity relationship . *Curr. Med. Chem.* 12, 2601-2623.
- Karvets, a., Hu, Z., Miralem, T., Torno, M. D., Maines, M. D., (2004). Biliverdin reductase, a novel regulator for induction of activating transcription factor-2 and heme oxygenase-1. *J. Biological chemistry*, 279(19):19916-19923.
- Kregel, K. C., (2002). Heat shock proteins: modifying factors in physiological stress responses and acquired thermotolerance, *J. Appl. Physiol*, 92, 2177–2186.
- Kultz, D., (2005). Molecular and evolutionary basis of the cellular stress response. *Ann. Rev. Physiology*, 67, 225-257.
- Kuhn, W., Roebroek, R., van Oppenraaij, D., Przuntek, H., Kretschmer, A., Buttner, T., Woitalla, D., & Muller, T., (1998). Elevated plasma levels of homocysteine in Parkinson's disease, *Eur. Neurol*, 40, 225–227.
- Kurland, J. F., Voehringer, D.W., Meyn, R. E., (2003) The MEK/ERK pathway acts upstream of NF kappa B1 (p50) homodimer activity and Bcl-2 expression in a murine B-cell lymphoma cell line. MEK inhibition restores radiation-induced apoptosis, *J. Biol. Chem*, 278, 32465–32470.
- Kumar, S., A. B., and Gélinas, C., (1992). The RxxRxRxxC motif conserved in all Rel/kappa B proteins is essential for the DNA-binding activity and redox regulation of the v-Rel oncoprotein, *Mol. Cell. Biol.*, 12, 3094–3106.
- Kvale, D., and Holme, (1996). Intercellular adhesion molecule-1 (ICAM-1; CD54) expression in human hepatocytic cells depends on protein kinase, C. *Journal of Hepatology*, 25, 67-676.

Kwak, M. K., Itoh, K., Yamamoto, M., Sutter, T. R., Kensler, T. W., (2001). Role of transcription factor Nrf2 in the induction of hepatic phase 2 and antioxidative enzymes in vivo by the cancer chemoprotective agent, 3H-1, 2-dimethiole-3-thione, *Mol Med* 7(2):135–145.

Kwak, M., Wakabayashi, N., Greenlaw, J., Yamamoto, M., and Kensler, T., (2003) Antioxidants enhance mammalian proteasome expression through the Keap1-Nrf2 signaling pathway, *Mol Cell Biol*, 23, 8786–8794.

Landry, J., Chre'tien, P., Lambert, H., Hickey, E., and Weber, L. A., (1989). Heat shock resistance conferred by expression of the human HSP27 gene in rodent cells. *J. Cell Biol*, 109, 7–15.

Lahti, A., Kankaanranta, H., Moilanen, E., (2002). P38 mitogen-activated protein kinase inhibitor SB203580 has a bi-directional effect on iNOS expression and NO production. *European Journal of Pharmacology*, 454(2–3): 115–123.

Lang, D., Hubrich, A., Dohle, F., Terstesse, M., Saleh, H., Schmidt, M., Pauels, H. G., & Heidenreich, S., (2000). Differential expression of heat shock protein 70 (hsp70) in human monocytes rendered apoptotic by IL-4 or serum deprivation. *Journal of Leukocyte Biology*, 68, 729-736.

Lazo, P. S., Ramos, S., Vincristine, (2007). Regulates the phosphorylation of the antiapoptotic protein HSP27 in breast cancer cells, *Cancer Lett* , 247, 273-282.

Lee, Y., Shacter, E., (1997). Bcl-2 does not protect Burkitt's lymphoma cells from oxidant-induced cell death. *Blood*, 89(12):4480–4492.

Lee, J. M., Calkins, M. J., Chan, K., Kan, Y. W., and Johnson, J. A., (2003). Identification of the NF-E2-related factor-2-dependent genes conferring protection against oxidative stress in primary cortical astrocytes using oligonucleotide microarray analysis, *J Biol Chem*, 278,12029–12038.

Lee, J. M., Hanson, J. M., Chu, W. A., and Johnson, J. A., (2001). Phosphatidylinositol 3-kinase, not extracellular signal-regulated kinase, regulates activation of the antioxidant-responsive element in IMR-32 human neuroblastoma cells, *J Biol Chem*, 276, 20011–20016.

Lee, J. R., J. T., McCubrey, J. A., (2002). The Raf/MEK/ERK signal transduction cascade as a target for chemotherapeutic intervention in leukemia, *Leukemia*,16, 486–507.

Lee, T. S., Chau, L. Y., (2002). Heme oxygenase-1 mediates the anti-inflammatory effect of interleukin-10 in mice, *Nature Med*, 8, 240– 246.

Lennon, S. V., Martin, S. J. and Cotter, T. G. (1991). Dose-dependent induction of apoptosis in human tumour cell lines by widely diverging stimuli. *Cell Prolif*. 24, 203-214.

Lentz, S. R., (2005). Mechanisms of homocysteine-induced atherothrombosis, *J Thromb Haemost*, 3(8):1646-54.

Li, G. C., Webb, Z., (1982). Correlation between synthesis of heat shock proteins and development of thermotolerance in Chinese hamster fibroblasts, *Proc Natl Acad Sci USA*, 79, 3218–3222.

Liao, D-F., Jin, Z-G., Arnold S., Daum, G., Steven P. Gygi, Aebersold, R., and Bradford, C., (2000). Purification and Identification of Secreted Oxidative Stress-induced Factors from Vascular Smooth Muscle Cells, *The Journal of Biological chemistry*, 275, 189–196.

Lione, F., PhD thesis (2009) University of Chester.

Lin, A., Karin, M., (2003). NF-kappaB in cancer: a marked target, *Semin Cancer Biol*, 13, 107–114.

Ling, C. T. & Chow, B. F. (1953). *J. biol. Chem.* 202,445.

Levrant S, Pacher P, Pesse B, Rolli J, Feihl F, Waeber B, Liaudet L. (2007) Homocysteine induces cell death in H9C2 cardiomyocytes through the generation of peroxynitrite. *Biochem Biophys Res Commun.* 359(3):445-50.

LI, G.C. & WEBB, Z. (1982). Correlation between synthesis of heat shock proteins and development of thermotolerance in Chinese hamster fibroblasts. *Proc. Natl Acad. Sci.*, 79, 3218.

Lee JS, Surh YJ (2005) Nrf2 as a novel molecular target for chemoprevention. *Cancer Lett* 224:171–184

Lindquist, S., (1986). The heat-shock response. *Annu. Rev. Biochem*, 55, 1151–1191

Liu, L., Zhang, X. J., Jiang, S. R., Ding, Z. N., Ding, G. X., Huang, J., Cheng, Y. L., (2007) Heat shock protein 27 regulates oxidative stress-induced apoptosis in cardiomyocytes: mechanisms via reactive oxygen species generation and Akt activation. *Chin Med J (Engl)*, 20,120(24):2271-7.

Liu, X. M., Peyton, K. J., Ensenat, D., Wang, H., Schafer, A. I., Alam, J., (2005). Endoplasmic reticulum stress stimulates heme oxygenase-1 gene expression in vascular smooth muscle - Role in cell survival, *Journal of Biological Chemistry*, 280(2): 872-877.

Liu, Y., Liu, W., Song, X. D., & Zuo, J. (2005). Effect of GRP75/mthsp70/PBP74/mortalin overexpression on intracellular ATP level, mitochondrial membrane potential and ROS accumulation following glucose deprivation in PC12 cells, *Molecular and cellular Biochemistry*, 268(1-2): 45-51

Loscalzo, J., (1996). The oxidant stress of hyperhomocysteinemia. *J. of Clinical investigation*, 98(1):5-7.

Lu, Q., Qiu, X., Hu, N., Wen, H., Su, Y., & Richardson, B. C., (2006). Epigenetics, disease and therapeutic interventions. *Ageing research reviews*, 5, 449-467.

Lucock, M. D., Daskalakis, I.G., Wild, J., Anderson, A., Schorah, C. J., Lean, M. E., Levene, M. I., (1996). The influence of dietary folate and methionine on the metabolic disposition of endotoxic homocysteine, *Biochem. Mol. Med*, 59, 104–111.

Luchsinger, J. A., Tang, M. X., Miller, J., Green, R., & Mayeux, R., (2007). Relation of higher folate intake to lower risk of Alzheimer disease in elderly. *Arch. Neurol.*, 64, 86-92.

Lyle, A. N., & Griendling, K.K., (2006). Modulation of vascular smooth muscle signaling by reactive oxygen species. *Physiology*, 21(4):269-280.

Maines, M. D., (1997). The heme oxygenase system: a regulation of second messenger gases. *Ann. Rev. Pharmacological toxicology*, 37, 517-554.

Maines, M. D., (2005). New insights into biliverdin reductase functions: linking heme metabolism to cell signaling. *Physiology*, 20(6):382-389.

Maines, M. D., & Gibbs P. E. M., (2005). 30 some years of heme oxygenase: from a molecular wrecking ball to a mesmerizing trigger of cellular events. *Biochemical and biophysical research communications*, 338, 568-577.

Maino, G., & Joris, I., (1995). Apoptosis, necrosis and necroptosis. An overview of cell death. *Am. J. Pathology*, 146, 3-15.

Marie-Thérèse S. Al., Elie, H., Claea B., Diaz-Latoud, C., Claude, L., Rousson, R., Arrigo, A. P., and Rodriguez-Lafrassw, C., (2008). Protective role of Hsp27 protein against gamma radiation-induced apoptosis and radiosensitization effect of Hsp27 gene silencing in different human tumor cells, *Int. J. Radiation Oncology Biol. Phys.*, 70 (2):543–553.

Malinow, M. R., Kang, S. S., Taylor, L. M., Wong, P. W., Coull, B., Inahara, T., Mukerjee, D., Sexton, G., Upson, B., (1989). Prevalence of hyperhomocystinemia in patients with peripheral arterial occlusive disease, *Circulation* 79, 1180–1188.

Malinow, M. R., (1990). Hyperhomocyst(e)inemia. A common and easily reversible risk factor for occlusive atherosclerosis, *Circulation*, 81, (6):2004-6

Mark, B., Hampton, Orrenius, S., (1997). Dual regulation of caspase activity by hydrogen peroxide: implications for apoptosis, *FEBS Letters*, 414, 552-556.

Mark, W., Mush, Aditya K., and Eugene B. Chang, (2004). Heat shock protein 72 binds and protects dihydrofolate reductase against oxidative injury, *Biochemical and biophysical research communication*, 313, 185-192.

Marks-Konczalik, J., Chu, S. C., Moss, J., (1998). Cytokine-mediated transcriptional induction of the human inducible nitric oxide synthase gene requires both activator protein 1 and nuclear factor kappaB-binding sites, *Journal of Biological Chemistry*, 273 (35): 22201–22208.

Marla, S. S., Lee, J., Groves, J. T., (1997). Peroxynitrite rapidly permeates phospholipid membranes. *Proc Natl Acad Sci USA*, 94(26):14243-8.

Martindale, J. L., Holbrook, N. J., (2002). Cellular response to oxidative stress: signaling for suicide and survival, *J Cell Physiol*, 192, 1–15.

Martin, D., Rojo, A., Salinas, M., Diaz, R., Gallardo, G., Alam, J., Galarreta, C. M., and Cuadrado, A., (2003). Regulation of heme oxygenase-1 expression through the phosphatidylinositol 3-kinase/Akt pathway and the Nrf2 transcription factor in response to the antioxidant phytochemical carnosol, *J Biol Chem*, 279, 8919–8929.

Mason, P., Kalinowski, L., Jacob, R. F., Jacoby, A. M., and Malinski, T., (2005). Nebivolol reduces nitroxidative stress and restores nitric oxide bioavailability in endothelium of African Americans, *Circulation*, 112, 3795–3801.

Matsuzaki, H., Tamatani, M., Mitsuda, N., Namikawa, K., Kiyama, H., Miyake, S., Tohyama, M., (1999). Activation of Akt kinase inhibits apoptosis and changes in Bcl-2 and Bax expression induced by nitric oxide in primary hippocampal neurons, *J. Neurochem*, 73, 2037–2046.

Matthews, J. R., Wakasugi, N., Virelizier, J.-L., Yodoi, J., and Hay, R.T., (1992). Thioredoxin regulates the DNA binding activity of NF-kappa B by reduction of a disulphide bond involving cysteine 62., *Nucleic Acids Res.*, 20, 3821–3830.

Matthews, J. R., Kaszubska, W., Turcatti, G., Wells, T.N.C. and Hay, R. T., (1993). Role of cysteine62 in DNA recognition by the P50 subunit of NF-kappa B , *Nucleic Acids Res.*, 21, 1727–1734.

Mattson, M. P., (2003) Gene-diet interactions in brain aging and neurodegenerative disorders, *Ann Intern Med*, 139, 441–444.

Mattson, M. P., Shea, T. B., (2003). Folate and homocysteine metabolism in neural plasticity and neurodegenerative disorders, *TINS*, 26, 137–146.

Mattson, M. P., Kruman, Duan, W., (2002). Folic acid and homocysteine in age-related disease, *Ageing Res Rev*, 1, 95–111.

Mattson, M. P., Chan, S. L., Camandola, S., (2001). Presenilin mutations and calcium signaling defects in the nervous and immune systems. *Bioessays*, 23(8):733-44.

Mayer, B., Hemmens, B., (1997). Biosynthesis and action of nitric oxide in mammalian cells, *Trends in Biochemical Sciences*, 22(12): 477–481.

Mayer, M. P., & Bukau, B., (1998). Hsp70 chaperone system: Diversity of cellular functions and mechanism of action. *Biological chemistry*, 379(3):261-268.

McCubrey, J. A., Lahair, M. M., Franklin, R. A., (2006). Reactive oxygen species-induced activation of the MAP kinase signaling pathways, *Antioxid. Redox Signal.* 8, 1775–1789.

McCaddon, A., (2006). Homocysteine and cognition - A historical perspective, *J. Alzheimer's Disease.*, 9(4): 361-380.

McCaddon, A., Cobalz Limited, (2001). A method of treating an individual with metabolic evidence of vitamin B12 deficiency and co-existing dementia or other neuropsychiatric abnormality, and to medical compositions for use in said method. U.K. patent application 0110336.5.

McCaddon, and Davies, G., (2005). Co-administration of N-acetylcysteine, vitamin B12 and folate in cognitively impaired hyperhomocysteinaemic patients, *Int. J. Geriatr. Psychiatry*, 20, 998–1000.

McCully, K. S., (2005). Hyperhomocysteinemia and arteriosclerosis: historical perspectives, *Clin Chem Lab Med*, 43(10): 980-6.

McMahon, M., Itoh, K., Yamamoto, M., Chanas, S. A., Henderson, C. J., McLellan, L. I., (2001). The Cap'n'Collar basic leucine zipper transcription factor Nrf2 (NF-E2 p45-related factor 2) controls both constitutive and inducible expression of intestinal detoxification and glutathione biosynthetic enzymes, *Cancer Res*, 61(8):3299–3307.

McNulty H, Cuskelly GJ, Ward M (2000). Response of red blood cell folate to intervention: implications for folate recommendations for the prevention of neural tube defects, *Am J Clin Nutr.* 71(5 Suppl):1308S-11S

H., McNulty, L. R., C. Dowey, J. J., Strain, A., Dunne, M., Ward, A. M., Molloy, L. B., McAnena, J. P., Hughes, M., Hannon-Fletcher, J. M., Scott, (2006). Riboflavin Lowers Homocysteine in Individuals Homozygous for the *MTHFR* 677C3T Polymorphism. *Circulation*. 113,74-80.

McNulty, H., Pentieva, K., Hoey, L., Ward M., (2008). Homocysteine, B-vitamins and CVD. *Proceedings of the Nutrition Society*, 67, 232–237

McNulty, H., Cuskelly, G. J., Ward, M., (2009). Response of red blood cell folate to intervention: implications for folate recommendations for the prevention of neural tube defects. *Am J Clin Nutr*, 71 (suppl):1308S–11S

Mosser, D. D., Caron, A. W., Bourget, L., Densi-Larose, C. and Massie, B.(1997). Role of the human heat shock protein hsp70 in protection against stress-induced apoptosis. *Mol. Cell. Biol.* 17, 5317-5327.

McCaddon A, Hudson P (2007) Alzheimer's disease, oxidative stress and B-vitamin depletion. *Future Neurology* 2(5):537-47

Mehlen, P., Briolay, J., Smith, L., Diaz-Latoud, C., Fabre, N., Pauli, D., and Arrigo, A. P., (1993). Analysis of the resistance to heat and hydrogen peroxide stresses in COS cells transiently expressing wild type or deletion mutants of the *Drosophila* 27-kDa heat shock protein, *Eur. J. Biochem*, 215, 277–284.

Mehlen, P., Kretz-Remy, C., Preville, X., and Arrigo, A. P., (1996). Human hsp27, *Drosophila* hsp27 and aB-crystallin expression-mediated increase in glutathione is

essential for the protective activity of these proteins against TNF α -induced cell death. *EMBO J.*, 15, 2695–2706.

Mehlen, P., Preville, X., Chareyron, P., Briolay, J., Klemenz, R., Arrigo, A. P., (1995). Constitutive expression of human hsp27, *Drosophila* hsp27, or human alpha B-crystallin confers resistance to TNF- and oxidative stress-induced cytotoxicity in stably transfected murine L929 fibroblasts. *J Immunol*, 154, 363-374.

Mémet, S., (2006). NF-kappaB functions in the nervous system: from development to disease, *Biochem Pharmacol*, 72(9):1180-95.

Menoret, A., Chaillot, D., Callahan, M, & Jacquin, C. (2002). Hsp70, an immunological actor playing with the intracellular self under oxidative stress. *International Journal of Hyperthermia*, 18(6): 490-505.

Miller, J. W., (1999). Homocysteine and Alzheimer's disease, *Nutr. Rev*, 57, 126–129.

Blandini, F., Fancellu, R., Martignoni, E., Mangiagalli, A., Pacchetti, C., Samuele, A., & Minowada, G., Welch, W. J., (1995). Clinical implications of the stress response, *J. Clin. Invest*, 95, 3–12.

Mitchell, J. B., Russo, A., (1983) Thiols, thiol depletion, and thermosensitivity. *Radiat Res*, 95, 471–485.

Miyazawa, K., Mori, A., Miyata, H., Akahane, M., Ajisawa, Y., and Okudaira, H. (1998). Regulation of interleukin-1 β -induced interleukin-6 gene expression in human fibroblast-like synoviocytes by p38 mitogen-activated protein kinase, *J. Biol. Chem*, 273, 24832–24838.

Momose, I., Terashima, M., Nakashima, Y., Sakamoto, M., Ishino, H., Nabika, T., Moncada, S., Higgs, E.A., (1991). Endogenous nitric oxide: physiology, pathology and clinical relevance, *European Journal of Clinical Investigation*, 21(4): 361–374.

Morita, T., (2005). Heme oxygenase and atherosclerosis. Arteriosclerosis, thrombosis and vascular Biology, 25, 1786-1795.

Motterlini, R., Foresti, R., Intaglietta, M., and Winslow, R. M., (1996). NO-mediated activation of heme oxygenase: endogenous cytoprotection against oxidative stress to endothelium, *Am. J. Physiol. Heart Circ. Physiol*, 270, H107-H114.

Mujumdar, V. S., Aru, G. M., Tyagi, S. C., (2001). Induction of oxidative stress by homocyst(e)ine impairs endothelial function. *J Cell Biochem*, 82, (3):491-500

Müller, C. W., Rey, F. A., Sodeoka, M., Verdine, G. L. and Harrison, S. C. (1995). Structure of the NF-kappa B p50 homodimer bound to DNA, *Nature*, 373, 311–317

Muller, M. R., Pfannes, S. D., Ayoub, M., Hoffmann, P., Bessler, W. G., Mittenbuhler, K., (2001). Immunostimulation by the synthetic lipopeptide P3CSK4: TLR4-independent activation of the ERK1/2 signal transduction pathway in macrophages, *Immunology*, 103(1): 49–60.

Muslin, A. J., (2005). Role of raf proteins in cardiac hypertrophy and cardiomyocyte survival, *Trends Cardiovasc. Med*, 15, 225–229.

Muslin, A. J., (2008). MAPK signalling in cardiovascular health and disease: molecular mechanisms and therapeutic targets, *Clinical Science*, 115, 203–218.

Musch, M. W., Ciancio, M., Sarge, K., Chang, E. B., (1996). Induction of heat shock protein 70 protects intestinal epithelial IEC-18 cells from oxidant and thermal injury, *Am. J. Physiol*, 270, C429–C436.

Musch, M. W., Sugi, K., Straus, D. Chang, E. B., (1999). Heat-shock protein 72 protects against oxidant-induced injury of barrier function of human colonic epithelial Caco2/bbe cells, *Gastroenterology*, 117, 115–122.

Nagaraja, D., Noone, M. L., Bharatkumar, V. P., Christopher, R., (2008). Homocysteine, folate and vitamin B(12) in puerperal cerebral venous thrombosis, *J Neurol Sci*, 272(1-2):43-7.

Nakaso, K., Yano, H., Fukuhara, Y., Takeshima, T., Wada-Isoe, K., Nakashima, K., (2003). PI3K is a key molecule in the Nrf2-mediated regulation of antioxidative proteins by hemin in human neuroblastoma cells, *FEBS Lett*, 546, 181–184.

Nakano, H., Nakajima, A., Sakon-Komazawa, S., Piao, J. H., Xue, X., Okumura, K., (2006). Reactive oxygen species mediate crosstalk between NF-kappaB and JNK. *Cell Death Differ*, 13(5):730-7.

Nappi, G., (2001). Plasma homocysteine and L-DOPA metabolism in patients with Parkinson disease, *Clin. Chem*, 47, 1102–1104.

Nathan, C., Xie, Q. W., (1994). Regulation of biosynthesis of nitric oxide. *J Biol Chem*, 269(19):13725–13728.

Nathan, C., (1992). Nitric oxide as a secretory product of mammalian cells. *FASEB J*, 6, 3051–3064.

Ng, D. C., Bogoyevitch, M. A., (2000). The mechanism of heat shock activation of ERK mitogen-activated protein kinases in the interleukin 3-dependent ProB cell line BaF3, *J Biol Chem*, 275, 40856–40866.

Nguyen, T., Sherratt, P. J., and Pickett, C. B., (2003). Regulatory mechanisms controlling gene expression mediated by the antioxidant response element, *Annu Rev Pharmacol Toxicol*, 43,233–260.

Nicotera, P., Melino, G., (2004). Regulation of the apoptosis-necrosis switch. *Oncogene*, 23(16):2757-65.

Nishioka, M., T. Araib, K., Yamashitac, M. Sasada, H., Morib, H., Ishiib, K., Tajimaa, K., Makinoe, K., Fukud., (2003). *Life Sciences* 73, 221–231.

Nioi, P., and Hayes, J. D., (2004). Contribution of NAD(P)H:quinone oxidoreductase 1 to protection against carcinogenesis, and regulation of its gene by the Nrf2 basicregion leucine zipper and the arylhydrocarbon receptor basic helix-loop-helix transcription factors, *Mutat Res*, 555,149–171.

Numazawa, S., Ishikawa, M., Yoshida, A., Tanaka, S., Yoshida, T., (2003). A typical protein kinase C mediates activation of NF-E2-related factor 2 in response to oxidative stress, *Am. J. Physiol. Cell. Physiol*, 285, 334–342.

Nyunoya, T., Coleman, M., Spitz, D. R., Hunninghake, G.W., (2008). Constitutive ERK MAPK activity regulates macrophage ATP production and mitochondrial integrity, *J.Immunol*, 80:7485–7496.

Obeid, R., & Herrmann, W., (2006). Mechanisms of homocysteine neurotoxicity in neurodegenerative diseases with special reference to dementia. *FEBS Lett*, 580, 2994-3005

Obermeier, F., Gross, V., Scholmerich, J., Falk, W., (1999). Interleukin-1 production by mouse macrophages is regulated in a feedback fashion by nitric oxide. *Journal of Leukocyte Biology*, 66(5):829–836.

Ohkawara, T., Takeda, H., Nishiwaki, M., Nishihira, J., Asaka, M., (2006). Protective effects of heat shock protein 70 induced by geranylgeranylacetone on oxidative injury in rat intestinal epithelial cells. *Scand J Gastroenterol* , 41, 312-317.

Ortega, M. A., Aleixandre de Artinano, A. M., (2000). Nitric oxide reactivity and mechanisms involved in its biological effects. *Pharmacol Res* , 42: 421–427.

Otani, S., Otaka, M., Jin, M., Okuyama, A., Itoh, S., Iwabuchi, A., Sasahara, H., Itoh, H., Tashima, Y., Masamune, O., (1997). Effect of preinduction of heat shock proteins on acetic acid-induced colitis in rats. *Dig Dis Sci*, 42, 833-846.

Otterbein, L. E., & Choi, A. M. K., (2000). Heme oxygease:colors defense against cellular stress. *Am. J. Pysiol Lung Cell Mol Physiol*, 279(6):L1029-1054.

Pamplona, R. & Barja, G., (2006). Mitochondrial oxidative stress againg and caloric restriction: the protein and methionine connection. *Biochimica et biophysica Acta (BBa)*.

Pandey, P., Farber, R., Nakazawa, A., (2000). Hsp27 functions as a negative regulator of cytochrome c-dependent activation of procaspase-3, *Oncogene*,19, 1975–1981.

Patel, R. P., Moellering, D., Murphy-Ullrich, J., Jo, H., Beckman, J. S., & Darley-Usmar V. M., (2000). Cell signaling by reactive nitrogen and oxygen speacies in arthrosclerosis. *Free radical biology and medicine*, 28, (12): 1780-1794.

Pearl, L. H., & Prodromou, C., (2002). Structure, function and mechanism of the hsp90 molecular chaperone. *Adv. Protein chem.* 59, 157-186.

Peng, H.-B., Rajavashisth, T.B., Libby, P., and Liao, J. K., (1995a). Nitric oxide inhibits macrophage-colony stimulating factor gene transcription in vascular endothelial cells, *J. Biol.Chem.*, 270, 17050–17055.

Peng, H.-B., Libby, P., and Liao, J. K., (1995b). Induction and stabilization of I kappa B alpha by nitric oxide mediates inhibition of NF-kappa B, *J. Biol. Chem.*, 270,14214–14219.

Perkins, N. D., (2006). Post-translational modifications regulating the activity and function of the nuclear factor kappa B pathway, *Oncogene*, 25, 6717–6730.

Pezacka, E. H., (1993). Identification and characterization of two enzymes involved in the intracellular metabolism of cobalamin. Cyanocobalamin beta-ligand transferase and microsomal cob(III)alamin reductase. *Biochim Biophys Acta*, 1157(2):167-77

Pezacka, E., Green, R., Jacobsen D. W., (1990). Glutathionylcobalamin as an intermediate in the formation of cobalamin coenzymes, *Biochem Biophys Res Commun*, 169:(2)443-50.

Pham, C. G., Bubici, C., Zazzeroni, F., Papa, S., Jones, J., Alvarez, K., (2004). Ferritin heavy chain upregulation by NF-kappaB inhibits TNFalpha-induced apoptosis by suppressing reactive oxygen species, *Cell* , 119,529–542.

Picerno, I., Chirico, C., Condello, S., Visalli, G., Ferlazzo, N., Gorgone, G., Caccamo, D., Ientile, R., (2006). Homocysteine induces DNA damage and alterations in proliferative capacity of T-lymphocytes: a model for immunosenescence? *Biogerontology*, 8, (2):111-9.

Pietarinen-Runtti, P., Lakari, E., Raivio, K. O., and Vuokko, L., Kinnula., (2000). Expression of antioxidant enzymes in human inflammatory cells. *Am J Physiol Cell Physiol*, 278,118-125.

Pischke, S. E., Zhou, Z., Song, R., Ning, W., Alam, J., Ryter, S. W., and Choi, A. M., (2005). Phosphatidylinositol 3-kinase/Akt pathway mediates heme oxygenase-1 regulation by lipopolysaccharide, *Cell Mol Biol*, 51, 461–470.

Pinsky DJ, Patton S, Mesaros S, Brovkovich V, Kubaszewski E, Grunfeld S, Malinski T (1997). Mechanical transduction of nitric oxide synthesis in the beating heart *Circ Res*. 81(3):372-9.

Pockley, A. G., (2003). Heat shock proteins as regulators of the immune response. *Lancet*, 362, 469-476.

Prasad, M. V., Dermott J. M., Heasley, L. E., Johnson, G. L., Dhanasekaran, N., (1995). Activation of Jun kinase/stress-activated protein kinase by GTPase-deficient mutants of Ga12 and Ga13, *J Biol Chem*, 270, 18655–18659.

Pratt, W. B., & Toft, D. O., (2003). Regulation of signaling protein function and trafficking by the Hsp90/hsp70-based chaperone machinery. *Exp. Biol. Med. (Maywood)*, 228, 111-133.

Preville, X., Salvemini, F., Giraud, S., Chaufour, S., Paul, C., Stepien, G., (1999). Mammalian small stress proteins protect against oxidative stress through their ability to increase glucose-6-phosphate dehydrogenase activity and by maintaining optimal cellular detoxifying machinery, *Exp Cell Res*, 247, 61-78.

Prohaszka, Z., & Fust, G.,(2004). Immunological aspects of heat-shock proteins- the optimum stress of life, *Molecular Immunology*, 41, 29-44.

Qin, S., Chock, P. B., (2003). Implication of phosphatidylinositol 3-kinase membrane recruitment in hydrogen peroxide-induced activation of PI3K and Akt, *Biochemistry* 42, 2995–3003.

Quinlivan, E. P., McPartlin, J., McNulty, H., Ward, M., Strain, J. J., Weir, D. G., Scott, J. M., (2001). Importance of both folic acid and vitamin B12 in reduction of risk of vascular disease. *Lancet*, 359, 227–228

Raingeaud, J., Whitmarsh, A. J., Barrett, T., Derijard, B., and Davis, R. (1996). MKK3- and MKK6-regulated gene expression is mediated by the p38 mitogen-activated protein kinase signal transduction pathway, *Mol. Cell. Biol.* 16, 1247–1255.

Raingeaud, J., Gupta, S., Rogers, J., Dickens, M., Han, J., Ulevitch, R. J., and Davis, R. J., (1995). Pro-inflammatory cytokines and environmental stress cause p38 mitogen-activated protein kinase activation by dual phosphorylation on tyrosine and threonine, *J. Biol. Chem.* 270, 7420–7426.

Raman, M., Chen, W. and Cobb, M. H., (2007). Differential regulation and properties of MAPKs. *Oncogene* 26, 3100–3112.

Reed, J. C., (2000). Mechanism of apoptosis (Warner/Lambert Award), *Amer. J. Pathol*, 157, 1415-1430.

Refsum, H., Ueland, P. M., Nygard, O., Vollset, S. E., (1998). Homocysteine and cardiovascular disease, *Annu. Rev. Med*, 49, 31–62.

Refsum, H., (2001). Folate, vitamin B12 and homocysteine in relation to birth defects and pregnancy outcome, *Br. J. Nutr*, 85(Suppl. 2):S109–S113.

Ren, H., Musch, M. W., Kojima, K., Boone, D., Ma, A., Chang E. B., (2001). Short-chain fatty acids induce intestinal epithelial heat shock protein 25 expression in rats and IEC 18 cells, *Gastroenterology*, 121, 631-639.

Ryter SW, Choi AM (2002) Heme oxygenase-1: molecular mechanisms of gene expression in oxygen-related stress. *Antioxid Redox Signal* 4: 625–632.

Rushmore TH, Morton MR, Pickett CB (1991). The antioxidant responsive element. Activation by oxidative stress and identification of the DNA consensus sequence required for functional activity. *J.Biol. Chem.* 266: 11632-11639.

Rincon, M., Enslen, H., Raingeaud, J., Recht, M., Zapton, T., Su, M. S., Penix, L. A., Davis, R. J., and Flavell, R. A., (1998). Interferon-gamma expression by Th1 effector T cells mediated by the p38 MAP kinase signaling pathway, *EMBO J.* 17, 2817–2829.

Ritossa, F.(1962). New puffing pattern induced by temperature shock and DNP in *Drosophila*. *Experientia*, 18(12): 571-573.

Rogalla, T., Ehrnsperger, M., Preville, X., Kotlyarov, A., Lutsch, G., Ducasse, C., Paul, C., Wieske, M., Arrigo, A. P., Buchner, J., and Gaestel, M., (1999). Regulation of Hsp27 oligomerization, chaperone function, and protective activity against oxidative stress/tumor necrosis factor alpha by phosphorylation, *J Biol Chem* 274,18947–18956.

Roigas, J., Wallen, E. S., Loening, S. A., Moseley, P. L., (1998). Effects of combined treatment of chemotherapeutics and hyperthermia on survival and the regulation of heat shock proteins in Dunning R3327 prostate carcinoma cells. *Prostate*, 34,195–202

Ropeleski, M. J., Tang, J., Walsh-Reitz, M. M., Musch, M. W., Chang E. B.,(2003). Interleukin-11-induced heat shock protein 25 confers intestinal epithelial-specific cytoprotection from oxidant stress, *Gastroenterology*, 124, 1358-1368.

Rosenberg, I. H., (2007). Challenges and opportunities in the translation of the science of vitamins, *Am J Clin Nutr*, 85 (1):325S-327.

Ruchalski, K., Mao, H. P., Li, Z. J., Wang, Z. Y., Gillers, S., Wang, Y. H., Mosser, D. D., Gabai, V., Schwartz, J. H., & Borkan, S. C. (2004). Regulation of monocyte migration by ampterin (HMGB1). *Blood*, 104(4):1174-1182.

Ruffels, J., Griffin, M., Dickenson, J. M., (2004). Activation of ERK1/2, JNK and PKB by hydrogen peroxide in human SH-SY5Y neuroblastoma cells: role of ERK1/2 in H₂O₂-induced cell death, *Eur. J. Pharmacol*, 483, 163–173.

Ryter, S., Kim, H. P., Hoetzel, A., Park, J. W., Nakahira, K., Wang, X., (2007). Mechanisms of Cell Death in Oxidative Stress. *Antioxidants & Redox Signaling*, 9(1):49-89.

Saito, Y., Nishio, K., Ogawa, Y., Kimata, J., Kinumi, T., Yoshiday, Y., Noguchi, N., & Niki, E., (2006). Turning point in apoptosis/necrosis induced by hydrogen peroxide, *Free Radical Research*, 40(6):619–630.

Saleh, A., Srinivasula, S. M., Balkir, L., Robbins, P. D., Alnemri, E. S., (2000). Negative regulation of the Apaf-1 apoptosome by Hsp70, *Nat Cell Biol*, 2(8): 476-83.

Salina, M., Diaz, R., Abraham, N. G., Ruiz de Galarreta, C. M., and Cuadrado, A., (2003). Nerve growth factor protects against 6-hydroxydopamine-induced oxidative

stress by increasing expression of heme oxygenase-1 in a phosphatidylinositol 3-kinase-dependent manner, *J Biol Chem*, 278, 13898–13904.

Samali, A., Robertson, J. D., Peterson, E., Manero, F., van Zeijl, L., Paul, C., Cotgreave, I. A., Arrigo, A. P. and Orrenius, S. (2001). Hsp27 protects mitochondria of thermotolerant cells against apoptotic stimuli. *Cell Stress Chaperones* 6, 49-58.

Samali, A., and Cotter, T. G., (1996). Heat shock proteins increase resistance to apoptosis, *Exp. Cell Res*, 223, 163–170.

Sassa, S., (2004). Why heme needs to be degraded to iron, biliverdin IXalpha, and carbon monoxide? *Antioxid Redox Signal*. 6(5):819-24

Scalabrino, G. (1999). Epidermal growth factor as a local mediator of the neurotrophic action of vitamin B12 (cobalamin) in the rat central nervous system, *FASEB J*, 13, 2083–2090.

Scalabrino, G., (2005). Cobalamin in subacute combined degeneration and beyond traditional interpretations and novel theories. *Experimental neurology*, 192(2): 463-479.

Schilb, A., Riou, V., Schoepfer, J., Ottl, J., Müller, K., Chene, P., Mayr, L. M., Filipuzzi, I., (2004). Development and implementation of a highly miniaturized confocal 2D-FIDA-based high-throughput screening assay to search for active site modulators of the human heat shock protein 90beta. *J Biomol Screen*. 9(7):569-77.

Schwartz, L. M., Smith, S. W., Jones, M. E., Osborne, B. A., (1993). Do all programmed cell deaths occur via apoptosis? *Proc Natl Acad Sci USA*, 90, 980–984.

Schwartz, S. M., Hemark, R. L., & Majesky, M. W., (1990). Developmental mechanisms underlying pathology of arteries, *Physiological Reviews*, 70(4):1177-1209.

Schweichel, J., & Merker, H., (1973). The morphology of various types of cells death in prenatal tissues, *teratology*, 7(3):253-266.

Selhub, J., Jacques, P. F., Bostom, A. G., (2000). Relationship between plasma homocysteine and vitamin status in the Framingham study population, Impact of folic acid fortification, *Public Health Rev*, 28, 117–145.

Sennequier, N., Stuehr, D. J., (1996). Analysis of substrate-induced electronic, catalytic, and structural changes in inducible NO synthase. *Biochemistry*, 35(18):5883–5892.

Seshadri, S., Beiser, A., Selhub, J., (2002). Plasma homocysteine as a risk factor for dementia and Alzheimer's disease, *N Engl J Med* , 346, 476–483.

Singh, R. and Czaja, M. J., (2007). Regulation of hepatocyte apoptosis by oxidative stress, *J Gastroenterology and Hepatology*, 22, Suppl. 1; S45–S48.

Smith L., Fantes K. H., Ball S., Waller J. G., Emery W. B., Anslow W. K. and Walker A. D., *Biochem. J.*, 1952, 52, 389–395.

Shane, B., (2000). Folic acid, vitamin B12 and vitamin B6. Philadelphia, Saunders, W. B.

Shi, Y. H., Mosser, D. D., & Morimoto, R. I. (1998). Molecular chaperone as HSF-1 specific transcription repressor. *Genes & Development*, 12(5): 654-666.

Shibahara, S., (2003). The heme oxygenase dilemma in cellular homeostasis: new insights for the feedback regulation of heme catabolism. *Tohoku J. Exp. Medicine*, 200(4):167-186.

Sies H., Glutathione and its role in cellular functions (1999). *Free Radic Biol Med.* 27; 9-10:916-21.

Shin-ichi, Y., Mikio, K., and Kazuhiro, N., (2000). Benzylidene Lactam Compound, KNK437, a Novel Inhibitor of Acquisition of Thermotolerance and Heat Shock Protein Induction in Human Colon Carcinoma Cells, *Cancer research*, 60, 2942–2948

Siow, R., Sato, h., & Mann, G., (1999). Heme oxygenase carbon monoxide signaling pathway in atherosclerosis: anti-atherogenic action of bilirubin and carbon monoxide? *Cardiovascular research*, 41(2): 385-394.

Stocker, R., McDonagh, A. F., Glazer, A. N., Ames, B. N., (1990). Antioxidant activities of bile pigments: biliverdin and bilirubin, *Methods Enzymol.* 186:301– 309.

Soares, M. P., Usheva, a., Brouard, s., Berberat, P. O., Gunther, L., Tobiasch, E., & bach, F. H., (2002). Modulation of endothelial cell apoptosis by heme oxygenase-1 derived carbon monoxide, *Antioxidants & redox signaling*, 4(2):321-329.

So-Hyun, P., Jung-Hee, Jang, Mei-Hua, L., Hye-Kyung, N. A., Young-Nam, Cha, and Young-Joon, S., (2007). *Antioxidants & Redox signaling*, 9, 12.

Son, G. H., Geum, D., Chung, S., Park, E., Lee, K. H., Choi, S., (2005). A protective role of 27-kDa heat shock protein in glucocorticoid-evoked apoptotic cell death of hippocampal progenitor cells, *Biochem Biophys Res Commun*, 338, 1751-1758.

Sriram, M., Osipiuk, J., Freeman, B. C., Morimoto, R. I., & Joachimiak, A. (1987). Human Hsp70 molecular chaperone binds two calcium ions within the ATPase domain. *Structure*, 5(3):403-414.

Stadtman, E. R., (2004). Role of oxidant species in aging. *Curr. Med. Chem.* 11, 1105-1112.

- Strasser, A., O'Connor, L., Dixit, V. M., (2000). Apoptosis signaling. [*Annu Rev Biochem*](#), 69,217-45.
- Stuehr, D. J., Kwon, N. S., Nathan, C. F., Griffith, O. W., Feldman, P. L., Wiseman, J., (1991). N omega-hydroxy-L-arginine is an intermediate in the biosynthesis of nitric oxide from L-arginine. *Journal of Biological Chemistry*, 266(10):6259–6263.
- Suarez-Moreira, E., Yun, J., Birch, C. S., Williams, J. H. H., McCaddon, A., and Brasch, N. E., (2006). Vitamin B₁₂ and redox homeostasis: Cob(II)alamin reacts with superoxide at rates approaching superoxide dismutase (SOD).
- Sun, Z., Zhang, S., Chan, J. Y., Zhang, D. D., (2007). Keap1 controls postinduction repression of the Nrf2-mediated antioxidant response by escorting nuclear export of Nrf2. *Mol Cell Biol*, 27(18): 6334–6349.
- Sun, B., and Karin, M., (2008). NF-KB signaling, liver disease and hepatoprotective agents, *Oncogene*, 27, 6228–6244.
- Sun, A. Y., Simonyi, A., Sun, G. Y., (2002). The French paradox and beyond: neuroprotective effect of polyphenols, *Free radic Bio Med.*, 32(4):314-318.
- Szeto, Y. T., Benzie, I. F., (2002). Effects of dietary antioxidants on human DNA ex vivo, *Free Radic Res*, 36, 113–118.
- Szabo, C., (2005). Roles of poly(ADP-ribose)polymerase activation in pathogenesis of diabetes mellitus and its complication: Pharmacological approach of DNA damage and repair: the PARO pathways. *Pharmacological research*, 52(1):60-71.
- Tavaria, M., Gabriele, T., Kola, I. & Anderson, R. L., (1995). A hitchiker's guide to the human Hsp70 family. *Cell stress & chaperones*, 1 (1):23-28.
- Tian, W., Bonkovsky, H. L., Shibahara, S., and Cohen, D. M., (2001) *Am. J.Physiol. Renal Physiol.* 281, F983-F991.
- Tissieres A, Mitchell HK and Tracey UM (1974) Proteins synthesis in salivary glands of *D. melanogaster*. Relation to chromosome puffs. *J Mol Biol* 84: 389-398
- Tulis DA, Durante W, Peyton KJ, Evans AJ, Schafer AI (2001) Heme oxygenase-1 attenuates vascular remodelling following balloon injury in rat carotid arteries. *Atherosclerosis* 155: 113–122.
- Trinklein, N. D., Murray, J. I., Hartman, S. J., Botstein, D., & Myers, R. M., (2004). Genome- wide regulation of mammalian heat shock response. *Mol. Biol. Cell*, 15, 1254-01261.
- Torres, M., Forman, H. J., (2003). Redox signalling and the MAP kinase pathways, *Biofactors*, 17,287–296.

Toledano, M. B., Ghosh, D., Trinh, F. and Leonard, W. J. (1993). N-terminal DNA-binding domains contribute to differential DNA-binding specificities of NF-kappa B p50 and p65, *Mol. Cell. Biol.*, 13, 852–860.

Toyuz, R. M., Schiffrin, E. L. (2004). Reactive oxygen species in vascular biology implication in hypertension. *Histochem cell Biol.* 122: 339-52.

Tsuchiya, A., Tashiro, E., Yoshida, M., Imoto, M., (2005). Involvement of nuclear accumulation of heat shock protein 27 in leptomycin B-induced apoptosis in HeLa cells. *J Antibiot*, 58: 810-816.

Tyagi, N., Ovechkin, A. V., Lominadze, D., Mosal, K. S., Tyagi, S. C. (2006). Mitochondrial mechanism of microvascular endothelial cells apoptosis in hyperhomocysteinemia, *J. cell Biochem*, 98(5):1150-62.

Tytell, M., (2005). Release of heat shock proteins (Hsps) and the effects of extracellular Hsps on neural cells and tissues. *International Journal of hyperthermia*, 21(5): 445-455.

Uchiyama, T., Engelman, R.M., Maulik, N., Das, D.K., (2004). Role of Akt signaling in mitochondrial survival pathway triggered by hypoxic preconditioning, *Circulation*, 22, 3042–3049.

Uchiyama, T., Astuta, H., Utsugi, T., Oguri, M., Haasegawa, A., Nakamura, T., Nakai, A., Nakata, M., Maruyama, I., & Tomura, H., (2007). HSF1 and constitutively active HSF1 improve vascular endothelial function (heat shock proteins improve vascular endothelial function. *Atherosclerosis*, 190(2): 321-329.

Valko, M., Rhodes, C. J., Moncol, J., Izakovic, M., & Mazur, M., (2006). Free radical metals and antioxidants on oxidative stress-induced cancer, *chemico-biological Interaction*, 160(1): 1-40.

Vanags, D. M., Poörn-Ares, M. I., Coppola, S., Burgess, D. H., and Orrenius, S., (1996). Protease involvement in fodrin cleavage and phosphatidylserine exposure in apoptosis, *J. Biol. Chem*, 271, 31075-31085.

Verhoef, P., Stampfer, M. J., Buring, J. E., Gaziano, J. M., Allen, R. H., Stabler, S. P., Reynolds, R. D., Kok, F. J., Hennekens, C. H. & Willett, W. C., (1996). Homocysteine metabolism and risk of myocardial infarction: relation with vitamins B6, B12, and folate. *Am. J. Epidemiol*, 143, 845–859.

Vermeulen, E. G., Stehouwer, C. D., Twisk, J. W., van der Berg, M., de Jong, S. C., Mackaay, A. J., van Campen, C. M., Visser, F. C., Jakobs, C. A., Bulterjys, E. J., Rauwerda, J. A., (2000). Effect of homocysteine-lowering treatment with folic acid plus vitamin B6 on progression of subclinical atherosclerosis: a randomised, placebo-controlled trial, *Lancet*, 355, (9203): 517–22.

Wallace, J. M.W., Bonham, M. P., Strain, J. J., Duffy, E. M., Robson, P. J., Ward, M., McNulty, H., Davidson, P. W., Myers, G. J., Shamlaye, C. F., Clarkson, T. W., Molloy, A. M., Scott, J. M., Ueland P. M., (2008). Homocysteine concentration,

related B vitamins, and betaine in pregnant women recruited to the Seychelles Child Development Study. *Am J Clin Nutr.* 87(2): 391–397.

Wang, B. S., Lin, J. K., Lin-Shiau, S. Y., (1999). Role of tyrosine kinase activity in 2,2V,2-tripyridine-induced nitricoxide generation in macrophages, *Biochemical Pharmacology*, 57, (12):1367–1373.

Wang, X., Martindale, J. L., Liu, Y., Holbrook, N. J., (1998). The cellular response to oxidative stress: influences of mitogen-activated protein kinase signaling pathways on cell survival, *Biochem J.*, 333, 291–300.

Wang X. (2001). The expanding role of mitochondria in apoptosis. *Genes Dev.* 15;15(22):2922-33.

Wellbrock C, Karasarides M, Marais R. (2004). The RAF proteins take centre stage. *Nature Reviews. Molecular Cell Biology*, 5(11), 875-85.

Weinberg, J. B., Chen, Y., Beasley, B. E., Ghosh, D. K., (2005). Cobalamins and cobinamides inhibit nitric oxide synthase enzymatic activity, *Blood* , 627.

Ward, M., McNulty, H., McPartlin, J., Strain, J. J., Weir, D. G., Scott, J. M., (1997). Plasma homocysteine, a risk factor for cardiovascular disease, is lowered by physiological doses of folic acid. *Q J Med* , 90:519–524

Ward, M., (2001). Homocysteine, folate, and cardiovascular disease. *Int J Vitam Nutr Res.* 71(3):173-8

Weinberg, J. B., Chen, Y., Jiang, N., Beasley, B. E., John, C., Salerno, Ghosh, D. K. E., (2009). Inhibition of nitric oxide synthase by cobalamins and cobinamides, *Free Radical Biology & Medicine*, 46,1626–1632

Wen, Z. K., Xu, W., Xu, L., Cao, Q. H., Wang, Y., Chu, Y. W. and Xiong, S. D., (2007). DNA hypomethylation is crucial for apoptotic DNA to induce systemic lupus erythematosus-like autoimmune disease in SLE-non-susceptible mice. *Rheumatology*, 46,1796–1803

Westwick, J. K., Weitzel, C., Minden, A., Karin, M., Brenner, D. A., (1994). Tumor necrosis factor alpha stimulates AP-1 activity through prolonged activation of the c-Jun kinase, *J Biol Chem*, 269, 26396–26401.

Wheatley, C., (2007). The return of the Scarlet Pimpernel: cobalamin in inflammation II-cobalamins can both selectively promote all three nitric oxide synthases (NOS), particularly iNOS and eNOS, and, as needed, selectively inhibit iNOS and nNOS. *Journal of Nutritional & Environmental Medicine*, 16(3–4): 181–211.

Widmann, C., Gibson, S., Jarpe, M. B., Johnson, G. L., (1999). Mitogen-activated protein kinase: conservation of a three-kinase module from yeast to human. *Physiol. Rev.* 79, 143–180.

- Wolj, S. P., (1994). *Methods Enzymol*, 233,182-189.
- Woo, K. S., Chook, P., Lolín, Y. I., Sanderson, J. E., Metreweli, C., Celermajer, D. S., (1999). Folic acid improves arterial endothelial function in adults with hyperhomocystinemia, *J Am Coll Cardiol*, 34 (7): 2002–2006.
- Wheeler, D. S., & Wong, H. r., (2007). Heat shock response and acute lung injury. *Free radical Biol. Med.*, 42, 1-14
- Whitesell, L., Lindquist, S. L., (2005). HSP90 and the chaperoning of cancer, *Nat Rev Cancer*, 5, 761–772.
- Whitmarsh, A. J., Yang, S. H., Su, M. S. S., Sharrocks, A. D., and Davis, R. J.(1997) *Mol. Cell. Biol.* 17, 2360–2371.
- Xia, Z., Dickens, M., Raingeaud, J., Davis, R. J., Greenberger, M. E., (1995). Opposing effects of ERK and JNK-p38 MAP kinases on apoptosis, *Science*, 270,1326–1331.
- Xia, Y. F., Liu, L. P., Zhong, C. P., Geng, J. G., (2001). NF-kappaB activation for constitutive expression of VCAM-1 and ICAM-1 on B lymphocytes and plasma cells, *Biochemical and Biophysical Research Communications*, 289 (4):851–856.
- Yamakawa, H., Ito, Y., Naganawa, T., Banno, Y., Nakashima, S., Yoshimu, S., Sawada, M., Nishimura, Y., Nozawa, Y., Sakai, N., (2000). Activation of caspase-9 and -3 during H₂O₂-induced apoptosis of PC12 cells independent of ceramide formation, *Neurol. Res*, 22, 556– 564.
- Yamada, K., Gravel, R. A., Toraya, T., & Matthews, R. G., (2006). Human methionine synthase reductase is a molecular chaperone for human methionine synthase, *Proc Natl Acad Sci U S A*, 103 (25):9476-81
- Ymaguchi, T., Shioji, I., Sugimoto, A., & Masayuki, Y., (2002). Psychological stress increases bilirubin metabolites in human urine. *Biochemical and Biophysical Research Comm.* 293, 517-520.
- Yet, S.-F., Tiang, R., Layne, M. D., Hsieh, C.-M., Maemura, K., Solovyeva, M., Ith, B., Melo, L. G., Zhang, L., Ingwall, J. S., Dzau, V. G., Lee, M.-U., and Perrella, M. A., (2001). *Circ. Res.* 89, 168–173.
- Yasui, K., Kowa, H., Nakaso, K., Takeshima, T., & Nakashima, K., (2000). Plasma homocysteine and MTHFR C677T genotype in levodopa-treated patients with PD., *Neurology* 55, 437–440.
- Yla-Herttuala, S., Nikkari, T., Hirvonen, J., Laaksonen, H., Mottonen, M., Pesonen, E., Raekallio, J., (1986). Biochemical composition of coronary arteries in Finnish children, *Arteriosclerosis*, 6, 230–236
- Yang Z, Barnes CJ & Kumar R. (2004) *Clin. Cancer Res.* 10: 3621-3628.

Yung, J. Y., Yoo, C. I., Kim, H. T., Kwon, C. H., Park, J. Y., Kim, Y. K., (2007). Role of mitogenactivated protein kinase (MAPK) in troglitazone-induced osteoblastic cell death, *Toxicology*, 234,73–82.

Zanotto-Filho, A., Delgado-Cañedo, A., Schröder, R., Becker, M., Klamt, F., Moreira, J. C., (2009). The pharmacological NFkappaB inhibitors BAY117082 and MG132 induce cell arrest and apoptosis in leukemia cells through ROS-mitochondria pathway activation, *Cancer Lett.*

Zhao, R., Davey, M., Hsu, Y. C., Kaplanek, P., Tong, A., Parsons, A. B.,(2005). Navigating the chaperone network: an integrative map of physical and genetic interactions mediated by the hsp90 chaperone, *Cell*, 120, 715–727.

Zhao, B., Guo, Q., & Xin, W., (2001). Free radical scavenging by green tea polyphenols: methods in enzymology. *Flavonoids & other polyphenols*. 2177-231.

Zhao, C. Q., Young, M. R., Diwan, B. A., Coogan, T. P., and Waalkes, M. P. (1997). Association of arsenic-induced malignant transformation with DNA hypomethylation and aberrant gene expression. *Proc. Natl Acad. Sci.* 94, 10907-10912.

Zhang, Y., Gordon, G.B., (2004). A strategy for cancer prevention: stimulation of the Nrf2-ARE signaling pathway. *Mol. Cancer Ther.* 3, 885–893.

Zhang, D. D., and Hannink, M. (2003). Distinct cysteine residues in Keap1 are required for Keap1-dependent ubiquitination of Nrf2 and for stabilization of Nrf2 by chemopreventive agents and oxidative stress, *Mol Cell Biol*, 23, 8137–8151.

Zhang, P., Omaye, S. T., (2001). Antioxidant and prooxidant roles for beta-carotene, alpha-tocopherol and ascorbic acid in human lung cells, *Toxicol, In Vitro*, 15, 13–24.

Zhang, X., Chen, S., Li, L., Wang, Q., Le, W., (2008). Folic acid protects motor neurons against the increased homocysteine, inflammation and apoptosis in SOD1 G93A transgenic mice, *Neuropharmacology*, 54 (7) :112-9.

Zou, J., Guo, Y., Guettouche, T., Smith, D. F., & Voellmy, R., (1998). Repression of heat shock transcription factor 1 activation by Hsp90 that form a stress-sensitive complex with HSF-1. *Cell*, 94, 471-480.